Charles University in Prague

Department of Physiology

and

Institute of Physiology AS CR, Prague

Biochemistry of Membrane Receptors

Postnatal development of $GABA_B$–receptors in the frontal rat brain cortex

Mgr. Dmytro Kagan

PhD Thesis

2014

Supervisor:

Doc. RNDr. Petr Svoboda, DrSc.

Institute of Physiology AS CR, Prague

Biochemistry of Membrane Receptors

Declaration by candidate.

I hereby declare that this thesis is my own work and it has not been submitted anywhere for any award. Where the sources of information have been used, they have been acknowledged.

In Prague, August 10, 2014 ……

Mgr. Dmytro Kagan

Acknowledgements.

First and foremost I would like to express my sincere gratitude to my advisor Doc. RNDr. Petr Svoboda, DrSc. for his continuous support of my Ph.D. study and research.

I am also very grateful to my colleagues from the Department who contributed immensely to my professional and personal time at the Institute of Physiology.

Lastly, I would like to thank my family for all their love and encouragement.

ABSTRACT

In this work, the detailed analysis of $GABA_B$–R/G protein coupling in the course of pre– and postnatal development of rat brain cortex indicated the significant intrinsic efficacy of $GABA_B$–receptors already shortly after the birth: at postnatal day 1 and 2. Subsequently, both baclofen and SKF97541–stimulated G protein activity, measured as the high–affinity [^{35}S]GTPγS binding, was increased. The highest level of agonist–stimulated [^{35}S]GTPγS binding was detected at postnatal days 14 and 15. In older rats, the efficacy, i.e. the maximum response of baclofen– and SKF97541–stimulated [^{35}S]GTPγS binding was continuously decreased so, that the level in adult, 90–days old rats was not different from that in newborn animals.

The potency of G protein response to baclofen stimulation, characterized by EC_{50} values, was also high at birth but unchanged by further development. The individual variance among the agonists was observed in this respect, as the potency of SKF97541 response was decreased when compared in 2–days old and adult rats.

The highest plasma membrane density of $GABA_B$–R, determined by saturation binding assay with specific antagonist [^{3}H]CGP54626A, was observed in 1–day old animals. The further development was reflected in *decrease* of receptor number. The adult level was ≈3–fold lower than in new born rats.

The ontogenetic development of Na^+/K^+–ATPase, which was used as marker of the overall brain development, was completely different from that observed in the study of $GABA_B$–R–signaling cascade: plasma membrane density of Na^+/K^+–ATPase was continuously increased in the course of the whole postnatal period; the adult level was ≈3–fold higher than in new born (1–day–old) rats.

The high level of lipofuscin like pigments (LFP) was generated in rat brain cortex during the first 5 days of postnatal life. Maximum level of LFP was detected on the postnatal day 2. Starting from the postnatal day 10, LFP concentration returned down to the prenatal level. A new rise in LFP concentration was observed in 90–days old animals. This second increase of LFP may indicate the beginning of the aging process in rat brain cortex.

ABSTRAKT

Byla provedena detailní analýza spřažení $GABA_B$-R s G proteinem během prenatálního a postnatálního vývoje mozkové kůry potkana, která ukázala významnou vnitřní účinnost $GABA_B$-R hned po narození (1. a 2. den). Následně byla zjištěna stimulovaná funkční aktivita G proteinů baklofenem i SKF97541 (agonisté $GABA_B$-R), která byla měřena pomocí vazby [^{35}S] GTPγS, jejíž nejvyšší hodnota byla detekována během 14. a 15. dne postnatálního vývoje. Účinnost, tj. maximální odpověď baklofenem a SKF97541 stimulované vazby [^{35}S] GTPγS, se u starších potkanů stále snižovala tak, že její hodnota měřená u devadesátidenních potkanů se nelišila od hodnot u novorezených zvířat.

Velikost odpovědi G proteinů na stimulaci baklofenem (vyjádřena jako EC_{50}) byla také zvýšena po narození a během dalšího vývoje se neměnila. Na rozdíl od baklofenu se síla odpovědi SKF97541 zmenšovala (při porovnání dvoudenních mláďat a dospělých potkanů).

Nejvyšší zastoupení $GABA_B$-R v plazmatické membráně stanovené pomocí saturačních vazebných pokusů s použitím specifického antagonisty [^{3}H] CGP54626A bylo detekováno u jednodenních zvířat. Další vývoj byl charakterizován *snížením* počtu receptorů. Ve srovnání s novorozenými potkany byla hladina u dospělých jedinců 3x nižší.

Ontogenetický vývoj Na^+/K^+-ATPázy (která slouží jako standard celkového vývoje mozku) se zcela lišil ve srovnání s vývojem signalizační kaskády $GABA_B$-R: množství Na^+/K^+-ATPázy ve frakcích plazmatických membrán se neustále zvyšovalo v průběhu celé ontogeneze; hladina u dospělých zvířat byla až 3x vyšší než u mláďat.

V mozkové kůře se vytvářela vysoká hladina lipofuscinových pigmentů (LFP) během prvních pěti dnů od narození. Maximální množství LFP bylo detekováno u dvoudenních zvířat. Po 10 dnech se koncentrace LFP vrátila na prenatální hodnotu. Nový vzestup LFP byl zaznamenán u devadesátidenních potkanů. Toto další zvýšení obsahu LFP může představovat začátek procesu stárnutí mozkové kůry potkana.

CONTENTS

1. LIST OF AUTHOR'S PUBLICATIONS

1. Bourova, L., Vosahlikova, M., **Kagan, D.**, Dlouha, K., Novotny, J. and Svoboda, P. (2010): Long–term adaptation to high doses of morphine causes desensitization of mu–OR– and delta–OR–stimulated G protein response in forebrain cortex but does not decrease the amount of G protein alpha subunits. Medical Science Monitor 16, BR260–270 (IF = 1.543).

2. Ujcikova, H., Dlouha, K., Roubalova, L., Vosahlikova, M., **Kagan, D.** and Svoboda P. (2011): Up–regulation of adenylylcyclases I and II induced by long–term adaptation of rats to morphine fades away 20 days after morphine withdrawal. Biochimica et Biophysica Acta 1810, 1220–1229 (IF = 3.990).

3. Wilhelm, J., Ivica, J., **Kagan, D.** and Svoboda P. (2011) Early postnatal development of rat brain is accompanied by generation of lipofuscin–like pigments. Molecular and Cellular Biochemistry 347, 157–162 (IF = 2.168).

4. **Kagan, D.**, Dlouhá, K., Roubalová, L. and Svoboda, P. (2012): Ontogenetic development of GABA(B)–receptor signaling cascade in plasma membranes isolated from rat brain cortex; the number of GABA(B)–receptors is high already shortly after the birth. Physiological Research 61, 629–635 (IF = 1.531).

5. Dlouhá, K., **Kagan, D.**, Roubalová, L., Ujčíková, H. and Svoboda, P. (2013) Plasma membrane density of GABAB–R1a, GABAB–R1b, GABA–R2 and trimeric G proteins in the course of postnatal development of rat brain cortex. Physiological Research 62, 547–559 (IF = 1.555).

6. Ujčíková H., Brejchová J., Vošahlíková M., **Kagan D.**, Dlouhá K., Sýkora J., Merta L., Drastichová Z., Novotný J., Ostašov P., Roubalová L., Hof M. and Svoboda P. (2014): Opioid–Receptor (OR) Signaling Cascades in Rat Cerebral Cortex and Model Cell Lines: the Role of Plasma Membrane Structure. Physiological Research, 63, Suppl. 1, 165–176 (IF = 1.555).

7. Ujcikova, H., Eckhardt, A., **Kagan, D.**, Roubalova, L. and Svoboda, P. (2014): Proteomic analysis of post–nuclear supernatant fraction and Percoll–purified membranes prepared from brain cortex of rats exposed to increasing doses of morphine. Proteome Science, 12:11 (IF = 1.88).

2. ABBREVIATIONS

BPM – bulk of plasma membranes

DRM – detergent–resistant membrane domain

cAMP – cyclic adenosine monophosphate

EDTA – Ethylenediaminetetraacetic acid

GABA– γ–aminobutyric acid

$GABA_B$–R – $GABA_B$ receptors

GDP – guanozine diphosphate

GPCR – G protein coupled receptor

α–GPDH – α–glycerolphosphate

GSH/GSSG – reduced glutathione/oxidised glutathione

GTP – guanozine triphosphate

IP_3 – inositol triphosphate

HEK293 – human embryonal kidney cells

HEPES – 4–(2–hydroxyethyl)–1–piperazineethanesulfonic acid

HPLC – high performance liquid chromatography

mGluR – metabotropic glutamate receptor

nAChR – nicotinic acetylcholine receptor

LPM – low density membrane fragments

LFP – lipofuscin–like pigments

MDCK – Madin–Darby canine kidney cells

PM – plasma membranes

rpm – rounds per minute

ROS – reactive oxygen species

SKF – 1–[2–(4–Methoxyphenyl)–2–[3–(4–methoxyphenyl)propoxy]ethyl]imidazole

SDH – succinate dehydrogenase

TM – transmembrane

Tris – tris–(hydromethyl)–aminomethan

VIP–PACAP – Vasoactive intestinal peptide – Pituitary adenylate cyclase–activating polypeptide

3. AIMS OF THE THESIS

1) ***The first aim*** of my work was to improve and refine the method for isolation of plasma membrane fraction (PM) from frontal brain cortex. The main problem in the past was to find an optimum compromise between the amount of protein applied per density gradient and the purity of PM preparation. Application of the high amount of protein in post–nuclear fraction (PNS) resulted in PM contaminated to the higher or lower degree by mitochondrial fragments. Furthermore, the recovery of PM protein, when compared with the starting homogenate or post–nuclear fraction, was not always reproducible and standard. The improved method was subsequently used for studies of opioid– and $GABA_B$–receptor signaling in frontal brain cortex (Bourova *et al.*, 2010; Ujcikova *et al.*, 2011, Ujcikova *et al.*, 2014).

I have also participated in testing the effect of non–ionic detergents Triton–X100 and Brij58 on brain cortex PM and compared flotation of Percoll–purified PM in the presence or absence of low–concentrations of these detergents. This procedure has been introduced in our laboratory by Drs. V. Lisy, L. Rudajev and J. Stohr and at present time, it may be used for preparation of membrane domains/ rafts with unchanged or even higher efficacy of coupling between $GABA_B$–R and the cognate G protein of Gi/Go family, than the original, detergent–untreated domains (**Figs. 22–25**).

2) ***The second aim*** of my work was to introduce the new method for determination of the number of $GABA_B$–R in PM prepared form the frontal rat brain cortex. This can not be done by radiolabelled GABA itself because of the low–affinity of GABA for these receptors. Therefore, I have introduced the two radioligands, agonist [^{3}H]baclofen and antagonist [^{3}H]CGP54626A, carried out the direct saturation binding assays with increasing concentrations of these specific and highly radioactive ligands and determined the maximum number (Bmax) and dissociation constant (Kd) of their binding sites in various PM preparations (Kagan *et al.*, 2012). The Bmax values of [^{3}H]baclofen– and [^{3}H]CGP54626A–binding in PM were determined in parallel with [^{3}H]ouabain binding, which was used as an estimate of PM density of prototypical PM marker, Na^+/K^+–ATPase (Dlouha *et al.*, 2012). PM content of Na^+/K^+–ATPase was also used as a general marker of forebrain cortex development and maturation of PM protein composition.

3) Determination of the number of $GABA_B$–receptors at different stages of ontogenetic development is not sufficient to characterize the function of $GABA_B$–R signaling cascade as the primary signal represented by binding of GABA to receptor sites oriented at the extracellular side of plasma membrane is transmitted into the cell interior by trimeric G proteins. These proteins transmit the signal further down–stream but also terminate and regulate the functioning of $GABA_B$–R pathway. For ***this third aim*** of my work I used the high–affinity [^{35}S]GTPγS binding assay adapted to analysis of the brain tissue. This methodological improvement was based on the usage of relatively high GDP concentrations (20–30 μM) which suppressed the high basal level of [^{35}S]GTPγS binding (Roubalova *et al.*, 2010; Kagan *et al.*, 2012).

4) Potent $GABA_B$–R agonist SKF97541 was described as a useful agent in treatment of at least some forms of epileptic seizures. Therefore, I have compared the ontogenetic profile of baclofen– and SKF–stimulated [^{35}S]GTPγS binding with the aim to define even the small difference between these two agents when stimulating the cognate G proteins. The maximum of baclofen–stimulated [^{35}S]GTPγS binding was detected at postnatal day 10, while the maximum of SKF–stimulated [^{35}S]GTPγS binding was measured at postnatal day 15. Thus, the effect of these two agonists on functional activity of $GABA_B$–R in the course of postnatal period was not the same (Kagan *et al.*, 2012).

5) Finally, I have participated in studies of formation of lipofuscin–like pigments (LFP) in frontal rat brain cortex in the neonatal period and during the early postnatal period. The generation of LFP represents an important test/ marker of oxidative damage of the brain tissue by free oxygen radicals. Analysis of LFP was made first in the whole tissue homogenates (Wilhelm at al., 2011), subsequently, LFP were determined in different subcellular membrane fractions: nuclear sediment, post–nuclear supernatant, mitochondria, microsomes, crude plasma membranes and cytosol (**Fig. 35**). Our results indicate that the highest accumulation of oxidative products takes place immediately after the birth; our results also indicate that brain LFP constitute a complex mixture of many chemical compounds whose composition is changing during development.

4. INTRODUCTION

4.1. G protein coupled receptors

The extracellular signals such as the light, hormones, neurotransmitters, pheromones, odorants and also Ca^{2+} cations interact with and bind to the large family of the plasma membrane receptors which are functionally coupled with guanine–nucleotide binding regulatory proteins (G proteins), G protein–coupled receptors.

Hormones and neurotransmitters bind primarily to the stereo–specific site of the receptor molecule which is located at the cell surface and exposed to extracellular side of plasma membrane and a surrounding water space. The binding reaction represents the first step in complicated sequence of molecular events transmitting the signal from the extracellular side of plasma membrane into the cell interior. Therefore, the final physiological response of a given cell type is initiated and regulated by the primary molecular events proceeding in plasma membrane at receptor level. In *all* GPCR–initiated signaling cascades, the hormone or neurotransmitter binding induces conformational change of receptor molecule, which is transmitted to G protein and induces dissociation of trimeric G protein–complex (non–active) into the free (active) Gα and Gβγ subunits. Subsequently, both Gα and Gβγ activate a numerous enzyme activities (effectors) or ionic channels which then regulate the intracellular concentrations of secondary messengers such as cAMP, cGMP, IP_3, diacylglycerol (DAG), arachidonic acid, sodium, potassium or calcium cations **(Fig. 1**).

Fig. 1 Structural and functional organization of G protein–coupled receptors (GPCRs) in plasma membrane

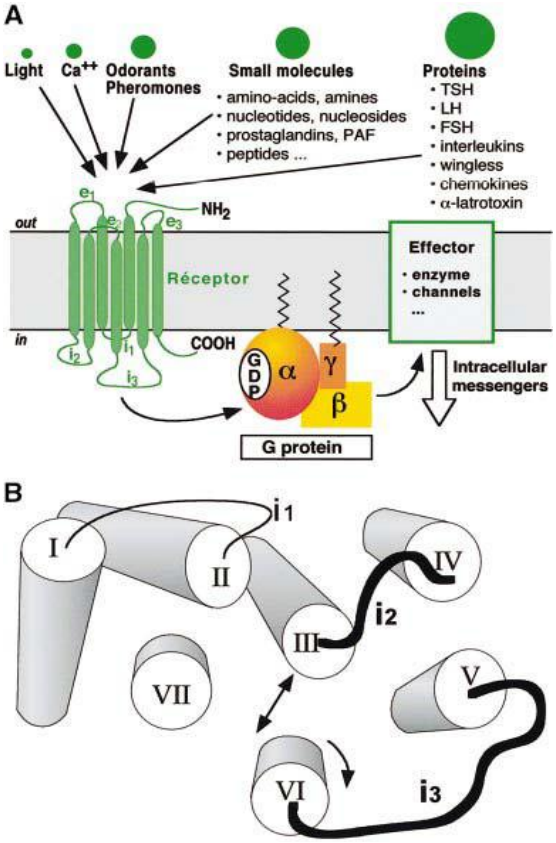

From Bockaert, J., Pin J. P. (1999) Molecular tinkering of G protein–coupled receptors: an evolutionary success. The EMBO Journal 18, 1723–1729

(**A**) GPCRs have a central common core made of seven transmembrane helices (TM1–TM7) connected by three intracellular (i1, i2, i3) and three extracellular (e1, e2, e3) loops. The diversity of messages which activate these receptors is an illustration of their evolutionary success.

(**B**) Illustration of the central core of rhodopsin. The core is viewed from the cytoplasm. The length and orientation of the TMs are deduced from the two–dimensional crystal of bovine and frog rhodopsin. The N– and C–terminal and i3 are included in TM3 and TM6. The core is represented in its *active conformation*. The TM6 and TM7 lean out of the structure, the TM7 turn by 30% on its axis (clockwise as viewed from the cytoplasm). This opens a cleft in the central core in which G proteins can find their way. The i2 and i3 loops are the two main loops engaged in G protein recognition and activation.

4.2. Classification and diversity of GPCRs

Three main families of GPCRs were recognized by comparison of amino–acid sequences of individual receptor proteins. Receptors from different families share no sequence similarity. This indicates a remarkable example of molecular convergence in the course of evolution (**Fig. 2**).

Family 1 contains most GPCRs including receptors for odorants. **Group 1a** contains GPCRs for small ligands including rhodopsin and β–adrenergic receptors. The binding site is localized within the seven TMs. **Group 1b** contains receptors for peptides whose binding site includes the N–terminal, the extracellular loops and the superior parts of TMs. **Group 1c** contains GPCRs for glycoprotein hormones. It is characterized by a large extracellular domain and a binding site which is mostly extracellular but at least with contact with extracellular loops e1 and e3.

Family 2 GPCRs have a similar morphology to group Ic GPCRs, but they do not share any sequence homology. Their ligands include high molecular weight hormones such as glucagon, secretine, VIP–PACAP and the Black widow spider toxin, α–latrotoxin (Krasnoperov *et al.*, 1997; Davletov *et al.*, 1998).

Family 3 contains mGluRs, Ca^{2+}–sensing receptors, $GABA_B$–receptors and a group of putative pheromone receptors coupled to the G protein Go (termed VRs and Go–VN) became new members of this family.

Family 4 comprises pheromone receptors (VNs) associated with Gi.

Family 5 includes the ‘frizzled’ and the ‘smoothened’ (Smo) receptors involved in embryonic development and in particular in cell polarity and segmentation. The cAMP receptors (cAR) have only been found in *D. discoıdeum* but its possible expression in vertebrate has not yet been reported.

Fig. 2 **Classification and diversity of GPCRs**

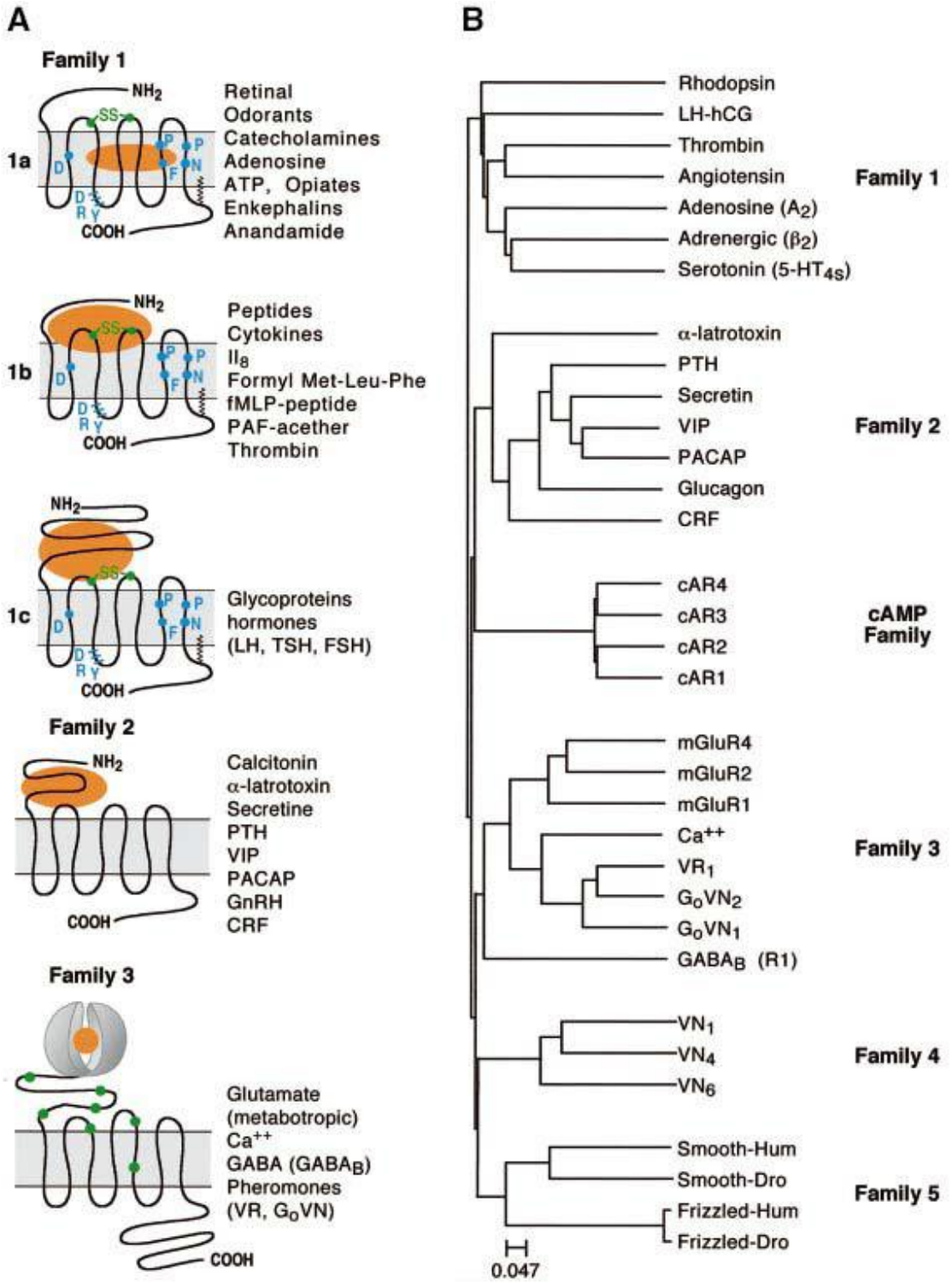

From Bockaert J., Pin, J.P. (1999) Molecular tinkering of G protein–coupled receptors: an evolutionary success. The EMBO Journal 18, 1723–1729

4.3. Receptors for γ–aminobutric acid (GABA)

The main inhibitory system in the brain uses γ–aminobutyric acid (GABA) as a transmitter. γ–aminobutyric binds to three types of receptors – $GABA_A$ (Olsen and Venter, 1986), $GABA_B$ (Bowery *et al.* 1989, 1991, 1993) and $GABA_C$ (Bormann and Feigenspan 1995). *$GABA_A$ receptor* is a part of supra–molecular complex $GABA_A$ chloride ionophore and a consequence of its activation is opening of chloride channel and hyperpolarization of membrane potential (Olsen and Venter, 1986). The subunit composition of $GABA_A$ receptor has sequence homology with the neural type of nicotinic acetylcholine receptor (nACh–R). It is organized as a pentamer of five different subunits (α, β, γ, δ and ε). Each subunit group has different subtypes, e.g. six different α, four β, four γ and two δ were identified. Like neuronal nACh–R, these subunits mix in a heterogeneous fashion to produce a wide array of $GABA_A$ receptors with different pharmacological and electrophysiological properties (Vicini, 1991).

Historically, *$GABA_B$ receptors* were pharmacologically distinguished from $GABA_A$ receptors as bicuculine–insensitive sites for GABA for which specific agonist is (–)–baclofen (Hill and Bowery (1981); Bowery *et al.* (1983, 1984, 1985, 1987); Hill (1985)). After discovery of specific antagonists, $GABA_B$ receptors were defined as a class of bicuculine–insensitive GABA receptors for which (–)–baclofen is a specific agonist and phaclofen and 2–hydrox–saclofen specific antagonist (Kerr and Ong, 1995). These receptors are not physically bound to an ionic channel and belong to the family of G protein coupled receptors, GPCR (Bowery *et al.* 1989, 1991, 1993; Kerr and Ong, 1995). Thus, the signal initiated by binding of GABA to $GABA_B$–R is transmitted further down–stream by trimeric G proteins. Increased concentrations of GTP favor the dissociation of activated G proteins from the high affinity state of the receptor driving it towards lower affinity state what results in a reduction of $GABA_B$ receptor binding (Hill *et al.*, 1981, 1984). This result provided the first evidence that $GABA_B$ receptors are linked to G proteins.

The functional $GABA_B$ receptor is a hetero–dimer formed by a GABA B1 and B2 subunit (**Fig. 3**). Each of the subunits possesses extracellular N–termini, seven–transmembrane domains, and intracellular C–termini. The functional receptors heterodimerize via a C–terminal coiled–coil domain that shields an ER retention motif on B1, promoting cell surface expression. Two splice variants of the B1 subunit (1A and 1B) exist, differing by the presence of two “sushi” axonal targeting domains in the 1a subunit. Activation of the receptor

occurs when ligand (GABA or baclofen) binds to the N–termini of the B1 subunit in a venus flytrap mode of ligand binding (zoom panel). Essential ligand–binding amino acids have been highlighted. The B2 subunit then confers functional activity coupling to Gi/o G proteins via its intracellular loops.

Fig. 3 **$GABA_B$–receptor structure**

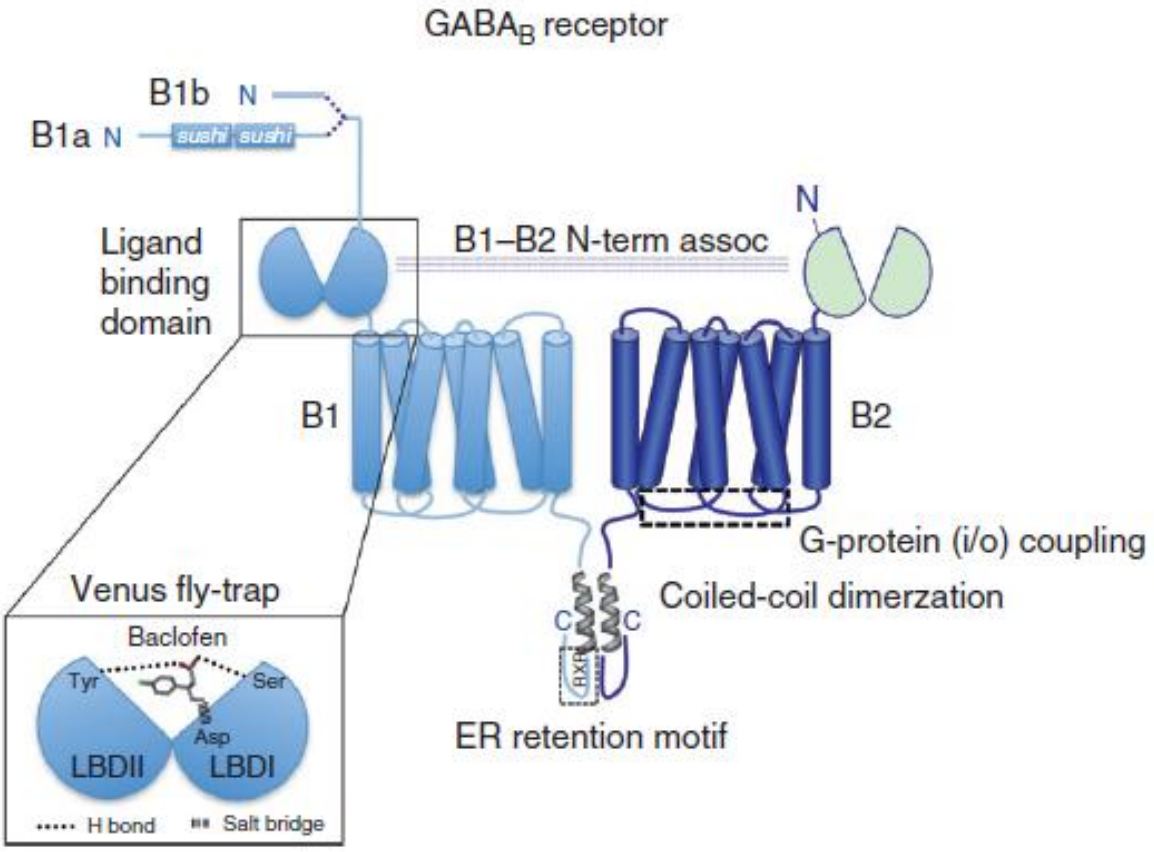

From Pagnet and Slezinger (2010) $GABA_B$ receptor coupling to G proteins and Ion channels. Advances in Pharmacology 58, 123–147

4.4. Trimeric G proteins and GDP/GTP exchange in guanine–nucleotide binding site of Gα subunits (G protein cycle)

From the structural point of view, trimeric G proteins are composed from three subunits, Gα and Gβγ (Rodbell, 1980; Gilman, 1987; Birnbaumer, 1990; Birnbaumer at al., 1990; Kaziro *et al.*, 1991; Helmreich and Hofman, 1996). Binding of an agonist to receptor molecule induces an exchange of GDP (which is in the resting state tightly bound to the Gα) for GTP. G protein complex containing Gα–GTP dissociates quickly into free Gα–GTP and Gβγ subunits. Both Gα–GTP and Gβγ subsequently stimulate or inhibit numerous enzymes and ionic channels at intracellular side of plasma membrane. Shortly after the dissociation of G protein complex Gαβγ into the free Gα–GTP and Gβγ, an endogenous GTPase activity of Gα subunit is activated and Gα–GTP is hydrolyzed to Gα–GDP. Gα subunits in GDP–liganded state (Gα–GDP) exhibit high–affinity towards free Gβγ. Therefore, Gα–GDP bind Gβγ and the non–active, trimeric G protein complex Gαβγ is formed again and the whole cycle may start again after encounter with activated, i.e. an agonist–bound receptor, **Fig. 4** (Gilman, 1987; Kaziro *et al.*, 1991; Helmreich and Hofman, 1996).

Fig. 4 **Trimeric G protein cycle; the general scheme**

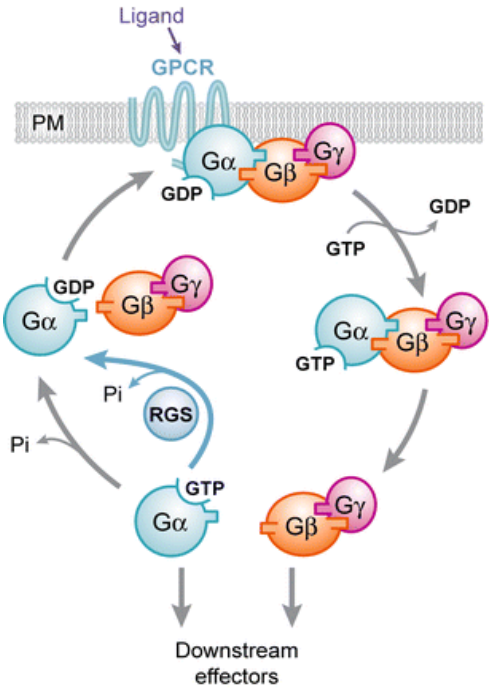

From Li L, Wright SJ, Krystofova S, Park G, Borkovich KA (2007) Heterotrimeric G protein signalling in filamentous fungi. Annual Rev Microbiol 61, 423–452

4.5. Classification and function of G proteins

G protein classification is based on similarity of amino acid sequence/ structure of Gα subunits (Kaziro *et al.*, 1991). The four major families of Gα subunits were identified.

1) G_s/G_{olf} family (four splice variants of $G_s\alpha$ and Gα protein of olfactory bulb, $G_{olf}\alpha$); Gα subunits of G_s/G_{olf} family stimulate adenylyl cyclase (AC) activity in cholera–toxin sensitive manner.

2) G_i/G_o family [$G_i1\alpha$, $G_i2\alpha$, $G_i3\alpha$, $G_o1\alpha$, $G_o2\alpha$, $G_t1\alpha$ (R) in retinal rodes, $G_t2\alpha$ (C) in retinal cones, $G_q\alpha$ (gustducin), $G_z\alpha$]. Gα subunits of G_i/G_o family inhibit adenylyl cyclase, stimulate phospholipase Cβ3 or affect ionic channels in pertussis–toxin (PTX) sensitive manner.

3) $G_q/G_{11}\alpha$ family ($G_q\alpha$, $G_{11}\alpha$, $G_{14}\alpha$, $G_{15}\alpha$, $G_{16}\alpha$). Gα subunits of $G_q/G_{11}\alpha$ family proteins inhibit adenylyl cyclase or stimulate phospholipase Cβ3 in PTX–insensitive manner,

4) $G_{12}\alpha/G_{13}\alpha$ family. Gα subunits of $G_{12}\alpha/G_{13}\alpha$ family activate small, monomeric G proteins of Rho family and regulate intracellular membrane traffic (Riobo and Manning, 2005).

4.6. $GABA_B$–receptors and PTX–sensitive G proteins of Gi/Go family

Pertussis–toxin (PTX), exotoxin produced by Bordetella Pertussis, ADP–ribosylates and uncouples the Gi and Go proteins from G protein coupled receptors, which revert to low–affinity state, by catalyzing the ADP–ribosylation of the Galpha–subunits (Katada and Ui, 1982). This covalent modification, proceeding at the C–terminus cystein –4 of the alpha–subunit of Gi/Go proteins, blocks the interaction with the activated receptor (occupied by an agonist) so, that the alpha–subunit remains in non–active, GDP–liganded state and it is unable to enter the GTP–GDP cycle initiated by GDP–GTP exchange reaction. High–affinity [^{3}H]GABA binding to $GABA_B$ sites is reduced and low–affinity binding is increased by treatment of brain membranes with PTX, whilst PTX and N–ethylmaleinimide uncouple $GABA_B$ receptors from G proteins, an effect which is reversed by the addition of purified Gi–proteins (Asano a spol., 1985; Asano a Ogasavara, 1986).

Increased concentration of GTP favors the dissociation of activated G proteins from the high affinity state of the receptor. Receptors are driven to the low–affinity state what results in a reduction of agonist binding to $GABA_B$–R (Hill *et al.*, 1981, 1984). This result provided the *first evidence* that $GABA_B$–R are linked to G proteins. $GABA_B$–agonist stimulation of high–

affinity [^{32}P]GTPase was the *second experimental evidence* supporting the idea, that the effect of $GABA_B$ agonists was mediated via trimeric G proteins (Bowery *et al.*, 1987) and close correlation between baclofen–stimulated GTPase and regional distribution of $GABA_B$–R in the brain also supported this idea. Baclofen–stimulated GTPase activity in vitro was significantly inhibited by pertussis toxin (PTX) and also by specific antipeptide antisera oriented against $G_i\alpha$ subunit proteins (Sweeney and Dolphin, 1992). The electrophysiological analysis using the specific antisera indicated that both PTX–sensitive $G_i\alpha$ and $G_o\alpha$ proteins were effected by $GABA_B$–R agonists (Dolphine, 1990, 1991).

4.7. G protein turnover affects $GABA_B$–receptor function

Agonist activation of $GABA_B$ receptor ($GABA_{B1/B2}$–R) leads to GTP exchange for GDP on $G_{i/o}\alpha$. The activated heterotrimeric complex ($G_{i/o}\alpha$–GTP$\beta\gamma$) then signals to different effectors (e.g., adenylyl cyclase, GIRK, and CaV). The intrinsic GTPase activity of $G_{i/o}\alpha$ hydrolyzes GTP to GDP, allowing the inactive heterotrimer ($G_{i/o}\alpha$–GDP–G$\beta\gamma$) to reform. The presence of RGS accelerates the GTPase activity of $G_{i/o}\alpha$, leading to less $G_{i/o}\alpha$–GTP–G$\beta\gamma$ and G$\beta\gamma$, leading to desensitization of GIRK and CaV currents, and shift in the GABAB coupling efficiency to higher concentrations (**Fig. 5**).

Fig. 5 G protein turnover affects $GABA_B$–receptor function

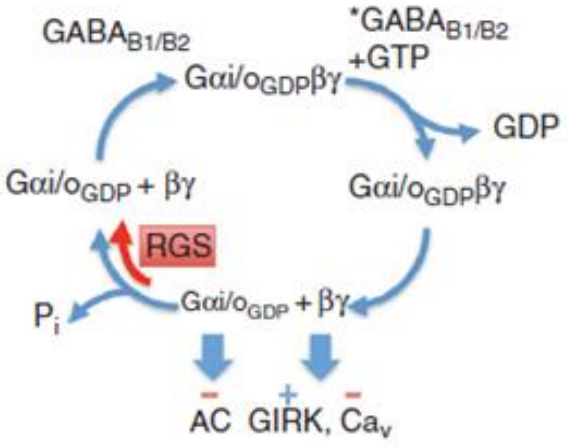

From Padgett and Slezinger (2010) $GABA_B$ receptor coupling to G proteins and Ion channels. Advances in Pharmacology 58, 123–147

4.8. Effectors and physiological functions of $GABA_B$–receptors

As described in the previous paragraphs, $GABA_B$–receptors modulate their effectors via the activated free Gα and Gβγ subunits released from trimeric Gαβγ complex. The first $GABA_B$–R effector characterized was *adenylcyclase* whose activity was shown to be inhibited by free Gα subunits of G_i/G_o family (Xu and Wojcik, 1986). The physiological significance of AC inhibition in brain, however, is difficult to outline in uneqivocal way because the numerous different AC isoforms I–X were discovered (**Fig. 6**) and shown to exhibit widely different responsiveness to individual Gα or Gβ subunit proteins (**Figs. 7 and 8**) (Simonds, 1999; Sunahara and Taussig, 2002). Even at present time, the physiological consequences of inhibition of AC activity are poorly understood and include effects on transcription factors, kinases and intracellular Ca^{2+} signaling (Couve *et al.*, 2002; New *et al.*, 2006; Ren and Mody, 2003; Steiger *et al.*, 2004).

Fig. 6 **Structure and membrane topology of adenylcyclase**

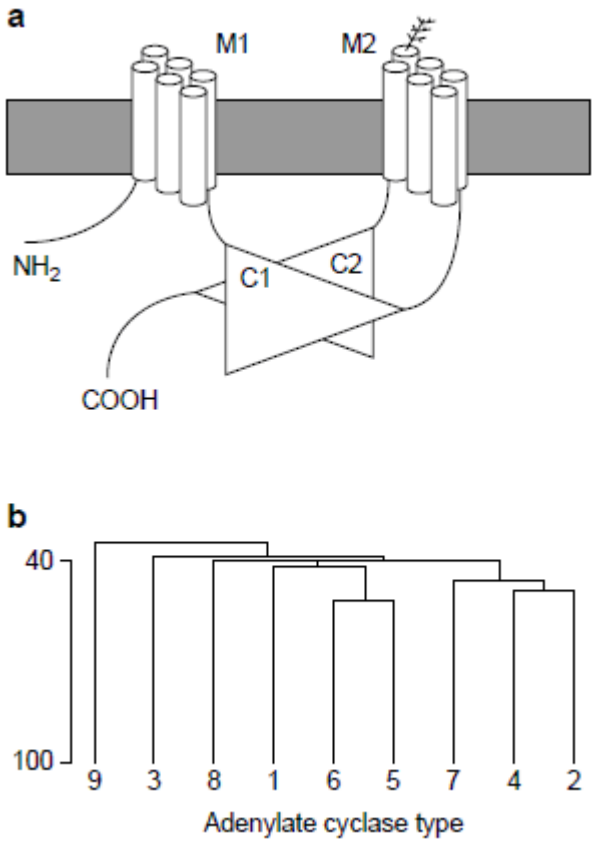

Legend to Fig. 6

a) Schematic diagram of the proposed membrane topology of the adenylyl cyclases (AC) based on hydropathy analysis and the terminology of $G_o\alpha$ by A. G. Gilman. The grey rectangle represents the plasma membrane into which the clusters M1 and M2 of six transmembrane spanning α–helical segments anchor the enzyme. The cytosolic domains include the N–terminal region, the homologous ~25 kDa catalytic domains C1 and C2 interacting in a head–to–tail manner and the C–terminus. The cDNAs for all nine principal cyclase isoforms predict sites of N–linked glycosylation in M2 (branching tuft) and the glycoprotein nature of several AC isoforms has been proven by glycohydrolytic analysis.

b) Sequence relationships among the nine AC isoforms are represented in a dendrogram generated by the program PILEUP in which the vertical distance is proportional to the similarity between sequences. A scale approximating the percent sequence similarity is provided on the left, in which the similarity between AC9 and AC3 determined by the program GAP is indicated as 40%.

Fig. 7 **Distribution in AC isoforms in mammalian tissues**

Table 1. Mammalian isforms of adenylate cyclase

Adenylate cyclase (AC) type	Size (no. of amino acids)	mRNA expression	Refs
AC1	1134	Brain, retina, adrenal medulla	5, 6
AC2	1090	Brain, olfactory bulb > lung	6, 7
AC3	1144	Olfactory neurones, brain, retina, aorta, lung, testis	8–10
AC4	1064	Kidney, brain, heart, liver, lung	11
AC5	1184	Heart > brain > kidney	12, 13
AC6	1165	Heart, brain > kidney, testis, spleen, liver	13–16
AC7	1099	Lung, heart, spleen, kidney, brain	17, 18
AC8	1248	Brain[a]	14, 19
AC9	1353	Skeletal muscle, brain > kidney lung, liver, heart	20, 21

[a]Northern blotting[13], demonstrated the expression of AC8 message in brain, while reverse transcriptase (RT)–PCR identified AC8 mRNA in brain, but not in heart, liver, kidney, testis or skeletal muscle[14].

Fig. 8 Functional responsiveness of different AC isoforms to G protein activation

Table 2. Adenylate cyclase: type-specific patterns of regulation

Adenylate cyclase type	Regulatory signal											
	$G_i\alpha$		$G\beta\gamma$		PKA		PKC[d]		Ca^{2+}/CaM		Other Ca^{2+}-mediated effects	
	Effect	Refs	Effect	Refs	Effect	Refs	Effect	Refs	Effect	Refs	Effect	Refs
AC1	↓	a	↓	25, 26			↑	a, 30, 31	↑	35	↓	g
AC2	–	b	↑	25–27			↑	27, 32–34	–	7		
AC3	↓	22	–	25			↑	30, 31	↑	36	↓	h
AC4			↑	11			↓	f	–	11		
AC5	↓	23			↓	28			–	12	↓	i
AC6	↓	22, 24	–	13	↓	29	–	30	–	16	↓	j
AC7			(↑)	c			↑	17, 18	–	17		
AC8									↑	19	–	g
AC9			–	20					–	20	↓	i

[a]Inhibition of adenylate cyclase type 1 (AC1) by $G_i\alpha$ evident with forskolin or calcium/calmodulin (Ca^{2+}/CaM) stimulation but less effective on $G_s\alpha$-stimulated activity[22]. [b]Inhibition of AC2 by $G_i\alpha$ not evident using purified components[24], although experiments using COS7 cells co-transfected with AC2 and mutationally activated $G_i\alpha$ suggest an inhibitory effect[22]. [c]Indirect evidence in transfected HEK293 cells suggest that AC7 might be positively regulated by $G_{\beta\gamma}$ (Ref. 56). [d]Note that in many of the experiments cited under this heading the effect of protein kinase C (PKC) is inferred from treatment of intact cells with phorbol esters. [e]Phorbol ester potentiation of AC1 in transfected cells seen only to Ca^{2+}/CaM stimulation[30]. [f]Inhibition of AC4 by PKCα not of basal activity, but of $G_s\alpha$-stimulated component[22]. [g]AC1 but not AC8 is inhibited by CaM kinase IV (Ref. 74). [h]AC3 is inhibited by constitutively active CaM kinase II (Ref. 75). [i]AC5 is inhibited by calcium in a CaM-independent fashion[12]. [j]In membrane preparations AC6 is inhibited by submicromolar calcium concentrations in a CaM-independent fashion[15] and can be inhibited in intact cells by calcium ionophores[14]. [k]Enhanced cAMP production in response to immunosuppressant blockers of calcineurin suggest negative regulation of AC9 by this Ca/CaM-activated phosphatase[21].

In comparison to Gα–mediated signaling, Gβγ–mediated signaling is much better understood. The main Gβγ–dependent effectors of presynaptic $GABA_B$ receptors are *P/Q–and N–type voltage–dependent Ca^{2+} channels* (Barral *et al.*, 2000; Bussieres and El Manira, 1999; Chen and van den Pol, 1998). $GABA_B$ receptors inhibit these Ca^{2+} channels at excitatory and inhibitory terminals, thereby restricting neurotransmitter release. By definition, $GABA_B$ *autoreceptors* inhibit GABA release while $GABA_B$ *heteroreceptors* decrease the release of other neurotransmitters, including, for example, glutamate, dopamine, adrenaline, or serotonin. Depending on whether the terminal releases an inhibitory or excitatory neurotransmitter, presynaptic $GABA_B$ receptors increase or decrease the excitability of the postsynaptic neuron.

Presynaptic $GABA_B$–receptors restrict the neurotransmitter release not only by inhibiting $Ca2^+$ channels but also by retarding the recruitment of synaptic vesicles (Sakaba and Neher, 2003). Recent evidence also suggests that presynaptic $GABA_B$ receptors couple to inwardly rectifying Kir3–type K^+ channels (also designated GIRK channels) to inhibit glutamate release (Fernandez–Alacid *et al.*, 2009; Ladera *et al.*, 2008). However, Kir3 channels are generally considered as the main effectors of postsynaptic $GABA_B$ receptors (Luscher *et al.*, 1997; Wagner and Dekin, 1993). $GABA_B$–mediated activation of Kir3 channels produces slow inhibitory postsynaptic potentials (IPSPs) by inducing K^+ efflux, which hyperpolarizes the membrane and shunts excitatory currents. Postsynaptic $GABA_B$ receptors also down–regulate Ca^{2+} channels, which inhibit dendritic $Ca2^+$–spike propagation (Perez–Garci *et al.*, 2006). The alteration of membrane potential by activated $GABA_B$–R by means of opening

the Ca^{2+} or K^+ channels is explained in details in **Fig. 9.**

Activation of the G protein coupled $GABA_B$–receptor stimulates GTP–dependent G protein (Gi/o) dissociation of the Gα and Gβγ dimer. The Gα i/o subunit has been shown to inhibit adenylyl cyclase while the Gβγ dimer is capable of modulating voltage–gated Ca^{2+} (v) or G protein–gated inwardly rectifying K^+ (GIRK) channels, resulting in potent neuronal inhibition. Effector specificity may be regulated by hetero–complex formation, guided by targeting protein partners and subcellular localization.

Fig. 9 $GABA_B$–R signaling via K^+ (GIRKs) and $Ca2^+$ (v) channels

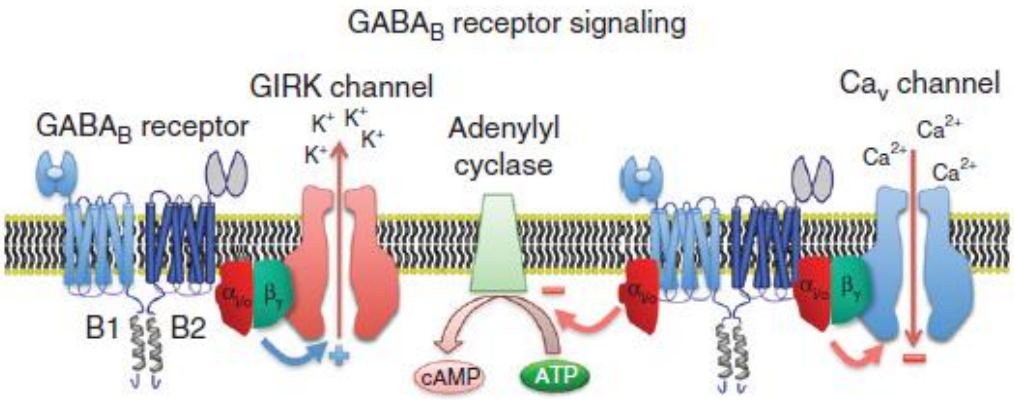

From Padgett and Slezinger (2010) $GABA_B$ receptor coupling to G proteins and Ion channels. Advances in Pharmacology 58, 123–147

The cell interior is negatively charged in comparison with the extracellular space. The **Ca^{2+} (v) channels** (voltage–dependent calcium channels) are activated (opened) in the course of depolarization of cell membrane. Opening of Ca_V channels causes *depolarization* of the membrane. Calcium cations enter intracellular compartment (pre–synaptic part) and induce fusion of neurotransmitter containing vesicles with plasma membrane and release of neurotransmitter into synaptic cleft. $GABA_B$–R via Gβ block the opening of **Ca^{2+} (v) channels** and in this way inhibit the neuro–transmitter release.

Transport of potassium cations by G protein gated inwardly rectifying **K^+ channels (GIRKs)** out from the cell interior induces *hyperpolarization* of cell membrane, generates "slow inhibitory postsynaptic potentials (IPSPs) and shunts the excitatory currents. In this

way it inhibits excitation. Post–synaptic $GABA_B$–R open GIRKs channels, again via Gβ subunits, and in this way increase excitability at post–synaptic level. $GABA_B$–auto–receptors inhibit release of its own neurotransmitter, i.e. GABA. $GABA_B$–heteroreceptors inhibit release of other neutransmitters such as glutamate or serotonine.

The present state of knowledge about the plasma membrane part of $GABA_B$–receptor signaling cascade may be therefore described as a mutually interrelated regulatory network of receptors, G proteins, AC isoforms and ionic channels proceeding as positive or negative feed–back regulatory loops (Pinard *et al.*, 2010). The final out–come of these regulatory circuits depends on expression level and activity of individual proteins in a given cell population present in a given brain area. *Therefore, when considering GABA as the main inhibitory neurotransmitter of mammalian brain, activation of pertussis–toxin sensitive G proteins of G_i/G_o family by $GABA_B$–receptors represents the crucial primary regulatory mechanism for an optimum of function of the brain.*

4.9. Subcellular fractionation of the frontal rat brain cortex and isolation of plasma membranes from mammalian cells; *historical perspective*

The original methods for subcellular fractionation of the rat brain tissue and isolation of plasma membrane fragments in density gradients were using the highly hypertonic solutions of sucrose (De Robertis at al., 1962a, b; Whittacker *et al.*, 1964; Lisy *et al.*, 1971). A synthetic polymer of sucrose Ficoll (Amersham Pharmacia Biotech, Uppsala, Sweden) was subsequently introduced to overcome the problem of the high osmotic pressure (Holter and Moller, 1958; Pertoft, 1966). This has been successfully made and Ficoll is used up to now for isolation of lymphocytes, other blood cells and separation of different cell populations in general, but is unappropriate for fractionation of subcellular membrane particles because of the very high viscosity of its aqueous solutions (Pertoft, 2000).

The more advanced methods (De Pierre and Karkowsky, 1973; Whittacker, 1984; Rickwood, 1984, Hollingsworth *et al.*, 1985; Fisher *et al.*, 1986; Dunkley *et al.*, 1986; Maloteaux *et al.*, 1995; Luabeya *et al.*, 1997; Pertoft, 2000) were using aqueous solutions of Percoll and Iodixanol (OptiPrep). These organic macromolecules, when diluted to proper concentration and supported by salts, represented much less damaging environment for isolation of the whole cells or subcellular membrane fragments/ vesicles. The rather complicated and sophisticated isolation of small synaptosomal vesicles enriched in trimeric G proteins (Ahnert–Hilger at al., 1993) as well as existence of aggregated forms of trimeric G

proteins isolated in the presence of mild detergents such as digitonin or Lubrol PX (Jahangeer and Rodbell, 1993) should be also noticed. The difficulties of how to overcome the toxicity, osmotic pressure changes and penetration of density gradient media into the particles have been discussed by Rickwood (1984). The detailed methodological advices of how to use OptiPrep were presented by Graham (2002).

4.10. Isoosmotic density gradient media

Various density gradient media were developed for specific applications of centrifugational techniques. These media, if possible, should not alter the cells or particles to be separated and should provide a proper density range for separation of one type of cells (or subcellular) membrane particles from another. The difficulties which have to be overcomed when viewed from the general point of view are represented by toxicity, osmotic pressure changes and penetration of a given chemical used for preparation density gradient medium into the particles which are being isolated or separated form each other (Rickwood, 1984).

Sucrose

The main disadvantages of sucrose solutions are some of their physico–chemical properties. Sucrose solutions in high concentration range have a high osmolarity and are also highly viscous. Cells and subcellular particles, which are osmotically sensitive, will band at a density which differ from their physiological density. Furthermore, due to the low molecular weight, the sucrose may penetrate into the cells and an to envelope the intracellar particles.

Polysucrose

A synthetic polymer of sucrose (Ficoll; Amersham Pharmacia Biotech, Uppsala, Sweden) was introduced early to overcome the problem of high osmotic pressure inherently combined with usage of sucrose itself (Holter and Moller, 1958). However, Ficoll of molecular weight 400,000 also gives measurable osmotic effects at high concentrations; this problem had to be compensated by addition of salts into the density gradient media with the aim to to keep iso–osmotic conditions throughout the centrifuge tube (Pertoft, 2000).

Iodinated compounds

Iodinated compounds are widely used as centrifugation media (Iodixanol, Optiprep^{TM}) (Graham, 2002). In Optiprep^{TM} solutions, the cells band isopycnically without being subject to the high osmotic stress existing in sucrose gadients (Rickwood, 1984).

Colloidal silica

The use of colloidal silica was first reported by Mateyko and Kopac (1995). They

reported the osmotic pressure effects, the ability to separate cells, permeation into the particles and solubility in aqueous solutions used for preparation of density gradient media. Of all substances tested, none came closer to providing all the desired characteristics than colloidal silica. However, it was found that a pure silica sol was toxic to cells and caused hemolysis of red blood cells. At the time when polysaccharides were introduced to stabilize colloidal silca gradients they were also found to inhibit toxic effects of the silica (Pertoft, 1966). The introduction of absorbed polymers to silica particles to obtain iso–osmotic, pH–neutral and high density solutions led to introduction of Percoll in 1977 (Amersham Pharmacia Biotech, Uppsala, Sweden).

It follows that Percoll has proved to be the density gradient medium of choice since it fulfils almost all criteria for an ideal density gradient medium. Therefore, Percoll was used by us for subcellular fractionation of the brain tissue as well as cell homogenates prepared from HEK293 cell lines.

4.11. Structural organization of trimeric G proteins in plasma membrane*; membrane domains and multimeric structures of G proteins*

The multimeric structures of trimeric G proteins in brain membranes have been originally described by Jahangeer and Rodbell (1993). The functional evidence for the existence of non–uniformly or non–randomly organized, clustered forms of signaling units containing G proteins has been originally formulated by Neubig (1994). This early idea had subsequently induced a large experimental attention which was oriented to the detailed biochemical analysis of plasma membrane preparations isolated from stably transfected cell lines (specifically expressing the given type of GPCR), primary tissue culture cells or natural tissues. Subsequently, a large number of reports dealing with the plasma membrane sub–compartments denominated as *membrane domains or rafts* was published (Jacobson and Dietrich, 1999; Smart *et al.*, 1999; Simons and Tomre, 2000; Brown and London, 2000, Babichuk and Draeger, 2006; Allen *et al.*, 2007). The biochemical preparations of membrane domains were found to be enriched in cholesterol, glycolipids, sphingolipids and trimeric G proteins (for general reviews see Jacobson and Dietrich, 1999; Smart *et al.*, 1999; Simons and Tomre, 2000; Brown and London, 2000, Babichuk and Draeger, 2006; Allen *et al.*, 2007). The content of GPCR in membrane domains was relatively low (Moravcova *et al.*, 2004; Svoboda *et al.*, 2004; Rudajev *et al.*, 2005).

However, these studies were performed under the widely different methodological conditions. The usage of high detergent concentrations for preparation of membrane domains, in this case designated as detergent–resistant membrane domains (DRMs) (Sargiacomo *et al.*, 1993; Lisanti *et al.* 1994 a, b), resulted in preparations exhibiting the very low or zero agonist efficacy for stimulation of GDP/GTP exchange reaction of G proteins. This has been demonstrated first in stably transfected HEK293 cell lines stably expressing δ–OR–Gi1α (I^{351}–C^{351}) fusion protein (Bourova *et al.*, 2003). The same was truth when using the "alkaline–treatment" protocol based on sonication and extraction of the cell homogenate in highly alkaline solution of 0.5–1 M Na_2CO_3 (Song *et al.* 1996a, b).

According to experimental results collected over the years in our laboratory, the best of the so–far described methods/ protocols for preparation of membrane domains is that of Smart *et al.* (1995, 1999). The views what the term *membrane domains* actually means from methodological, structural and functional point of view were reviewed by Pike (2004). The sometimes controversial viewpoints about the size and physiological meaning of *membrane domains* were expressed by Pike (2006a, b) and Shaw (2006).

4.12. Biochemical methods for preparation of membrane domains

The disadvantage of the method of Smart *et al.* (1995, 1999) using the sequence of three types of density gradients is, however, the very low amount of protein recovered in the final preparation of pure "domains" – about 0.2–0.5% of the original amount present in the starting material, i.e. the cell homogenate. Therefore, when trying to find some compromise between purity and quantity of the final preparation, we have combined centrifugation in Percoll gradient followed by the "flotation" in sucrose density gradient. Plasma membrane enriched fraction was prepared from the rat brain cortex by centrifugation at 116,000xg for 35 min in Percoll^R gradient (Beckman Ti60 rotor), subsequently, the low–density membrane fragments (LPM) were separated from the bulk of plasma membranes (BPM) by flotation in a step–wise 15/20/25/30/35/40% w/v sucrose gradient (**Fig. 10**).

Fig. 10 Isolation of plasma membranes in Percoll gradient followed by separation of LPM (low–density PM fragments) and BPM (bulk of plasma membranes) by flotation in sucrose density gradient; *subcellular fractionation of rat brain cortex under detergent–free conditions* (Drastichova *et al.*, 2008)

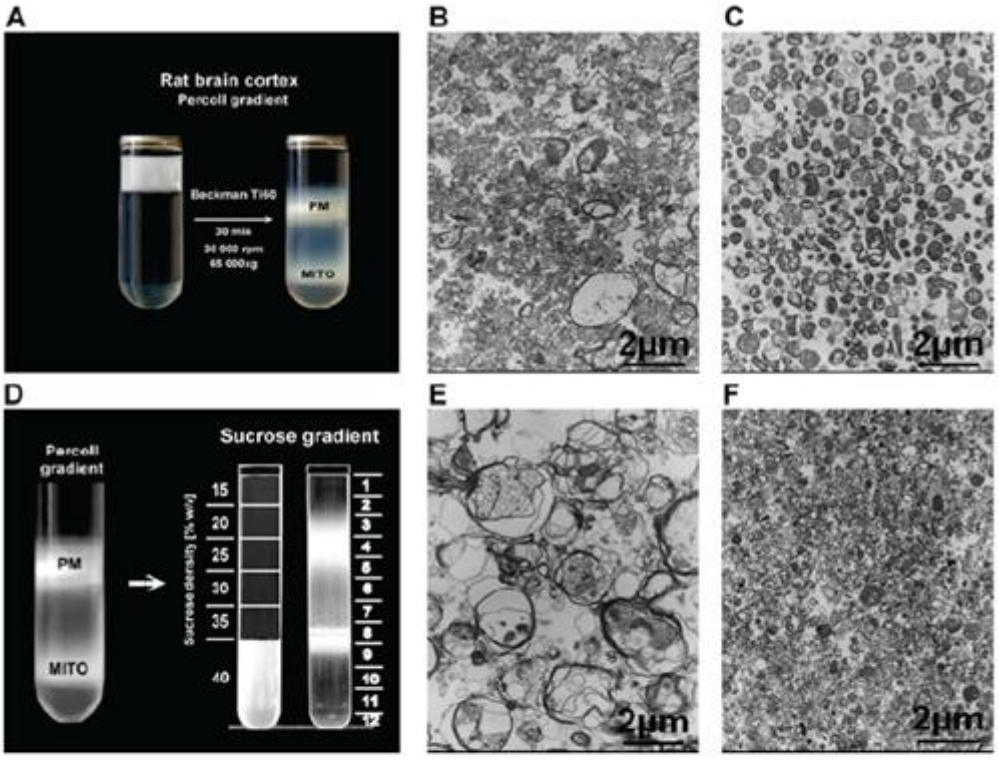

Subcellular fractionation of rat brain cortex. **A**, *Separation of plasma membrane and mitochondrial fractions in Percoll® gradient.* Post-nuclear supernatant was prepared from cerebral cortex of the rat and fractionated in Percoll® gradient. The upper layer of plasma membranes (PM) was separated from lower layer of mitochondria (MITO). **B**, plasma membrane fraction represented mixture of large and small vesicular structures together with sheets of myelin; **C**, in mitochondrial fraction, pure mitochondria were detected. **D**, *Flotation of plasma membrane fraction in sucrose gradient.* The upper layer collected from Percoll® gradient (PM) was fractionated by flotation in 15/20/25/30/35/40 % w/v sucrose gradient. Low-density plasma membrane (LPM), represented by hazy area in 15/20 % sucrose (fractions 3-5), were resolved from bulk of PM observed as distinct, optically dense band in 35 % sucrose or at 35/40 % sucrose interface (fractions 7-8). **E**, LPM were composed from large synaptosomal membrane particles and myelin; **F**, Bulk of plasma membrane (BPM) contained heterogeneous mixture of small vesicular structures (magnification 11700x).

Subsequently, we tried to prepare, from the frontal rat brain cortex, the detergent–resistant membrane domains which would exhibit the functional coupling between GPCRs and trimeric G proteins and compare the characteristics of neurotransmitter activation of $GABA_B$–R and other GPCRs in detergent–treated (DRMs) and detergent–untreated low–density PM fragments (LPM).

Figures **11–17**, accompanying text and the *comments* to these figures demonstrate how this goal was achieved.

Fig. 11 Subcellular fractionation of the rat brain cortex in the absence and presence of high (1% w/v) concentration of non/ionic detergent Triton X–100

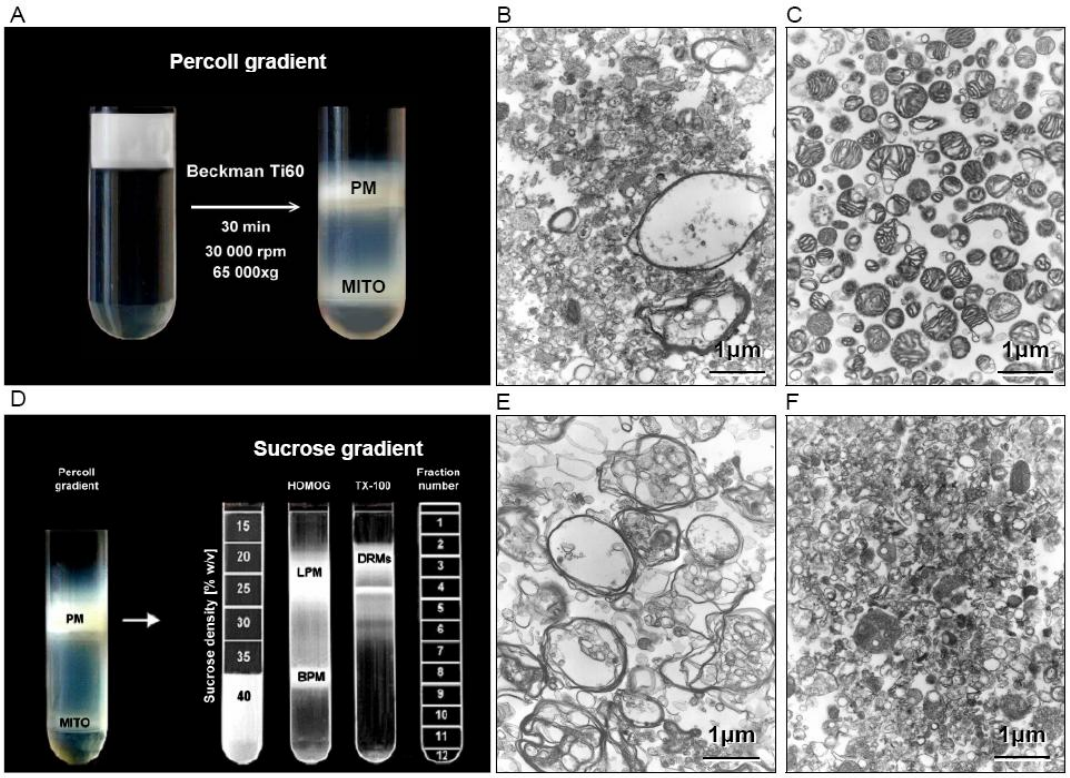

From PhD Thesis of Dr. Vladimír Rudajev, Charles University in Prague, Faculty of Natural Science, Department of Physiology, 2006

Legend to Fig. 11. A, separation of plasma membrane (PM) and mitochondrial (MITO) fractions in Percoll gradient; **B**, plasma membrane fractions represents a mixture of small and large (synaptomes) vesicles; **C**, mitochonrial fractions contains mitochondria; **D**, fractionation of PM by flotation in sucrose gradient; **E**, the low–density PM fragments (LPM) are enriched in synaptosomes; **F**, bulk of plasma membranes (BPM) contains the small vesicles.

As demonstrated in **Fig. 11**, the addition of 10% v/v Triton X–100 to Percoll–purified PM in the final concentration of 1% v/v and a subsequent resolution of TX–100 solubilized PM fragments by flotation in 15/20/25/30/35/40 % w/v sucrose density gradient for 24 hours at 118,000xg in Beckman SW41, results in flotation (of relatively small part when expressed as recovery of protein) **up**, i.e. to the low–density area of sucrose gradient. TX–100–resistant PM fragments exhibiting the low–density are localised in fractions 2–5. These fractions were collected from the top to the bottom of centrifuge tube, mixed together and represented the so–called detergent–resistant membrane domains, DRMs.

Unfortunately, as demonstrated in the following sequence of results presented in **Figs. 12–16**, DRMs prepared according to this protocol were not functional in the terms of functional coupling between $GABA_B$–R and G proteins of Gi/Go family. The ability of $GABA_B$–R agonist baclofen to stimulate G protein was diminished at the high detergent concentrations.

Fig. 12 Sucrose density gradient profile of plasma membrane marker Na^+/K^+–ATPase; *comparison of the detergent–untreated and TX–100–treated low–density membrane fragments (LDM)*

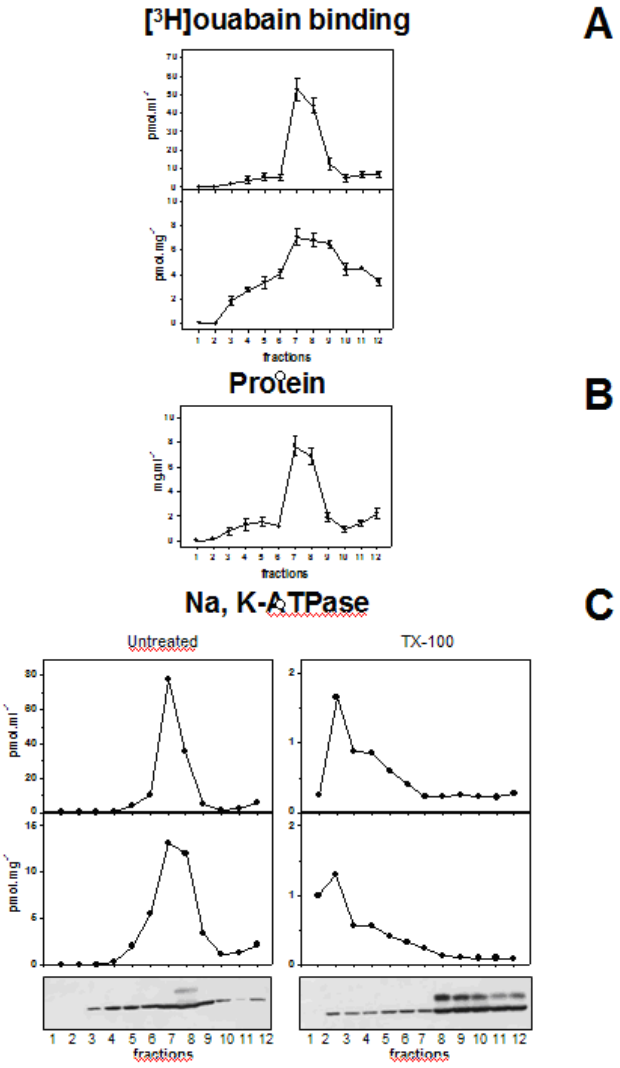

From PhD Thesis of Dr. Vladimír Rudajev, Charles University in Prague, Faculty of Natural Science, Department of Physiology, 2006

Legend to Fig. 12.

A) Distribution of prototypical plasma membrane marker Na^+/K^+–ATPase along the sucrose density gradient was determined by [^{3}H]ouabain binding assay. **B)** The protein

content in sucrose fractions 1–12 collected form the top to bottom of the centrifuge tube (Beckman SW 41) was determined by Lowry method. **C**) Distribution of Na^+/K^+–ATPase along the gradient was determined by imunoblot analysis with specific antibodies oriented against the alpha subunit of Na^+/K^+–ATPase and compared in detergent–untreated (**Untreated**) and Triton X–100 (0.5 %)–treated (**TX–100**) fractions. The results represent typical fractionation procedure.

Fig. 13 **Distribution of GPCR along sucrose density gradient**; detection by specific agonist and antagonist radioligand binding assays

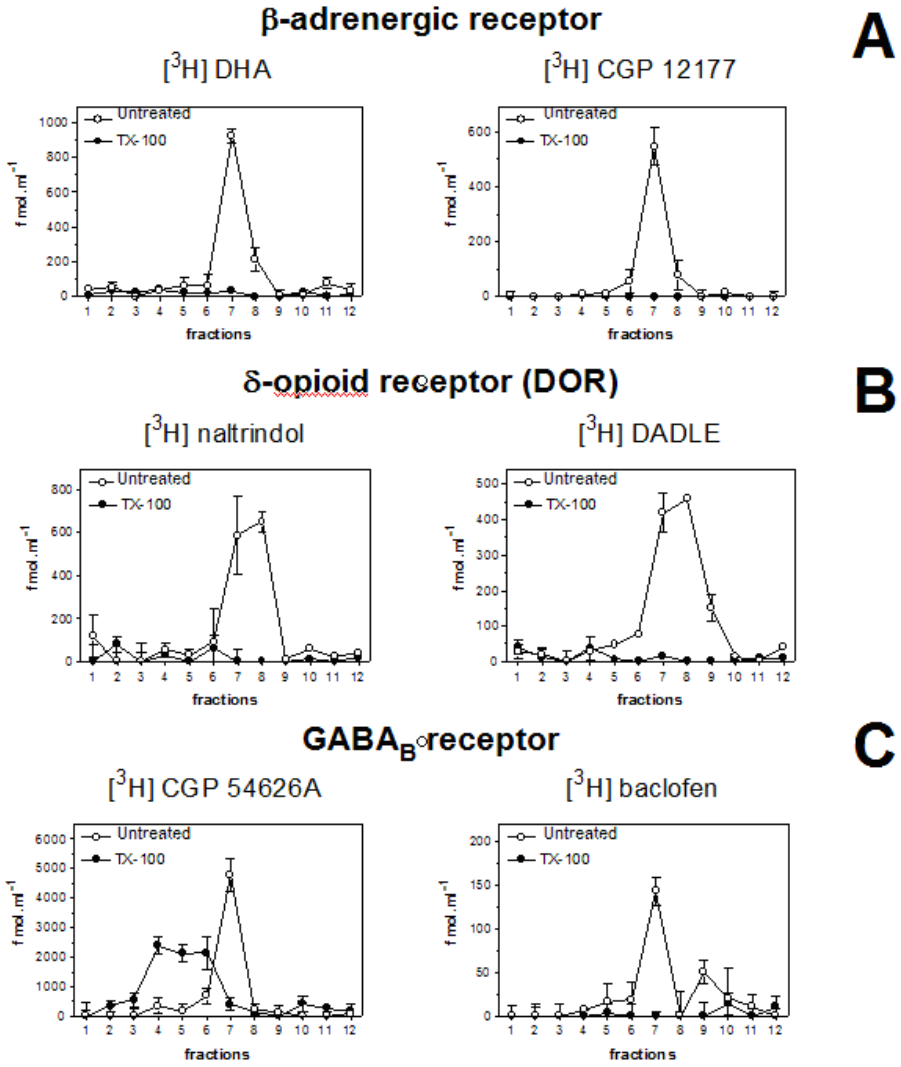

From PhD Thesis of Dr. Vladimír Rudajev, Charles University in Prague, Faculty of Natural Science, Department of Physiology, 2006

Legend to Fig. 13. Receptor content in sucrose fractions 1–12 (collected form the top to bottom of the centrifuge tube of Beckman SW 41) was determined by specific agonist and antagonist radioligand binding assays. In the contrary to β–AR and δ–OR, $GABA_B$–receptors were highly

enriched in TX–100–resistant membrane domains, DRMs.

Fig. 14 Distribution of GPCR along sucrose density gradient*; detection by immunoblot analysis with specific antibodies*

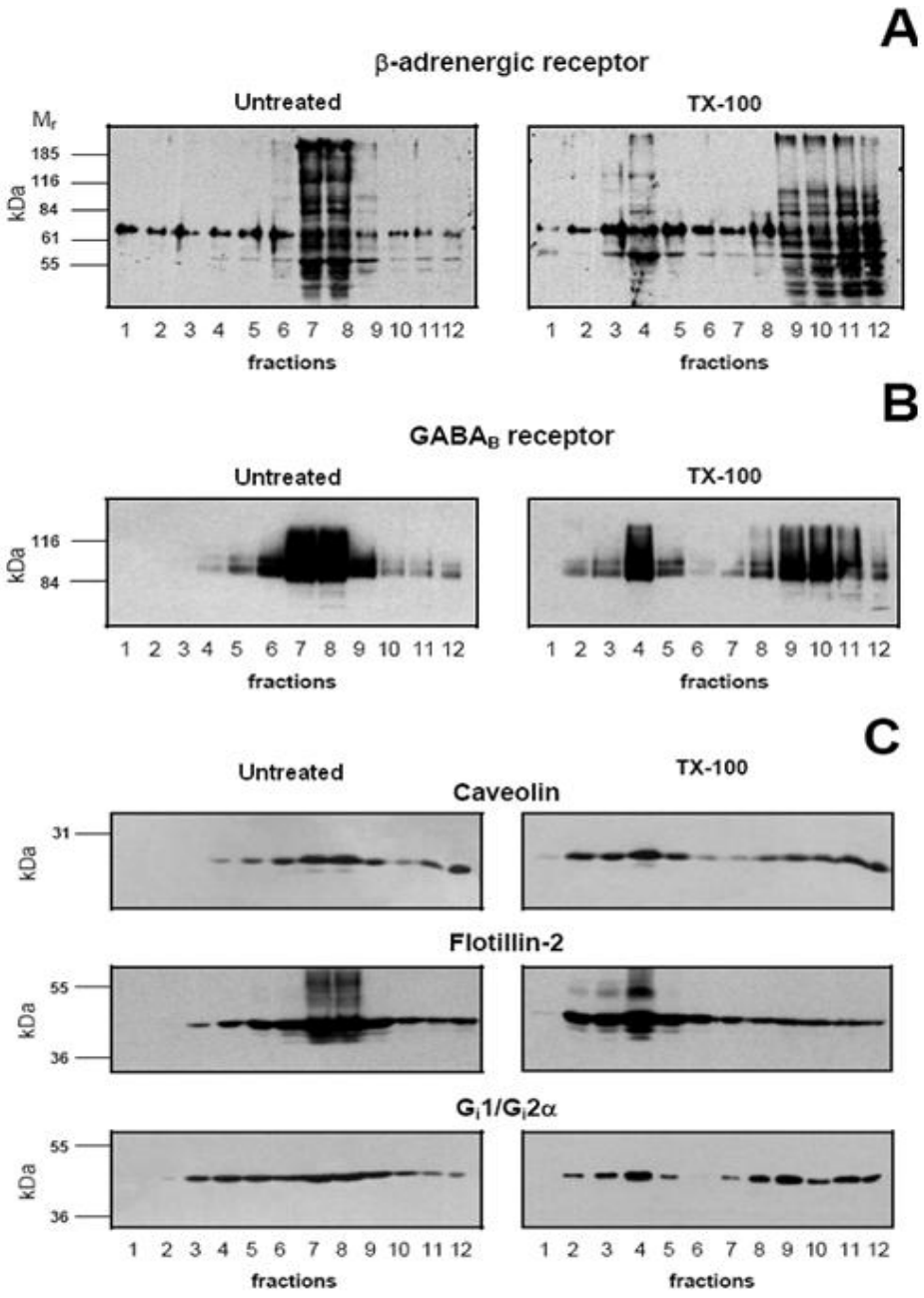

From PhD Thesis of Dr. Vladimír Rudajev, Charles University in Prague, Faculty of Natural Science, Department of Physiology, 2006

Legend to Fig. 14. Receptor content in sucrose fractions 1–12 collected form the top to bottom of the centrifuge tube (Beckman SW 41) was determined by specific agonist and antagonist radioligand binding assays. In the contrary to β–AR and δ–OR, $GABA_B$–receptors were highly enriched in TX–100–resistant membrane domains, DRMs.

Fig. 15 Deleterious effect of the high detergent concentration on functional activity of $GABA_B$–R

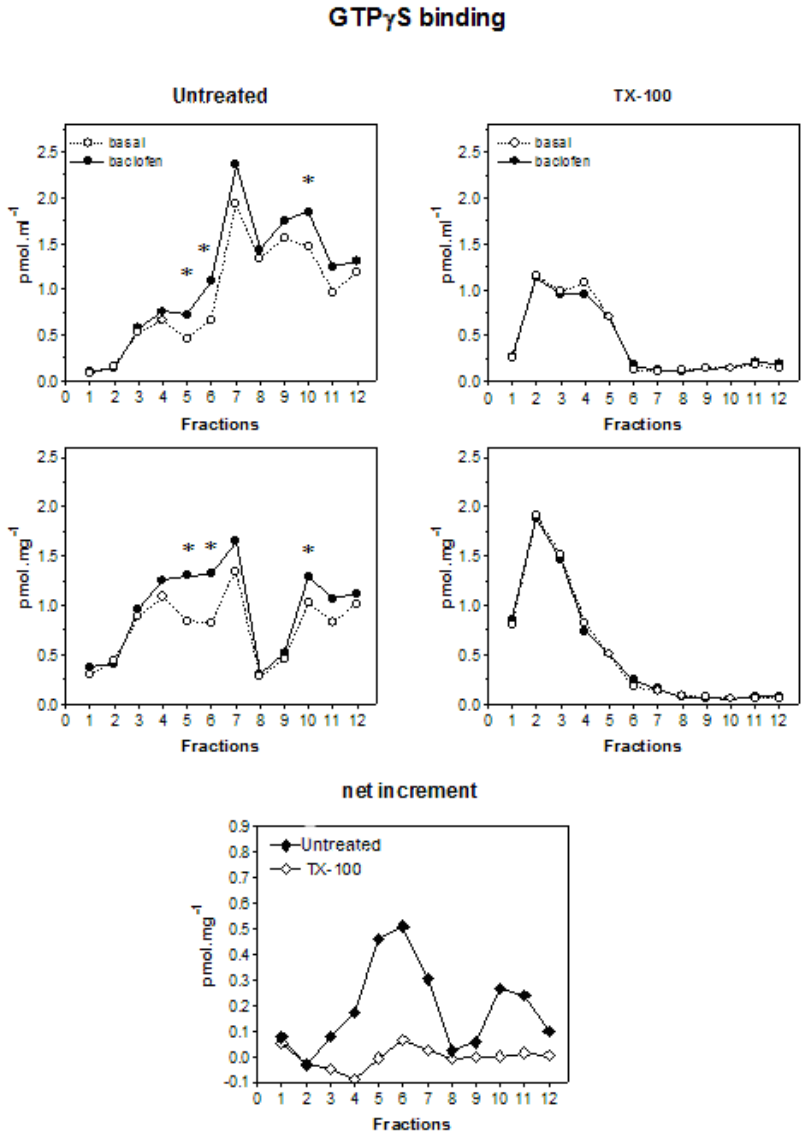

From PhD Thesis of Dr. Vladimír Rudajev, Charles University in Prague, Faculty of Natural Science, Department of Physiology, 2006

Legend to Fig. 15. Percoll purified plasma membranes were prepared from the brain cortex of adult rats and divided into two identical portions. The first portion was intensively mixed and represented the detergent–untreated PM sample; to the second portion, 10% v/v Triton–X100 was added to final concentration of 1 % w/v. Exactly 2 ml of these two PM preparations were mixed with 2 ml of 80% w/v sucrose and fractionated by flotation in 15/20/25/30/35/40 % w/v sucrose gradient (centrifugation for 24 hours at 116,000xg, Beckman SW41). The low–density fractions 1–5 (1 ml each) which were collected from the top of the centriguge tubes and combined together represented the detergent–untreated (LPM) and detergent–treated (TX–100) preparation of membrane domains.

Functional activity of G proteins was measured by high–affinity [^{35}S]GTPγS binding assay using the single concentration of baclofen (0.1 mM) as a stimulating agonist.

Fig. 16 Comparison of dose–response curves of baclofen–stimulated [^{35}S]GTPγS binding in detergent–untreated (LPM) and TX–100 (1 % v/v)–treated–plasma membranes; *agonist stimulation is diminished at high detergent concentration*

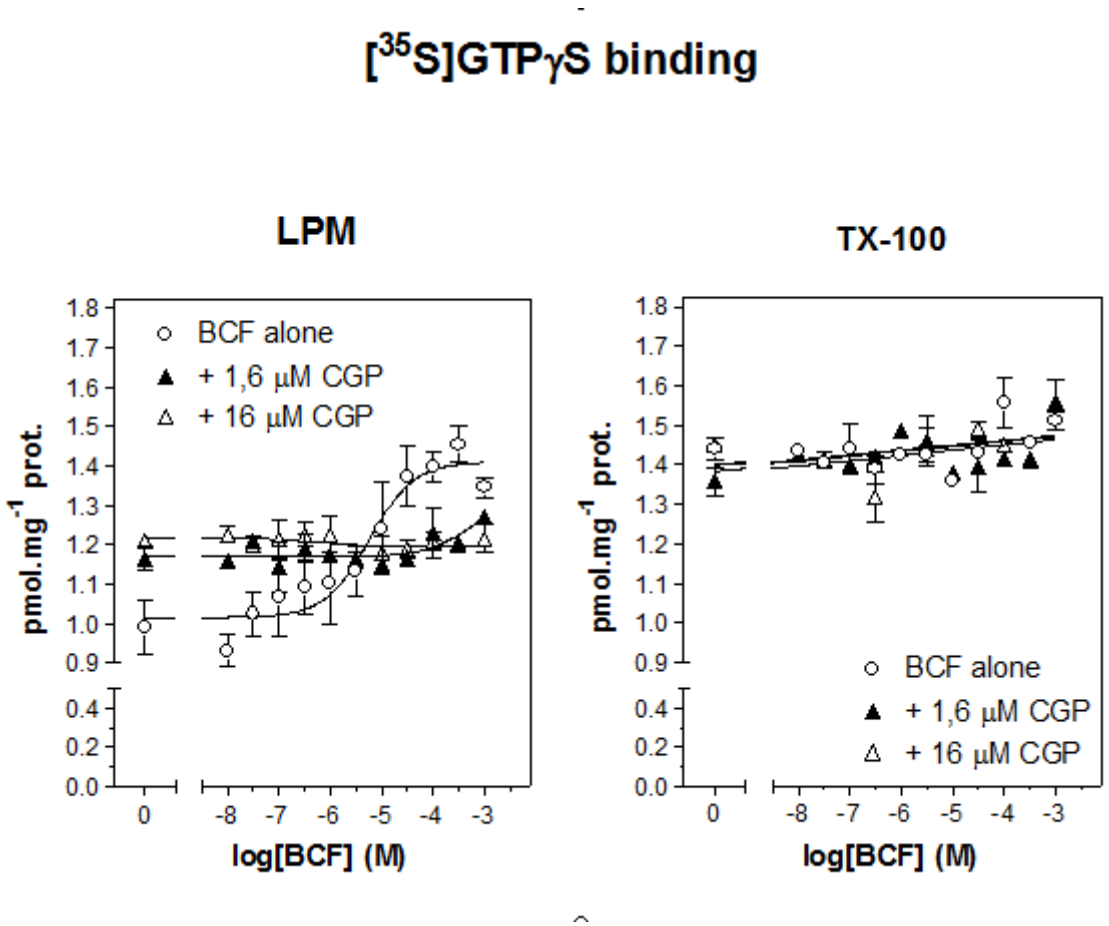

From PhD Thesis of Dr. Vladimír Rudajev, Charles University in Prague, Faculty of Natural Science, Department of Physiology, 2006

Legend to Fig. 16. The same legend as in Fig. 16. The functional activity of G proteins was measured by high–affinity GTPγS binding assay using the increasing concentrations of baclofen as a stimulating agonist (○), baclofen plus 1.6 µM CGP54626A (▲) or baclofen plus 16 µM CGP54626A (Δ).

Detergent–untreated membrane domains (LPM) exhibited the full responsiveness towards baclofen (BCF); contrarily, baclofen–stimulated [^{35}S]GTPγS binding was diminished in TX–100–resistant membrane domains prepared by addition of 10 % v/v Triton X–100 to

post–nuclear fraction to final concentration of 1 % v/v and subsequent flotation of detergent–treated PNS for 24 hours in 15/20/25/30/35/40 % w/v sucrose gradient.

With the aim to find a better procedure for preparation of DRMs, PM were exposed to increasing concentrations of non–ionic detergent Brij58 for 30 min at 0 ºC and assayed for baclofen–stimulated, high–affinity [^{33}S]GTPγS binding. Results presented in **Fig. 17** indicated that in relatively narrow range of detergent concentrations (0.01–0.1% w/v), the net–increment of baclofen–stimulated [^{33}S]GTPγS binding very high.

Fig. 17. The effect of increasing concentrations of Brij–58 on baclofen–stimulated, [^{33}S]GTPγS binding in Percoll–purified plasma membranes prepared from rat brain cortex.

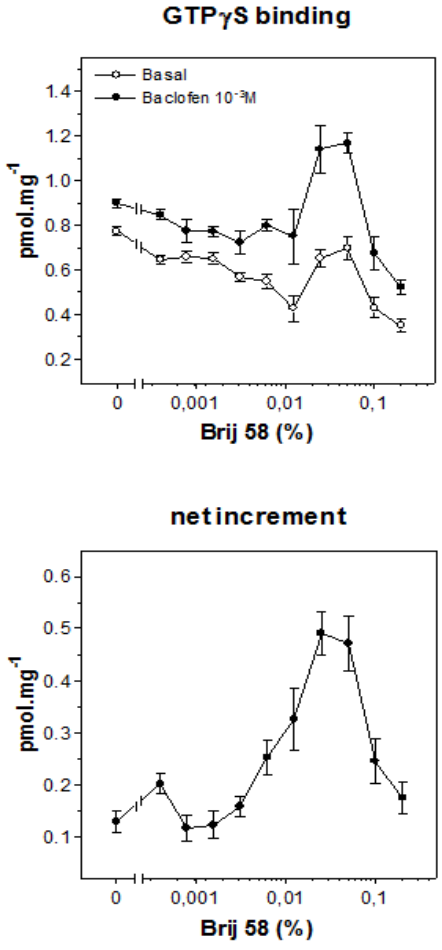

From PhD Thesis of Dr. Vladimír Rudajev, Charles University in Prague, Faculty of Natural Science, Department of Physiology, 2006

Based on this result, detergent–extraction of PM at 0 ºC was carried out in 0.025, 0.05% and 0.1% Brij58 and resulting PM fragments were separated by flotation in sucrose gradient

as described before. Distribution of Brij58–treated PM fragments was compared with distribution of detergent–untreated PM by measurement of the amount of protein in fractions 1–12 collected from the top to bottom of centrifuge tube (**Fig. 18**). We have also measured the distribution of membrane domain (caveolin and flotilin) and plasma membrane ($GABA_B$–R and Na^+/K^+–ATPase) markers in fractions 1–12 (**Fig. 19**) and compared distribution of Brij58–treated PM fragments with those formed by extraction of PM at the same concentrations of Triton X–100 (**Fig. 20**). Finally, baclofen–stimulated high–affinity [^{35}S]GTPase was measured in sucrose fractions 1–12 collected from Brij58–treated and Triton X–100–treated PM as an assay of baclofen–stimulated G protein activity (**Fig. 21**).

Fig. 18 Comparison of protein distribution in sucrose density gradients fractions prepared by flotation of *detergent–untreated (A) or Brij–58–treated (B) plasma membranes from rat brain cortex*

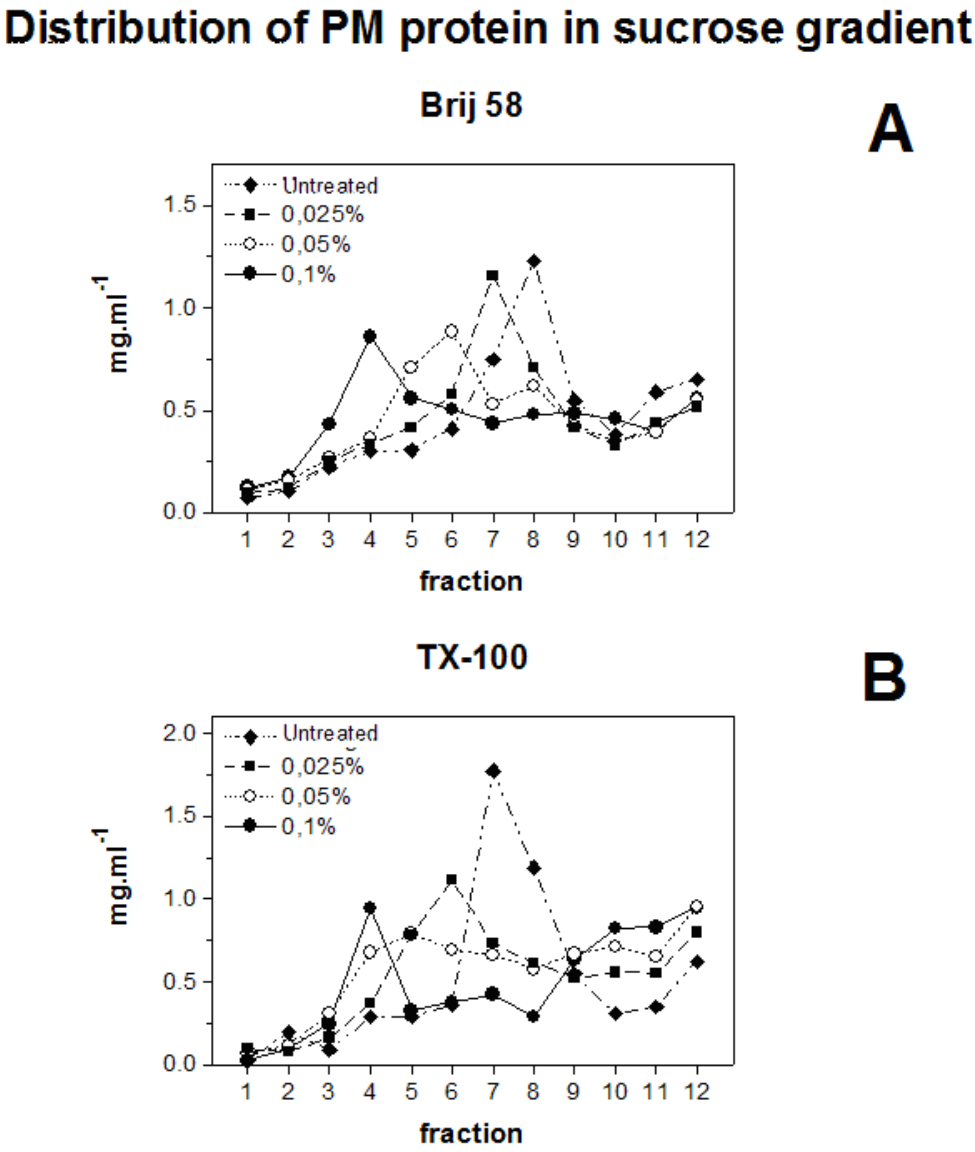

From PhD Thesis of Dr. Vladimír Rudajev, Charles University in Prague, Faculty of Natural Science, Department of Physiology, 2006

Legend to Fig. 18. Percoll–purified plasma membranes were prepared from brain cortex of adult rats and divided into four identical portions. The first portion was intensively mixed and represented the detergent–untreated PM sample (**Untreated**); to the second, third and fourth portion, the 10% w/v Brij58 was added to final concentration of 0.025, 0.05 and 0.1% w/v Brij–58. Exactly 2 ml of these four PM preparations were mixed with 2 ml of 80% w/v sucrose and fractionated by flotation in 15/20/25/30/35/40 % w/v sucrose gradient

(centrifugation for 24 hours at 116,000xg, Beckman SW41). The protein amount in fractions 1–12 collected from the top to the bottom of Beckman SW41 centrifuge tube was determined by Lowry method.

Fig. 19 Distribution of the membrane domain (caveolin–1, flotillin–2)– and plasma membrane (Na^+/K^+–ATPase and $GABA_B$–R) markers in sucrose density gradient; *the effect of increasing concentrations of Brij–58*

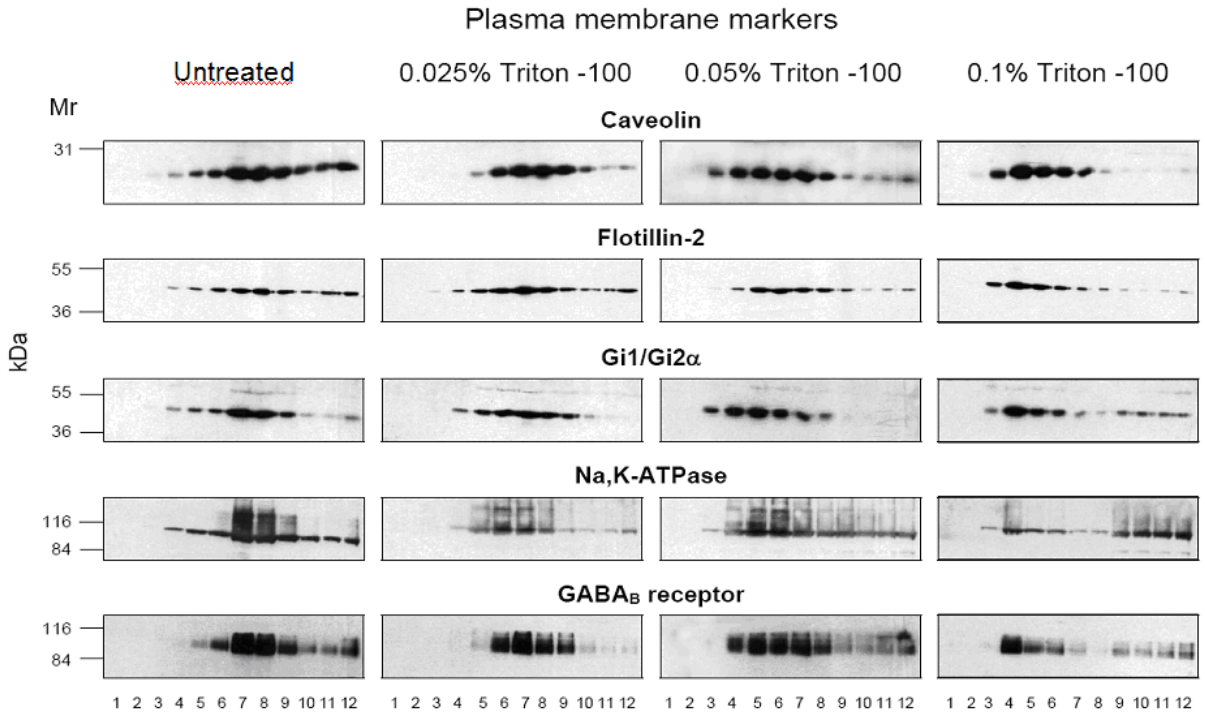

From PhD Thesis of Dr. Vladimír Rudajev, Charles University in Prague, Faculty of Natural Science, Department of Physiology, 2006

Legend to Fig. 19. Distribution of caveolin–1, flotillin–2, Gi1/Gi2α, α–subunit of Na^+/K^+–ATPase and $GABA_B$–R in sucrose density gradient was determined by TCA precipitation (6% TCA, 60 min on ice) of constant volume aliquots of fractions 1–12, SDS–PAGE and immunobloting with specific antibodies.

Fig. 20 Distribution of the membrane domain (caveolin–1, flotillin–2)– and plasma membrane (Na^+/K^+–ATPase and $GABA_B$–R) markers in sucrose density gradient; *the effect of increasing concentrations of Triton–X100.*

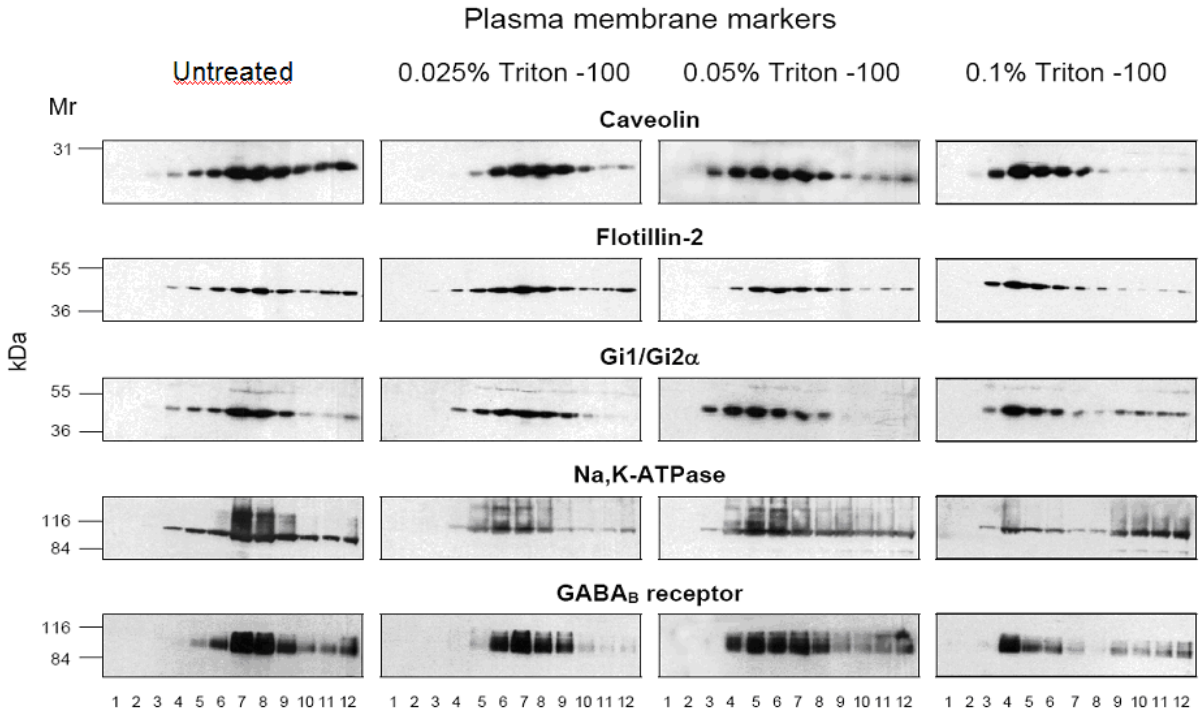

From PhD Thesis of Dr. Vladimír Rudajev, Charles University in Prague, Faculty of Natural Science, Department of Physiology, 2006

Legend to Fig. 20

Distribution of caveolin–1, flotillin–2, Gi1/Gi2α, α–subunit of Na^+/K^+–ATPase and $GABA_B$–R in sucrose density gradient was determined by TCA precipitation (6% TCA, 60 min on ice) of constant volume aliquots of fractions 1–12, SDS–PAGE and immunobloting with specific antibodies.

Fig. 21 Distribution of baclofen–stimulated, high–affinity[^{32}P]GTPase along the sucrose denisty gradient; *the effect of increasing concentrations of Brij–58 (A) and Triton X–100 (B)*

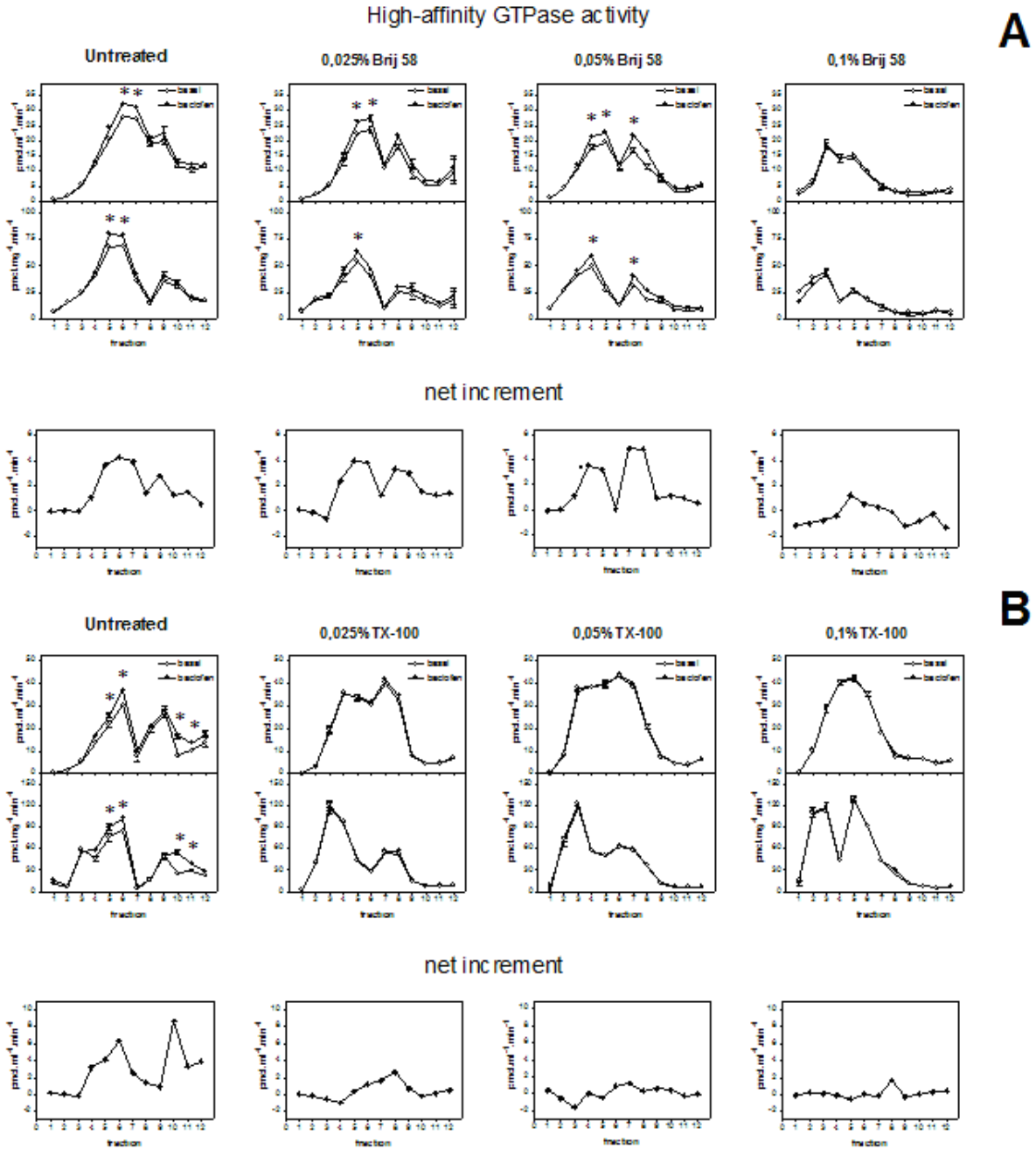

From PhD Thesis of Dr. Vladimír Rudajev, Charles University in Prague, Faculty of Natural Science, Department of Physiology, 2006

Legend to Fig. 21

Baclofen–stimulated high–affinity [^{35}S]GTPase was measured in sucrose fractions 1–12 collected from Brij58–treated– and Triton X–100–treated PM as an assay of baclofen–stimulated G protein activity.

Data presented in **Figs. 17–21** indicated, that the detergent–resistant membrane domains prepared in the presence of low concentrations of non–ionic detergent Brij58 exhibit baclofen–stimulated activity of G proteins. The optimum range of detergent concentrations was found to be in 0.025–0.05 % w/v range; at higher concentration, the agonist–stimulated component of G protein activity was attenuated due to the inhibitory action of the high detergent concentrations.

The reader might ask why the basal activity of G proteins is so high, much higher than of baclofen–stimulated component. The high basal, agonist–independent activity of G proteins is an inherent property PM prepared form natural tissues like brain or heart muscle. In natural tissues, the basal activity of G proteins is enhanced by RGS proteins which increase GTPase activity of Gα subunits and in this way increase the overall activity of G protein cycle (compare with **Fig. 4**). RGS proteins, under resting conditions residing in cytoplasmic space, are navigated to the inner side of plasma membrane by free Gβ subunits which appear on the inner side of plasma membrane shortly after agonist stimulation of receptor molecules.

4.13. Reactive oxygen species (ROS)

The earth began its life without free oxygen in its atmosphere (Dole, 1965). Oxygen accumulation is a consequence of the establishment and propagation of photosynthesizing archea and bacteria on this planet (Campbell and Reece, 2005).With the arrival of the world's first de facto pollutant (i.e., oxygen), approximately 3 billion years ago there evolved organisms that reductively metabolized oxygen to produce ATP in mitochondria (Rich, 2003) (i.e., aerobic respiration). Mitochondrial energymetabolism yields several reactive oxygen species (ROS) including oxygen ions (O_2^-, the primary ROS), free radicals, and peroxides (inorganic and organic). The presence of ROS produced profound consequences for life on earth, both beneficial and deleterious. For example, awealth of evidence suggests that high levels of ROS are intimately linked to the appearance of neuronal death in various neurological disorders. These include chronic diseases (Parkinson's disease or Alzheimer's disease) (Guglielmotto, 2009), acute injury of the brain (brain trauma and cerebral ischemia) (Chen et al, 2011; Valko et al, 2007), or psychiatric disorders (autism, attention deficit hyperactivity disorder, depression, and schizophrenia) (Michel et al, 2012). An increase in oxidative and nitrooxidative stress and a decrease in the antioxidant capacity of the brain are key factors involved in the etiology of neuropsychiatric diseases.

An increase in oxidative and nitro–oxidative stress and a decrease in the antioxidant capacity of the brain are key factors involved in the etiology of neuropsychiatric diseases.

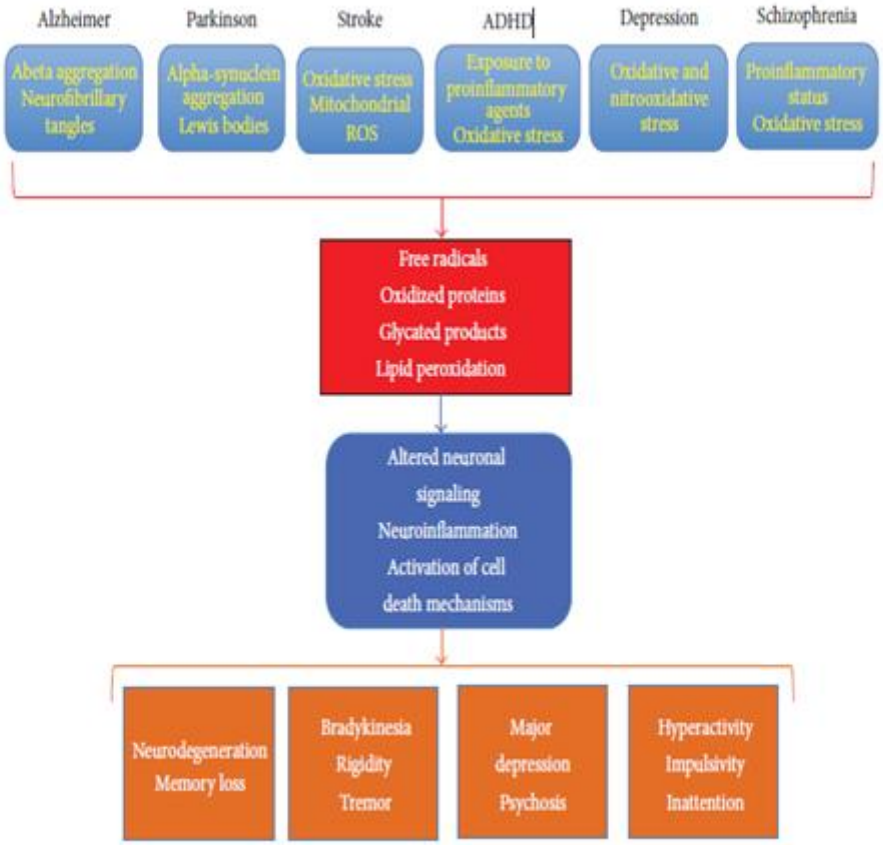

Schematic representation of oxidative stress-related mechanisms underlying disease development in Alzheimer's disease (AD), Parkinson disease (PD), stroke, attention deficit and hyperactivity disorders (ADHD), schizophrenia, and depression.

Besides the pathological states mentioned above, the generation of ROS may proceed largely shortly after the birth of mammals, as the newly born organism is suddenly exposed to much higher concentration of oxygen than in the mothers womb. Furthermore, in the brain of mammals (like the rat) which are born at relatively low level of maturation, the mitochondrial respiratory chain is not fully functional. Therefore, the possibility for the high production of ROS shortly after the birth of is high.

4.14. Lipofuscin–like pigments (LFP) as the end–products of free radical mediated membrane lipid oxidation

LFP are autofluorescent, liposoluble compounds which may be separated from cells or tissues by chloroform extraction. They represent the end–products of reactions involving free radical attack on biological molecules and can be formed, for example, in reactions between lipid peroxidation products, mainly unsaturated aldehydes, with compounds containing free

amino groups. Their characteristic emission maximum was found to be at 420–470 nm after being excited at 340–390 nm. The mechanism of their formation and chemical identity has been revealed in many in vitro studies, in which reactive aldehydes were incubated with amino group–containing molecules. Owing to their intrinsic fluorescent properties and molecular stability these products are easily measured by means of spectrofluorimetry and are used as **biomarkers of oxidative stress caused by various triggers**.

As relatively stable end–products of lipid peroxidation, LFP are good markers of free radical production and of consequent damage to lipids. Moreover, they are used not only as markers of lipid degradation but also to estimate amino acid and protein loss due to cross–linking. So far, LFP have been mostly used as robust markers of oxidative damage without defining the specific chemical identity of compounds representing these pigments. *In such cases, the fluorescent pigments are simply markers of free radical production under different circumstances.*

5. MATERIALS AND METHODS

5.1. Materials

$GABA_B$–receptor agonists baclofen (β–p–chlorophenyl–GABA), SKF97541 [3–aminopropyl (methyl) phosphinic acid] and antagonist [^{3}H]CGP54626A (41.5 Ci/mmol, cat. no. R1088) were purchased from Tocris. [^{35}S]GTPγS (1250 Ci/mmol) was from Perkin–Elmer (NEG030H). Complete protease inhibitor cocktail was from Roche Diagnostic (cat. no. 1697498). All other chemicals were of highest quality available.

All experiments were approved by Animal Care and Use Committee of the Institute of Physiology, Academy of Sciences of the Czech Republic to be in agreement with Animal Protection Law of the Czech Republic as well as European Community Council directives 86/609/EEC.

5.2. Isolation of plasma membrane–enriched fraction from rat brain cortex

The first goal of my work was to standardize the technique for preparation of Percoll–purified plasma membranes from the rat brain cortex. The first problem which I had to solve was to find an optimum compromise between the amount of protein applied per density gradient and quantity and purity of plasma membrane (PM) preparation. Application of the high amount of protein in post–nuclear fraction (PNS) resulted in PM preparation contaminated with mitochondria and lysosomes which are present in brain tissue in extraordinary high amounts. The final version of this procedure is out–lined in the following paragraph.

Rat brain cortex was minced with razor blade on pre–cooled plate and diluted in STEM medium containing 250 mM sucrose, 20 mM Tris–HCl, 3 mM $MgCl_2$, 1 mM EDTA, pH 7.6, fresh 1 mM PMSF plus protease inhibitor cocktail. It was then homogenized mildly in loosely–fitting Teflon–glass homogenizer for 5 min (2 g w.w. per 10 ml) and centrifuged for 5 min at 3500 rpm. Resulting post–nuclear supernatant (PNS) was filtered through Nylon nets of decreasing size (330, 110 and 75 mesh, Nitex) and applied on top of Percoll in Beckman Ti70 tubes (30 ml of 27.4 % Percoll in STE medium). Centrifugation for 60 min at 30000 rpm (65000 x g) resulted in the separation of two clearly visible layers (Bourova *et al.* 2009).

The upper layer represented plasma membrane fraction (PM); the lower layer contained mitochondria (MITO). The upper layer was removed, diluted 1:3 in STEM medium and centrifuged in Beckman Ti70 rotor for 90 min at 50000 rpm (175000 x g). Membrane sediment was removed from the compact, gel–like sediment of Percoll, re–homogenized by hand in a small volume of 50 mM Tris–HCl, 3 mM $MgCl_2$, 1 mM EDTA, pH 7.4 (TME medium), snap frozen in liquid nitrogen and stored at –80 °C.

5.3 Subcellular fractionation of rat brain cortex by flotation in sucrose density gradient; isolation of detergent–untreated and detergent–resistant membrane domains

The second goal of my work was to extend and test the reproducibility of the methods which were used previously in our laboratory for isolation of detergent–untreated and detergent–resistant membrane domains (DRMs). The usage of high detergent concentrations for preparation of membrane domains (Sargiacomo *et al.*, 1993; Lisanti *et al.* 1994 a, b) resulted in membrane fragments exhibiting the very low or zero agonist efficacy for stimulation of GDP/GTP exchange reaction of G proteins (Bourova *et al.*, 2003). Using other words, DRMs isolated in the presence of high detergent concentrations were inactive as far as stimulation of GPCR was involved. The same was truth when using the "alkaline–treatment" protocol based on sonication and extraction of the cell homogenate in highly alkaline solution of 0.5–1 M Na_2CO_3 (Song *et al.* 1996a, b).

According to experimental results collected over the years in our laboratory, the best of the so–far described methods/ protocols for preparation of membrane domains is that of Smart *et al.* (1995, 1999). The views what the term *membrane domains* actually means from methodological, structural and functional point of view were reviewed by Pike (2004). The sometimes controversial viewpoints about the size and physiological meaning of *membrane domains* were expressed by Pike (2006a, b) and Shaw (2006).

The disadvantage of the method of Smart *et al.* (1995, 1999) using the sequence of three types of density gradients is, however, the very low amount of protein recovered in the final preparation of pure "domains" – about 0.2–0.5% of the original amount present in the starting material, i.e. the cell homogenate. Therefore, when trying to find some compromise between purity and quantity of the final preparation, centrifugation in Percoll gradient was followed by the "flotation" in sucrose density gradient.

Plasma membrane enriched fraction was prepared from the rat brain cortex by

centrifugation at 116,000xg for 35 min in Percoll^{R} gradient (Beckman Ti60 rotor) as described in Methods (compare with **Figs. 10** and **11**) and subsequently, the low–density membrane fragments (LPM) were separated from the bulk of plasma membranes (BPM) by flotation in a step–wise 15/20/25/30/35/40% w/v sucrose gradient (Roubalova *et al.*, 2009). The protein profile of sucrose density gradient was clearly dependent on detergent concentration (**Fig. 23** and **24**): when increasing detergent concentration, the PM band recovered in the lower part of centrifugation tube (at zero concentration of the detergent) was transferred up, towards the low–density end of the gradient.

Measurement of functional activity of $GABA_B$–R as baclofen–stimulated, high–affinity [^{35}P]GTPase (**Fig. 20**) indicated the best results when using 0.025% or 0.05% w/v Brij58. At these concentrations, the baclofen–stimulated, high–affinity [^{35}P]GTPase in DRMs was comparable with that in detergent–untreated PM. Based on these results, the 5 main areas of the sucrose density gradient were distinguished: **area I**, the top of gradient containing no protein; **area II**, low–density PM fragments; **area III**, plasma membranes (PM); **area IV**. An intermediate area between PM band and gradient pellet; **area V**, gradient pellet containing PM fragments exhibiting the higher density than 40% w/v sucrose (**Fig. 23**). Reproducibility of the sucrose density gradient profiles obtained after flotation of detergent–untreated samples was satisfactory (**Fig. 24**).

Fig. 22 Preparation of detergent resistant membrane domains (DRMs) from rat brain cortex by extraction of Percoll–purified plasma membranes at low detergent concentrations; *dependence on detergent / protein ratio*

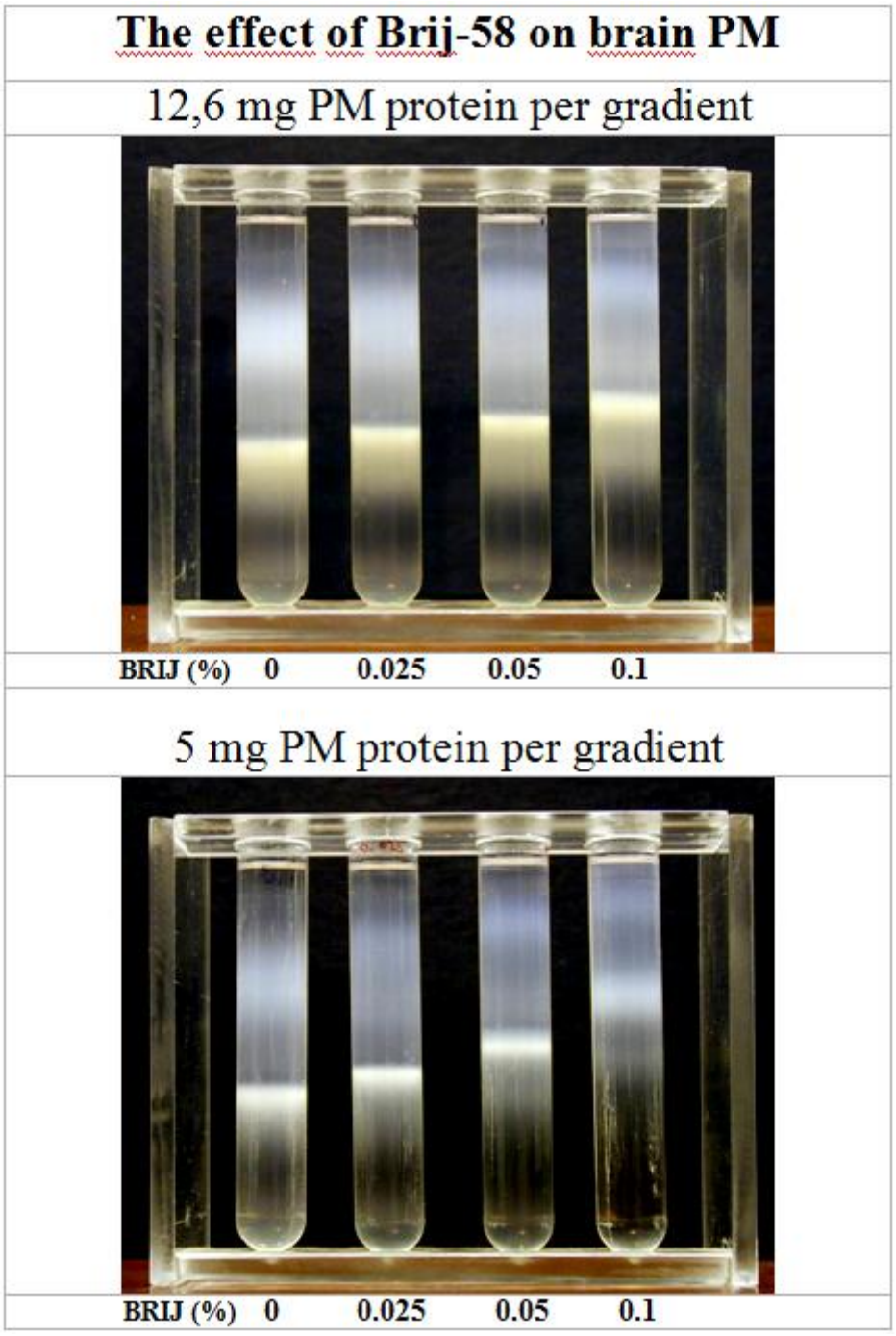

Fig. 23 Preparation of functional DRMs from rat brain cortex by extraction of Percoll–purified plasma membranes at low detergent concentrations; *the five main area sucrose density gradient*

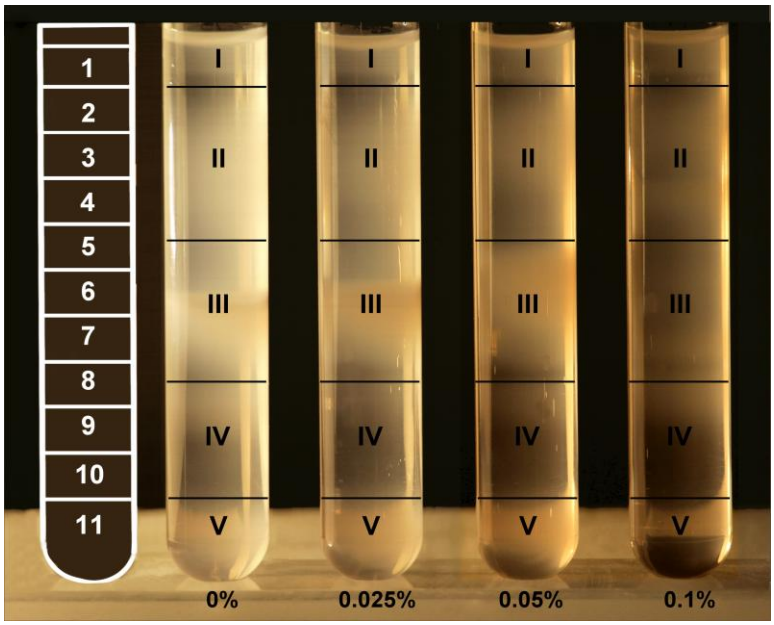

Fig. 24 Reproducibility of sucrose density gradients profiles; *fractionation of rat brain cortex under the detergent–free conditions*

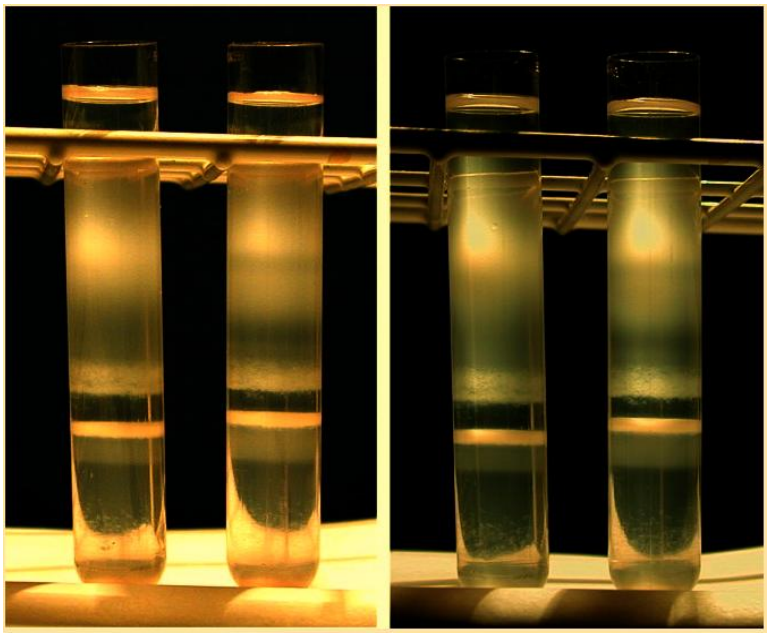

As demonstrated in **Fig. 25**, I have also tested the effect of the short–term ultrasound exposure (sonication) of 5s, 10s and 20s duration on distribution of PM fragments in flotation sucrose density. The short–term sonication resulted in an alteration of distribution of PM fragments: the broad distribution of PM fragments visualized as a wide band in the lower part of cuvette was transformed into the narrow, more restricted distribution pattern. To avoid this effect, I have not used sonication for subcellular fractionation of rat brain tissue and preparation of LDM and PM.

Fig. 25 Effect of the short–tem sonication on macroscopical profile of sucrose density gradient

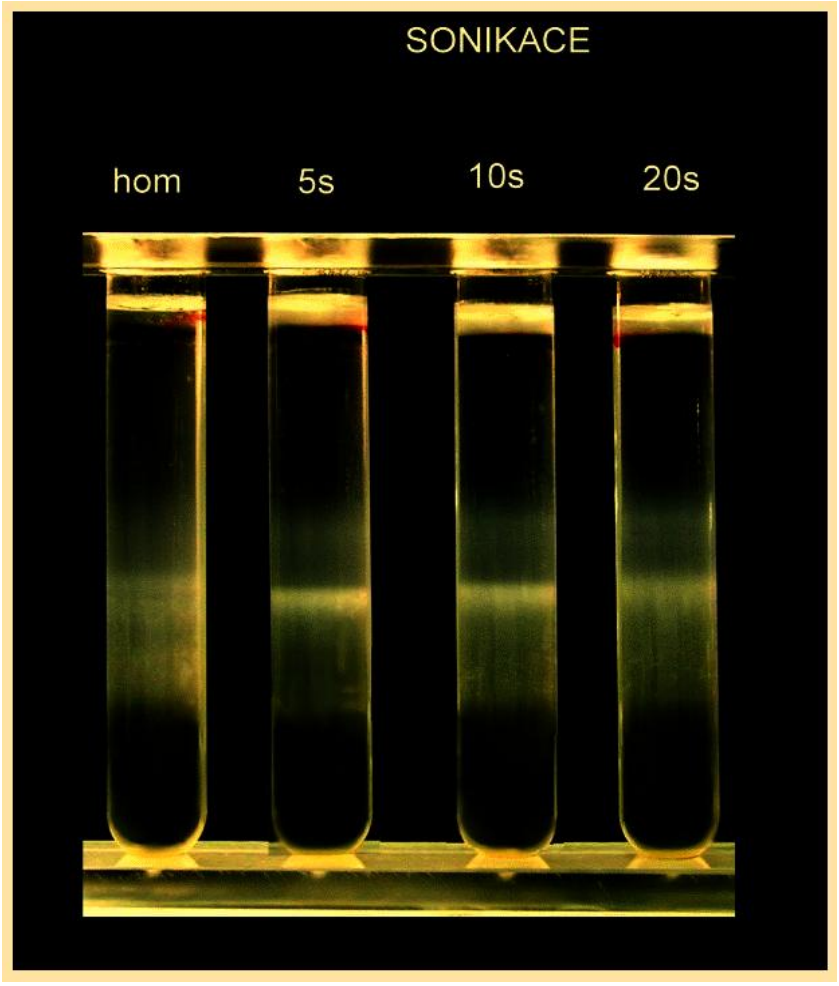

5.4. Agonist–stimulated [^{35}S]GTPγS binding; *dose–response curves*

Measurement of agonist–stimulated, high–affinity binding of non–hydrolysable analog of GTP, [^{35}S]GTPγS, represents a general and widely used method for determination of the effect of GPCR agonists on G protein activity. This method is based on agonist–induced exchange of GDP for GTP. The radioactive analog of GTP enters the ligand binding pocket within the short time–period when it is opened after interaction of G protein with agonist–bound, i.e. activated receptor. However, in natural tissues such as brain, the high basal level [^{35}S]GTPγS binding exists in the absence of GDP and this type of binding is not effected by agonist (**Fig. 27**). The strategy how to reveal the agonist–stimulated component of [^{35}S]GTPγS binding is to mimic the conditions in living cell most closely. That means to include GDP in reaction mix (i.e. in assay buffer) and, by means of increasing GDP concentration, to reveal the high–affinity component which responds to a given agonist. This component is otherwise hidden in the overall [^{35}S]GTPγS binding.

Fig. 26 Dependence of [^{35}S]GTPγS binding to the brain cortex PM on GDP concentration

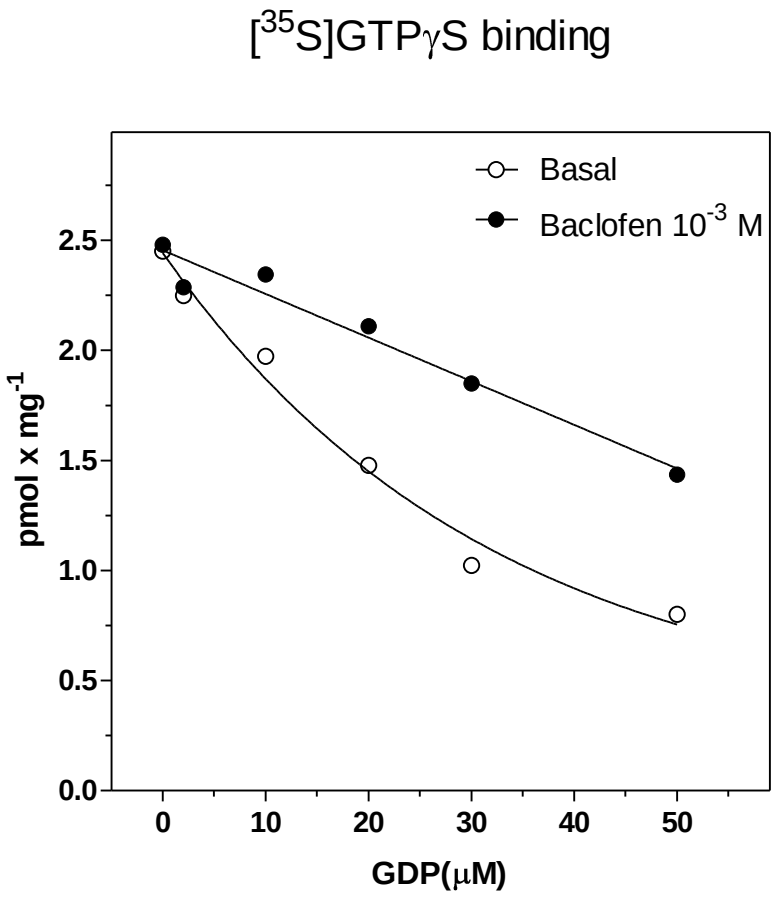

Based on results presented in **Fig. 26**, I have chosen the 20 μM concentration of GDP as that one, which will be included in [^{35}S]GTPγS binding assay mix in my studies of ontogenetic development of functional coupling between $GABA_B$–R and the cognate G proteins in rat brain cortex. At this GDP concentration, baclofen–stimulation of the basal level of [^{35}S]GTPγS binding was much higher than in previous studies of detergent–untreated PM (**Fig. 21**) which were performed in our laboratory. Therefore, the measurement of functional activity of $GABA_B$–R by determination of baclofen–stimulated, high–affinity [^{35}S]GTPγS binding, could be measured with higher accuracy.

Membranes prepared from 2–, 14– and 90–day–old rats of selected ages were incubated with (total binding, B_{total}) or without (basal binding, B_{basal}) increasing concentrations of $GABA_B$–R agonists baclofen and SKF97541 (10^{-10}–10^{-3} M) in final volume of 100 μl of reaction mix containing 20 mM HEPES, pH 7.4, 3 mM $MgCl_2$, 100 mM NaCl, 20 μM GDP, 0.2 mM ascorbate and [^{35}S]GTPγS (about 100–200,000 dpm per assay) for 30 min at 30 °C. The binding reaction was terminated by dilution with 3 ml of ice–cold 20 mM HEPES, pH 7.4, 3 mM $MgCl_2$ and filtration through Whatman GF/C filters on Brandel cell harvester. Radioactivity remaining on the filters was determined by liquid scintillation using Rotiszcint Eco Plus cocktail. Non–specific binding was determined in parallel assays containing 10 μM unlabelled GTPγS. Data were analyzed by GraphPad Prism 4 (GraphPad Software, San Diego, CA, USA) and B_{basal}, B_{max} and EC_{50}, values calculated according to the method of least–squares by fitting the data with sigmoidal dose–response curve.

5.5. Agonist–stimulated [^{35}S]GTPγS binding; one–point assay

With the aim to screen PM prepared from all age intervals under the same assay conditions, membranes (20 μg protein per assay) were incubated with ($B_{agonist}$) or without (B_{basal}) 1 mM baclofen or 100 μM SKF97541 in final volume of 100 μl of reaction mix containing 20 mM HEPES, pH 7.4, 3 mM $MgCl_2$, 20 μM GDP, 0.2 mM ascorbate and [^{35}S]GTPS (1–2 nM) for 30 min at 30 °C. The binding reaction was discontinued by dilution with 3 ml of ice–cold 2 mM HEPES, pH 7.4, 0.15 mM $MgCl_2$ and immediate filtration through Whatman GF/C filters on Brandel cell harvester. Radioactivity remaining on the filters was determined by liquid scintillation using Rotiszcint Eco Plus cocktail. Non–specific

GTPγS binding was determined in parallel assays containing 10 μM GTPγS. The binding data were analyzed by GraphPad Prism 4 and represent an average ± S.E.M. of 3 experiments.

5.6. [^{3}H]CGP54626A binding; saturation binding study

Membranes (100 μg protein per assay) were incubated with increasing concentrations of $GABA_B$–antagonist [^{3}H]CGP54626A (0.06–36.8 nM) in final volume of 100 μl of binding mix containing 50 mM Tris–HCl (pH 7.4) plus 2.5 mM $CaCl_2$ for 60 min at 30 °C. The bound and free radioactivity was separated by filtration through Whatman GF/B filters in Brandel cell harvestor. Filters were washed 3x with 3 ml of ice–cold incubation buffer and radioactivity remaining and placed in 5 ml of scintillation cocktail (Rotiszint Eco Plus). The non–specific binding was determined in the presence of 1 mM GABA in binding mix. Data were analyzed by GraphPad Prism 4 and K_d and B_{max} values calculated according to the method of the least–squares by fitting the data with rectangular hyperbola.

5.7. Na^+/K^+–ATPase; *[^{3}H]ouabain binding*

Sodium plus potassium–activated, oubain–dependent Na^+/K^+–ATPase (E.C. 3.6.1.3) was determined by "one–point" [^{3}H]ouabain binding assay according to Svoboda *et al.* (1988). Membranes (50 μg of protein) were incubated with 20 nM [^{3}H]ouabain in a total volume of 0.45 ml of 5 mM $NaHPO_4$, 5 mM $MgCl_2$, 50 mM Tris–HCl, pH 7.6 (Mg–Pi buffer) for 90 min at 30 ºC. The bound and free radioactivity was separated by filtration through Whatman GF/B filters in Brandel cell harvester. Filters were washed 3× with 3 ml of ice–cold incubation buffer and placed in 4 ml of scintillation cocktail (CytoScint, ICN). Radioactivity remaining on filters was determined after 10 h at room temperature by liquid scintillation. Non–specific binding was determined in the presence of 1 μM unlabelled ouabain.

5.8. Protein determination

The method of Lowry was used for determination of membrane protein (Lowry et al, 1951). Bovine serum albumin (Sigma, Fraction V) was used as standard. Data were calculated by fitting the data with calibration curve as quadratic equation.

5.9. Measurement of lipofuscin like pigments

The technique described by Goldstein and McDonagh (Goldstein and Mc Donagh, 1976), modified in (Wilhelm and Herget, 1999), was used for the analysis of LFP in brain

homogenates. Approximately 30 mg of frozen brain sample was weighed, chopped to fine pieces, and transferred into a glass–stoppered test tube containing 6 ml of chloroform–methanol mixture (2:1, v/v). After 1–h extraction on a motor–driven shaker, 2 ml of double distilled water was added, the sample was agitated, and the ensuing mixture was centrifuged (400 g, 10 min). After centrifugation, the lower chloroform phase was separated and used for measurement of fluorescence.

Fluorescence excitation and synchronous spectra were measured in Aminco–Bowman 2 spectrofluorometer. Recordings and analysis was performed by AB–2 computer program, which was also used for organization of the spectra into tridimensional spectral arrays. The *excitation spectra* were measured in the range of 250–400 nm for emission adjusted between 400 and 500 nm in steps of 10 nm. The quantitative estimation of LFP was based on excitation and emission maxima found in tridimensional spectral arrays. The three major fluorophores F325/380, F335/410, and F355/440 (excitation/emission, nm) were identified. The fluorometer was calibrated based on the standard No. 5 of the instrument manufacturer, and the LFP concentration was expressed in arbitrary units per mg tissue wet weight. The statistical evaluations were made using ANOVA with Scheffe post–hoc test, and the results are shown as means ± SEM. The synchronous *emission spectra* were measured in the range of 350–550 nm, with a constant difference of 50 nm between excitation and emission wavelengths. Their second derivatives were obtained using the AB–2 software.

5.10. HPLC analysis

Brain chloroform extracts were evaporated under the stream of nitrogen. The evaporated sample was dissolved in approximately 1 ml of running phase used in isocratic HPLC separation. A mixture of acetonitrile–methanol– water (50:10:40, v/v) was used for separation of LFP. A Jasco HPLC instrument equipped with fluorescence detector was set at the excitation and emission maxima of the three major fluorophores. A C18 column (4 x 250 mm) was used for the analysis. Isocratic elution gave optimum separation at 0.2 ml/min.

6. RESULTS

6.1. The ontogenetic development of $GABA_B$–receptor signaling cascade

6.1.1. Functional coupling of $GABA_B$–R with G proteins

The efficacy (maximum of G protein response) and potency (affinity of G protein response) of $GABA_B$–receptors in plasma membranes isolated from brain cortex of 2–, 14– and 90–days old rats was determined as baclofen– and SKF97541–stimulated, high–affinity [^{35}S]GTPγS binding in the presence of 20 μM GDP. The addition of 20 μM GDP into the assay mix was necessary to suppress the high basal level of binding of this non–hydrolysable analog of GTP with the aim to reveal the agonist–stimulated component of G protein activity (compare with **Fig. 26**). Dose–response curves were measured in 0.1 nM–1 mM range of baclofen or SKF97541 concentrations and the significance of difference among PM prepared from 2–(PD2), 14– (PD14) and 90–days (PD90) old rats was analyzed by one–way ANOVA followed by Bonferroni's *post–hoc* comparison test using GraphPad Prism 4 software.

Surprisingly, baclofen exhibited the significant ability to increase the basal level of [^{35}S]GTPγS binding measured in the absence of agonist (B_{basal}) already in 2–day–old animals (PD2). This ability was further increased in the course of the first two weeks of postnatal life (**Fig. 27**), but virtually unchanged when viewed over the whole period of brain development as the averaged dose–response curve measured in 2–days–old animals was not significantly different from that measured in adult rats (90–days old). The basal level of [^{35}S]GTPγS binding was also significantly increased between PD2 and PD14 and subsequently decreased to the adult level. The same result applied to the net–increment of agonist stimulation expressed as the difference between baclofen–stimulated and the basal level of [^{35}S]GTPγS (**Table 1**). The % of baclofen–stimulation over the basal level of binding was unchanged.

The developmental alteration of dose–response curves of SKF97541–stimulated [^{35}S]GTPγS binding, analyzed in an independent set of PM preparations, was similar to that of baclofen, however, a substantial difference between the two agonists was also noticed. SKF97541 exhibited the significant ability to increase the basal level of [^{35}S]GTPγS binding already in 2–day–old animals. The maximum response of SKF97541 was increased between PD2 (B_{max} = 1.13 pmol x mg^{-1}) and PD14 (B_{max} = 1.51 pmol x mg^{-1}) and further development was reflected in decrease of SKF97541–stimulated [^{35}S]GTPγS binding to the level in 90–days–old animals (B_{max} = 1.08 pmol x mg^{-1}), which was not significantly different from that in 2–days–old animals.

The significant difference, however, was observed when comparing the basal level of binding in 2–days–old (B_{basal} = 0.83 pmol x mg^{-1}), 14–days–old (B_{basal} = 1.02 pmol x mg^{-1}) and 90–days–old (B_{basal} = 0.66 pmol x mg^{-1}) animals: PD2 versus PD14, p<0.01, **; PD14 versus PD90, p<0.01,**; PD2 versus PD90, p<0.01,** (**Table 1).** The % of SKF97541–stimulation over the basal level was unchanged. Comparison of SKF97541– and baclofen–stimulated [^{35}S]GTPγS binding data indicated, that usage of different animals for preparation of PM was associated with the difference in the basal level of binding in the absence of agonist.

The potency (EC_{50} values) of G protein response to baclofen was not significantly different in membranes prepared from 2–, 14– and 90–day–old rats, but decreased from the birth to adulthood in the case of SKF97541 (**Table 1**). This finding was compatible with electrophysiological studies of brain maturation indicating an altered sensitivity to different $GABA_B$–R agonists in the course of brain development (Bernasconi *et al.* 1992, Hosford *et al.* 1992, Marescaux *et al.* 1992, Lin *et al.* 1993, Kubová *et al.* 1996, Mareš 2008).

Fig. 27 Dose–response curves of baclofen and SKF97541–stimulated [^{35}S]GTPγS binding in PM isolated from 2–, 14– and 90–day–old rats

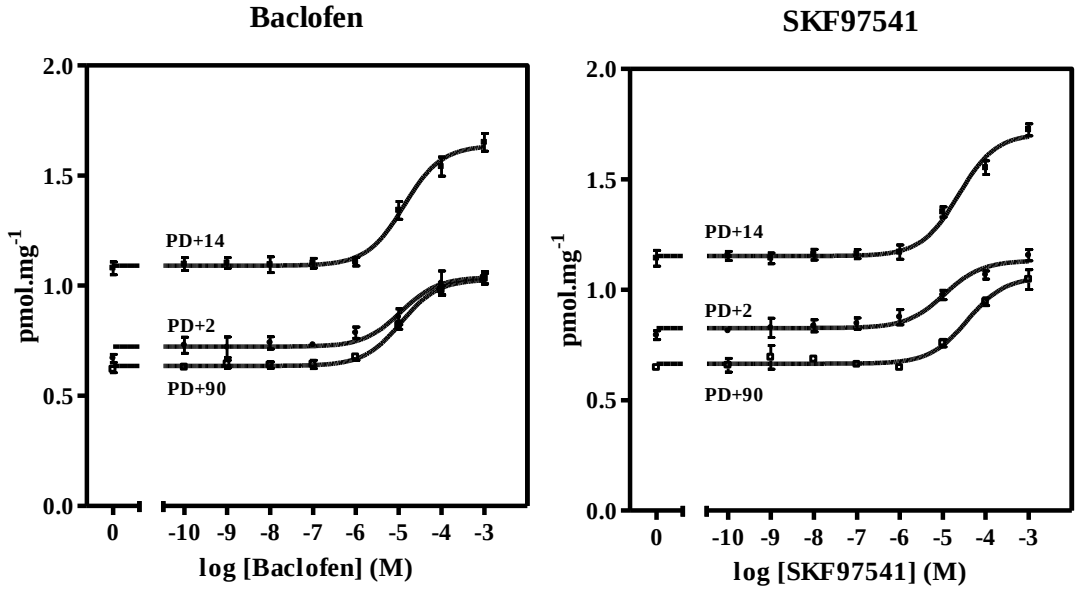

Legend to Fig. 27. PM were isolated in parallel from brain cortex of 2 (●)–, 14 (○)– and 90 (■)–days–old rats and the high–affinity [^{35}S]GTPγS binding was measured in the presence of

increasing concentrations of $GABA_B$–R agonists (–)–baclofen (left) or (–)–SKF97541 (right panel) in different age groups as described in Methods. The binding data were fitted by sigmoidal dose–response curves using GraphPad *Prism 4* and represent the average of three experiments ± S.E.M. Differences between the averaged dose–response curves corresponding to PM prepared from 2–(PD2), 14–(PD14) and 90–days (PD90) old rats were statistically analyzed by one–way ANOVA followed by Bonferroni's post–hoc comparison test. The results of this analysis are presented in **Table1.**

Table 1. Maximum response (B_{max}) and affinity (EC_{50}) of baclofen– and SKF97541–stimulated [^{35}S]GTPγS binding in PM isolated from 2–, 14– and 90–days old rats.

A(–)–baclofen	**2–days**	**14–days**	**90–days**
Bbasal	0.72 ± 0.01	1.09 ± 0.02	0.64 ± 0.01
Bmax	1.04 ± 0.03	1.64 ± 0.03	1.03 ± 0.01
Bmax – Bbasal	0.31	0.62	0.40
100 x Bmax / Bbasal	152 %	152 %	166 %
EC_{50} *(μM)*	9.00 (4.46–18.15)	13.35 (7.80–22.85)	13.26 (9.96–17.65)
B(–)–SKF97541			
Bbasal	0.83 ± 0.01	1.15 ± 0.01	0.66 ± 0.01
Bmax	1.13 ± 0.02	1.71 ± 0.02	1.08 ± 0.02
Bmax – Bbasal	0.30	0.49	0.42
100 x Bmax / Bbasal	142 %	152 %	168 %
EC_{50} *(μM)*	9.79 (5.30–18.10)	23.40 (14.31–38.25)	36.51 (21.87–60.95)

B_{basal} (pmol · mg^{-1}), binding in the absence of agonist; B_{max} (pmol · mg^{-1}), binding at saturating agonist concentration; = B_{max} – B_{basal}, net–increment of agonist stimulation; 100 x B_{max} / B_{basal}, % stimulation of the basal level by agonist. EC_{50} (μM), agonist concentration inducing half–maximum stimulation (95 % confidence

limit). B_{max}, B_{basal} and EC_{50} values were determined by analysis of the sigmoidal dose–response curves of baclofen– (**A**) and SKF97541– (**B**) stimulated [^{35}S]GTPγS binding presented in Figure 1 by GraphPad Prism 4 and represent the average of three experiments ± S.E.M. The significance of difference between B_{basal}, B_{max} and EC_{50} values in PM prepared from 2 (PD2)–, 14 (PD14)– and 90 (PD90)–days–old rats was determined by one–way ANOVA followed by Bonferroni's *post–hoc* comparison test.

The significance of difference between Bbasal, Bmax and EC50 values in PM prepared from 2 (PD2)–, 14 (PD14)– and 90 (PD90)–days–old rats was determined by one–way ANOVA followed by Bonferroni's post–hoc comparison test.

A (baclofen).

Bbasal (PD2 versus PD14, p<0.0001, ***; PD14 versus PD90, p<0.0001, ***; PD2 versus PD90, p>0.05, not significant. **Bmax** (PD2 versus PD14, p<0.001, ***; PD14 versus PD90, p<0.001, ***; PD2 versus PD90, p>0.05, not significant. **EC50** (PD2 versus PD14, p>0.05, NS; PD14 versus PD90, p>0.05, NS; PD2 versus PD90, p>0.05, NS.

B (SKF97541).

Bbasal (PD2 versus PD14, p<0.0001, ***; PD14 versus PD90, p<0.0001, ***; PD2 versus PD90, p=0.0022, **. **Bmax** (PD2 versus PD14, p<0.0001, ***; PD14 versus PD90, p<0.0001, ***; PD2 versus PD90, p>0.05, NS. **EC50** (PD2 versus PD14, p>0.05, NS; PD14 versus PD90, p>0.05, NS; PD2 versus PD90, p<0.01, **).

Determination of the dose–response curves of baclofen– and SKF9754–stimulated [^{35}S]GTPγS binding in 1–, 15– and 90–days old rats was followed by the detailed analysis of ontogenetic profile of agonist–stimulated G protein activity in fetuses (–1) and in PM prepared from 1–, 2–, 4–, 5–, 9–, 10–, 14–, 15–, 25–, 30–, 35–, 42–, 47– and 90–days old rats. Data presented in **Fig. 28** indicated clearly the existence of maximum of baclofen– and SKF97541–stimulated G protein activity at PD14 and PD15. Baclofen–stimulated, SKF9754–stimulated and the basal level of [^{35}S]GTPγS binding in adult animals were not significantly different from those detected in 2–days–old animals (PD2). Accordingly, the peak value of [^{3}H]GABA binding was detected at PD14 in rat brain cortical slices by quantitative autoradiography and this high level of [^{3}H]GABA binding subsequently declined to the adult level (Turgeon and Albin 1994).

Fig. 28 Baclofen– and SKF97541–stimulated [^{35}S]GTPγS binding; *one–point assay*

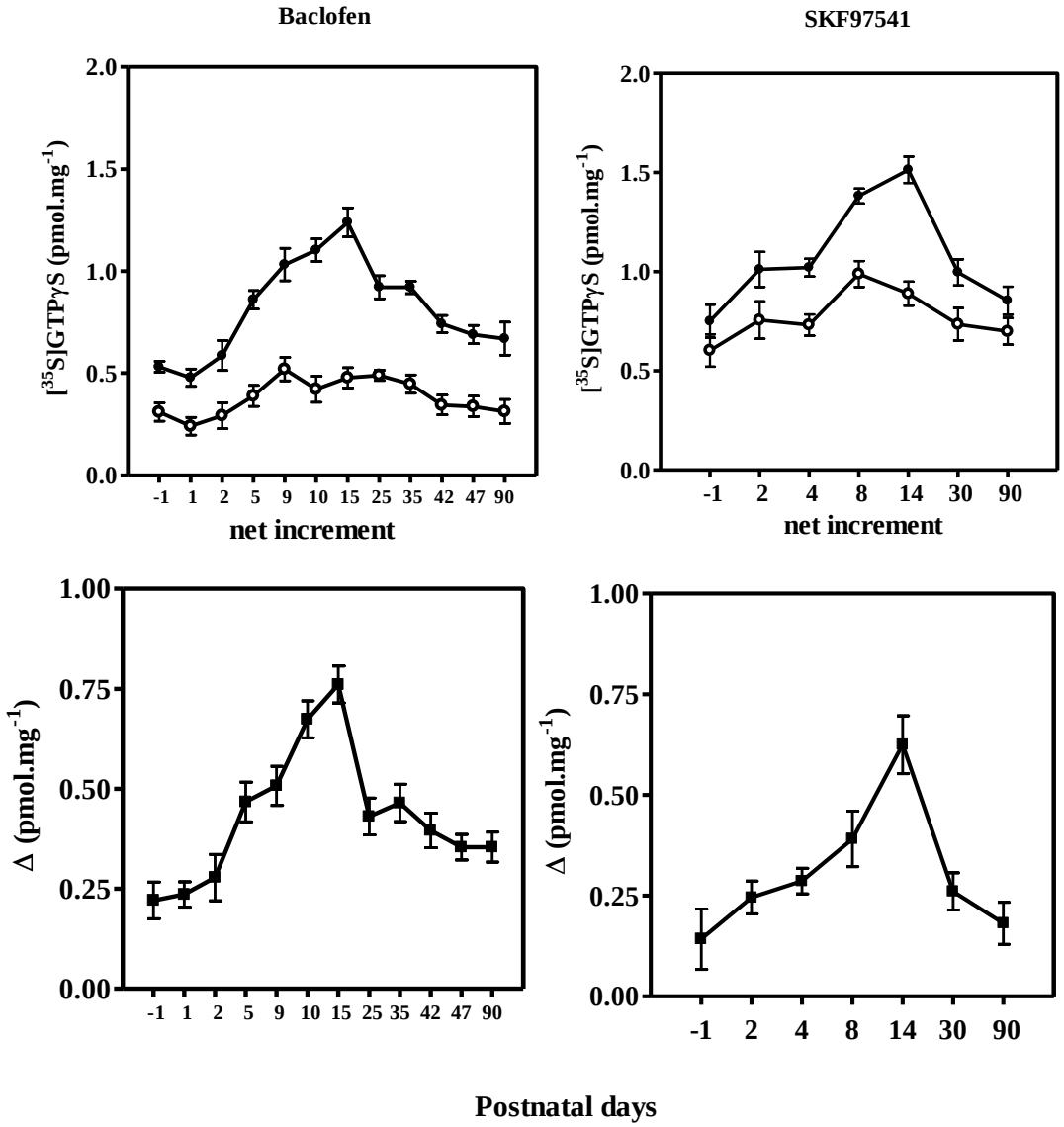

Legend to Fig. 28.

Upper panels. PM were isolated from fetuses (–1) and from 1–, 2–, 4–, 5–, 8–, 9–, 10–, 14–, 15–, 25–, 30–, 35–, 42–, 47– and 90–days old rats, frozen in liquid nitrogen and used only once. Baclofen– and SKF97541–stimulated [^{35}S]GTPγS binding was determined in different age groups as described in Methods in the presence (●, $B_{agonist}$) or absence (○, B_{basal}) of 1 mM baclofen (left) or 100 μM SKF97541 (right panel).

The significance of difference between the two sets of data ($B_{agonist}$ versus B_{basal}) at all age intervals was analyzed by Student s t–test using GraphPad Prism 4: baclofen, $p < 0.001$, ***; SKF97541, $p < 0.0022$, **. The same type of comparison ($B_{agonist}$ versus B_{basal}) was also performed at individual age intervals: **baclofen** [day –1 (*), PD2 (**), PD5(***), PD9(***),

$^{+}$10(***), PD15(**), PD25(***), PD35(****), PD42(***), PD47(**), PD90(***)]. **SKF97541** [day –1 (NS), PD2 (NS), PD4(*), PD8(*), PD14(**), PD30(NS), PD90(NS)].

Lower panels. Difference between agonist–stimulated ($B_{agonist}$) and basal (B_{basal}) level of binding was expressed as the net–increment of agonist stimulation $\Delta = B_{agonist} - B_{basal}$. Data represent the average ± S.E.M. of three experiments.

The existence of the sharp maximum of $GABA_B$–R agonist–stimulated [^{35}S]GTPγS binding at PD15 and PD14 **(Fig. 28)** was fully consistent with our previous data indicating the striking maximum of basal, manganese–, fluoride– and forskoline–stimulated AC activity in 12–day–old rats (Ihnatovych *et al.* 2002). Thus, the increase of baclofen– and SKF97541–stimulated G protein activity during the first two weeks of postnatal life, its maximum in 14–15–day–old rats and the subsequent decrease is correlated in time with the maximum of AC activity. The question to what extend the maximum of AC activity observed at PD12 precedes the peak of activity of G proteins can not be decided at the present stage of our experimentation, as AC activity was determined at PD12 and PD18 only, i.e. not in the period between these two age intervals.

6.1.2 Number and affinity of $GABA_B$–R; *direct saturation binding study with antagonist [^{3}H]CGP54626A*

Plasma membrane density of $GABA_B$–R at different age intervals was determined by saturation binding study with specific antagonist [^{3}H]CGP54626A. Data presented in **Fig. 29** indicated clearly that the highest PM density of $GABA_B$–R, estimated as the maximum binding capacity (B_{max}) of [^{3}H]CGP54626A binding sites, was detected in PM samples prepared from 1–day–old rats (2.27±0.08 pmol · mg^{-1}). The further development was reflected in a marked decrease of [^{3}H]CGP54626A binding as the B_{max} values of 1.38±0.05 and 0.93±0.04 pmol · mg^{-1} were determined in PM isolated from 13– and 90–days old rats, respectively. The dissociation constant (K_d) was increased from 11.8 nM (PD1) to 15.3 nM (PD13) and 22.1 nM (PD90), indicating the decreased affinity and qualitative change of $GABA_B$–R binding sites towards this antagonist in the course of rat brain cortex maturation. The decrease in affinity of [^{3}H]CGP54626AA binding (expressed as 1 / K_d), observed together with the decrease in affinity of SKF97541–response of G proteins (**Fig. 27**), suggests a partial agonistic nature of [^{3}H]CGP54626AA interaction with $GABA_B$–R which would be altered in the course of brain cortex ontogenesis.

Fig. 29. Saturation of [^{3}H]CGP54626AA binding sites in PM isolated from 1–, 13– and 90–day–old rats

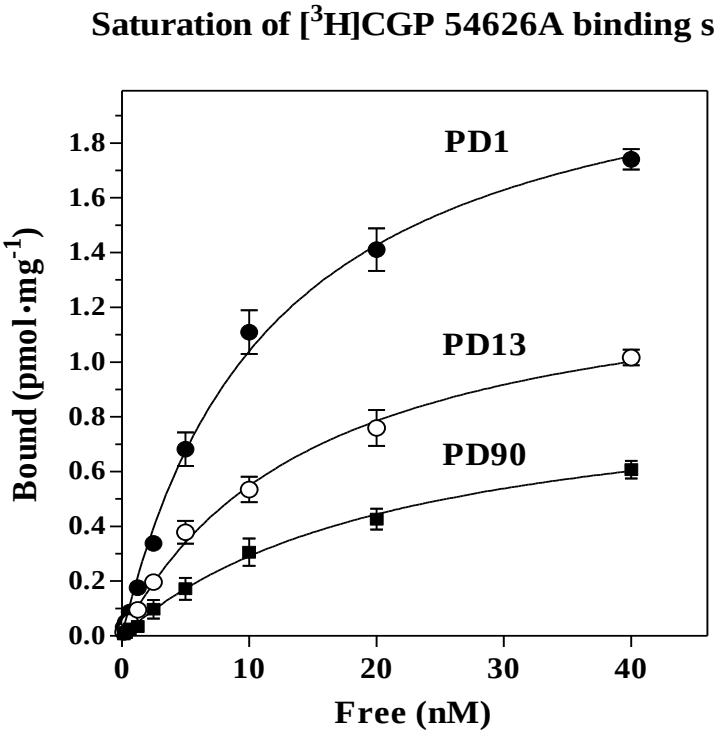

Legend to Fig. 29. Maximum number (B_{max}) and affinity (K_d) of specific [^{3}H]CGP54626AA binding sites was determined in PM isolated in parallel from brain cortex of 1 (●)–, 13 (○)– and 90 (■)–days old rats by direct saturation binding assay as described in Methods. B_{max} (maximum binding capacity) and K_d (dissociation constant) of specific [^{3}H]CGP54626AA binding sites were calculated by fitting the data by 1–site hyperbola by GraphPad *Prism 4* and represent the average ± S.E.M. of 3 experiments. One–way ANOVA followed by Bonferroni's post–hoc comparison test was used for statistical analysis of the difference between B_{max} or K_d values in PM prepared from rats of different ages. **B_{max}** : PD1 versus PD13, $p < 0.01$, **; PD13 versus PD90, $p < 0.001$, ***; PD13 versus PD90, $p < 0.05$, *. **K_d** : PD1 versus PD13, $p > 0.05$, NS; PD13 versus PD90, $p < 0.01$, **; PD13 versus PD90, $p < 0.05$, *.

6.1.3. Ontogenetic development of sodium plus potassium activated, ouabain dependent Na^+/K^+–ATPase (EC 3.6.1.3)

Postnatal development of $GABA_B$–R–G protein coupling and antagonist ligand binding to $GABA_B$–R was substantially different from maturation of the prototypical plasma membrane marker, Na^+/K^+–ATPase (**Fig. 30A, B**). Membrane density of Na, K–ATPase, determined by immunoblotting with specific antibodies oriented against the affinity purified α–subunit of this enzyme, was low around the at birth (PD–1, PD1 and PD2) and further development was reflected in a marked increase of this protein. The major increase occurred between the birth and PD25. Since this age interval, PM content of Na, K –ATPase was not significantly different in PM isolated from 35–, 42– and 90–day–old rats.

The intensity of average immunoblot signal in adult rats (PD90) was 3.5–times higher than around the birth, i.e. in PM samples prepared from foetuses 1–day before the birth or from 1– and 2–days–old animals (PD1 and PD2). This result indicated a marked increase of plasma membrane density of Na,K–ATPase molecules in the course of brain cortex development.

Virtually the same result was obtained when selective inhibitor [^{3}H]ouabain was used for determination of the number of Na^+/K^+–ATPase molecules in PM (**Fig. 30C**). The major increase of [^{3}H]ouabain binding in PM was noticed between the birth and PD25. Since PD25, the binding of this radioligand was not significantly different from the adult animals. [^{3}H]ouabain binding in 90–day–old rats (13.89 pmol.mg^{-1}) was 1.6x higher than in 15–day–old rats (8.64 pmol.mg^{-1}) and 2.6x higher than in fetuses 1 day before the birth (5.44 pmol.mg^{-1}).

Thus, the postnatal development of plasma membrane density of Na^+/K^+–ATPase molecules proceeded in completely different way when compared with maturation of $GABA_B$–R signaling cascade. The highest number of $GABA_B$–R was observed around the birth and further development was reflected in 2.4–fold decrease of $GABA_B$–receptor binding sites for specific antagonist [^{3}H]CGP54626AA while the amount of Na^+/K^+–ATPase molecules was increased ≈3–fold between the birth and adulthood (90–days old rats).

Fig. 30 Plasma membrane density of Na^+/K^+–ATPase determined by immunoblot analysis (A, B) and [^{3}H]ouabain binding (C)

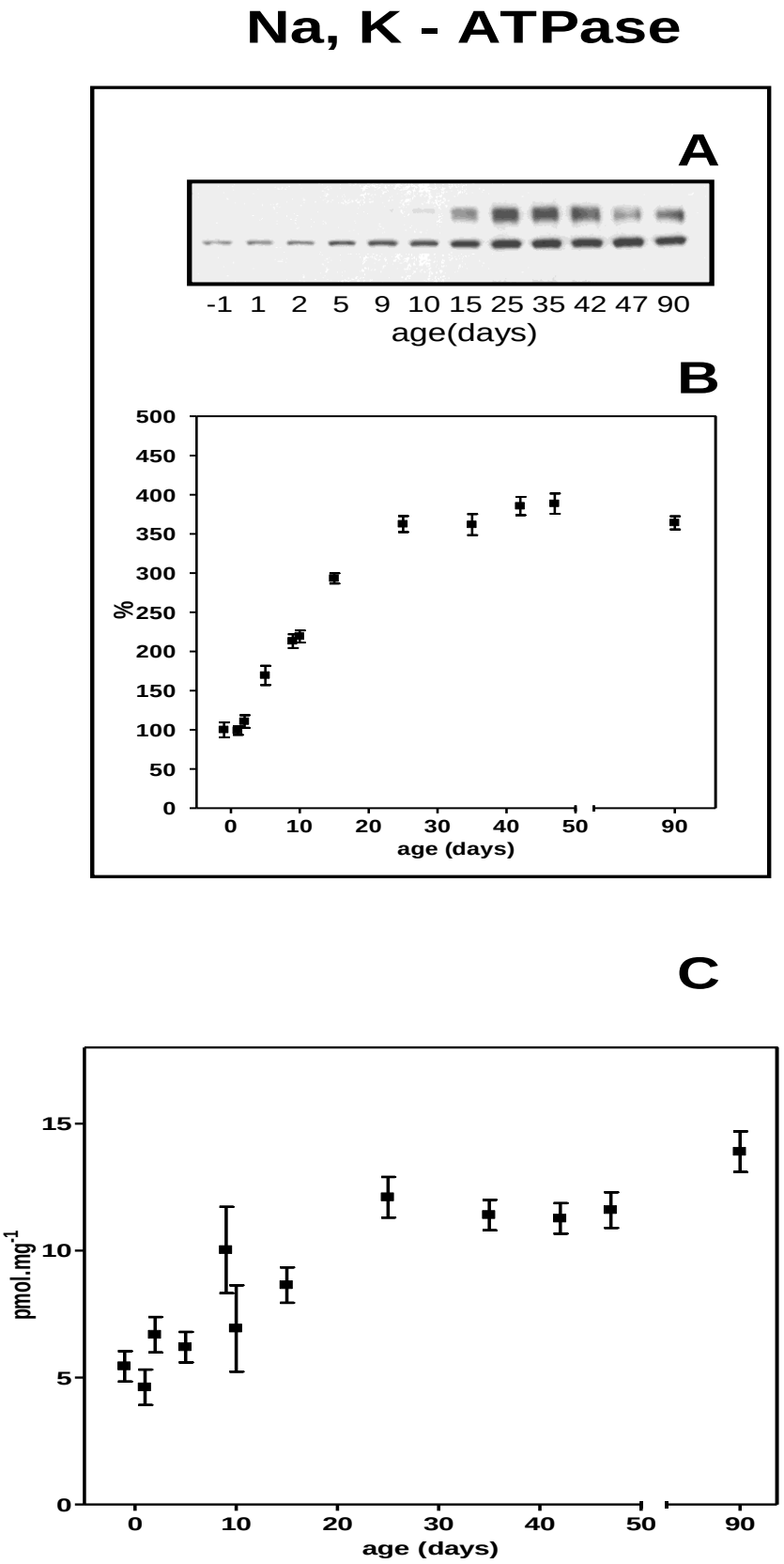

Immunoblot detection of α–subunit of Na^+/K^+–ATPase was performed by polyclonal Ab (Santa Cruz, sc–28800). **(A)** Typical immunoblot. **(B)** Average of 5 immunoblots. The significance of the difference between the immunoblot signal determined in fetuses 1–day before the birth (100%) and signals determined at different ages (PD1, PD2, PD5, PD9, PD10, PD15, PD25, PD35, PD42, PD47, PD90) was analyzed by one–way ANOVA followed by Bonferroni's test using GraphPad Prism 4. Since PD5, the increase of Na^+/K^+–ATPase was highly significant (**, $p < 0.01$). **(C)** [^{3}H]ouabain binding was measured as described in Methods. Data represent the average ± S.E.M. of three experiments performed in triplicates. Significance of the difference between the binding at different age intervals was analyzed by one–way ANOVA followed by Bonferroni's test: fetuses D–1 versus PD15 (*, $p<0.05$), D–1 versus PD25 (**, $p<0.01$), D–1 versus PD90 (**, $p<0.01$), PD15 versus PD25 (*, $p<0.05$), PD15 versus PD90 (**, $p<0.01$), PD25 versus PD90 (NS, $p>0.05$).

6.2. The ontogenetic development of oxidative damage of the brain; *generation of lipofuscin–like pigments (LFP)*

6.2.1. Study of lipofuscin–like pigments in brain tissue homogenates.

The aim of our first study of LFP production in rat brain (Wilhelm at al., 2011) was to get information about free oxygen radical damage proceeding in rat rain cortex before and shortly after the birth. We have also analyzed the whole postnatal period up to the postnatal–day–90 (PD90). Our studies were performed with the tissue homogenates prepared from animals of different ages: *group A*, 7 days before birth; *group B*, 1 day before birth; *group C*, postnatal day 1; *group D*, postnatal day 2; *group E*, postnatal day 5; *group F*, postnatal day 10; *group G*, postnatal day 15; *group H*, postnatal day 25; *group I*, postnatal day 35; *group J*, 90–days–old animals. For a detailed characterization of fluorescent properties of LFP, we used the fluorescence spectroscopy methods comprising the 3–dimensional spectral arrays with synchronous screening of the fluorescence spectra. Furthermore, the total LFP were resolved into several fractions by means of chloroform–metanol 3 : 1 extraction followed by HPLC with fluorescence detection.

We have shown that the brain LFP constitute a complex mixture of very many different chemical compounds (fluorophores) whose composition is changing in the course of brain development, **Figs. 31, 32 and 33).** Our results also indicated that the *highest*

accumulation of oxidative products in the forebrain, when tested by detection of LFP, occurred immediately after the birth, at PD2 and PD5 (**Fig. 32**). This result may be interpreted as indication of the high oxidative damage proceeding in rat brain shortly after the birth.

Fig. 31. Examples of 3D–fluorescence excitation spectra determined in brain chloroform extracts. (A) 7 days before birth, (D) 2 days after the birth, (J) 90 days after the birth

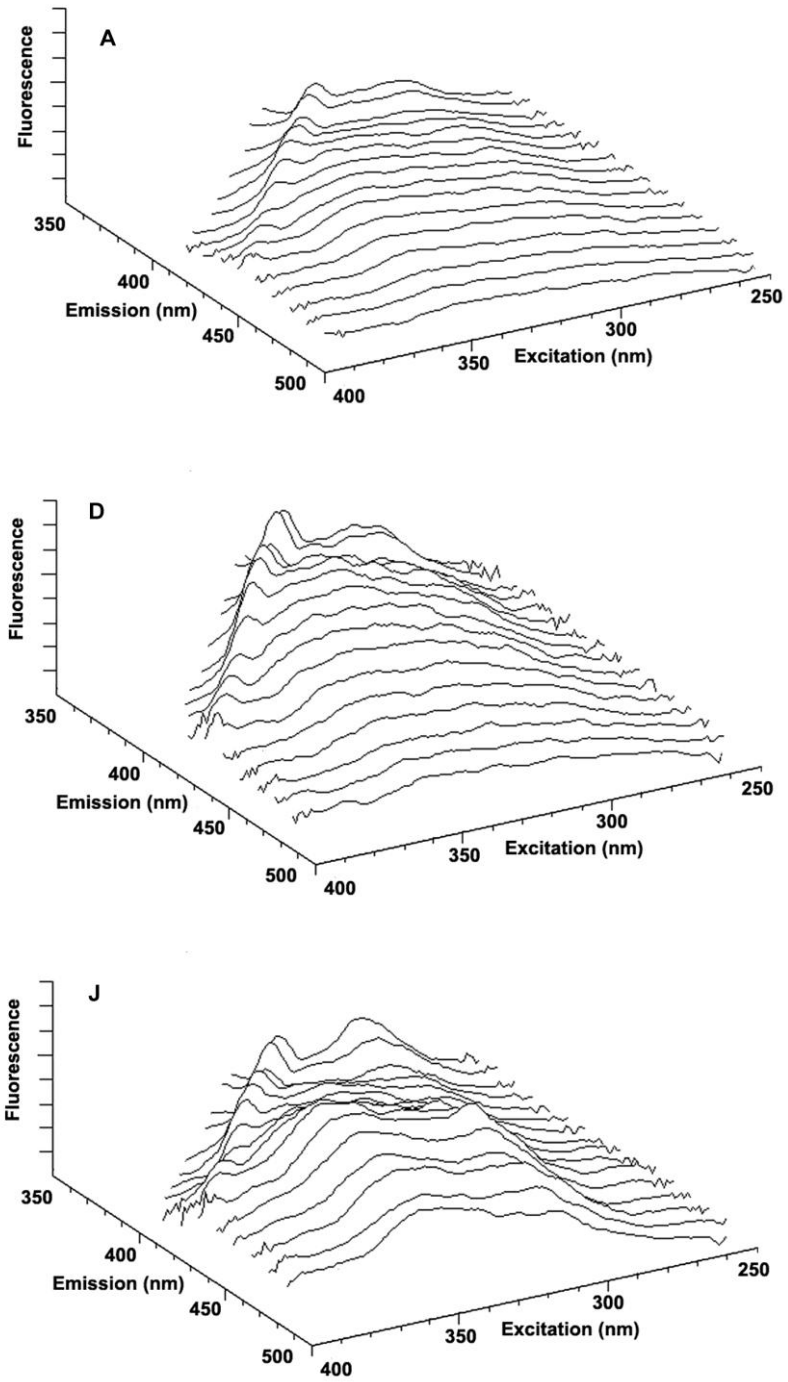

Legend to Fig. 31.

A total of 70 pregnant female Wistar rats were used throughout the experiments. They had free access to water and standard laboratory diet. The offspring's of both sexes were divided into 10 groups. Group **A** (110 fetuses) was sampled 7 days before birth, group **B** (110 fetuses) 1 day before birth, group **C** (50 animals) on postnatal day 1, group **D** (50 animals) on postnatal day 2, group **E** (50 animals) on postnatal day 5, group **F** (50 animals) on postnatal day 10, group **G** (50 animals) on postnatal day 15, group H (30 animals) on postnatal day 25, group **I** (30 animals) on postnatal day 35, and group **J** (20 animals) 3 months after birth.

Fig. 32. Quantitative determination of three major LFP fluorophores found in 3D spectra.

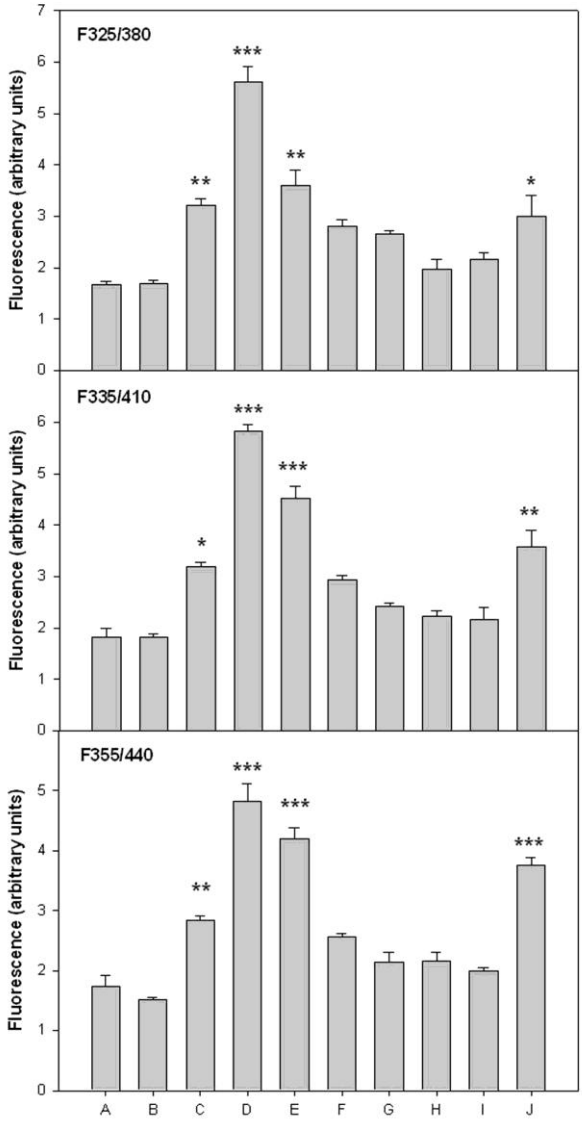

Legend to Fig. 32. Group **A**, 7 days before birth; group **B**, 1 day before birth; group **C**, postnatal day 1; group **D**, postnatal day 2; group **E**, postnatal day 5; group **F**, postnatal day 10; group **G**, postnatal day 15; group **H**, postnatal day 25; group **I,** postnatal day 35; group **J**, 3 months old animals. Statistical significance was related to group A:

* P< 0.05, ** P<0.01, *** P< 0.001.

Fig. 33. Examples of synchronous fluorescence spectra (left–hand panels) and their 2nd derivatives (right–hand panels). (A) 7 days before the birth; (D) postnatal day 2; (E) postnatal day 5; (J) 3 month old animals.

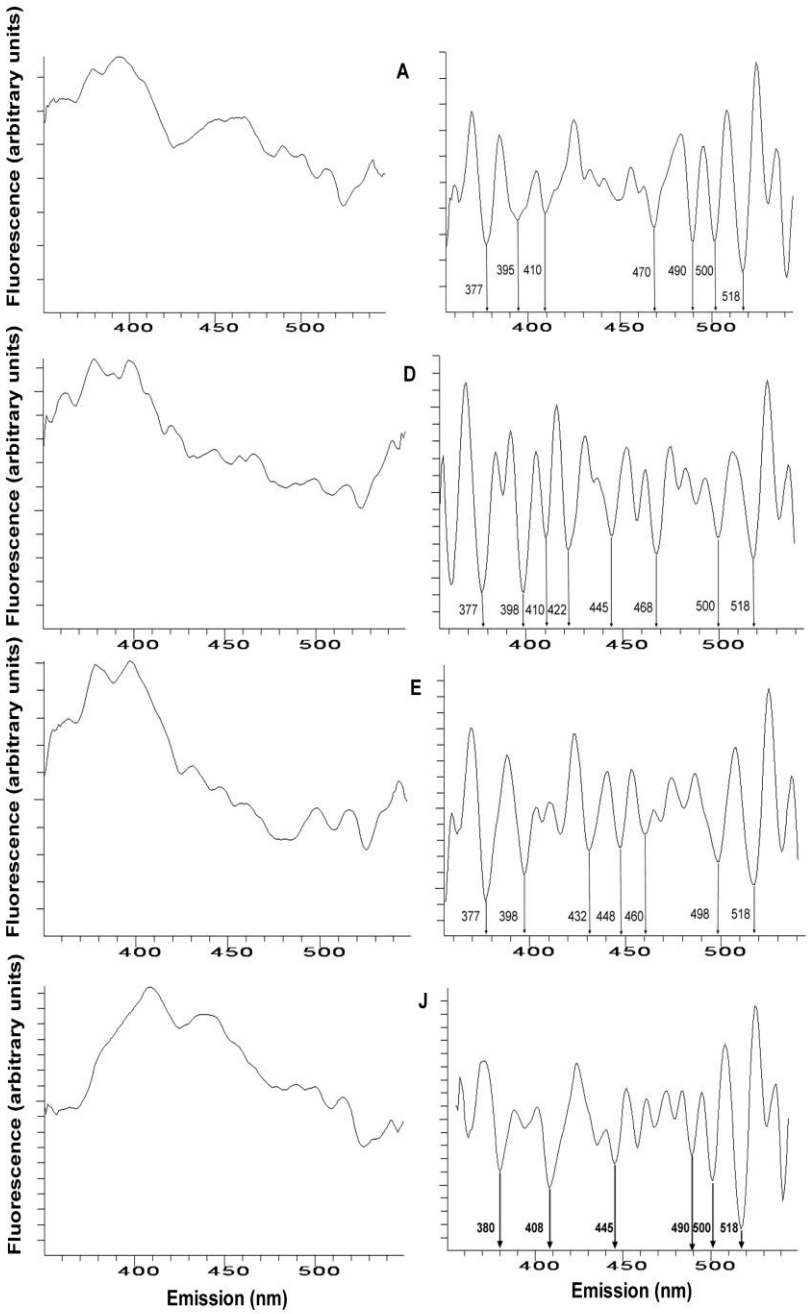

Legend to Fig. 33. Vertical arrows in the 2nd derivatives of the spectra indicate the emission maxima of the resolved fluorophores.

Fig. 34. Examples of the HPLC tracings of fluorophore F355/410 in brain chloroform extracts prepared from of animals of different ages. A) 7 days before birth, D) postnatal day 2, E) postnatal day 5, J) 3 month old animals.

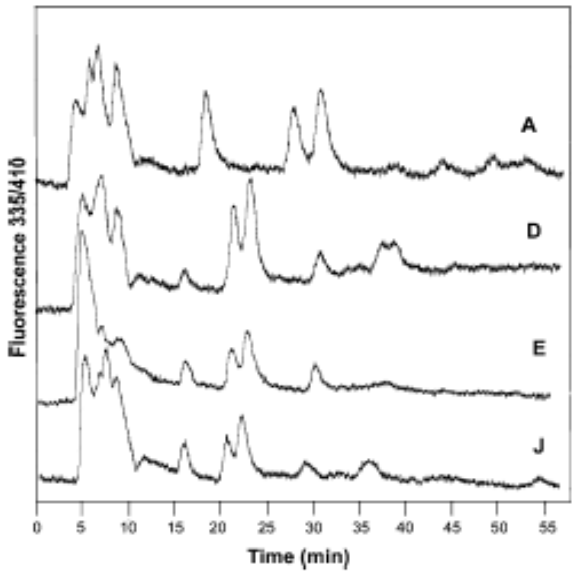

Legend to Fig. 34. Brain chloroform extracts were evaporated under the stream of nitrogen. The evaporated sample was dissolved in approximately 1 ml of running phase used in isocratic HPLC separation. A mixture of acetonitrile–methanol–water (50:10:40, v/v) was used for separation of LFP. A Jasco HPLC instrument equipped with fluorescence detector was set at the excitation and emission maxima of the three major fluorophores. A C18 column (4 x 250 mm) was used for the analysis. Isocratic elution gave optimum separation at 0.2 ml/ml.

6.2.2. Study of lipofuscin–like pigments in subcellular membrane fractions.

The aim of our second study of LFP in the brain (Wilhelm at al., 2014; manuscript in preparation) was to determine the ontogenetic development of LFP production in different subcellular membrane fractions (post–nuclear fraction, mitochondria, miscrosomes, crude plasma membranes, cytosol) and to compare the ontogenetic patterns observed in these membranes with data obtained by analysis of the whole tissue homogenates. The LFP level in fetuses was taken as a reference value corresponding to 100%. The LFP content in different membrane fractions collected at different time intervals of brain development were expressed as percentage of this value. The results are presented in **Fig. 35**.

Fig. 35. LFP levels in brain homogenate and subcellular fractions during development. Foetal homogenate level was taken as 100%. Statistical significance: * P< 0.05, ** P< 0.01, *** P< 0.001

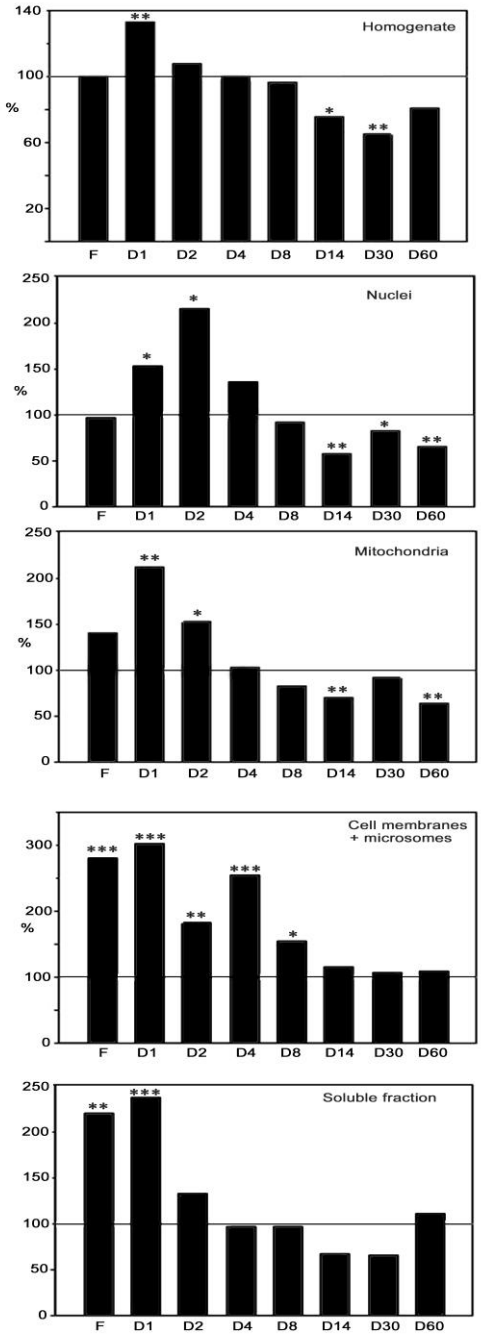

Judged from an overall point of view, the results were in full accordance with our previous study of tissue homogenates (Wilhelm et. al. 2011). However, analysis of LFP in 5 subcellular fractions has also brought some unexpected observations. First, it was found that

the high LFP levels were detected already in the foetal brain in ***soluble*** *fraction* (220%) and in ***crude*** *plasma membrane* fraction (CM) representing the mixture of vesicles derived from plasma membrane and microsomes (282%), whilst the LFP level in other fractions was not increased. The soluble fraction was still increased on PD1 (236%) and then returned to the control level and stayed unchanged throughout the whole time scale of experiment. *In the soluble fraction, we might expect lipoproteins containing the oxidized lipids with characteristics of LFP. Apparently, these lipoproteins are quickly decomposed after birth.*

In "crude plasma membranes" containing the small vesicular fragments derived from plasma membrane, endoplasmic reticulum and Golgi, the increased LFP level stayed until PD8. This was a unique observation when compared with other membrane types, as the LFP levels in other fractions were increased only up to PD2. Detection of this prolonged LFP increase in CM might indicate a change of this cell structure proceeding well beyond the birth.

LFPs in mitochondria were increased on PD1 (212%) and PD2 (152%). Afterwards, they returned to normal levels and were further decreased on PD14 (70%) and PD60 (64%). Thus, and as already noticed in our previous analysis of brain tissue homogenates (Wilhelm *et al.*, 2011), the increase of LFPs immediately after birth (PD1 and PD2) may be interpreted as an indication of an intensive aerobic metabolism accompanied by free radical production and consequent damage of membrane structures. The decrease of mitochondrial and nuclear LFP in samples collected from older rats (PD8–PD14) might be an indication of the high mitochondrial turnover proceeding in this period. The newly formed mitochondria, containing the low amount of LFP appear and dilute the concentration of these substances in the whole MITO fraction.

In nuclei, LFP was increased at PD1 (152%) and PD2 (215%). This increase was followed by decrease below the control value observed at PD14 (58%), PD30 (82%) and PD60 (65%). Nuclear membrane contains the electron transfer system analogical to that of endoplasmic reticulum which can be the source of free radicals and LFP. In similarity to mitochondria, the decrease of LFP level at PD8 and PD14 might be caused by an intensive cell proliferation, when the newly formed nuclei, containing less LFP, are merged into the overall pool detected in nuclear fraction.

7. DISCUSSION

7.1. The ontogenetic development of $GABA_B$–receptor signaling cascade

The highest maximum response (efficacy) of baclofen– and SKF97541–stimulated [^{35}S]GTPγS binding was measured at postnatal day 14 and 15 and afterward, the ability of these two $GABA_B$–R agonists to increase activity of G proteins decreased continuously towards the adult level (**Fig. 28**). Accordingly, the peak value of [^{3}H]GABA binding was detected at PD14 in rat brain cortical slices by quantitative autoradiography and this high level of [^{3}H]GABA binding subsequently declined to the adult level (Turgeon and Albin 1994).

The existence of the maximum of coupling efficacy between $GABA_B$–R and G proteins, which was observed in "opening of eyes period" at PD14 and PD15, may be interpreted as an overlap between the two opposite regulatory effects: the stimulation which is stronger at age intervals before this period and inhibition, which prevails in older rats.

Data presented in my work (**Figs 27 and 28**) indicated a noticeable extent of compatibility of our present results with experimental data obtained before by functional assays of adenylyl cyclase (AC) activity in the presence or absence of $GABA_B$–R agonists, (Ihnatovych *et al.* 2002). Maximum activation of baclofen– and SKF97541–stimulated [^{35}S]GTPγS binding at PD14 and PD15 coincided with the developmental profile of AC activity. The maximum of agonist–stimulated G protein activity (**Fig. 28**) as well as basal, fluoride–, GTP– and forskoline–stimulated AC was found in the same period of brain development, i.e. between PD10 and PD15. However, a marked difference between the two sets of data was noticed as well. Maturation of functional coupling of $GABA_B$–R with G proteins preceded maturation of AC system because AC activity was very low at birth while both baclofen and SKF97541 exhibited significant efficacy already at PD2 (**Fig. 27**).

The highest plasma membrane density of $GABA_B$–R determined by saturation binding study with specific antagonist [^{3}H]CGP54626A was observed shortly after the birth (at PD1) and subsequently decreased in 13– and 90–day–old rats (**Fig. 29**). It may be therefore suggested that the physiological significance of the high receptor number and significant efficacy of coupling of $GABA_B$–R with G proteins shortly after the birth (at PD1 and PD2) is related to some other effectors but AC–cAMP system. Ionic channels regulated by the free $G_o\alpha$ and Gβ subunits represent the primary candidates for such effectors (Newberry *et al.* 1984a,b, Gähwiler *et al.* 1985, Bormann 1988, Bowery *et al.* 1989).

Comparison of EC_{50} values of baclofen–stimulated [^{35}S]GTPγS binding indicated no

significant difference in PM samples isolated from 2–, 14– and 90–day–old rats. Contrarily, the EC_{50} values of G protein stimulation by SKF97541 were clearly increased from the birth to adulthood (**Table 2**). This result suggests a developmental decrease in affinity of $GABA_B$–R response for the latter agonist and it is compatible with electrophysiological studies of brain function indicating the differences in sensitivity of $GABA_B$–R to different agonists (Bernasconi *et al.* 1992, Hosford *et al.* 1992, Lin *et al.* 1992, Marescaux *et al.* 1992). Furthermore, epileptological studies of brain function indicated that anticonvulsant action of baclofen was unchanged during postnatal period (Kubová *et al.* 1996); simultaneously, the ontogenetic profile of anticonvulsant action of SKF97541 was not identical with that of baclofen (Mareš 2008). Thus, the time–span between PD12 and PD18 represented the most critical period from this point of view.

7.2. The ontogenetic development of Na^+/K^+–ATPase

The ontogenetic development of Na^+/K^+–ATPase[1] was completely different from that obtained in studies of $GABA_B$–R–signaling cascade (**Fig. 30**). Membrane density of Na^+/K^+–ATPase molecules, determined by immunodetection of the α–subunit of this enzyme, was increased 3.5–fold in PM isolated from adult, 90–days–old animals when compared with PM isolated from foetuses 1–day before the birth. The similar increase (2.6–fold) was detected in [^{3}H]ouabain binding studies. Thus, the overall maturation of the brain cortex, which was in our studies monitored by a developmental study of prototypical plasma membrane marker Na^+/K^+–ATPase, proceeds between the birth and the adulthood. *The increase of Na^+/K^+–ATPase molecules in PM proceeds in striking contrast to ontogenetic change of number of $GABA_B$–R which is in this period decreased 2.4–fold.*

1, Sodium plus potassium activated, magnesium dependent adenosinetriphosphatase (EC 3.6.1.3) represents a crucial enzyme for preservation of the continuous neuronal activity as it is catalyzing the active, ATP–dependent transport of sodium and potassium cations across plasma membrane. The 3 sodium cations are transported from the cell interior to the extracellular space in exchange of 2 potassium cations which pumped into the cell. The single cycle of Na^+/K^+–ATPase catalytical activity results in transfer of one positive charge out from the cell.

7.3. Postnatal ontogenesis of oxidative damage of the brain

LFP were used as a tool to assess the extent of ROS formation in brain cortex of rats during early postnatal development. The highest accumulation of these compounds was found immediately after birth and the level of these compounds was subsequently falling down to the three months of age, which is believed to represent a period when ageing starts in rats.. Although the increased free radical production shortly after the birth is to be expected because

of the rapid increase in oxygen concentration in the brain of new born animals and absence of fully functional mitochondria at this age interval, the detection of the final products of peroxidative damage (LFP) has not been analyzed before in the detailed manner, i.e. on the day by day basis.

When considering the up–to–date literature data from the broader scope of view, ROS–mediated oxidative damage of DNA was demonstrated in rat brain, liver, kidney and skin during the first few hours after the birth (Randerath *et al.* 1997). Lungs were not affected. The brain lesions were considered as substantial and were similar to or even greater than the lesions in senescent, 24–month old rats. The concept of oxidative stress generated after the normal birth was also supported by the finding of a pronounced neonatal decreases in the hepatic GSH/GSSG ratio in rats (Sastre *et al.* 1994, Pellardo *et al.* 1991). Also the product of membrane lipid peroxidation, malonaldehyde, exhibited a transient rise after the birth in rat liver and kidney (Gunther *et al.* 1993). The tissue specificity of manifestation of oxidative damage may be easily explained by differences in balance between the intensity of oxidative metabolism and antioxidant protection existing in a given tissue. *Up to now, no such studies were undertaken in the brain.*

Our results indicated a transient accumulation of LFP in neonatal rat brain: LFP, were increased on the day 1 after the birth (PD1), reached the maximum level on the day 2 (PD2) and decreased to the prenatal level already on postnatal day 5 (PD5) (**Fig. 35;** Wilhelm *et al.*, 2011). A new rise of LFP production was found in 3–month–old animals (PD90). As already mentioned, results presented in our work correlated with the demonstration of oxidative damage of DNA (Randerath *et al.* 1997). The fact that all fluorophores had similar ontogenetic pattern supported the physiological relevance of our results as this finding may be interpreted to mean that LFPs are generated by the same process or are localized in the same subcellular membrane compartment.

Wihelm and Ostadalova (2012) investigated the ontogenetic profile of generation of LFPs in neonatal rat heart and found that the observed changes were similar to those obtained in frontal brain cortex. Mitochondria are the first suspected source for ROS production when considering the brain. This interpretation is supported by the previously published data (Svoboda and Lodin 1972, 1973) indicating the low activity of α–glycerolphosphate and succinate dehydrogenases in immature brain: the activity of both enzymes was very low before and shortly after the birth. The temporary activation of α–GPDH (maximum at PD4–8) faded away before PD10. The major increase of these mitochondrial enzyme activities proceeded between PD10 and PD20 and was not completed before PD30. Thus, the presence

of immature respiratory chain of mitochondria in brain cortex of newborn animals may explain the increase of LFP immediately after the birth.

Besides mitochondria, the high LFP production in brain of new–born animals may be also interpreted as an indication for the presence of the high amount of microglia phagocytosing the apoptosed brain cells. In mice, the maximum phagocytosis associated with significant ROS production, occurred on postnatal day 3 (Marı´n–Teva *et al.* 2004). This time period corresponds well with the maximum of LFP production measured in our experiments: between PD1 and PD5. Thus, at least some part of the early production of LFP in the brain may be cell specific and functionally related to activity of microglia. Transition from hypoxia to normoxia and increase of oxygen partial pressure was also shown to increase production of free radicals (Wilhelm *et al.* 1999). It is therefore possible that the hypoxic/ normoxic transition proceeding in the newly born rats contributes to the process of LFP formation.

The pattern of 3D–spectral arrays, synchronous spectra and their derivatives (all together) indicate the presence of many fluorescent species belonging to the category of LFP. Each of these spectrally characterized species can be further resolved into several chromatographically distinct compounds (**Fig. 31, 32, 33**; Wilhelm *et al.*, 2011). Taken together, LFP may originate from hundreds, may be thousands, of unknown compounds which are functionally related to or produced by the brain oxidative damage after the birth. We assume that a formation of LFPs in 3–month–old animals, when aging starts in rats, is based primarily on ROS generated by mitochondria (Kann and Kovacs, 2007). Since that time, these products only accumulate (Brunk and Terman, 2002).

8. CONCLUSIONS

1) The significant intrinsic efficacy of $GABA_B$–receptors was detected in rat brain cortex already shortly after the birth: at postnatal day 1 and 2. Subsequently, both baclofen and SKF97541–stimulated G protein activity, measured as the high–affinity [^{35}S]GTPγS binding, was increased. The highest level of agonist–stimulated [^{35}S]GTPγS binding was detected at postnatal days 14 and 15. In older rats, the efficacy, i.e. the maximum response of baclofen– and SKF97541–stimulated [^{35}S]GTPγS binding was continuously decreased so, that the level in adult, 90–days old rats was not different from that in newborn animals. This profile of ontogenetic development of functional coupling between $GABA_B$–R and the cognate G proteins was similar to the maturation of adenylyl cyclase activity (Ihnatovych *et al.* 2002).

The existence of maximum of coupling efficacy between $GABA_B$–R and G proteins, observed in "opening of eyes period" at PD14 and PD15, may be interpreted as an overlap between the two opposing / counter–acting regulatory effects: stimulatory which is stronger at age intervals before this period and inhibitory effect, which prevails in older rats.

2) The potency of G protein response to baclofen stimulation, characterized by EC_{50} values, was also high at birth but unchanged by further development. The individual variance among different agonists was observed in this respect as the potency of SKF97541 response was decreased when compared in 2– and 90–days old rats.

3) Plasma membrane density of $GABA_B$–R, determined by saturation binding assay as maximum binding capacity (B_{max}) of specific antagonist [^{3}H]CGP54626A, was highest in 1–day old animals. The further maturation of rat brain cortex was reflected in decrease of PM density of $GABA_B$–R observed in 13– and 90–days old animals.

4) The ontogenetic development of Na^+/K^+–ATPase was completely different from that obtained in studies of $GABA_B$–R–signaling cascade. In contrast to the number of $GABA_B$–R, plasma membrane density of Na^+/K^+–ATPase molecules was increased ≈ 3–fold when compared in new born (1–day–old) and 90–days–old rats.

5) The high level of lipofuscin like pigments (LFP) was generated in rat brain cortex during the first 5 days of postnatal life. Maximum level of LFP was detected on the postnatal day 2. Starting from the postnatal day 10, LFP concentration returned down to the prenatal level. A new rise in LFP concentration was observed in 90–days old animals. This second increase of LFP may indicate the beginning of the aging process in rat brain cortex.

9. REFERENCES

AHNERT–HILGER, G., SCHAFER, T., SPICHER, K., GRUND, CH., SCHULZ, G. and WIEDENMANN, B. (1993) Detection of G protein heterotrimers on large dense core and small synaptic vesicles of neuroendocrine and neuronal cells. *Eur. J. Cell Biol. 65*, 26–38

ALLEN, J.A., HALVERSON–TAMBOLI, J.A. and RASENICK, M.M. (2007) Lipid raft microdomains and neutrotransmitter signalling. *Neuroscience 8*, 128–140ASANO, T. and OGASAWARA, N. (1986) Uncoupling of gamma–aminobutyric acid B receptors from GTP–binding proteins by N–ethylmaleimide: effect of N–ethylmaleimide on purified GTP–binding proteins. *Mol. Pharmacol. 29*, 244–249

ASANO, T., UI, M. and OGASAWARA, N. (1985) Prevention of the agonist binding to gamma–aminobutyric acid B receptors by guanine nucleotides and islet–activating protein, pertussis toxin, in bovine cerebral cortex. Possible coupling of the toxin–sensitive GTP–binding proteins to receptors. *J. Biol. Chem. 260*, 12653–12658

BABIYCHUK, E.R. and DRAEGER, A. (2006) Biochemical characterisation of detergent–resistant membranes: a systematic approach. *Biochem. J.*, 407–416

BARRAL, J., TORO, S., GALARRAGA, E. *et al.* (2000). GABAergic presynaptic inhibition of rat neostriatal afferents is mediated by Q–type Ca(2^+) channels. *Neuroscience Letters 283*, 33–36

BERNASCONI, R., LAUBER, J., MARESCAUX, C., VERGNES, M., MARTIN, P., RUBIO, V., LEONHARDT, T., REYMANN, N. and BITTIGER, H. (1992) Experimental absence seizures: potential role of gamma–hydroxybutyric acid and $GABA_B$ receptors. *J. Neural. Transm. 35*, 155–177

BIRNBAUMER, L. (1990) Transduction of receptor signal into modulation of effector activity by G proteins. *FASEB J. 4*, 3178–3188

BIRNBAUMER, L., ABRAMOWITZ, J., and BROWN, A.M. (1990) Receptor–effector coupling by G proteins. *Biochim. Biophys. Acta 1031*, 163–224

BLOCH–TARDY, M., ROLLAND, B. and GONNARD, P. (1971) Ontogenetic evolution of the molecular forms of 4–aminobutyrate 2–oxoglutarate aminotransferase in rat brain and liver. *J. of Neurochem. 18*, 1779–1781

BOCKAERT J. and PIN, J.P. (1999) Molecular tinkering of G protein–coupled receptors: an evolutionary success. *The EMBO Journal 18*, 1723–1729

BORMANN, J. (1988) Electrophysiology of $GABA_A$ and $GABA_B$ receptor subtypes. *Trends Neurosci. 11*, 112–116

BORMANN, J. and FEIGENSPAN, A. (1995) $GABA_C$ receptors. *TiNS 18*, 515–519

BOUROVA, L., KOSTRNOVA, A., HEJNOVA, L., MORAVCOVA, Z., MOON, H.E., NOVOTNY, J., MILLIGAN, G. and SVOBODA, P. (2003). Delta–opioid receptors exhibit high efficiency when activating trimeric G proteins in membrane domains. *J. Neurochem. 85*, 34–49

BOUROVA, L., STOHR, J., LISY, V., RUDAJEV, V., NOVOTNY, J. and SVOBODA, P. (2009) Isolation of plasma membrane compartments from rat brain cortex; detection of agonist–stimulated G protein activity. *Med. Sci. Monit. 15*, 111–122

BOUROVA, L., VOSAHLIKOVA, M., KAGAN, D., DLOUHA, K., NOVOTNY, J. and SVOBODA, P. (2010) Long–term adaptation to high doses of morphine causes desensitization of mu–OR– and delta–OR–stimulated G protein response in forebrain cortex but does not decrease the amount of G protein alpha subunits. *Med. Sci. Monit. 16 (8)*, 260–270

BOWERY, N. G., HILL, D. R. and HUDSON, A. L. (1983) Characterization of $GABA_B$ receptor binding sites on rat whole brain synaptosomes. *Br. J. Pharmacol.* 78, 191–206

BOWERY, N. G., PRICE, G. W., HUDSON, A. L., HILL, D. R. and WILKIN, G. P., TURNBULL, M. J. (1984) GABA receptor multiplicity. *Neuropharmacology 23*, 219–231, 1984

BOWERY, N. G., HILL, D. R. and HUDSON, A. L. (1985) [^{3}H](–)Baclofen: an improved ligand for $GABA_B$ sites. *Neuropharmacology 24*, 207–210

BOWERY, N. G., HUDSON, A. L. and PRICE, G. W. (1987) $GABA_A$ and $GABA_B$ receptor site distribution in the rat central nervous system. *Neuroscience 20*, 365–383

BOWERY, N. G. (1989) $GABA_B$ receptors and their significance in mammalian pharmacology. *TiPS 10*, 401–407

BOWERY, N.G., MAGUIRE, J.J. and PRATT, G.D. (1991) Aspects of molecular pharmacology of GABA receptors. *Semin. Neurosci. 3*, 241–249

BOWERY, N. G. (1993) $GABA_B$ receptor pharmacology. *Ann. Rev. Pharmacol. Toxicol. 33*, 109–147

BROWN, D.A. and LONDON, E. (2000) Structure and function of sphingolipid– and cholesterol–rich membrane rafts. *J. Biol. Chem. 275*, 17221–17224

BRUNK, U.T. and TERMAN, A. (2002) Lipofuscin: mechanisms of age–related accumulation and influence on cell function. *Free Radic Biol Med 33*, 611–619

BUSSIERES, N. and EL MANIRA, A. (1999) $GABA_B$ receptor activation inhibits N–and P/Q–type calcium channels in cultured lamprey sensory neurons. *Brain Research 847*, 175–185

CAMPBELL, N. A. and REECE, J. B. (2005) *Biology*, Pearson–Benjamin Cummings, 7th edition

CHANCE, B., SIES., H., CHEN, G., and van den POL, A. N. (1998). Presynaptic GABAB autoreceptor modulation of P/Qtype calcium channels and GABA release in rat suprachiasmatic nucleus neurons. *Journal of Neuroscience 18*, 1913–1922

CHEN, S. D., YANG, D. I., LIN, T. K., SHAW, F. Z., LIOU, C. W. and CHUANG, Y. C. (2011) Roles of oxidative stress, apoptosis, PGC–1 and mitochondrial biogenesis in cerebral ischemia. *Int. J. of Mol. Sci. 12 (10),* 7199–7215

COUVE, A., THOMAS, P., CALVER, A. R. , HIRST, W. D., PANGALOS , M. N., WALSH, F. S., SMART , T. G. and MOSS, S. J. (2002) Cyclic AMP–dependent protein kinase phosphorylation facilitates GABA(B) receptor–effector coupling. *Nat. Neurosci. 5,* 415–424

DAVLETOV, B. A., MEUNIER, F. A., ASHTON, A. C., MATSUSHITA, H., HIRST, W. D. *et al.* (1998) Vesicle exocytosis stimulated by alpha–latrotoxin is mediated by latrophilin and requires both external and stored Ca^{2+}. *EMBO J. 17 (14),* 3909–3920

DE PIERRE, J.W. and KARNOVSKY, M.L. (1973) Plasma membranes from mammalian cells. A review of methods fro their characterisation and isolation. *J. Cell Biol. 56*, 275–303

DE ROBERTIS, E., DE IRALDI, A.P., DE LORES ARNAIZ, G.R. and SALGANICOFF, L. (1962a) Isolation and subcellular distribution of acetylcholine and acetylcholine esterase. *J. Neurochem. 9*, 23–35

DE ROBERTIS, E., DE LORES ARNAIZ, G.R. and DE IRALDI, A.P. (1962b) Isolation of synaptic vesicles from the rat brain. *Nature (Lond.) 194*, 794–795

DLOUHA, K., KAGAN, D., ROUBALOVA, L., UJCIKOVA, H. and SVOBODA, P. (2013) Plasma membrane density of GABA(B)–R1a, GABA(B)–R1b, GABA–R2 and trimeric G proteins in the course of postnatal development of rat brain cortex. *Physiol. Res. 62 (5)*, 547–559

DOLE, M. (1965) Thenatural history of oxygen. *Journal of General Physiology 49 (1),* 5–27

DOLPHIN, A.C. (1990) G protein modulation of calcium currents in neurons. *Ann. Rev. Physiol. 52*, 243–255

DOLPHIN, A.C. (1991) Regulation of calcium channel activity by GTP binding proteins and secondary messengers. *Biochim. Biophys. Acta 1091*, 68–80

DUNKLEY, P. R., JARVIE, P. E., HEATH, J. W., KIDD, G. J. and ROSTAS, J. A.

(1986) A rapid method for isolation of synaptosomes on Percoll gradients. *Brain Res. 372*, 115–129

FERNANDEZ–ALACID, L., AGUADO, C., CIRUELA, F. *et al.* (2009). Subcellular compartment–specific molecular diversity of pre–and post–synaptic GABA–activated GIRK channels in Purkinje cells. *Journal of Neurochemistry 110*, 1363–1376.

FISHER, T.E., TUCHEK, J.M. and JOHNSON, D.D. (1986) A comparison of methods for removal of endogenous GABA from brain membranes prepared for binding assays. *Neurochem. Res. 11*, 1–8

GÄHWILER B. H. and BROWN, D.A. (1985) $GABA_B$–receptor–activated K^+ current in voltage–clamped CA3 pyramidal cells in hippocampal cultures. *Proc. Natl. Acad. Sci. U S A 82*, 1558–1562

GILMAN, A.G. (1987) G proteins: transducers of receptor–generated signals. *Ann. Rev. Biochem. 56*, 615–649

GOLDSTEIN, B.D. and MCDONAGH, E.M. (1976) Spectrofluorescent detec–tion of in vivo red cell lipid peroxidation in patients treated with diaminodiphenylsulfone. *J. Clin. Investig. 57*, 1302–1307

GRAHAM, J. (2002) Fractionation of Golgi, endoplasmic reticulum, and plasma membrane from cultured cells in a preformed continuous iodixanol gradient. *The Sci World 2*, 1435–1439

GRAHAM, J. (2002) Homogenization of mammalian cultured cells. *The Sci. World 2*, 1630–1633

GRAHAM, J. (2002) OptiPrep^{tm} density gradient solutions for mammalian organelles. *The Sci. World 2*, 1440–1443

GRAHAM, J. (2002) Peparation of preformed iodixanol gradients. *The Sci. World 2*, 1351–1355

GRAHAM, J. (2002) Preparation of crude subcellular fractions by differential centrifugation. *The Sci. World 2*, 1638–1642

GRAHAM, J. (2002) Purification of lipid rafts from cultured cells. *The Sci. World 2*, 1662–1666

GRAHAM, J. (2002) Rapid purification of nuclei from animal and plant tissues and cultured cells. *The Sci. World 2*, 1551–1554

GRAHAM, J. (2002) Separation of membrane vesicles and cytosol from cultured cells and bacteria in a preformed discontinuous gradient. *The Sci. World 2*, 1555–1559

GRAVE, G. D., KENNEDY, C. and SOKOLOFF, L. (1971) Impairment of growth and

development of the rat brain by xypoxia at atmospheric pressure. *J. of Neurochem. 19*, 187–194

GROSSFIELD, R.M and SHOOTER, E. M. (1971) A study of the changes in protein composition of mouse brain during ontogenetic development. *J. of Neurochem. 18*, 2265–2277

GUGLIELMOTTO, M., TAMAGNO, E. and DANNI, O. (2009) Oxidative stress and hypoxia contribute to Alzheimer's disease pathogenesis: two sides of the same coin. *The Scientific World Journal 9 (1)*, 781–791

GUNTHER, T., HOLLRIEGL, V. and VORMANN, J. (1993) Perinatal development of iron and antioxidant defense systems. *J. Trace Elem. Electrolytes Health Dis*. *7*, 47–52

GUROFF, G. and Brodsky, M. (1971) Enzymes of nucleic acid metabolism in the brains of young and andult rats. *J. of Neorochem. 18*, 2077–2084

HELMREICH, J. M. and HOFMANN, K.– P. (1996) Structure and function of proteins in G protein coupled signal transfer. *Biochim. Biophys. Acta 1286*, 285–322

HILL, D. R. (1985) $GABA_B$ receptor modulation of adenylate cyclase activity in brain slices. *Br. J. Pharmacol. 84*, 249–257

HILL, D. R. and BOWERY, N. G. (1981) ^3H–Baclofen and ^3H–GABA bind to bicuculine–insensitive $GABA_B$ sites in rat brain. *Nature 290*, 149–152

HILL, D. R., BOWERY, N. G. and HUDSON, A. L. (1984) Inhibition of $GABA_B$ receptor binding by guanyl nucleotides. *J. Neurochem. 42*, 652–657

HOLLINGSWORTH, E.B., MCNEAL, E.T., BURTON, J.L., WILLIAMS, R.J., DALY, J.W. and CREVELING, C.R. (1985) Biochemical characterization of a filtered synaptoneurosome preparation from guinea pig cerebral cortex: cyclic adenosine 3':5'–monophosphate–generating systems, receptors and enzymes. *J. Neurosci. 5*, 2240–2253

HOLTER H. and MOLTER K. M. (1958) A substance for aqueous density gradients. *Exp. Cell Res. 15*, 631–632

HOLTER, H. and MOLTER, K. M. (1958) A substance for aqueous density gradients. *Exp. Cell Res. 15*, 631–632

HOSFORD, D. A., CLARK, S., CAO, Z., WILSON, W. A. jr, LIN, F. H., MORRISETT, R. A. and HUIN, A. (1992) The role of $GABA_B$ receptor activation in absence seizures of lethargic (lh/lh) mice. *Science 257*, 398–401

JACOBSON K. and DIETRICH, C. (1999) Looking at lipid rafts? *Cell biology 9*, 87–91

JAHANGEER, S. and RODBELL, M. (1993) The disaggregation theory of signal transmission revisited: further evidence that G proteins are multimeric and disaggregate to

monomers when activated. *Proc. Nat. Acad. Sci. U S A 90*, 8782–8786

JAHANGEER, S. and RODBELL, M. (1993) The disaggregation theory of signal transmission revisited: further evidence that G proteins are multimeric and disaggregate to monomers when activated. *Proc. Nat. Acad. Sci. U S A 90*, 8782–8786

KAGAN, D., DLOUHA, K., ROUBALOVA, L. and SVOBODA, P. (2012) Ontogenetic development of GABA(B)–receptor signaling cascade in plasma membranes isolated from rat brain cortex; the number of GABA(B)–receptors is high already shortly after the birth. *Physiol. Res. 61 (6)*, 629–635

KANN, O. and KOVA´CS, R. (2007) Mitochondria and neuronal activity. *Am. J. Physiol. Cell Physiol 292*, C641–C657

KATADA, T. and UI, M. (1982a) ADP ribosylation of the specific membrane protein of C6 cells by islet–activating protein associated with modification of adenylate cyclase activity. *J. Biol. Chem. 257*, 7210–7216

KATADA, T. and UI, M. (1982b) Direct modification of the membrane adenylate cyclase system by islet–activating protein due to ADP–ribosylation of a membrane protein. *Proc Natl Acad Sci U S A 79*, 3129–3133

KAZIRO, Y., YTOH, H., KOZASA, M., NAKAFUKU, M. and SATOH, T. (1991) Structure and function of signal–transducing GTP–binding proteins. *Ann. Rev. Biochem. 60*, 349–400

KAZIRO, Y., YTOH, H., KOZASA, M., NAKAFUKU, M. and SATOH, T. (1991) Structure and function of signal–transducing GTP–binding proteins. *Ann. Rev. Biochem. 60*, 349–400

KERR, D. I. B. and ONG J. (1995) $GABA_B$ receptors. *Pharmac. Ther. 67*, 187–246

KRASNOPEROV, V. G., BITTNER, M. A., BEAVIS, R., KUANG, Y., SALNIKOW, K. V. *et al.* (1997) α–Latrotoxin stimulates exocytosis by the interaction with a neuronal G protein–coupled receptor. *Neuron 18 (6)*, 925–937

KUBOVÁ, H., HAUGVICOVÁ, R. and MAREŠ, P. (1996) Moderate anticonvulsant action of baclofen does not change during development. *Biol. Neonate 69*, 405–412

LADERA, C., DEL CARMEN GODINO, M., JOSE CABANERO, M. *et al.* (2008). Pre–synaptic GABA receptors inhibit glutamate release through GIRK channels in rat cerebral cortex. *Journal of Neurochemistry 107*, 1506–1517

LADURON, P.M. (1984) Axonal transport of receptors: coexistence with neurotransmitter and recycling. *Biochemical Pharmacology 33*, 897–903

LI L, WRIGHT S.J., KRYSTOFOVA S., PARK G. and BORKOVICH K.A. (2007)

Heterotrimeric G protein signalling in filamentous fungi. *Annual Rev. Microbiol. 61*, 423–452

LIN, F. H., CAO, Z., and HOSFORD, D. A. (1993) Increased number of $GABA_B$ receptors in lethargic (lh/lh) mouse model of absence epilepsy. *Brain Res. 608,* 101–106

LISANTI, M.P., SCHERER, P.E., TANG, Z. and SARGIACOMO, M., (1994) Caveolae, caveolin and caveolin–rich membrane domains: a signalling hypothesis. *Trends. Cell. Biol. 4*, 231–235

LISANTI, M.P., SCHERER, P.E., VIDUGIRIENE, J., TANG, Z.L., VOSATKA, A.H., TU, Y.–H., COOK, R.F. and SARGIACOMO, M. (1994b) Characterisation of caveolin–rich membrane domains isolated from an endothelial rich source: implications for human disease. *J. Cell. Biol. 126,* 111–126

LISY, V., KOVARU, H., FALTIN, J. and LODIN, Z. (1971) Activity of succinate dehydrogenase and acetylcholine esterase in synaptic endings isolated from neuropil and cerebral cortex. *Phys. Res. 20,* 229–234

LOWRY, O.H., ROSEBROUGH, N.J., FARR, A.L. and RANDALL, R.J. (1951). Protein measurement with the Folin phenol reagent. J Biol Chem 193 (1), 265–275

LUABEYA, M. K., VANISBERG M.A., JEANJEAN A.P., BAUDHUIN, P., LADURON, P.M. and MALOTEAUX, J.M. (1997) Fractionation of human brain by differential and isopycnic equilibration techniques. *Brain Res. Protocols 1,* 83–90

LUSCHER, C., JAN, L. Y., STOFFEL, M. *et al.* (1997). G protein–coupled inwardly rectifying K^+ channels (GIRKs) mediate postsynaptic but not presynaptic transmitter actions in hippocampal neurons. *Neuron 19*, 687–695

MALOTEAUX, J.M., LUABEYA, M.K., VANISBERG, M.A., JEANJEAN, A.P., BAUNHUIN, P., SCHERMAN, D. and LADURON, P.M. (1995) Subcellular distribution of receptor sites in human brain: differentiation between heavy and light structures of high and low density. *Brain Res. 687*, 155–166

MAREŠ, P (2008) Anticonvulsant action of $GABA–_B$ receptor agonist SKF97541 differs from that of baclofen. *Physiol. Res. 57*, 789–792

MARESCAUX, C., VERGNES, M., BERNASCONI, R. (1992) $GABA_B$ receptor antagonists: potential new anti–absence drugs. *J. Neural. Transm. Suppl. 35*, 179–188

MARI´N–TEVA, J.L., DUSART, I., COLLIN, C. et al (2004) Microglia promote the death of developing Purkinje cells. *Neuron 41*, 535–547

MATEYKO G. M. and KOPAC, M. J. (1959) Isopycnic cushioning for density gradient centrifugation. *Exp. Cell Res. 17*, 524–526

MICHEL, T. M., PÜLSCHEN, D. and THOME, J. (2012) The role of oxidative stress in

depressive disorders. *Current Pharmaceutical Design 18 (36),* 5890–5899

MORAVCOVÁ, Z., RUDAJEV, V., NOVOTNÝ, J., ČERNÝ, J., MATOUŠEK, P., PARENTI, M., MILLIGAN, G. and SVOBODA, P. (2004) Long–term agonist stimulation of IP prostanoid receptor depletes the cognate $G_s\alpha$ protein from membrane domains but does not affect the receptor level. *Biochem. Biophys. Acta,* 1691, 51–65

NEUBIG, R. R. (1994) Membrane organisation in G protein mechanism. *FASEB J. 8,* 939–946

NEW, D. C., AN, H., IP, N. Y. and WONG, Y. H. (2006) GABAB heterodimeric receptors promote $Ca2^{+}$ influx via store–operated channels in rat cortical neurons and transfected Chinese hamster ovary cells. *Neuroscience 137,* 1347–1358

NEWBERRY, N. R. and NICOLL, R. A. (1984a) Direct hyperpolarizing action of baclofen on hippocampal pyramidal cells. *Nature 308,* 450–452

NEWBERRY, N. R. and NICOLL, R. A. (1984b) A bicuculline–resistant inhibitory post–synaptic potential in rat hippocampal pyramidal cells in vitro. *J. Physiol., 348,* 239–254

OLIANAS, M.C. and ONALI, P. (1999) GABA(B) receptor–mediated stimulation of adenylyl cyclase activity in membranes of rat olfactory bulb. Br J Pharmacol. 126, 657–664

OLSEN, R.W. and VENTER, C.J. (eds): Benzodiazepine/GABA Receptors and Chloride Channels: Structural and Functional Properties. Alan R. Liss, New York (1986)

PADGETT, C.L. and SLESINGER P. A. (2010) $GABA_B$ receptor coupling to G proteins and Ion channels. *Advances in Pharmacology 58,* 123–147

PELLARDO, F.V., SASTRE, J., ASENSI, M. et al (1991) Physiological changes in glutathione metabolism in fetal and newborn liver. *Biochem J. 274,* 891–893

PÉREZ–GARCI, E., GASSMANN, M., BETTLER, B. *et al.* (2006). The GABAB1b isoform mediates long–lasting inhibition of dendritic Ca^{2+} spikes in layer 5 somatosensory pyramidal neurons. *Neuron 50,* 603–616

PERTOFT, H. (1966) Gradient centrifugation in colloidal silica–polysaccharide media. *BBA 126,* 594–596

PERTOFT, H. (1966) Gradient centrifugation in colloidal silica–polysaccharide media. *BBA 126,* 594–596

PERTOFT, H. (2000) Fractionation of cells and subcellular particles with Percoll. *J. Biochem. Biophys. Methods 44,* 1–30

PERTOFT, H. (2000) Fractionation of cells and subcellular particles with Percoll. *J. Biochem. Biophys. Methods 44,* 1–30

PERTOFT, H. (2000) Fractionation of cells and subcellular particles with Percoll. *J.*

Biochem. Biophys. Methods 44, 1–30

PIKE, L. J. (2004) Lipid rafts: heterogeneity on the high seas. *Biochem. J. 378*, 281–292

PIKE, L. J. (2006) Rafts defined: a report on the Keystone symposium on lipid rafts and cell function. *J. Lipid Res. 47*, 1597–1598

PINARD, A., SEDDIK, R. and BETTLER, B. (2010) $GABA_B$ receptors: Physiological functions and mechanism of diversity. *Advances in Pharmacology 58*, 231–255

RANDERATH, E., ZHOU, G. D. and RANDERATH, K. (1997) Organ–specific oxidative DNA damage associated with normal birth in rats. *Carcinogenesis 18*, 859–866

RAYCHAUDHURI , C. and DESAI, I. D. (1972) Regulation of lysosomal enzymes. IV. Changes in enzyme activities of liver, kidney, and brain during development. *Int. J. of Biochem. 3 (15)*, 309–314

REN, X. and MODY, I. (2003) Gamma–hydroxybutyrate reduces mitogen–activated protein kinase phosphorylation via $GABA_B$ receptor activation in mouse frontal cortex and hippocampus. *J. Biol. Chem. 278*, 42006–42011

RICH, P.R. (2003) The molecular machinery of Keilin's respiratory chain. Biochem. *Soc. Transactions 31 (6)*, 1095–1105

RICKWOOD, D. (1984) Centrifugation, a practical approach. Oxford, IRL Press

RIOBO, N. A. and MANNING, D. R. (2005) Receptors coupled to heterotrimeric G proteins of G_{12}/G_{13} family. *Trends Phrmacol. Sci. 26 (3)*, 146–154

RODBELL, M. (1980) The role of hormone receptors and GTP–regulatory proteins in membrane transduction. *Nature 284*, 17–22

RUDAJEV, V., NOVOTNY, J., HEJNOVA, L., MILLIGAN, G. and SVOBODA, P. (2005) Thyrotropin–releasing hormone receptor is excluded from lipid domains. Detergent–resistant and detergent–sensitive pools of TRH receptor and $G_q\alpha/G_{11}\alpha$ protein. J. *Biochemistry (Jap) 138*, 111–125

SAKABA, T., and NEHER, E. (2003). Direct modulation of synaptic vesicle priming by GABA(B) receptor activation at a glutamatergic synapse. *Nature 424*, 775–778

SARGIACOMO, M., SUDOL, M., TANG, Z. and LISANTI, M.P. (1993) Signal transducing molecules and glycosyl–phosphatidylinositol–linked proteins form a caveolin–rich insoluble complex in MDCK cells. *J. Cell. Biol. 122*, 789–807

SASTRE, J., ASENSI, M., RODRIGO, F. et al (1994) Antioxidant admin–istration to the mother prevents oxidative stress associated with birth in the neonatal rat. *Life Sci 54*, 2055–2059

SCHWARK, W. S., SINGHAL, R. L. and LING, G. M. (1971) Glyceraldehyde–3–phosphate dehydrogenase activity in developing brain during experimental cretinism. *BBA 273*, 308–317

SHAW, A.S. (2006) Lipid rafts: now you see them, now you don't. *Nature Immunology 7 (11)*, 1139–1142

SIMONDS, W.F. (1999) G protein regulation of adenylate cyclase. *Trends Pharmacol. Sci. 20*, 66–73

SIMONS, K. and Toomre, K. (2000) Lipid rafts and signal transduction. *Nature Reviews 1*, 31–39

SMART, E. J., GRAF, G. A., MCNIVEN, M. A., SESSA, W. C., ENGELMAN, J. A., SCHERER, P. E., OKAMATO, T. and LISANTI, M. P. (1999) Caveolins, liquid–ordered domains and signal transduction. *Mol. Cell. Biol. 19*, 7289–7304

SMART, E. J., GRAF, G. A., MCNIVEN, M. A., SESSA, W. C., ENGELMAN, J. A., SCHERER, P. E., OKAMATO, T. and LISANTI, M. P. (1999) Caveolins, liquid–ordered domains and signal transduction. *Mol. Cell. Biol. 19*, 7289–7304

SMART, E.J., YING, Y.–S., MINEO, CH. and ANDERSON, R.G.W. (1995) A detergent–free method for purifiying caveolae membrane from culture cells. *Proc. Nat. Acad. Sci. U S A 92*, 10104–10108

SONG, K.S., . SCHERER, P.E, TANG, Z., OKAMOTO, T., LI, S. , CHAFEL, M. , CHU, C. , KOHTZ, D.S. and LISANTI, M.P. (1996b) Expression of caveolin–3 in skeletal, cardiac, and smooth muscle cells. Caveolin–3 is a component of the sarcolemma and co–fractionates with dystrophin and dystrophin–associated glycoproteins, *J. Biol. Chem. 271*, 15160–15165

SONG, K.S., LI, S., OKAMOTO, T., QUILLIAM, L. A., SARGIACOMO, M. and LISANTI, M. P. (1996a) Co–purification and direct interaction of Ras with caveolin, an integral membrane protein of caveolae microdomains. Detergent–free purification of caveolae microdomains. *J. Biol. Chem. 271*, 9690–9697

STEIGER, J. L., BANDYOPADHYAY, S., FARB, D. H. and RUSSEK, S. J. (2004) cAMP response element–binding protein, activating transcription factor–4, and upstream stimulatory factor differentially control hippocampal GABABR1a and GABABR1b subunit gene expression through alternative promoters. *J. Neurosci. 24*, 6115–6126

SUNAHARA, R. and TAUSSIG, R. (2002) Isoforms of mammalian adenylyl cyclase: multiplicities of signaling. *Mol. Interv. 2*, 168–184.

SVOBODA, P. and LODIN, Z. (1972) Postnatal development of some mitochondrial

enzyme activities of cortical neurons and glial cells. *Physiol. Bohemoslov. 21*, 457–465

SVOBODA, P. and LODIN, Z. (1973) Ontogenic development of oxidative capacity of the brain. *Physiol. Bohemoslov. 23*, 434

SVOBODA, P., TEISINGER, J., NOVOTNÝ, J., BOUŘOVÁ, L., DRMOTA, T., HEJNOVÁ, L., MORAVCOVÁ, Z., LISÝ, V., RUDAJEV, V., STOHR, J., VOKURKOVÁ, A., ŠVANDOVÁ, I. and DURCHÁNKOVÁ, D. (2004) Biochemistry of transmembrane signalling mediated by trimeric G proteins. *Physiol. Res. 53 (Suppl. 1)*, S141–S152

SWEENEY, M.I. and Dolphin, A.C. (1992) 1, 4–Dihydropyrines modulate GTPhydrolysis by Go in neuronal membranes. *FEBS Lett. 310*, 66–70

UJCIKOVA, H., DLOUHA, K., ROUBALOVA, L., VOSAHLIKOVA, M., KAGAN, D. and SVOBODA, P. (2011) Up–regulation of adenylylcyclases I and II induced by long–term adaptation of rats to morphine fades away 20 days after morphine withdrawal. *BBA 1810 (12)*, 1220–1229

UJCIKOVA, H., BREJCHOVA, J., VOSAHLIKOVA, M., KAGAN, D. et al (2014) Opioid–receptor (OR) signaling cascades in rat cerebral cortex and model cell lines: the role of plasma membrane structure. *Phys. Res. 63 (Suppl. 1),* 165–176

VALKO, M., LEIBFRITZ, D., MONCOL, J., CRONIN, M. T. D., MAZUR, M. and TELSER, J. (2007) Free radicals and antioxidants in normal physiological functions and human disease. *Int. J. of Biochem. And Cell Bio. 39 (1)*, 44–84

VICINI, S. (1991) Pharmacologic significance of the structural heterogeneity of the GAB_A receptor – chloride ion channel complex. *Neuropsychopharmacology 4*, 9–15

VOGEL, S.S., CHIN, G.J., SCHWARTZ, J.H. and REESE, T.S. (1991) Pertussis toxin–sensitive G proteins are transported toward synaptic terminals by fast axonal transport. *Proc. Nat. Acad. Sci. U S A 88*, 1775–1778

WAGNER, P. G., and DEKIN, M. S. (1993). GABAb receptors are coupled to a barium–insensitive outward rectifying potassium conductance in premotor respiratory neurons. *Journal of Neurophysiology 69*, 286–289

WHITTACKER, V.P. (1984) The structure and function of cholinergic synaptic vesicles *Biochemical Society Transactions (Lond.) 12*, 561–575

WHITTACKER, V.P., MICHAELSON, I.A. and KIRKLAND, R.J.A. (1964) The separation of synaptic vesicles from nerve ending particles (synaptosomes). *Biochem. J. 90*, 293–303

WILHELM, J. and HERGET, J. (1999) Hypoxia induces free radical damage to rat erythrocytes and spleen: analysis of the fluorescent end–products of lipid peroxidation. *Int. J.*

Biochem. Cell Biol. 31, 671–681

WILHELM, J., IVICA, J., KAGAN, D. and SVOBODA, P. (2011) Early postnatal development of rat brain is accompanied by generation of lipofuscin–like pigments. *Mol. Cell. Biochem. 347*, 157–162

WILHELM, J. and OSTADALOVA, I. (2012) Ontogenetic changes of lipofuscin–like pigments in the rat heart. *Phys. Res. 61*, 173–179

XU, J. and WOJCIK, W.J. (1986) Gamma aminobutyric acid B receptor–mediated inhibition of adenylate cyclase in cultured cerebellar granule cells: blockade by islet activating protein. *J. Pharmacol. Exp. Therapeutics 239*, 568–573

10. SUPPLEMENT (PUBLICATIONS)

© Med Sci Monit, 2010; 16(8): BR260-270
PMID: 20671607

Received: 2010.01.22
Accepted: 2010.05.04
Published: 2010.08.01

Long-term adaptation to high doses of morphine causes desensitization of μ-OR- and δ-OR-stimulated G-protein response in forebrain cortex but does not decrease the amount of G-protein alpha subunits

Authors' Contribution:
A Study Design
B Data Collection
C Statistical Analysis
D Data Interpretation
E Manuscript Preparation
F Literature Search
G Funds Collection

Lenka Bourova[1BCDE], Miroslava Vosahlikova[1BD], Dmytro Kagan[1,2B], Katerina Dlouha[1BD], Jiri Novotny[1,2BF], Petr Svoboda[1,2ACDEFG]

[1] Laboratory of Membrane Receptors, Institute of Physiology, Academy of Sciences of the Czech Republic, Prague, Czech Republic
[2] Department of Physiology, Faculty of Science, Charles University, Prague, Czech Republic

Source of support: This work was supported by Grant Agency of AS CR (IAA500110606), by Ministry of Education of the Czech Republic (projects LC 554 and MSM00 21620858) and by Academy of Sciences of the Czech Republic (AV0Z50110509)

Summary

Background: The functional activity of trimeric guanine-nucleotide-binding proteins (G-proteins) represents an essential step in linking and regulation of the opioid receptor (μ-, δ- and κ-OR)-initiated signaling pathways. Theoretical basis and/or molecular mechanism(s) of opioid tolerance and addiction proceeding in the central nervous system were not studied in the forebrain cortex of mammals with respect to quantitative analysis of opioid-stimulated trimeric G-protein activity.

Material/Methods: G-protein activity was measured in Percoll^{R}-purified plasma membranes (PM) isolated from the frontal brain cortex of control and morphine-treated rats by both high-affinity [^{32}P]GTPase and [^{35}S]GTPγS binding assays. Exposition to morphine was performed by intra-muscular application of this drug. Control animals were injected with sterile PBS.

Results: Both μ-OR (DAMGO)- and δ-OR (DADLE)-responses were clearly *desensitized* in PM isolated from morphine-treated rats; κ-OR (U-69593)- and baclofen ($GABA_B$-R)-stimulated [^{35}S]GTPγS binding was unchanged, indicating the specificity of the morphine effect. Under such conditions, the amount of G-protein alpha subunits was unchanged. The *order of efficacy* DADLE>DAMGO>U-69593 was the same in control and morphine-treated PM. Behavioral tests indicated that morphine-treated animals were fully drug-dependent and developed tolerance to subsequent drug addition.

Conclusions: Prolonged exposure of rats to high doses of morphine results in decrease of the over-all output of OR-stimulated G-protein activity in the forebrain cortex but does not decrease the amount of these regulatory proteins. These data support the view that the mechanism of the long-term adaptation to high doses of morphine is primarily based on desensitization of OR-response preferentially oriented to μ-OR and δ-OR.

key words: morphine • G-protein • forebrain cortex • plasma membranes • opioid receptors

Full-text PDF: http://www.medscimonit.com/fulltxt.php?ICID=881099

Word count: 5313
Tables: 3
Figures: 5
References: 58

Author's address: Lenka Bourova, Institute of Physiology, Academy of Sciences of the Czech Republic, Videnska 1083, 142 20 Prague 4, Czech Republic, e-mail: bourova@biomed.cas.cz

Background

Physiological action of opioid drugs requires an initial interaction with opioid receptors [1]. These receptors were classified as members of the rhodopsin family of G-protein coupled receptors, GPCR. Cloning of these receptors indicated that there are 3 distinct genes that code for 3 subtypes of opioid receptors, μ-OR, δ-OR and κ-OR [2–7]. Results from μ-OR knock-out mouse indicated that most if not all of the physiological effects of morphine are mediated via μ-OR [8].

All of these receptors are known to inhibit adenylyl cyclase activity in pertussis toxin-dependent manner by activation of G_i/G_o class of trimeric G-proteins [9]. These proteins (G_i1, G_i2, G_i3, G_o1, G_o2, G_o*) are present in the brain in large quantities, and inhibit adenylyl cyclase activity or regulate ionic channels in pertussis toxin-dependent manner [10–14]. More recent data have suggested the role of G_z protein, the only pertussis toxin-insensitive member of G_i/G_o family. The role of this G-protein, however, was demonstrated in the acute, *short-term* inhibitory effect of opioid drugs on AC activity, but not in generation of the state arising by long-term adaptation to morphine known as opioid tolerance [15].

Adenylyl cyclase (AC) is regulated by trimeric G-proteins, thus any significant change in AC activity should be preceded by alternation of trimeric G-protein activity. Several *in vitro* studies have indicated that the relationship between receptor occupancy and G-protein activation depends on the receptor density [16–18]; the magnitude of agonist-stimulated G-protein activity was proportional to the corresponding receptor densities in crude membrane preparations of monkey cortex and thalamus [19]. In our work, polytron homogenization resulted in degradation of abundant brain mitochondria and contamination of resulting PM fragments. To avoid this contamination, brain homogenization had to be performed mildly in a *loosely-fitting* teflon-glass Elvehjm-Potter homogenizer; furthermore, to preserve the full functional activity of G-proteins, membrane preparations should be snap frozen in liquid nitrogen and used only once [20]. Therefore, in this work, the purified PM preparation from brain cortex was used and DAMGO (μ-OR)-, DADLE (δ-OR)-, and U-69596 (κ-OR)-stimulated G-protein activity was compared in control and morphine-treated rats. Baclofen ($GABA_B$ agonist)-stimulated [^{35}S]GTPγS binding was used as a reference standard covering the activity of this highly expressed/abundant but unrelated brain GPCR as far as OR-induced signaling cascades are involved.

Material and Methods

Chemicals

DAMGO (2-D-alanine^2-4-methylphenylalanine-5-glycine-ol)-enkefalin = Tyr-D-Ala-Gly-N-methyl-Phe-Gly-ol (E7384), DADLE (2-D-alanine-5-D-leucine)-enkefalin = Tyr-D-Ala-Gly-Phe-D-Leu (Sigma E7384) and U-69593 (Sigma U-103) [(5α, 7α, 8β)-(–)-N-methyl-N-(7-(1-pyrrodinyl)-1-oxaspiro(4,5)dec-8-yl) benzeneacetamide were purchased from Sigma. [^{35}S] GTPγS (1115 Ci/mmol, SJ1320) and [21,22-^{3}H]ouabain (32 mCi/mmol; TRK 429) were from Amersham. [γ-^{32}P]GTP (1050 Ci/mmol, NEG 004) were purchased from Perkin-Elmer, NEN Life Sciences. Complete protease inhibitor cocktail was from Roche Diagnostic, Mannheim, Germany (cat. no. 1697498).

Antisera oriented against the brain $G_i\alpha1$, $G_i\alpha2$, $G_i\alpha3$ and Gβ subunit proteins were prepared as described previously [10–12,14]. Production of the rabbit primary polyclonal antipeptide sera anti-$G_s\alpha$, anti-$G_i\alpha$ 1, 2, anti-$G_i\alpha3$, anti-$G_q\alpha/G_{11}\alpha$ and anti-Gβ (B1) was performed according to [21–23] and [24–26]. We have also used $G_s\alpha$-(G-5040)-oriented antibodies from Sigma. The antisera prepared in our laboratory were previously characterized by Novotny et al. [27] and Ihnatovych et al. [28]. Caveolin-oriented antisera C13630 and C37120 were purchased from Transduction Laboratories (Nottingham, U.K.).

Animals

Male Wistar rats were killed by decapitation under ether narcosis (90-day-old, 160–180g), the frontal brain was rapidly removed and the cerebral cortex was quickly separated from white matter, snap frozen in liquid nitrogen and stored at –70° C until use.

Morphine treatment of experimental animals

Rats were exposed to morphine by intra-muscular application according to the following protocol: 10 mg/kg (day 1 and 2), 15 mg/kg (day 3 and 4), 20 mg/kg (day 5 and 6), 30 mg/kg (day 7 and 8), 40 mg/kg (day 9) and 50 mg/kg (day 10). Control animals were injected with sterile normal saline (0.9%NaCl). Control and morphine-treated animals were killed by decapitation under ether narcosis. The animals were sacrificed 24 hours after the last doses of morphine or normal saline. Brain cortex was removed, frozen in liquid nitrogen and stored in a –80° C freezer.

Isolation of plasma membrane fraction from rat brain cortex

Rat brain cortex was minced with a razor blade on a pre-cooled plate and diluted in STEM medium containing 250 mM sucrose, 20 mM Tris-HCl, 3 mM $MgCl_2$, 1 mM EDTA, pH 7.6, fresh 1 mM PMSF plus complete protease inhibitor cocktail. It was then homogenized mildly in a loosely-fitting Teflon-glass homogenizer for 5 min (2 g w.w. per 10 ml) and centrifuged for 5 min at 3500 rpm. The resulting post-nuclear supernatant (PNS) was filtered through nylon nets of decreasing size (330, 110 and 75 mesh, Nitex) and applied on top of Percoll^R in Beckman Ti70 tubes (30 ml of 27.4% Percoll in STE medium). Centrifugation for 30 min at 30000 rpm (65000×g) resulted in the separation of 2 clearly visible layers [29].The upper layer represented plasma membrane fraction (PM), while the lower layer contained mitochondria (MITO). The upper layer was removed, diluted 1:3 in STEM medium and centrifuged in a Beckman Ti70 rotor for 90 min at 50000 rpm (175000×g). Membrane sediment was removed from the compact, gel-like sediment of Percoll and rehomogenized by hand in a small volume of 50 mM Tris-HCl, 3 mM $MgCl_2$, 1 mM EDTA, pH 7.4 (TME medium).

Agonist-stimulated high-affinity GTPase

GTPase activity was measured in 3 assay incubation buffers containing i) [^{32}P]GTP plus 100 μM GTP (non-specific,

low-affinity GTPase), ii) [^{32}P]GTP + 0.5 μM GTP and iii) [^{32}P]GTP + 0.5 μM GTP + agonist as described previously [20,30]. Basal, high-affinity GTPase was calculated as the difference between GTPase activity measured at [^{32}P]GTP + 0.5 μM GTP and the low-affinity GTPase measured at 100 μM GTP; net increment of agonist-stimulation was calculated as the difference between [^{32}P]GTP + 0.5 μM GTP + agonist-stimulated GTPase (baclofen, DADLE, DAMGO, somatostatin, carbachol) and the basal, high-affinity GTPase measured at 0.5 μM GTP.

Agonist-stimulated [^{35}S]GTPγS binding

Membranes were incubated with (total) or without (basal) 1 mM baclofen ($GABA_B$-R agonist) in a final volume of 100 μl of reaction mix containing 20 mM HEPES, pH 7.4, 3 mM $MgCl_2$, 100 mM NaCl, 2 μM GDP, 0.2 mM ascorbate and 1 nM [^{35}S]GTPγS (about 100,000 dpm per assay) for 30 min at 30°C. The binding reaction was terminated by dilution with 3 ml of ice-cold 20 mM HEPES, pH 7.4, 3 mM $MgCl_2$ and filtration through Whatman GF/C filters on a Brandel cell harvester. Radioactivity remaining on the filters was determined by liquid scintillation using BioScint cocktail. Non-specific GTPγS binding was determined in parallel assays containing 10 μM unlabelled GTPγS.

[^{35}S]GTPγS binding was also measured in the absence (basal) or presence of a constant concentration of 1 mM baclofen ($GABA_B$-R) or 100 μM DAMGO (μ-OR agonist) plus increasing concentrations of GDP (2, 10, 20, 30, 50 and 100 μM). Assays were carried out as before (30 min at 30°C). The non-specific binding, defined as that remaining at 10 μM GTPγS, was subtracted from the basal ± agonist-stimulated level at each point.

Finally, the dose-response curves of agonist stimulation of [^{35}S]GTPγS binding [baclofen ($GABA_B$-R), DADLE (δ-OR agonist), DAMGO (μ-OR agonist) and U-69593 (κ-OR agonist)] were measured at a single [^{35}S]GTPγS concentration (1 nM) and 20 μM GDP in all binding assay media. The quantitative parameters of [^{35}S]GTPγS binding (EC_{50}) were analyzed by GraphPad Prism 4. The net increment (Δ) of agonist stimulation was calculated as the difference between agonist-stimulated and the basal level of binding.

SDS-PAGE and immunoblotting

The aliquots of membrane fractions (20 μg of proteins per sample) were mixed 1:1 with 2× concentrated Laemmli buffer (SLB) and heated for 3 min at 95°C. Standard SDS-PAGE (10% w/v acrylamide/0.26% w/v bis-acrylamide) was carried out as described before in detail [31–33]. Molecular mass determinations were based on pre-stained molecular mass markers (Sigma, SDS 7B). After SDS-PAGE, proteins were transferred to nitrocellulose and blocked for 1 h at room temperature in 3% (w/v) low-fat milk in TBS-Tween buffer [10 mM Tris-HCl, pH 8.0, 150 mM NaCl, 0.1% (v/v) Tween 20]. Antibodies were added in TBS-Tween containing 1% (w/v) low-fat milk and incubated for at least 2 h. The primary antibody was then removed and the blot washed extensively (3×10 min) in TBS-Tween. Secondary antibodies (donkey anti-rabbit IgG or sheep anti-mouse IgG conjugated with horse-radish peroxidase) were diluted in TBS-Tween containing 1% (w/v) low-fat milk, applied for 1 h and after 3 10-min washes the blots were developed by ECL technique using Super Signal West Dura (Pierce) as substrate. The developed blots were scanned with an imaging densitometer ScanJett 5370C (HP) and quantified by Aida Image Analyzer v. 3.28.

Behavioral tests

Morphine dependence was checked by evaluating the physical signs of *opiate abstinence syndrome* [34]. Morphine-induced *analgesic tolerance* was assessed by a modified *hot-plate* test [35] and *hind paw withdrawal* test [36]. All these tests were performed 24 h after the final dose of morphine or saline (control).

Analgesic tolerance (hot-plate test)

Rats were divided into 4 groups (3 animals each). Whereas control C_S and morphine-treated M_S rats were injected with saline (0.9% NaCl, i.p.), morphine (10 mg/kg, i.p.) was administered to control C_M and morphine-treated M_M animals 1 hour before commencement of the test. Rats were placed on an elevated 3 mm thick, clear glass plate, covered with a non-binding, clear Plexiglas cage, and were left to adapt to the testing environment for at least 10 min. A focused light source with a halogen bulb (50 W) delivering the heat stimuli was then located below the glass plate just under the plantar surface of 1 of the rat's hind paws and triggered together with a timer. The time for the first movement of the foot was noted. A test cut-off time of 30 s was chosen to avoid possible tissue damage. Each measurement was repeated 3 times, with at least a 5 min interval.

Analgesic tolerance (hind paw withdrawal test)

Rats were divided into 4 groups and injected with saline or morphine as described above. The hind paw withdrawal test in response to mechanical stimulation was performed in a standard way using *Frey filaments*. The rats were placed on an elevated plastic mesh (4×4 mm perforations) in a transparent cage that allowed full access to the paws from underneath. A series of 8 calibrated von Frey filaments (no. 1–8) with increasing bending force (equivalent to 10, 20, 35, 59, 80, 140, 290, and 370 mN) was used to determine mechanical sensitivity. Starting with the thinnest filament (no. 1), the filaments were successively applied from below perpendicularly to poke the plantar surface of each hind foot with sufficient force to cause slight bending. Each stimulus was repeated 6 times for each hind paw, with intervals of approximately 8–10 s. The number of positive responses (*paw withdrawal*) in each group of tested rats was recorded for each Frey filament.

Behavioral assessment of morphine withdrawal

The withdrawal syndrome was precipitated by naloxone added 24 h after the final dose of morphine. In this way, the physical dependence of experimental animals on morphine was indicated. Naloxone (2 mg/kg, i.p.) was administered to control and morphine-treated rats (3 animals in each group). Immediately after the injection of naloxone, control and morphine-treated rats were placed separately in clear Plexiglass cages with clean bedding and the following

Table 1. Agonist-stimulated GTPase in Percoll^R-purified PM isolated from brain cortex of control rats.

	pmol·min^{-1}·mg^{-1}	%
Basal	25.4±3.1	100±12
Baclofen	35.6±4.2	140±17*
Somatostatine	28.5±2.2	112±9 NS
Carbachol	29.0±3.0	114±12 NS
Isoprenaline	27.4±2.8	110±8 NS
DADLE	30.2±4.5	119±18 NS
DAMGO	29.3±3.1	115±12 NS

The difference between agonist-stimulated and basal level of high-affinity GTPase was measured in PM isolated from control rats and expressed as pmol per min per mg protein. Concentration of baclofen ($GAGA_B$-R), somatostatin, carbachol (mACh-R), isoprenaline (β-AR), DADLE (δ-OR) and DAMGO (μ-OR) was 100 μM. Data represent the mean ± SEM of three experiments; * – indicates significant difference between agonist-stimulated and basal level of enzyme activity, $p<0.05$; NS – non-significant.

selected behavioral parameters were observed continuously for 30 min: body shakes, teeth chatter and vacuous chewing. The number of these episodic types of behavior was recorded and an additional score was calculated based on multiplicities of 5 incidents: **0**, no incidents; **1**, 1–5 incidents; **2**, 6–10 incidents; and **3**, >11 incidents. Additionally, ptosis, irritability to touch and diarrhea were also observed. Because these withdrawal signs could not be defined in discrete episodes, these types of behavior were assessed using predefined anchor points on a 4-point scale: **0**, absent; **1**, mild; **2**, moderate; and **3**, marked.

Protein determination

The method of Lowry was used for determination of protein. Bovine serum albumin (Sigma, Fraction V) was used as standard. Data were calculated by fitting the data with calibration curve as quadratic equation.

Results

Agonist-stimulated GTPase in PM isolated from brain cortex of control, morphine-unexposed rats

Plasma membrane fraction (PM) was separated from the brain mitochondria in Percoll^R gradient according to Bourova et al. [29]. Comparison of the efficacy of different GPCR agonists when increasing high-affinity GTPase indicated that baclofen ($GABA_B$-R agonist) was the only ligand significantly increasing the basal level of enzyme activity: at 10 μg PM protein per assay, baclofen-stimulated GTPase represented 140% of the basal level (Table 1). The effect of other GPCR agonists was not significantly different from the basal level. This held for carbachol (mACh-R), somatostatin, and isoprenaline (β-AR), as well as OR agonists DADLE and DAMGO. Thus, under standard conditions of GTPase assay, OR-stimulated G-protein activity was undetectable.

Table 2. Increase of agonist-stimulated component of [^{35}S]GTPγS binding by increasing GDP concentrations.

A	Baclofen-stimulated [^{35}S]GTPγS binding		
GDP (μM)	%	Δ (pmol·mg^{-1})	p
2	102±5	0.038	NS
10	119±6	0.372	<0.05
20	143±12	0.631	<0.01
30	181±11	0.825	<0.01
50	179±16	0.635	<0.01
B	**DAMGO-stimulated [^{35}S]GTPγS binding**		
GDP (μM)	%	Δ (pmol·mg^{-1})	p
2	104±9	0.094	NS
10	95±8	–0.118	NS
20	115±12	0.265	<0.05
30	135±11	0.475	<0.01
50	141±16	0.387	<0.01

[^{35}S]GTPγS binding to PM isolated from control rats was measured as "*one-point*" assay at 1 nM [^{35}S]GTPγS in the presence of increasing concentration of GDP. Binding was measured in the absence (basal) or presence of 1 mM baclofen or 100 μM DAMGO. Agonist-stimulated level was expressed as % of the basal level (100%). Net increment of agonist stimulation was calculated as the difference between agonist-stimulated and basal level of binding and expressed as pmol·mg^{-1}. Data represent the mean ± SEM of binding assays performed in triplicates.

Baclofen-($GABA_B$-R) and DAMGO (μ-OR)-stimulated [^{35}S]GTPγS binding in brain cortex PM isolated from control rats

In the second part of our work, we tried to distinguish among different GTPγS binding sites with the aim to detect the agonist-responsive component of G-protein activity more clearly. [^{35}S]GTPγS binding was measured at 1 nM [^{35}S]GTPγS in the presence of increasing concentrations of GDP (Table 2). The constant, supra-maximal, 1 mM concentration of baclofen or 100 μM DAMGO (μ-OR agonist) were used for detection of the total level of binding (B_{total}); the basal level of binding (B_{basal}) was determined in parallel assays in the absence of these agonists.

Increase of GDP concentration in the binding mix was associated with the decrease of both agonist-stimulated (B_{total}) and the basal levels of [^{35}S]GTPγS binding (B_{basal}); however, the inhibitory effect of GDP on the basal level was more pronounced than on the total binding. In the absence of GDP, there was no significant difference between total and basal level of binding (NS). The same held for the data collected at 2 μM GDP (NS). The first significant stimulation was measured at 10 μM GDP for baclofen ($p<0.05$); the effect of DAMGO, being much smaller than of baclofen, was under these conditions not yet significant (NS). The data collected at 20, 30 and 50 μM GDP indicated a highly significant difference between B_{total} and B_{basal}

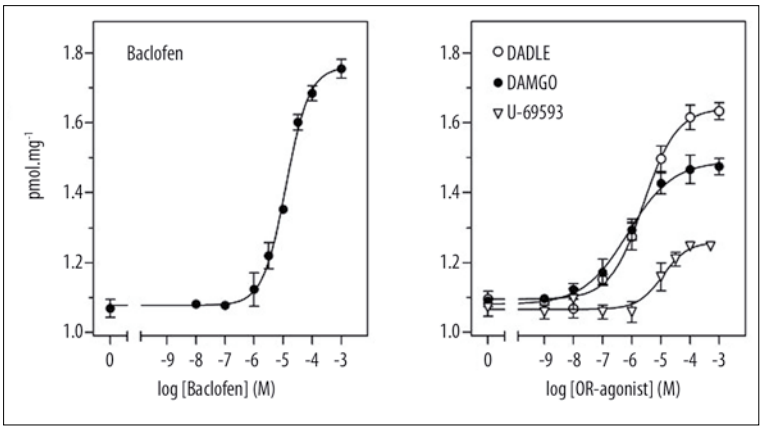

Figure 1. Dose-response curves of agonist-stimulation of [^{35}S]GTPγS binding in Percoll^{R}-purified PM isolated from brain cortex of control, morphine-untreated rats. [^{35}S]GTPγS binding reaction was performed at a single radioligand concentration (1 nM) in the absence (basal) or presence of increasing concentrations of baclofen ($GABA_B$-R), DADLE (δ-OR), DAMGO (μ-OR) or U-69593 (κ-OR). All assays were performed in the presence of 20 μM GDP and 10 μg of protein per tube. The binding reaction was started by transfer from 0°C to 30°C and continued for 30 min at 30°C. Non-specific binding was measured at 10 μM GTPγS and subtracted from the basal ± agonist-stimulated level at each point. Data represent the mean ±SEM of the single PM preparation analyzed in triplicates.

values ($p<0.01$) what indicated significant stimulation by both agonists (Table 2).

Further increase of GDP concentration to 100 μM was reflected in decrease of [^{35}S]GTPγS binding to the very low levels; the difference between B_{total} and B_{basal} (for both baclofen and DAMGO) became under such conditions smaller than at 20–50 μM GDP (data not shown). Thus, the optimum range of GDP concentrations for detection of agonist-stimulated [^{35}S]GTPγS binding in brain cortex PM was between 20 μM and 50 μM GDP. Under these conditions, agonist-stimulated component of total binding was clearly detectable as the positive difference between B_{total} and B_{basal} and could be expressed either as the net-increment of stimulation ($\Delta=B_{total}-B_{basal}$) or the ratio between baclofen-stimulated and basal level of binding (B_{total}/B_{basal}).

In this way (Table 2), the new methodology for detection of agonist-stimulated trimeric G protein activity was introduced in isolated plasma membranes from brain tissue. The very high basal level of G protein activity (GTPγS binding) had to be suppressed by excess of GDP. Under such conditions, i.e. in the presence of 20–30 μM GDP, the increase of the basal level of binding by agonist was high and nice dose-response curves could have been measured (Figures 1, 2). However, sensitivity of response was shifted by 2 orders of magnitude to the right because the active conformation of GPCR had to compete (when effecting the nucleotide binding site of G proteins in reaction mix), with this high concentration of GDP. GDP acts under such conditions as a "competitive inhibitory agent". Therefore, the high concentrations of agonists such as baclofen and DAMGO had to be used.

OR-stimulated [^{35}S]GTPγS binding in brain cortex PM isolated from control rats; ***dose-response curves***

Based on methodological improvements described in the previous section (Table 2), the next part of our work was aimed at analysis of the dose-response curves of OR agonists in PM isolated from control animals. The dose-response curves were measured at a single concentration of [^{35}S]GTPγS (1 nM) and 20 μM GDP in *all* binding assay media. Baclofen ($GABA_B$-agonist) was used as reference standard having significant effect when increasing high-affinity GTPase activity (Table 1) or [^{35}S]GTPγS binding (Table 2). The *efficacy* of agonist effect was judged as the difference between the maximum-stimulated and the basal level of binding (maximum net-increment, Δ_{max}).

Data presented in Figure 1 indicated highly significant stimulation of the basal level by all agonists ($p<0.01$); the maximum net increment (Δ_{max}) of stimulation decreased in the order: baclofen ($GABA_B$-R)>DADLE (δ-OR-DAMGO (μ-OR)>U-69593 (κ-OR) [0.69>0.54>0.38>0.18 pmol·mg^{-1}]; the ratio between agonist-stimulated and basal level of binding decreased in the same order: baclofen >DADLE>DAMGO>U-69593 [165>149>135>117%].

Comparison of OR-stimulated [^{35}S]GTPγS binding in brain cortex PM isolated from control and morphine-treated rats; *dose-response curves*

The dose-response curves of baclofen-, DADLE-, DAMGO- and U-69593-stimulated [^{35}S]GTPγS binding were subsequently measured and compared in PM isolated in parallel from both control and morphine-treated rats. As before, the 20 μM GDP was included in all binding assay media, and baclofen ($GABA_B$-R agonist) was used as a negative standard having significant effect on basal G-protein activity, whose action should not be affected by morphine-treatment of experimental animals.

PM isolated from morphine-treated rats exhibited significantly lower level of DADLE- and DAMGO-stimulated [^{35}S]GTPγS binding than membranes isolated from control, morphine-unexposed rats (Figure 2, middle panels). This difference was highly significant ($p<0.01$) and manifested in the whole range of DADLE or DAMGO concentrations; maximum net-increment Δ_{max} of OR stimulation was 0.35 and 0.26 pmol·mg^{-1} for DADLE and DAMGO, respectively. Morphine treatment caused the decrease of these values to 0.15 and 0.11 pmol·mg^{-1}. Baclofen-stimulated binding was unchanged; the stimulatory effect of κ-OR agonist U-69593 was also unchanged. Therefore, the data collected in all types of G-protein activity assays performed in this work could have been summarized as follows:

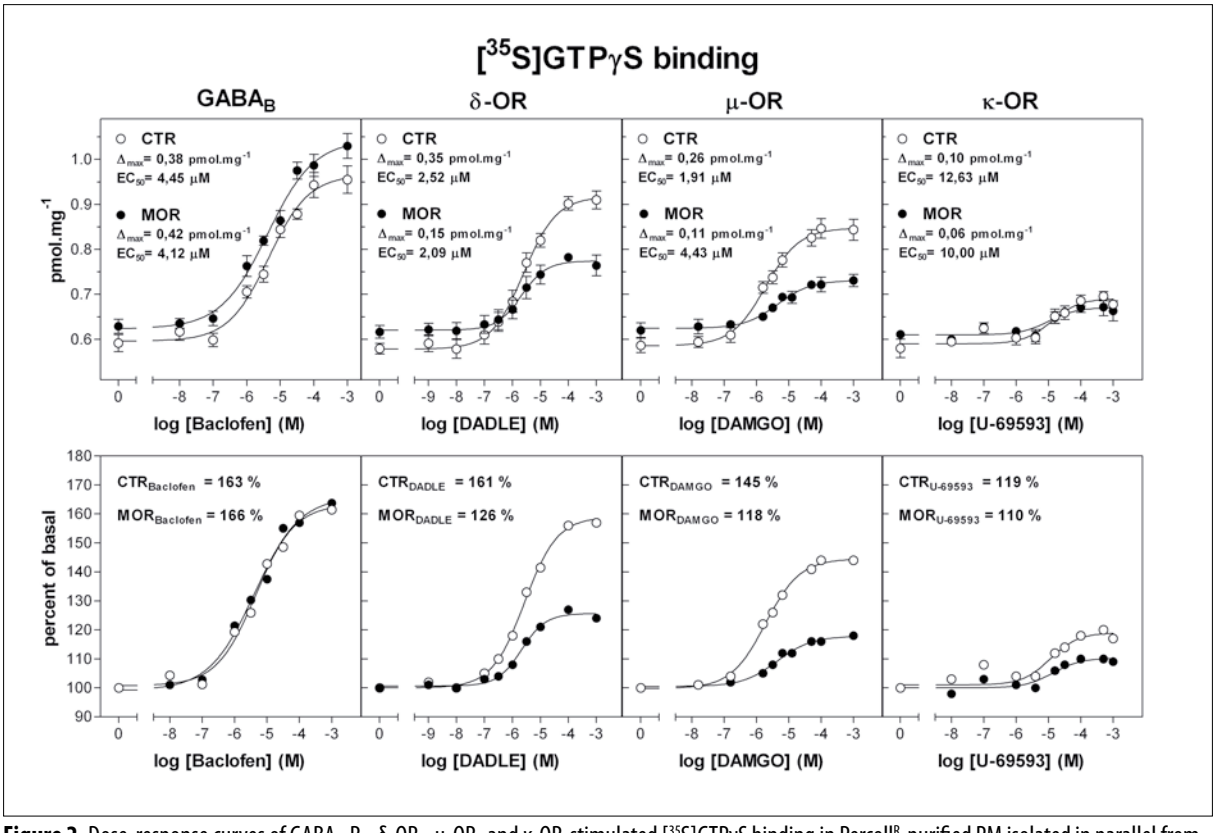

Figure 2. Dose-response curves of $GABA_B$-R-, δ-OR-, μ-OR- and κ-OR-stimulated [^{35}S]GTPγS binding in Percoll^R-purified PM isolated in parallel from control and morphine-treated rats. [^{35}S]GTPγS binding was performed at a single radioligand concentration (1 nM) in the absence (basal) or presence of increasing concentrations of agonists of $GABA_B$-R (baclofen), δ-OR (DADLE), μ-OR (DAMGO) or κ-OR (U-69593). All assays were performed in the presence of 20 μM GDP and 10 μg of protein per tube. The binding reaction was started by transfer from 0°C to 30°C and continued for 30 min at 30°C. Non-specific binding was measured at 10 μM GTPγS and subtracted from the basal ± agonist-stimulated level at each point. Δ_{max}, net increment of agonist stimulation was calculated as the difference between maximum agonist-stimulated and basal level of binding (pmol·mg^{-1} protein);% of stimulation was expressed as the ratio between agonist-stimulated and the basal level. Data represent the mean ±SEM of three PM preparations (± morphine), each analyzed in triplicates.

– OR-stimulated, high-affinity GTPase activity was undetectable in purified PM isolated from rat brain cortex PM (Table 1); the only GPCR agonist significantly increasing the basal level of GTPase activity was baclofen ($GABA_B$-R);
– analysis of [^{35}S]GTPγS binding in the presence of increasing concentrations of GDP indicated that the optimum range for detection of agonist effect was between 20 μM and 50 μμM GDP (Table 2);
– dose-response curves of agonist stimulation of [^{35}S]GTPγS binding in PM isolated from control animals indicated the order of efficacy: baclofen ($GABA_B$-R) >DADLE (δ-OR)>DAMGO (μ-OR) >U-69593 (κ-OR), Figure 1);
– comparison of the dose-response curves of different OR agonists in PM isolated in parallel from control and morphine-treated rats indicated the *highly significant decrease* of δ- and μ-opioid responses in PM isolated from morphine-treated rats (Figure 2);
– morphine treatment did not influence the dose-response curves of baclofen ($GABA_B$-R)-stimulated and U-69593 (κ-OR)-stimulated [^{35}S]GTPγS binding (Figure 2);
– the order of efficacy baclofen >DAMGO>DADLE>U69593 was the same in PM isolated from control and morphine-treated animals and thus unchanged by long-term adaptation to high-doses of morphine.

Comparison of G-protein density in PM isolated from control and morphine-treated rats

Determination G-protein activity presented in the previous paragraphs was accompanied by analysis of G-protein content in parallel PM samples. Data shown in Figure 3 indicated the unchanged level of the major class of OR-related trimeric G-proteins, $G_i1/G_i2\alpha$. A small increase of $G_i3\alpha$ protein was noticed (<120% of the control level). The pertussis toxin-insensitive member of G_i/G_o family, $G_z\alpha$ protein, was decreased, but no more than to 77% when compared with the control level, 100%. The OR-unrelated and ubiquitously expressed $G_q/G_{11}\alpha$ and $G_s\alpha$ proteins were unchanged. Thus, the decrease in activity of trimeric G-proteins was **not** accompanied by any significant change in membrane density of all the major classes of trimeric G-protein α subunits. This type of evidence may be regarded as additional support for a desensitization mechanism of morphine action, as the more drastic adaptation should be reflected in the decrease of the cognate G-protein alpha subunits in PM isolated from morphine-treated rats, *down-regulation* [37–40].

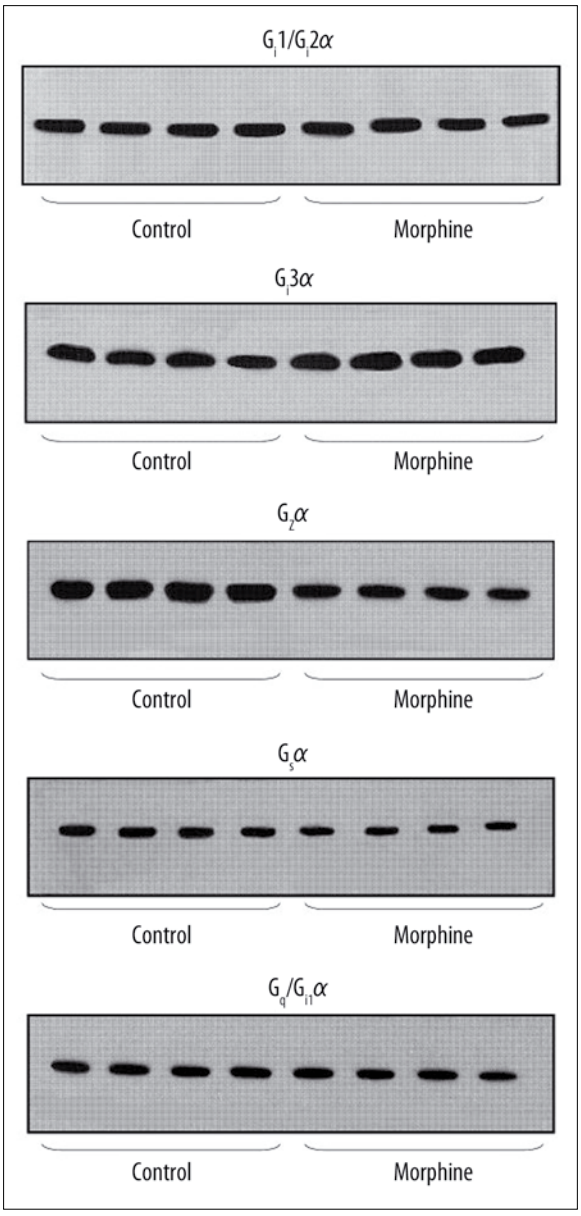

Figure 3. Comparison of G-protein content in PM isolated from control and morphine-treated rats; $G_i1/G_i2\alpha$, $G_i3\alpha$, $G_z\alpha$, $G_s\alpha$, $G_q/G_{11}\alpha$. The 20 µg of PM protein was resolved by SDS-PAGE and G-protein α subunits were identified by immunoblotting with specific antibodies, see Methods. **A**, $G_i1/G_i2\alpha$; **B**, $G_i3\alpha$; **C**, $G_z\alpha$; **D**, $G_s\alpha$; **E**, $G_q/G_{11}\alpha$. Left lanes, control samples; right lanes, morphine-treated samples. The difference between control and morphine-treated samples was analyzed by Student's t-test and expressed as% of control level (100%): $G_i1/G_i2\alpha$ (99±2%; NS), $G_i3\alpha$ (119±4%; $p<0.05$), $G_z\alpha$ (77±5%; $p<0.01$), $G_s\alpha$ (98±4%; NS), $G_q/G_{11}\alpha$ (96±4%; NS); NS, non-significant.

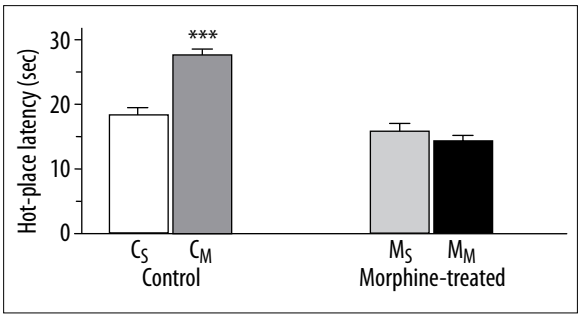

Figure 4. Hot-plate test. Rats were treated for 10 days with saline (C) or morphine (M) and 24 h after the final dose, anti-nociceptive effects of acute morphine administration were tested as described in Methods. One hour before testing their sensitivity to heat stimulation, control and morphine-treated rats were injected either with saline (C_S and M_S) or morphine (C_M and M_M). Data are expressed as means ±SEM (n=3 in each group). One-way ANOVA revealed a clear difference between C_M rats and all the other three tested groups (***, $p<0.001$).

Drug tolerance and dependence in rats treated with morphine under *in vivo* conditions. *Behavioral studies*

The biochemical studies of agonist-stimulated G-protein activity in isolated PM were extended by analysis of behavioral effects of morphine under *in vivo* conditions. These effects were analyzed by 2 tests of *tolerance* and a test of *dependence*. The day after administration of the last dose of morphine (see the Methods for detailed protocol of morphine additions), the tolerance to additional drug exposure was detected clearly *by hot-plate* and *hind paw withdrawal* tests (Figures 4, 5). The state of *dependence* of experimental animals, precipitated by intra-peritoneal administration of naloxone, was manifested by ptosis, chewing, diarrhea, increased sensitivity to touch and teeth chattering (Table 3).

There was no significant difference between control C_S and morphine-treated M_S rats in sensitivity to heat stimulation (*hot-plate test*), which was determined as delay in hind paw withdrawal (Figure 4). Acute administration of morphine did not change the sensitivity of morphine-treated rats (M_M), but it caused a highly significant analgesic effect in control C_M animals (Figure 4). These data indicated that the rats treated for 10 days with morphine developed a clear tolerance to this drug. This conclusion was also supported by the results of *hind paw withdrawal* test: there was no significant difference in sensitivity to mechanical stimulation between morphine-treated rats after acute injection of saline (M_S) or morphine (M_M) (Figure 5). In contrast, an acute dose of morphine totally blocked the response to stimulation by Frey filaments in control animals (Figure 5). Interestingly, morphine-treated rats were much more sensitive to mechanical stimulation as compared to control animals. Because the increased sensitivity to touch is considered as one of the main signs of opiate dependence (withdrawal state), the observed phenomenon can be ascribed to the development of **morphine dependence** in the tested morphine-treated animals.

Precipitation of morphine **withdrawal state** by naloxone resulted in a rapid and dramatic opiate abstinence syndrome in all tested morphine-treated rats. There were no such detectable signs of abstinence syndrome in the corresponding control animals. Characteristics of some morphine withdrawal behaviors are displayed in Table 3. All these observations confirmed that rats treated for 10 days with morphine developed a clear dependence on the drug.

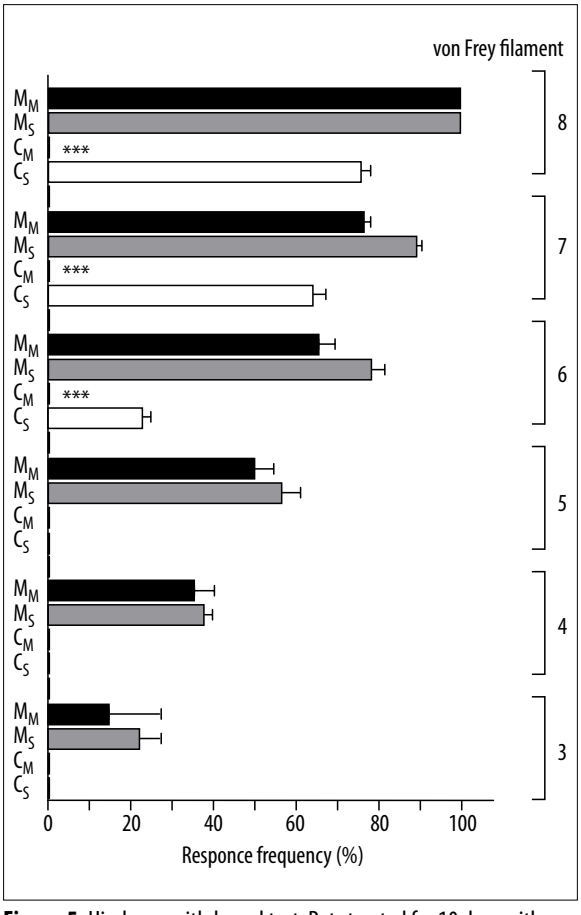

Figure 5. Hind paw withdrawal test. Rats treated for 10 days with saline (C) or morphine (M) were tested for their sensitivity to mechanical stimulation as described in Methods. Twenty-four hours after the final dose the rats were injected either with saline (C_S and M_S) or morphine (C_M and M_M) and one hour later they were poked with different von Frey filaments in their hind paws. Since there was a barely noticeable response to stimulation with very thin filaments (no. 1 and 2), only responses to filaments no. 3–8 are shown here. The occurrence of paw withdrawal was expressed as response frequency (i.e., number of trials accompanied by paw withdrawal/12×100). Values are plotted as means ±SEM (n=3 in each group). There was a clear and pronounced difference in sensitivity to mechanical stimulation between saline- and morphine-treated rats. The effect of acute administration of morphine to control animals was highly significant (***, $p<0.001$) when using von Frey filaments no. 6–8.

Discussion

Opioid *addiction* is a neurological disease symptomatically characterized by drug tolerance, dependence and craving. Data collected over the years aiming at characterization of this disease at cellular or molecular levels may be divided into 2 main hypotheses (for review see [1,41]). According to the *homeostatic* theory, the drug disturbs the cellular homeostasis and the effects are compensated by activation of **new** synthetic pathways that produce the opposite effects and thus restore homeostasis. The second theory considers the primary role of *drug-receptor interaction*, more specifically the

Table 3. Opiate withdrawal behavior in rats treated chronically with morphine

Behavior	Withdrawal score
Body shakes	0.7±0.3
Teeth clatter	2.7±0.3
Vacuous chewing	1.3±0.3
Ptosis	2.7±0.3
Irritability to touch	3.0±0.2
Diarrhoea	2.7±0.3

The values shown were calculated from scores of 0–3 for each behavior observed in morphine-treated rats during 30 min following administration of naloxone and represent the mean ±SEM. No withdrawal signs were observed in these animals before administration of naloxone except for a rather increased sensitivity to handling.

phenomenon of *desensitization* of hormone action proceeding at receptor level. The ability of the receptor to transmit the signal further down-stream becomes inactivated; the receptor becomes less sensitive to the drug. These 2 hypotheses are not mutually exclusive, as prolonged or repeated stimulation of target cells or tissues by a given GPCR agonist induces *desensitization* (decrease) of hormone responsiveness, which is compensated by re-sensitization (increase) proceeding on a longer-time basis. In a short-term scale, the OR induced increase in activity of inhibitory G-proteins (G_i/G_o) and inhibition of AC activity may be followed by increase of these activities proceeding in a long-term scale. The unequivocal difference between the 2 hypotheses/models is **not** in the sequence of counter-acting responses but in the simple fact that the *homeostatic* model involves an alteration in the amount of macromolecules, i.e., it implicitly involves synthesis of new protein molecules *de novo*, while the *change in drug-receptor* interaction model does not. It may be easily explained by a change in the activity of already existing signaling molecules such as receptors, G-proteins or adenylyl cyclases [1].

In this work we compared the opioid-stimulated G-protein activity in purified brain cortex PM isolated from control and morphine-treated rats. In the first part of our work we tried to analyze the high-affinity GTPase activity [42–47]. The ability of different GPCR agonists to stimulate the high-affinity GTPase was relatively low, and OR-agonists were unable to increase this activity in a statistically significant manner (Table 1). Baclofen, $GABA_B$-receptor agonist, was the only GPCR ligand significantly increasing GTPase activity by about 120–140% in different PM preparations. This result is in agreement with earlier data of Odagaki et al. [48] indicating that stimulation of high-affinity GTPase in frontal cortical membranes by several agonists other than $GABA_B$ receptor agonists was too low to quantify and was insufficient for comparing stimulation among different GPCR.

Therefore, in the second part of our work we tried to distinguish among different [^{35}S]GTPγS binding sites and improve methodological conditions for detection of agonist-stimulated component of G-protein activity. [^{35}S]GTPγS

binding was measured in the presence of increasing concentrations of GDP (2–100 μM) ± $GABA_B$-agonist baclofen or μ-OR agonist DAMGO. The results indicated that the optimum range for detection of agonist-stimulated component of [^{35}S]GTPγS binding was at 20–50 μM GDP (Table 2).

Subsequently, the dose-response curves of agonist-stimulation of [^{35}S]GTPγS binding were measured at a single concentration of [^{35}S]GTPγS (1 nM) plus 20 μM GDP in all binding assay media (Figure 1). Comparison of dose-response curves of baclofen ($GABA_B$-R)-, DADLE (δ-OR)-, DAMGO (μ-OR)- and U-69593 (κ-OR)-stimulated binding in PM isolated from control rats indicated that the highest *net increment* of agonist stimulation was detected with the order of efficacy: baclofen ($GABA_B$-R)>DADLE (δ-OR)>DAMGO (μ-OR)>U-69593 (κ-OR) [0.69>0.54>0.38>0.18 pmol·mg^{-1}]; the ratio between agonist-stimulated and basal level of binding decreased with the same order: baclofen >DADLE>DAMGO>U-69593 [165>149>135>117%].

Comparison of PM isolated from control and morphine-treated animals was performed in another, independent set of experiments (Figure 2). The data indicated the same order of efficacy in control and morphine-treated PM [baclofen ($GABA_B$-R)>DADLE (δ-OR)>DAMGO (μ-OR)>U-69593 (κ-OR)] and a *highly significant decrease* ($p<0.01$) of DADLE- and DAMGO-stimulated binding in morphine-treated rats (Figure 2, middle panels). The desensitization of G-protein response was manifested in the whole range of DADLE and DAMGO concentrations. Baclofen ($GABA_B$-R)- and U-69593 (κ-OR)-stimulated binding was **unchanged,** indicating the specificity of morphine-induced change.

The functional studies of G-protein activity indicating the desensitization of δ-OR and μ-OR responses were extended by analysis of the G-protein content (Figure 3). The unchanged level of the OR-related trimeric G-proteins $G_i1/G_i2\alpha$ was detected; the same result was found for the other 2 most widely expressed G-proteins $G_s\alpha$ and $G_q/G_{11}\alpha$. The decrease of $G_z\alpha$ protein, which has been reported to participate directly in the short-term mechanism of morphine action [15], and small increase of $G_i3\alpha$ were the only significant changes we were able to notice.

Behavioral studies performed under *in vivo* conditions in the last part of our work (Figures 4, 5, Table 3) indicated that the experimental animals were fully *drug dependent*, i.e., they developed tolerance to additional morphine exposure and much lower sensitivity to pain, as expected in an addicted state.

Desensitization of μ- and δ-opioid receptor response in frontal brain cortex of rats adapted to high doses of morphine for a prolonged period of time (10 days) is surprising, as the previous work using brain slices and quantitative [^{35}S]GTPγS autoradiography in this part of the brain did not indicate any difference [49]. DAMGO was highly effective when increasing the basal level of binding (191%), but the basal as well as DAMGO-stimulated binding was not different when compared in control and morphine-treated rats (exposed to increasing doses of morphine for 12 days, 10–320 mg/kg). Similar data has been published for heroine [50,51].

Decrease of both μ- and δ-OR-initiated signaling described in our present work is unlikely to arise from non-specific phenomena, because $GABA_B$-R- and κ-OR-stimulated [^{35}S]GTPγS binding was unchanged. Difference between results of Sim et al. [49], Sim-Selley et al. [50] and our data may be explained either by widely different GDP concentrations used in the binding assays (mM range in the case of autoradiographic studies), or by preparation of brain slices at high temperature (–35°C). The full preservation of agonist-stimulated G-protein activity is achieved only when the biological material is snap frozen in liquid nitrogen and used only once (after melting and storage at 0–4°C in the course of membrane isolation or G-protein activity assays). We have repeatedly experienced this fact in measurements of isoprenaline-sensitive adenylylcyclase in S49 lymphoma cells [52,53], DADLE-stimulated [^{35}S]GTPγS binding in HEK293 cells expressing DOR-G_i1 protein [20]or baclofen-stimulated high-affinity GTPase and [^{35}S]GTPγS binding in membranes from frontal brain cortex [30,54].

Previous extensive analysis of distribution of μ-, δ- and κ-OR and G-protein activity in rodent brain, together with the results indicating that morphine's analgesic and addictive properties, were abolished in mice lacking the μ-opioid receptor, has unambiguously demonstrated that μ-receptors mediate both the therapeutic and the adverse activities of this compound [8,55,56]. Therefore, our results demonstrating the order of efficacy DADLE (δ-OR)>DAMGO (μ-OR)>U-69593 (κ-OR) and desensitization of δ-OR mediated response at the level of G-protein activity bring new evidence which has so far not been noticed in the literature to date. Our results are compatible with findings indicating the relatively high density of δ-OR in adult rat forebrain [19,57] together with minor functional significance of κ-OR mediated cascade in this part of CNS [58].

It might be argued that G-protein activity measured in our biochemical work does not necessarily reflect the *in vivo* situation, however, behavioral studies performed under *in vivo* conditions (Figures 4, 5, Table 3) indicated that rats exposed to morphine according to our experimental protocol [increasing doses of morphine for 10 days: 10 mg/kg (day 1 and 2), 15 mg/kg (day 3 and 4), 20 mg/kg (day 5 and 6), 30 mg/kg (day 7 and 8), 40 mg/kg (day 9), 50 mg/kg (day 10)] developed tolerance and much lower sensitivity to pain in comparison with control animals.

Please note that determination of G-protein activity in our work was carried out under the *most simple assay conditions*, i.e., we did **not** use more sophisticated immuno-precipitation protocols, which might increase OR-stimulation of G-protein activity, but might also introduce artificial changes caused by differences in reactivity of G_i1-, G_i2- or G_i3-oriented antibodies. Alternation of antibody reactivity in the course of 10 days of morphine exposure cannot be excluded a priori. Therefore, the simple strategy based on isolation of subcellular membrane fraction enriched in and containing the major part of GPCR and G-proteins, i.e., of plasma membranes [29], together with the definition of the optimum range of GDP concentrations for detection of agonist-stimulated [^{35}S]GTPγS binding, appeared to be the better choice.

Desensitization of *both* μ-OR and δ-OR -stimulated G-protein responses in the *crucial* brain structure, frontal cortex, which has been unequivocally demonstrated in this work, supports the idea of the primary role of receptor-G-protein interaction

in genesis of addictive state [41,1]. Demonstration that desensitization of μ-OR and δ-OR-initiated G-protein pathways proceeds in the cerebral cortex, which has thus far been regarded as a less important brain area in drug addiction when compared with the brain stem, hippocampus and hypothalamus, suggests a more complex picture of integrative interactions among all parts of the brain in this severe phase of the addicted state. This conclusion seems logical, as dramatic changes in behavior of drug addicted animals (Figures 3, 4, Table 3) *should be* accompanied by detectable biochemical changes in the frontal brain cortex, representing the functionally uppermost part of the CNS.

Conclusions

Desensitization of μ-OR- and δ-OR-stimulated G-protein activity was measured in purified plasma membranes isolated from forebrain cortex of rats adapted to high doses of morphine for 10 days. Responsiveness to baclofen ($GABA_B$-R agonist) and U-69593 (κ-OR agonist) was unchanged, indicating the specificity of the morphine effect. Under these conditions the amount of G-protein alpha subunits was unchanged. Behavioral tests performed under *in vivo* conditions indicated that morphine-treated animals were fully drug-dependent and developed tolerance to subsequent drug addition. *These results support the view that the mechanism of addiction to morphine is primarily based on desensitization of OR response, which proceeds primarily at the level of G-protein functional activity.*

Acknowledgements

The authors thank Katarina Kluckova for valuable technical help.

References:

1. Law PY, Loh HH, Wei LN: Insights into the receptor transcription and signaling: implications in opioid tolerance and dependence. Neuropharmacology, 2004; 47(Suppl.1): 300–11
2. Evans CJ, Keith DE Jr., Morrison H et al: Cloning of a delta opioid receptor by functional expression. Science, 1992; 258: 1952–55
3. Kieffer BL, Befort K, Gaveriaux-Ruff C, Hirth CG: The delta-opioid receptor: isolation of a cDNA by expression cloning and pharmacological characterization. Proc Natl Acad Sci USA, 1992; 89: 12048–52
4. Chen Y, Mestek A, Liu J et al: Molecular cloning and functional expression of a mu-opioid receptor from rat brain. Mol Pharmacol, 1993; 44: 8–12
5. Chen Y, Mestek A, Liu J, Yu L: Molecular cloning of a rat kappa opioid receptor reveals sequence similarities to the mu and delta opioid receptors. Biochem J, 1993; 295: 625–28
6. Whistler JL, von Zastrow M: Morphine-activated opioid receptors elude desensitization by beta-arrestin. Proc Natl Acad Sci USA, 1998; 95: 9914–19
7. Whistler JL, Chuang HH, Chu P et al: Functional dissociation of mu opioid receptor signaling and endocytosis: implications for the biology of opiate tolerance and addiction. Neuron, 1999; 23: 737–46
8. Kieffer BL: Opioids: first lessons from knockout mice. Trends Pharmacol Sci, 1999; 20: 19–26
9. Carter BD, Medzihradsky F: Go mediates the coupling of the mu opioid receptor to adenylyl cyclase in cloned neural cells and brain. Proc Natl Acad Sci USA, 1993; 90: 4062–66
10. Gierschik P, Milligan G, Pines M et al: Use of specific antibodies to quantitate the guanine nucleotide-binding protein Go in brain. Proc Natl Acad Sci USA, 1986; 83: 2258–62
11. Goldsmith P, Gierschik P, Milligan G et al: Antibodies directed against synthetic peptides distinguish between GTP-binding proteins in neutrophil and brain. J Biol Chem, 1987; 262: 14683–88
12. Backlund PS Jr., Aksamit RR, Unson CG et al: Immunochemical and electrophoretic characterization of the major pertussis toxin substrate of the RAW264 macrophage cell line. Biochemistry, 1988; 27: 2040–46
13. Milligan G: Techniques used in the identification and analysis of function of pertussis toxin-sensitive guanine nucleotide binding proteins. Biochem J, 1988; 255: 1–13
14. Milligan G: Immunological probes and the identification of guanine nucleotide-binding proteins. in Houslay MD, Milligan G (eds.): G proteins as Mediators of Cellular Signalling Processes. New York: John Wiley & Sons. Ltd., 1990; 31–46
15. Tso PH, Wong YH: G(z) can mediate the acute actions of mu- and kappa-opioids but is not involved in opioid-induced adenylyl cyclase supersensitization. J Pharmacol Exp Ther, 2000; 295: 168–76
16. Selley DE, Liu Q, Childers SR: Signal transduction correlates of mu opioid agonist intrinsic efficacy: receptor-stimulated [^{35}S]GTP gamma S binding in mMOR-CHO cells and rat thalamus. J Pharmacol Exp Ther, 1998; 285: 496–505
17. Sim-Selley LJ, Daunais JB, Porrino LJ, Childers SR: Mu and kappa1 opioid-stimulated [^{35}S]guanylyl-5'-O-(gamma-thio)-triphosphate binding in cynomolgus monkey brain. Neuroscience, 1999; 94: 651–62
18. Maher CE, Selley DE, Childers SR: Relationship of mu opioid receptor binding to activation of G-proteins in specific rat brain regions. Biochem Pharmacol, 2000; 59: 1395–401
19. Ko MC, Lee H, Harrison C et al: Studies of mu-, kappa-, and delta-opioid receptor density and G protein activation in the cortex and thalamus of monkeys. J Pharmacol Exp Ther, 2003; 306: 179–86
20. Bourova L, Kostrnova A, Hejnova L et al: delta-Opioid receptors exhibit high efficiency when activating trimeric G proteins in membrane domains. J Neurochem, 2003; 85: 34–49
21. Mitchell FM, Griffiths SL, Saggerson ED et al: Guanine-nucleotide-binding proteins expressed in rat white adipose tissue. Identification of both mRNAs and proteins corresponding to G_i1, G_i2 and G_i3. Biochem J, 1989; 262: 403–8
22. Mullaney I, Milligan G: Identification of two distinct isoforms of the guanine nucleotide binding protein G_o in neuroblastoma X glioma hybrid cells: independent regulation during cyclic AMP-induced differentiation. J Neurochem, 1990; 55: 1890–98
23. Mitchell FM, Mullaney I, Godfrey PP et al: Widespread distribution of G_q alpha/G_{11} alpha detected immunologically by an antipeptide antiserum directed against the predicted C-terminal decapeptide. FEBS Lett, 1991; 287: 171–74
24. Mullaney I, Milligan G: Agonist activation of transfected human M1 muscarinic acetylcholine receptor in Chinese hamster ovary cells results in concurrent downregulation of G_q alpha and G_{11} alpha. Biochem Soc Trans, 1993; 21: 497S
25. Mullaney I, Mitchell FM, McCallum JF et al: The human muscarinic M1 acetylcholine receptor, when express in CHO cells, activates and downregulates both G_q alpha and G_{11} alpha equally and non-selectively. FEBS Lett, 1993; 324: 241–45
26. Mullaney I, Caulfield MP, Svoboda P, Milligan G: Activation, cellular redistribution and enhanced degradation of the G proteins G_q and G_{11} by endogenously expressed and transfected phospholipase C-coupled muscarinic m1 acetylcholine receptors. Prog Brain Res, 1996; 109: 181–87
27. Novotny J, Bourova L, Kolar F, Svoboda P: Membrane-Bound and cytosolic forms of heterotrimeric G proteins in young and adult rat myocardium: influence of neonatal hypo- and hyperthyroidism. J Cell Biochem, 2001; 82: 215–24
28. Ihnatovych I, Novotny J, Haugvicova R et al: Opposing changes of trimeric G protein levels during ontogenetic development of rat brain. Brain Res Dev Brain Res, 2002; 133: 57–67
29. Bourova L, Stohr J, Lisy V et al: Isolation of plasma membrane compartments from rat brain cortex; detection of agonist-stimulated G protein activity. Med Sci Monit, 2009; 15(4): BR111–22
30. Stohr J, Bourova L, Hejnova L et al: Increased baclofen-stimulated G protein coupling and deactivation in rat brain cortex during development. Brain Res Dev Brain Res, 2004; 151: 67–73
31. Matousek P, Novotny J, Svoboda P: Resolution of G(s)alpha and G(q) alpha/G(11)alpha proteins in membrane domains by two-dimensional electrophoresis: the effect of long-term agonist stimulation. Physiol Res, 2004; 53: 295–303
32. Moravcova Z, Rudajev V, Stohr J et al: Long-term agonist stimulation of IP prostanoid receptor depletes the cognate G(s)alpha protein in membrane domains but does not change the receptor level. Biochim Biophys Acta, 2004; 1691: 51–65

33. Matousek P, Novotny J, Rudajev V, Svoboda P: Prolonged agonist stimulation does not alter the protein composition of membrane domains in spite of dramatic changes induced in a specific signaling cascade. Cell Biochem Biophys, 2005; 42: 21–40
34. Guitart X, Kogan JH, Berhow M et al: Lewis and Fischer rat strains display differences in biochemical, electrophysiological and behavioral parameters: studies in the nucleus accumbens and locus coeruleus of drug naive and morphine-treated animals. Brain Res, 1993; 611: 7–17
35. Hargreaves K, Dubner R, Brown F et al: A new and sensitive method for measuring thermal nociception in cutaneous hyperalgesia. Pain, 1988; 32: 77–88
36. Miki K, Fukuoka T, Tokunaga A et al: Differential effect of brain-derived neurotrophic factor on high-threshold mechanosensitivity in a rat neuropathic pain model. Neurosci Lett, 2000; 278: 85–88
37. Svoboda P, Unelius L, Cannon B, Nedergaard J: Attenuation of G_s alpha coupling efficiency in brown-adipose-tissue plasma membranes from cold-acclimated hamsters. Biochem J, 1993; 295 (Pt 3): 655–61
38. Svoboda P, Milligan G: Agonist-induced transfer of the alpha subunits of the guanine-nucleotide-binding regulatory proteins G_q and G_{11} and of muscarinic m1 acetylcholine receptors from plasma membranes to a light-vesicular membrane fraction. Eur J Biochem, 1994; 224: 455–62
39. Svoboda P, Kim GD, Grassie MA et al: Thyrotropin-releasing hormone-induced subcellular redistribution and down-regulation of G_{11}alpha: analysis of agonist regulation of coexpressed G_{11}alpha species variants. Mol Pharmacol, 1996; 49: 646–55
40. Svoboda P, Unelius L, Dicker A et al: Cold-induced reduction in Gi alpha proteins in brown adipose tissue. Effects on the cellular hypersensitization to noradrenaline caused by pertussis-toxin treatment. Biochem J, 1996; 314 (Pt 3): 761–68
41. Tso PH, Wong YH: Molecular basis of opioid dependence: role of signal regulation by G-proteins. Clin Exp Pharmacol Physiol, 2003; 30: 307–16
42. Cassel D, Selinger Z: Catecholamine-induced release of [3H]-Gpp(NH)p from turkey erythrocyte adenylate cyclase. J Cyclic Nucleotide Res, 1977; 3: 11–22
43. Cassel D, Selinger Z: Mechanism of adenylate cyclase activation through the beta-adrenergic receptor: catecholamine-induced displacement of bound GDP by GTP. Proc Natl Acad Sci USA, 1978; 75: 4155–59
44. Koski G, Streaty RA, Klee WA: Modulation of sodium-sensitive GTPase by partial opiate agonists. An explanation for the dual requirement for Na+ and GTP in inhibitory regulation of adenylate cyclase. J Biol Chem, 1982; 257: 14035–40
45. Gierschik P, Sidiropoulos D, Steisslinger M, Jakobs KH: Na+ regulation of formyl peptide receptor-mediated signal transduction in HL 60 cells. Evidence that the cation prevents activation of the G-protein by unoccupied receptors. Eur J Pharmacol, 1989; 172: 481–92
46. Hilf G, Gierschik P, Jakobs KH: Muscarinic acetylcholine receptor-stimulated binding of guanosine 5'-O-(3-thiotriphosphate) to guanine-nucleotide-binding proteins in cardiac membranes. Eur J Biochem, 1989; 186: 725–31
47. Gierschik P, Moghtader R, Straub C et al: Signal amplification in HL-60 granulocytes. Evidence that the chemotactic peptide receptor catalytically activates guanine-nucleotide-binding regulatory proteins in native plasma membranes. Eur J Biochem, 1991; 197: 725–32
48. Odagaki Y, Nishi N, Ozawa H et al: Measurement of receptor-mediated functional activation of G proteins in postmortem human brain membranes. Brain Res, 1998; 789: 84–9.
49. Sim LJ, Selley DE, Dworkin SI, Childers SR: Effects of chronic morphine administration on mu opioid receptor-stimulated [35S]GTPgammaS autoradiography in rat brain. J Neurosci, 1996; 16: 2684–92
50. Sim-Selley LJ, Selley DE, Vogt LJ et al: Chronic heroin self-administration desensitizes mu opioid receptor-activated G-proteins in specific regions of rat brain. J Neurosci, 2000; 20: 4555–62
51. Maher CE, Martin TJ, Childers SR: Mechanisms of mu opioid receptor/G-protein desensitization in brain by chronic heroin administration. Life Sci, 2005; 77: 1140–54
52. Ransnas LA, Svoboda P, Jasper JR, Insel PA: Stimulation of beta-adrenergic receptors of S49 lymphoma cells redistributes the alpha subunit of the stimulatory G protein between cytosol and membranes. Proc Natl Acad Sci USA, 1989; 86: 7900–3
53. Svoboda P, Kvapil P, Insel PA, Ransnas LA: Plasma-membrane-independent pool of the alpha subunit of the stimulatory guanine-nucleotide-binding regulatory protein in a low-density-membrane fraction of S49 lymphoma cells. Eur J Biochem, 1992; 208: 693–98
54. Ihnatovych I, Novotny J, Haugvicova R et al: Ontogenetic development of the G protein-mediated adenylyl cyclase signalling in rat brain. Brain Res Dev Brain Res, 2002; 133: 69–75
55. Matthes HW, Maldonado R, Simonin F et al: Loss of morphine-induced analgesia, reward effect and withdrawal symptoms in mice lacking the mu-opioid-receptor gene. Nature, 1996; 383: 819–23
56. Contet C, Kieffer BL, Befort K: Mu opioid receptor: a gateway to drug addiction. Curr Opin Neurobiol, 2004; 14: 370–78
57. Kornblum HI, Hurlbut DE, Leslie FM: Postnatal development of multiple opioid receptors in rat brain. Brain Res, 1987; 465: 21–41
58. Maurer R: Multiplicity of opiate receptors in different species. Neurosci Lett, 1982; 30: 303–7

Physiol. Res. 62: 547-559, 2013

Plasma Membrane Density of $GABA_B$-R1a, $GABA_B$-R1b, GABA-R2 and Trimeric G-proteins in the Course of Postnatal Development of Rat Brain Cortex

K. DLOUHÁ[1], D. KAGAN[1], L. ROUBALOVÁ[1], H. UJČÍKOVÁ[1], P. SVOBODA[1]

[1]Institute of Physiology, Academy of Sciences of the Czech Republic, Prague, Czech Republic

Received April 11, 2013
Accepted June 18, 2013
On-line September 10, 2013

Summary

With the aim to understand the onset of expression and developmental profile of plasma membrane (PM) content /density of crucial components of $GABA_B$-R signaling cascade, $GABA_B$-R1a, $GABA_B$-R1b, $GABA_B$-R2, $G_i1/G_i2\alpha$, $G_i3\alpha$, $G_o\alpha$, $G_z\alpha$ and Gβ subunit proteins were determined by quantitative immunoblotting and compared in PM isolated from brain cortex of rats of different ages: between postnatal-day-1 (PD1) and 90 (PD90). PM density of $GABA_B$-R1a, $GABA_B$-R2, $G_i1/G_i2\alpha$, $G_i3\alpha$, $G_o\alpha$, $G_z\alpha$ and Gβ was high already at birth and further development was reflected in parallel decrease of both $GABA_B$-R1a and $GABA_B$-R2 subunits. The major decrease of $GABA_B$-R1a and $GABA_B$-R2 occurred between the birth and PD15: to 55 % (R1a, **) and 51 % (R2, **), respectively. Contrarily, PM level of the cognate G-proteins $G_i1/G_i2\alpha$, $G_i3\alpha$, $G_o\alpha$, $G_z\alpha$ and Gβ was unchanged in the course of the whole postnatal period of brain cortex development. Maturation of $GABA_B$-R cascade was substantially different from ontogenetic profile of prototypical plasma membrane marker, Na, K-ATPase, which was low at birth and further development was reflected in continuous increase of PM density of this enzyme. Major change occurred between the birth and PD25. In adult rats, membrane content of Na, K-ATPase was 3-times higher than around the birth.

Key words

$GABA_B$-R • Postnatal development • Rat brain cortex • G-proteins • Na, K-ATPase

Corresponding author

P. Svoboda, Institute of Physiology, Academy of Sciences of the Czech Republic, Vídeňská 1083, 142 20 Prague 4, Czech Republic. Fax: + 420-241062488. E-mail: svobodap@biomed.cas.cz

Introduction

$GABA_B$-receptors were defined as a class of bicuculline-insensitive GABA receptors for which (-)-baclofen is a specific agonist and phaclofen and 2-hydroxy-saclofen represent specific antagonists (Hill and Bowery 1981, Bowery *et al.* 1985, 1987, Kerr and Ong 1995). These receptors are not physically bound to ionic channels and belong to the family of G-protein coupled receptors, GPCR (Kerr and Ong 1995). Thus, the primary signal initiated by binding of GABA to $GABA_B$-R is transmitted further downstream by trimeric G-proteins.

The central nervous system is known to contain high levels of all trimeric Gα subunits. The three species of inhibitory G-proteins, $G_i\alpha1$, $G_i\alpha2$ and $G_i\alpha3$ (Mumby *et al.* 1988), the long ($G_s\alpha L$) and short ($G_s\alpha S$) variants of the stimulatory $G_s\alpha$ protein (Bray *et al.* 1986), phosphoinositidase C-linked $G_q\alpha$ and $G_{11}\alpha$ proteins (Milligan 1993) as well as representatives of $G_{12}\alpha/G_{13}\alpha$ family of G-proteins (Harhammer *et al.* 1994, 1996) were identified in brain tissue in high amounts. The major G-proteins of brain, however, are members of $G_o\alpha$ family. The two isoforms of $G_o\alpha$ subunits, $G_o\alpha1$ and $G_o\alpha2$, represent up to 1 % of the total membrane protein in the brain tissue (Giershick *et al.* 1986, Goldsmith *et al.* 1987, 1988, Milligan 1988, 1990). Accordingly, the content of Gβ subunits is very high in brain (Asano *et al.* 1988). It should be also mentioned that the complexity of biochemical composition of the brain tissue is not limited to G-proteins, but it is equally high for adenylylcyclase (AC) molecules because all the isoforms (ACI-X) of this

key regulatory enzyme of GPCR-initiated cascades were identified in CNS and their PM content was found to respond readily to physiological state of experimental animals (Ujcikova *et al*. 2011).

Regulation of the specificity and efficiency of coupling between GPCRs and trimeric G-proteins in natural tissue such as brain is therefore highly complex. GPCRs usually exert their action through activation of preferential G-proteins (in a given cell type), however, a single type of receptor can be also coupled to several G-proteins (Boege *et al.* 1991, Gerhardt and Neubig 1991, Raymond 1995, Dascal 1997, Gudermann *et al.* 1997, Hildebrandt 1997). Furthermore, the given type of G-protein may be activated by different receptors. Under such conditions, it is reasonable to assume that a complicated functional arrangement denominated as cross talk among individual members of G-protein-mediated cascades exists and provides an effective regulatory mechanism for the convergence or divergence of actions of a single neurotransmitter in nervous tissue.

Receptor-initiated activation of G-proteins results in the release of free Gα and Gβγ subunits from the non-active Gαβγ trimer; subsequently, both free Gα and Gβγ subunits mediate the signal transmission further downstream. Thus, besides the functional networks of Gi1α-, Gi2α-, Gi3α-, Go1α- and Go2α-mediated signaling, Gβγ-mediated cascades represent no less complicated regulatory circuits. The main Gβγ-regulated effectors of presynaptic $GABA_B$-receptors are P/Q-and N-type voltage-dependent Ca^{2+} channels (Chen and van den Pol 1998, Bussieres and El Manira 1999, Barral *et al.* 2000). $GABA_B$-receptors inhibit these Ca^{2+} channels at both excitatory and inhibitory terminals, thereby restricting neurotransmitter release. Depending on whether the terminal releases an inhibitory or excitatory neurotransmitter, the presynaptic $GABA_B$ receptors increase or decrease the excitability of the postsynaptic neuron (Pinard *et al.* 2010).

Presynaptic $GABA_B$ receptors restrict neurotransmitter release not only by inhibiting Ca^{2+} channels but also by retarding the recruitment of synaptic vesicles (Sakaba and Neher 2003). More recent evidence suggests that presynaptic $GABA_B$-receptors may couple to inwardly rectifying Kir3-type K^+ channels (also designated GIRK channels) to inhibit glutamate release (Ladera *et al.* 2008, Fernandez-Alacid *et al.* 2009); however, Kir3 channels are generally considered as the main effectors of postsynaptic $GABA_B$-receptors (Pinard *et al.* 2010).

Binding of GABA to postsynaptic $GABA_B$-R results in activation of Kir3 channels, induction of K^+ efflux and hyperpolarization of postsynaptic membrane. This change of membrane potential shunts excitatory currents in a non-specific way. Finally, under such conditions, the so-called slow inhibitory postsynaptic potentials (IPSPs) are generated. Activation of postsynaptic $GABA_B$-receptors was also found to decrease the activity of Ca^{2+} channels, which inhibit dendritic Ca^{2+}-spike propagation (Perez-Garci *et al.* 2006).

The present state of knowledge about the plasma membrane part of $GABA_B$-receptor signaling cascade in the brain may thus be described as a mutually interrelated regulatory network of $GABA_B$-R, PTX-sensitive G-proteins of $G_i/G_o\alpha$ family, various AC isoforms and ionic channels such as $GABA_A$-R (Xu and Wojcik 1986, Simonds 1999, Sunahara and Taussig 2002, Padgett and Schlesinger 2010, Pinard *et al.* 2010). Functionally, in this network, primary inhibitory signals proceeding at receptor level are followed by both positive and negative feedback regulatory loops tuning the whole regulatory circuit to an optimum output (Padgett and Schlesinger 2010, Pinard *et al.* 2010). These circuits are therefore highly complex and important for brain function as GABA represents the main inhibitory neurotransmitter of mammalian brain.

Our previous results indicated that the plasma membrane density of $GABA_B$-R, determined by a saturation binding assay with antagonist [^{3}H]CGP54626, was highest in 1-day-old animals and then it was dramatically decreased in 15- and 90-day-old rats (Kagan *et al.* 2012). Intrinsic efficacy of $GABA_B$-receptors, measured as agonist-stimulated, high-affinity [^{35}S]GTPγS binding, was also high at birth (PD1, PD2), however, it increased further during the first two weeks of postnatal life and reached the maximum between PD9 and PD15. In older rats, both baclofen- and SKF97541-stimulated [^{35}S]GTPγS binding was decreased so that the level in adult rats (PD90) was not different from that in newborn animals.

The aim of our present work was to establish the structural correlate to these functional studies of $GABA_B$-R ontogenesis by determination of PM density of $GABA_B$-R1a, $GABA_B$-R1b, $GABA_B$-R2, $G_i1/G_i2\alpha$, $G_i3\alpha$, $G_o\alpha$, $G_z\alpha$ and Gβ subunit proteins by quantitative immunoblottig with specific antibodies. We have also determined PTX-insensitive $G_{12}\alpha$ protein as a test of maturation of intracellular "membrane traffic", as

vesicular transport within the neuron is an important part of optimum functioning of CNS. The general trend of brain cortex maturation was screened by analysis of prototypical plasma membrane marker, ouabain-dependent Na, K-ATPase (EC 3.6.1.3).

Material and Methods

The experiments were approved by Animal Care and Use Committee of the Institute of Physiology, Academy of Sciences of the Czech Republic to be in agreement with Animal Protection Law of the Czech Republic as well as European Comunity Council directives 86/609/EEC.

Chemicals and radiochemicals

$GABA_B$-receptor agonists baclofen (β-p-chlorophenyl-GABA), SKF 97541 [3-aminopropyl (methyl) phosphinic acid] and antagonist [^{3}H]CGP 54626 (41.5 Ci/mmol, cat. no. R1088) were purchased from Tocris. [21, 22-^{3}H]ouabain (30 mCi/mmol; NET211001) was from Perkin Elmer. The complete protease inhibitor cocktail was from Roche Diagnostic (cat. no. 1697498). All other chemicals were of highest quality available.

Primary antisera and antibodies

$G_i1/G_i2\alpha$, $G_i3\alpha$ and $G_o1/G_o2\alpha$ subunit proteins were identified by antipeptide antibodies prepared as described originally by Gierschik *et al.* (1986), Goldsmith *et al.* (1987), Backlund *et al.* (1988) and Milligan (1988, 1990). These antisera were previously characterized in our laboratory (Ihnatovych *et al.* 2002a). Polyclonal antibodies oriented against $GABA_B$-R1 (R-300, sc-14006), $GABA_B$-R2 (H-300, sc-28792), Gβ (T-20, sc-378) $G_z\alpha$ (I-20, sc-388), $G_{12}\alpha$ (S-20, sc-409) and α subunit of Na, K-ATPase (H-300, sc-28800) were from Santa Cruz.

Isolation of plasma membrane-enriched fraction from rat brain cortex

Rat brain cortex was minced with a razor blade on a pre-cooled plate and diluted in STEM medium containing 250 mM sucrose, 20 mM Tris-HCl, 3 mM $MgCl_2$, 1 mM EDTA, pH 7.6, fresh 1 mM PMSF plus protease inhibitor cocktail. It was then homogenized mildly in loosely-fitting Teflon-glass homogenizer for 5 min (2 g w. w. per 10 ml) and centrifuged for 5 min at 3500 rpm. Resulting post-nuclear supernatant (PNS) was filtered through Nylon nets of decreasing size (330, 110 and 75 mesh, Nitex) and applied on top of Percoll in Beckman Ti70 tubes (30 ml of 27.4 % Percoll in STE medium). Centrifugation for 60 min at 30000 rpm (65000 x g) resulted in the separation of two clearly visible layers (Bourova *et al.* 2009). The upper layer represented plasma membrane fraction (PM); the lower layer contained mitochondria (MITO). The upper layer was removed, diluted 1:3 in STEM medium and centrifuged in Beckman Ti70 rotor for 90 min at 50000 rpm (175000 x g). Membrane sediment was removed from the compact, gel-like sediment of Percoll, re-homogenized by hand in a small volume of 50 mM Tris-HCl, 3 mM $MgCl_2$, 1 mM EDTA, pH 7.4 (TME medium), snap frozen in liquid nitrogen and stored at –80 °C.

SDS-PAGE and immunoblotting

Aliquots of PM were solubilised in NuPAGE SDS Sample Buffer (4x) with an addition of NuPAGE Sample Reducing Agent (10x) according to manufacturer's instructions. Samples were heated at 70 °C for 10 min, loaded at 10 μg/well and resolved by NuPAGE 4-12 % or 10 % Bis-Tris polyacrylamide gels (10 wells, 1 mm thick) using 3-(N-morpholino) propane sulfonic acid (MOPS), sodium dodecyl sulfate (SDS) running buffer with NuPAGE Antioxidant prior to blotting on nitrocellulose membranes (Protran, Schleicher & Schuell). Molecular mass determinations were based on pre-stained molecular mass markers (Sigma, SDS 7B).

After SDS-PAGE, the proteins were transferred to nitrocellulose and blocked for 1 h at room temperature in 5 % (w/v) low-fat milk in TBS-Tween buffer [10 mM Tris-HCl, pH 8.0, 150 mM NaCl, 0.1 % (v/v) Tween 20]. Antibodies were added in TBS-Tween containing 1 % (w/v) low-fat milk and incubated for at least 2 h. The primary antibody was then removed and the blot washed extensively (3 x 10 min) in TBS-Tween. Secondary antibodies (donkey anti-rabbit IgG conjugated with horseradish peroxidase) were diluted in TBS-Tween containing 1 % (w/v) low-fat milk applied for 1 h, and after three 10-min washes the blots were developed by ECL technique using Super Signal West Dura (Pierce) as substrate. The developed blots were scanned with an imaging densitometer ScanJett 5370C (HP) and quantified by Aida Image Analyzer v. 3.28 (Ray test).

[^{3}H]CGP54626 binding; one-point assay

Membranes (100 μg protein per assay) were incubated with 12 nM [^{3}H]CGP54626 in a final volume

of 100 µl of binding mix containing (A) 50 mM Tris-HCl (pH 7.4) alone, (B) 50 mM Tris-HCl (pH 7.4) plus 2.5 mM $CaCl_2$ or (C) 50 mM Tris-HCl (pH 7.4) plus 5 mM $MgCl_2$ for 60 min at 30 °C. The bound and free radioactivity was separated by filtration and determined by liquid scintillation as described. Non-specific binding was determined in the presence of 1 mM GABA.

Na, K-ATPase; [^{3}H]ouabain binding

Sodium plus potassium-activated, oubain-dependent Na, K-ATPase (E.C. 3.6.1.3) was determined by "one-point" [^{3}H]ouabain binding assay according to Svoboda *et al.* (1988). Membranes (50 µg of protein) were incubated with 20 nM [^{3}H]ouabain in a total volume of 0.45 ml of 5 mM $NaHPO_4$, 5 mM $MgCl_2$, 50 mM Tris-HCl, pH 7.6 (Mg-Pi buffer) for 90 min at 30 °C. The bound and free radioactivity was separated by filtration through Whatman GF/B filters in Brandel cell harvester. Filters were washed 3× with 3 ml of ice-cold incubation buffer and placed in 4 ml of scintillation cocktail (CytoScint, ICN). Radioactivity remaining on filters was determined after 10 h at room temperature by liquid scintillation. Non-specific binding was determined in the presence of 1 µM unlabelled ouabain.

Statistical analysis

The significance of difference between the immunoblot signal determined in fetuses 1-day before the birth (100 %) and signals determined at different age intervals (PD1, PD2, PD5, PD9, PD10, PD15, PD25, PD35, PD42, PD47, PD90) was analyzed by one-way test of variance ANOVA followed by Bonferroni's *post-hoc* comparison test using GraphPad*Prism4*.

One-way ANOVA followed by Bonferroni's *post-hoc* comparison test was also used for statistical analysis of the difference of [^{3}H]CGP54626 and [^{3}H]ouabain binding to PM isolated from 1-, 15- and 90-day-old rats.

Protein determination

Lowry method was used for determination of membrane protein using bovine serum albumin (Sigma, Fraction V) as a standard. Data were calculated by fitting the calibration curve as a quadratic equation.

Results

Our previous results indicated an early functional maturation of $GABA_B$-R signaling cascade in rat brain cortex (Kagan *at al.* 2012). Agonists baclofen and SKF97541 exhibited significant efficiency (both potency and efficacy) already at PD2 and the highest number of $GABA_B$-R, determined as maximum binding capacity (B_{max}) for specific antagonist [^{3}H]CGP54626, was determined in 1-day-old animals (PD1). In older rats, the number of [^{3}H]CGP54626 binding sites was decreased, in contrast to agonist-stimulated G-protein activity, which was increased during the first two weeks of postnatal life. The maximum of agonist-stimulated G-protein activity, measured as baclofen- or SKF97541-stimulated [^{35}S]GTPγS binding, was observed on PD14-15. Maximum of [^{35}S]GTPγS binding was followed by continuous decrease of G-protein activity till the adulthood (90-day-old rats).

Immunoblot analysis of plasma membrane density of $GABA_B$-R1a, $GABA_B$-R1b, $GABA_B$-R2 and of the cognate, PTX-sensitive G-proteins performed in this work (Fig. 1 and 2) indicated that expression level of $GABA_B$-R1a, $GABA_B$-R1b, $GABA_B$-R2 and of all individual members of G_i/G_o family ($G_i1/G_i2\alpha$, $G_i3\alpha$, $G_o\alpha$, $G_z\alpha$[1] and Gβ subunit proteins) was high already around the birth, i.e. in fetuses 1 day before the birth (D-1) and in 1- and 2-day-old rats (PD1 and PD2). Subsequently, membrane density of $GABA_B$-R1a, $GABA_B$-R1b and $GABA_B$-R2 was decreased more or less in parallel till PD15 (Fig. 1). At this age interval, the $GABA_B$-R subunits represented 55±15 % ($GABA_B$-R1a), 70±17 % ($GABA_B$-R1b) and 51±5 % ($GABA_B$-R2) of the level detected in newborn rats, 100 %. In early postnatal period (up to PD15), PM expression level of $GABA_B$-R1b was lower than of $GABA_B$-R1a.

By contrast, the membrane density of all G-proteins ($G_i1/G_i2\alpha$, $G_i3\alpha$, $G_o\alpha$, $G_z\alpha$, $G_{12}\alpha$[1] and Gβ) was unchanged in the course of the whole postnatal period, i.e. between PD2 and PD90 (Fig. 2). Expressed in more detail, the immunoblot signals of all G-proteins in PM samples containing the same amount of protein (10 µg) and prepared from fetuses 1 day before the birth and 1-, 2-, 5-, 9-, 10-, 15-, 25-, 35-, 42-, 47- and 90-day-old rats, were the same, i.e. not statistically different when compared with the control signal in fetuses 1 day before

[1] Though being insensitive to PTX and thus unrelated to $GABA_B$-R, the ontogenetic profile of $G_{12}\alpha$ protein was also measured with the aim to obtain information about the important group of G-proteins regulating membrane traffic (Harhammer *et al.* 1994, 1996, Hildebrant *et al.* 1997). The developmental change of these proteins was similar to that of other G-proteins. The prenatal level was high and afterwards, it decreased slowly and continuously till the adulthood.

the birth, 100 %. Thus, there was a clear disparity between development of receptor and G-proteins functionally participating in $GABA_B$-R signaling cascade: membrane density of $GABA_B$-R subunit proteins was substantially decreased between the birth and "opening of eyes" period, while the cognate, trimeric G-proteins of Gi/Go family were unchanged.

In the second part of our work, we have extended our recent results (Kagan *et al.* 2012) and compared antagonist [^{3}H]CGP54626 binding in ion-free, 2.5 mM $CaCl_2$ and 5 mM $MgCl_2$ containing incubation media (Fig. 3) in PM isolated from 1-, 13- and 90-days old rats. The use of ion-free incubation medium was introduced by Ko *et al*. (2003) for determination of the number of μ-, δ- and κ-opioid receptors in monkey brain cortex and hypothalamus. Comparison of the level of [^{3}H]CGP54626 binding in these media was performed by a "one-point assay" at the constant concentration of 15 nM of this radioligand.

The decrease of [^{3}H]CGP54626 binding was noticed in all incubation media, however, due the low level of binding, this decrease was not significant in ion-free medium (Fig. 3). The highly significant decrease was measured in 2.5 mM $CaCl_2$ ($p<0.001$) and 5 mM $MgCl_2$ ($p<0.01$) containing media. Please note that the level of binding in 2.5 mM $CaCl_2$ was much higher that in 5 mM $MgCl_2$. This result reflects and may be interpreted as a natural consequence of the presence of 2.5 mM calcium in extracellular medium surrounding $GABA_B$-R ligand binding site located on $GABA_B$-R1 (Padgett and Slesinger 2010, Pinard *et al.* 2010) and is in agreement with the previous agonist binding studies of $GABA_B$-R in rat brain cortex synaptosomes (Bowery *et al.* 1983). The decrease of $GABA_B$-R1a, $GABA_B$-R1b and $GABA_B$-R2 subunits (Fig. 1) proceeded in parallel with the decrease of antagonist binding (Fig. 3). However, it was terminated at PD15, while antagonist binding was decreased further till the adulthood (PD90).

Postnatal development of $GABA_B$-R1, $GABA_B$-R2, G-proteins and ligand binding to $GABA_B$-R was substantially different from maturation of the prototypical plasma membrane marker, Na, K-ATPase (Fig. 4A,B). Membrane density of α-subunit of Na, K-ATPase was low at birth (PD1, PD2) and further development was reflected in a marked increase of this protein. The major increase occurred between the birth and PD25. Since this age interval, PM content of Na, K-ATPase was not significantly altered in PM isolated from 35-, 42- and

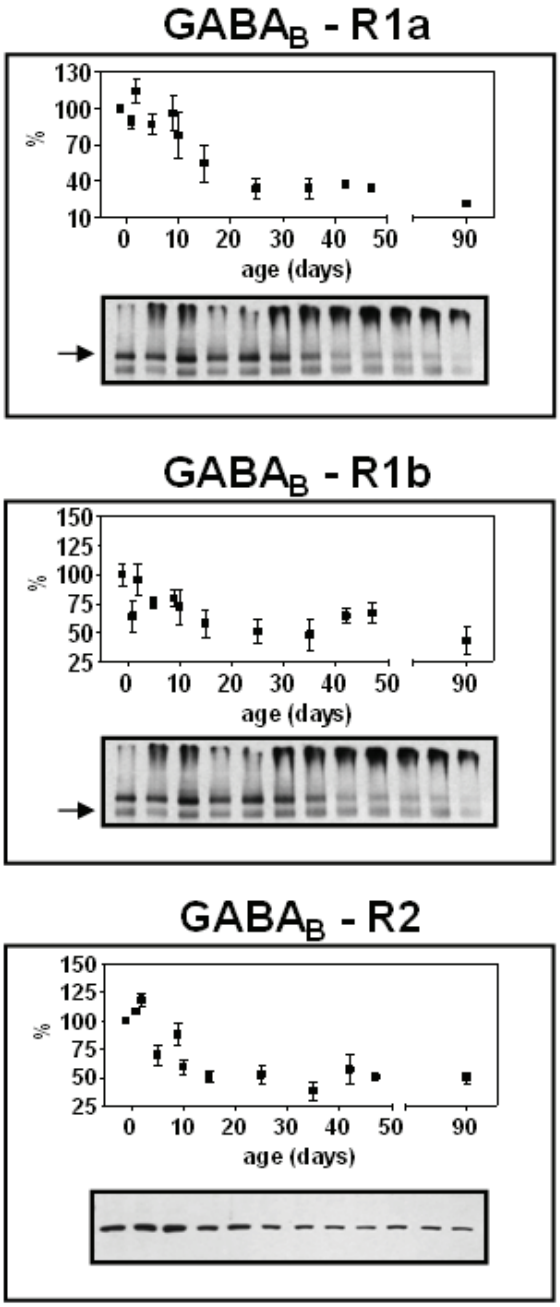

Fig. 1. Plasma membrane density of $GABA_B$-R1a, $GABA_B$-R1b, $GABA_B$-R2 subunit proteins; immunoblot analysis. PM proteins (10 μg per well) were resolved by Invitrogen NuPAGE system in 4-12 % gradient gel and identified by immunoblotting with specific antibodies as described in Methods. Data represent the average of five immunoblots ± SEM. Significance of the difference between the immunoblot signal determined in fetuses 1 day before the birth (D-1, 100 %) and signals determined at different ages (PD1, PD2, PD5, PD9, PD10, PD15, PD25, PD35, PD42, PD47, PD90) was analyzed by one-way ANOVA followed by Bonferroni's *post-hoc* comparison test using GraphPad*Prism4*. **$GABA_B$-R1a:** D-1 vs 15 (**, $P<0.01$), PD2 vs PD15 (**, $P<0.01$), PD2 vs PD90 (**, $P<0.01$), PD15 vs PD90 (NS, $P>0.05$). **$GABA_B$-R1b:** D-1 vs PD15 (NS, $P>0.05$), PD2 vs PD15 (NS, $P>0.05$), PD15 vs PD90 (NS, $P>0.05$), D-1 vs PD90 (**, $P<0.01$), PD2 vs PD90 (*, $P<0.05$). **$GABA_B$-R2:** D-1 vs PD15 (*, $P<0.05$), PD2 vs PD15 (**, $P< 0.01$), PD2 vs PD90 (**, $P< 0.01$), PD15 vs PD90 (NS, $P>0.05$).

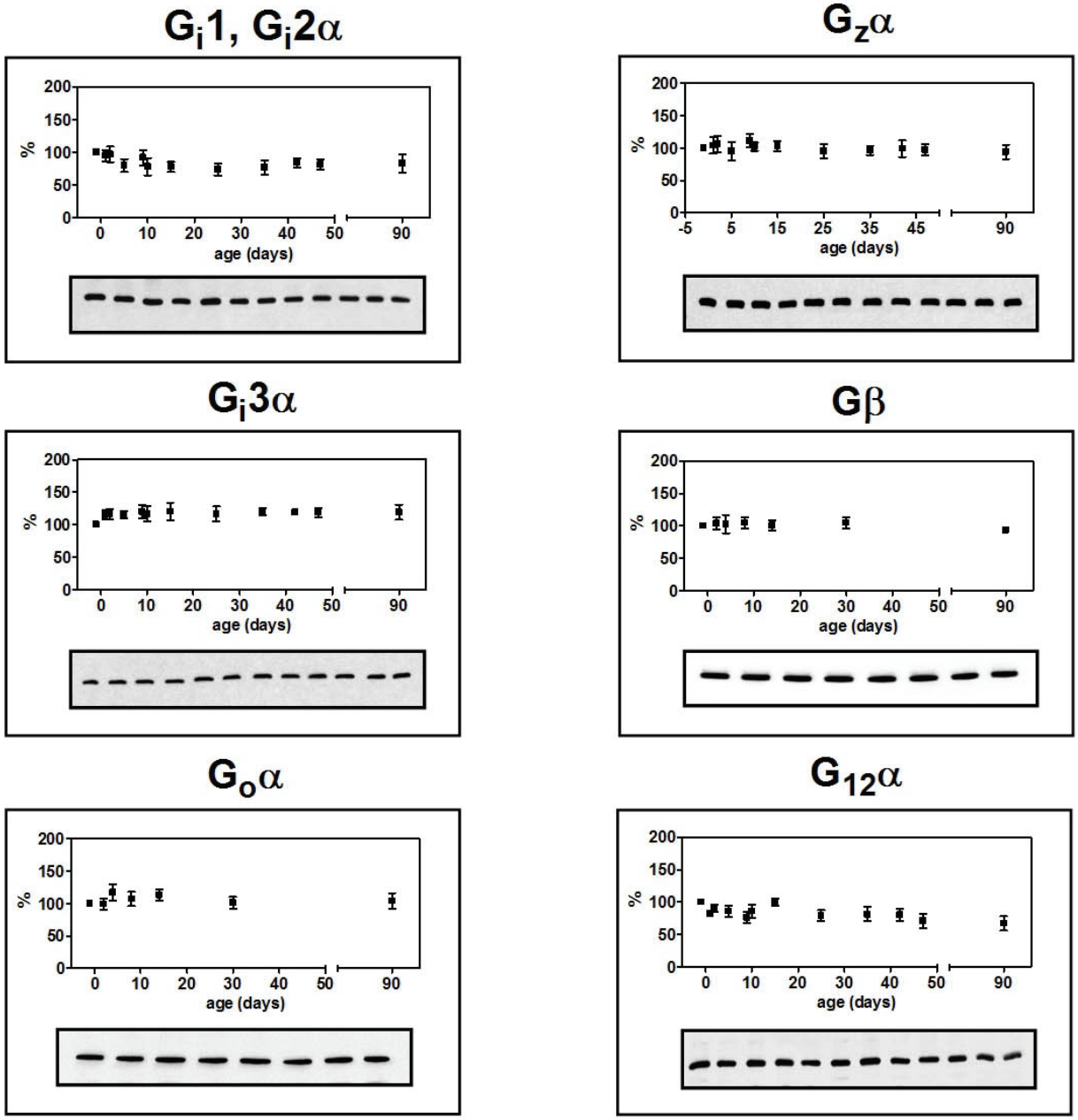

Fig. 2. Plasma membrane density of $G_i1/G_i2\alpha$, $G_i3\alpha$, $G_o\alpha$, $G_z\alpha$, $G\beta$ and $G_{12}\alpha$ subunit proteins; immunoblot analysis. The expression of G-proteins was analyzed in the same plasma membrane samples as those used for detection of $GABA_B$-R subunits. G-proteins were unchanged in the course of the whole postnatal period as there was no significant difference between immunoblot signals detected around the birth (D-1, PD1, PD2) and at all other ages: $G_i1/G_i2\alpha$ ($p>0.05$); $G_i3\alpha$ ($p>0.05$), $G_o\alpha$ ($p>0.05$), $G_z\alpha$ ($p>0.05$) and $G\beta$ ($p>0.05$) at all ages. $G_{12}\alpha$ was decreased between PD1 and PD90 (*, $p<0.05$).

90-day-old rats. The intensity of average immunoblot signal in adult rats (PD90) was 3.5-times higher than around the birth (day -1, PD1 and PD2).

Virtually the same results were obtained when selective inhibitor [^{3}H]ouabain was used for determination of Na, K-ATPase (Fig. 4C). The major increase of [^{3}H]ouabain binding in PM was noticed between the birth and PD25. Since PD25, the binding of this radioligand was not significantly different from the adult animals. [^{3}H]ouabain binding in 90-day-old rats (13.89 pmol.mg^{-1}) was 1.6x higher than in 15-day-old rats (8.64 pmol.mg^{-1}) and 2.6x higher than in fetuses 1 day before the birth (5.44 pmol.mg^{-1}). Thus, the overall maturation of brain cortex PM composition monitored by a developmental study of Na, K-ATPase molecules proceeds after the birth, while the level of $GABA_B$-signaling proteins is high at birth and further decreased ($GABA_B$-R) or unchanged (G-proteins).

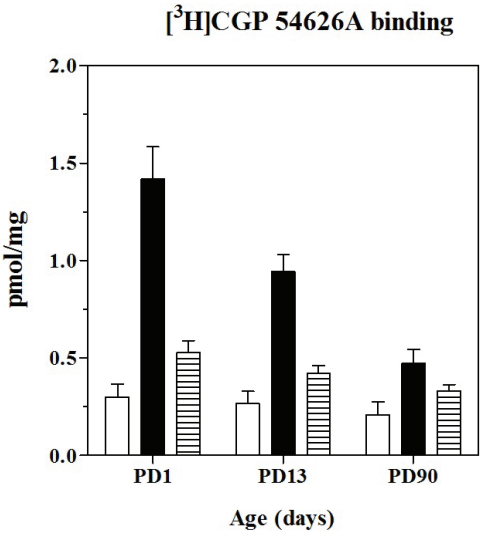

Fig. 3. Decrease of [^{3}H]CGP54626A binding in the course of postnatal ontogenesis. PM (100 μg protein per assay) isolated from 1-(PD1), 13-(PD13) and 90-(PD90)-day- old rats were incubated with 12 nM [^{3}H]CGP54626A in 50 mM Tris-HCl with no additions (□, open columns), in 50 mM Tris plus 2.5 mM $CaCl_2$ (■, full columns) or in 50 mM Tris-HCl plus 5 mM $MgCl_2$ (≡, hatched columns). Non-specific binding was determined in the presence of 1 mM GABA. Data represent the average of 3 binding assays performed in quadruplicates ± SEM. Comparison of binding data in PM isolated from PD1, PD13 and PD90 was performed by one-way ANOVA followed by Bonferroni's *post-hoc* comparison test. Open columns (□): PD1 versus PD13, NS, p>0.05; PD1 versus PD90, NS, p>0.05; PD13 versus PD90, NS, p>0.05. Full columns (■): PD1 versus PD13, **, p<0.01; PD1 versus PD90, ***, p<0.001; PD13 versus PD90, ***, p<0.001. Hatched columns (≡): PD1 versus PD13, NS, p>0.05; PD1 versus PD90, **, p<0.01; PD13 versus PD90, NS, p>0.05.

Discussion

In the brain, $GABA_B$-R-initiated signal transfer to G-proteins and from G-proteins to adenylyl cyclase (AC) represents a rather intricate trans-membrane process (Bormann 1988, Boege *et al.* 1991, Padgett and Slesinger 2010) because all its pivotal components occur in multiple isoforms with distinct functional properties, and the cognate G-proteins of G_i/G_o family exert both stimulatory and inhibitory effects on the overall AC activity, which represents the final outcome of the ten different isoenzymes, ACI-X (Backlund *et al.* 1988, Tang *et al.* 1992, Taussig *et al.* 1994, Simonds 1999, Sunahara and Taussig 2002). Our previous analysis of postnatal development of adenylyl cyclase in various brain areas indicated a marked activation of this enzyme in membranes prepared from 12-15-day-old rats (Ihnatovych *et al.* 2002b). The activity of the basal-, manganese-, fluoride-, GTP- and forskolin-stimulated AC was low at birth (PD1), increased sharply during the first two weeks of postnatal life, reached a maximum between

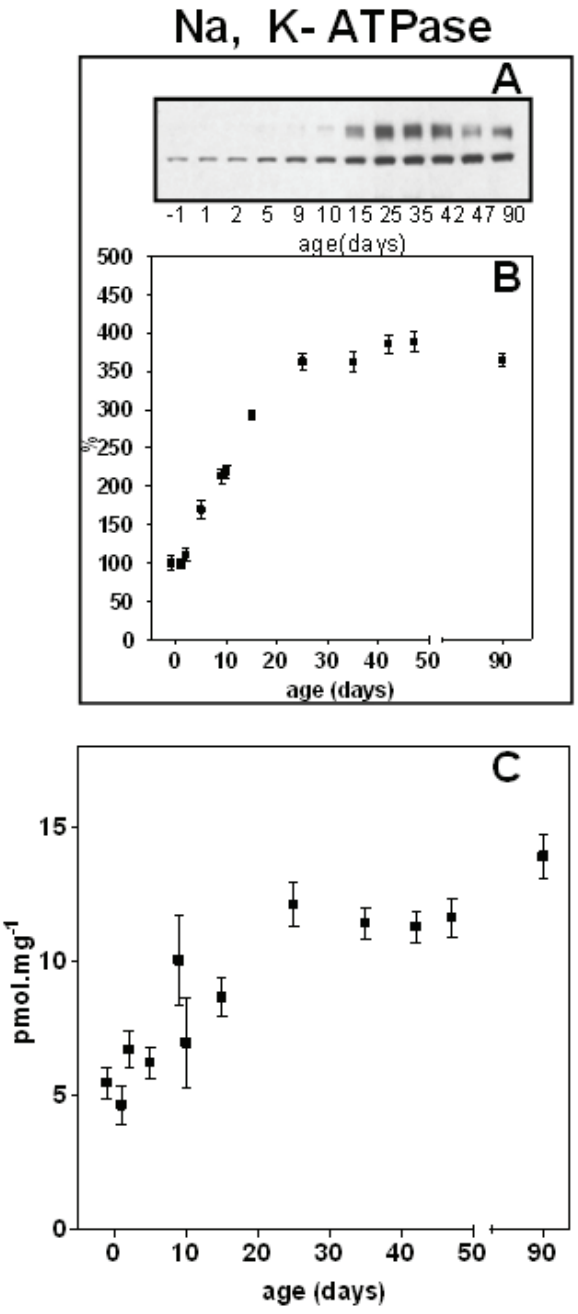

Fig. 4. Plasma membrane density of Na, K-ATPase; immunoblot analysis and [^{3}H]ouabain binding. Immunoblot detection of α-subunit of Na, K-ATPase was performed by polyclonal Ab (Santa Cruz, sc-28800). **(A)** Typical immunoblot. **(B)** Average of 5 immunoblots. The significance of the difference between the immunoblot signal determined in fetuses 1 day before the birth (100 %) and signals determined at different ages (PD1, PD2, PD5, PD9, PD10, PD15, PD25, PD35, PD42, PD47, PD90) was analyzed by one-way ANOVA followed by Bonferroni's test using GraphPad*Prism 4*. Since PD5, the increase of Na,K-ATPase was highly significant (**, p<0.01). **(C)** [^{3}H]ouabain binding was measured as described in Methods. Data represent the average ± SEM of three experiments performed in triplicates. Significance of the difference between the binding at different age intervals was analyzed by one-way ANOVA followed by Bonferroni's test: fetuses D-1 versus PD15 (*, p<0.05), D-1 versus PD25 (**, p<0.01), D-1 versus PD90 (**, p<0.01), PD15 versus PD25 (*, p<0.05), PD15 versus PD90 (**, p<0.01), PD25 versus PD90 (NS, p>0.05).

P12 and PD15 and then decreased to the level in 18-day-old rats. The maximum AC activities were roughly 4-times higher than those at birth. In older rats, AC activities were decreased further so that the level in adult animals (PD90) was about the same as that at birth (PD1). These results had also shown that there was a marked difference between the development of AC enzyme activity and protein content of individual AC isoforms. The immunoblot analysis indicated no significant change of ACI, but a continuous increase of ACII, IV and VI from PD1 to PD18. Since this age, membrane density of ACI, II, IV and VI was unchanged until the adulthood.

When considering other effectors of $GABA_B$-R but AC, presynaptic inhibition of voltage-gated Ca^{2+} channels (Ca_v) by $GABA_B$-R agonists has to be primarily considered (Dunlap and Fishbach 1981, Robertson and Taylor 1986, Dolphin 1990, 1991, Santos *et al.* 1995). Presynaptic inhibition of Ca_v by $GABA_B$-R agonists was demonstrated at early stages of postnatal development in rat somatosensory cortex at PD7 (Fukuda *et al.* 1993) and in hippocampus at PD6 (DiScenna *et al.* 1994). Postsynaptic $GABA_B$-receptors were found to be functioning in the cerebral cortex of rats only at postnatal day 17, i.e. 10 days later than presynaptic ones (Fukuda *et al.* 1993). It may be therefore suggested that the significant efficacy of baclofen and SKF97541 when activating G-proteins in newborn rat brain cortex (Kagan *et al.* 2012) is physiologically related to presynaptic inhibition of Ca_v channels mediated by G_o family of G-proteins. In accordance with this suggestion, PM density of $G_o\alpha$ and Gβ proteins was high already at PD1 and PD2 (Fig. 2).

G-protein regulated, inwardly rectifying potassium channels (GIRKs) represent another plausible candidate for interpretation of our data besides AC and voltage-gated Ca^{2+} channels (Ca_v). Activation of the $GABA_B$-R increases membrane conductance for potassium and reduces neuronal excitability by direct activation of the GIRK channels *via* free Gβγ subunits released from trimeric G-protein complex (Misgeld *et al.* 1995, Watts *et al.* 1996). The $GABA_B$-receptor was shown to be primarily K^+-linked in the hippocampus (Gahwiler and Brown 1985). GIRK channel activation by $G_{i/o}$-coupled GPCR results in hyperpolarization of the neuron and inhibition of neuronal activity (Dascal 1997). In this way, similarly to the $GABA_B$-Ca_V currents, the $GABA_B$-GIRK currents are considered as inhibitory ones. In similarity with $GABA_B$-R expression patterns, the $GABA_B$-GIRK currents have been identified in many brain regions including hippocampus, thalamus and cerebellum (Gahwiler and Brown 1985, Watts *et al.* 1996).

Functional characterization of individual $GABA_B$-R subunits in heterologous expression systems revealed a remarkable property of $GABA_B$-receptors: $GABA_B$-R1/$GABA_B$-R2 subunits must be co-expressed to form a functional $GABA_B$-receptor dimmer; when expressed individually, the subunits failed to form physiologically normal receptors (Jones *et al.* 1998, Couve *et al.* 1998, Kaupmann *et al.* 1998, Kuner *et al.* 1999, Galvez *et al.* 2001, Padgett and Slesinger 2010). It has been also discovered that the $GABA_B$-R1 subunit contains an endoplasmic reticulum (ER) retention signal, which prevents forward trafficking of this receptor subunit (Margeta-Mitrovic *et al.* 2000). Dimerization of $GABA_B$-R1 with the $GABA_B$-R2 shields ER retention signal and permits surface expression of both $GABA_B$-R1 and $GABA_B$-R2. Yeast two-hybrid analysis revealed that the C-terminus of $GABA_B$-R1 and $GABA_B$-R2 was an important pre-requisite for heterodimerization of these subunits (White *et al.* 1998). CD spectroscopic analysis of a 30 amino acid sequence in C-termini of these proteins revealed a coiled-coil domain between the $GABA_B$-R1 and $GABA_B$-R2, which was required for the subunit-specific formation of the functional receptor dimmer (Kammerer *et al.* 1999). Interestingly, the C-terminus of $GABA_B$-R2 subunit also regulates lateral diffusion of the receptor in hippocampal neurons suggesting that it helps to control receptor expression levels at the plasma membrane (Pooler and McIlhinney 2007).

In this work, the postnatal development of $GABA_B$-R1a, $GABA_B$-R1b and $GABA_B$-R2 was studied in plasma membranes isolated from brain cortex of rats of different ages by Western blotting. PM density of $GABA_B$-R1a, $GABA_B$-R1b and $GABA_B$-R2 was determined in parallel with trimeric Gα- and Gβ-subunits. Antagonist [^{3}H]CGP54626 binding was measured in the same membrane samples. Subsequently, data collected on $GABA_B$-R were compared with the ontogenetic profile of prototypical plasma membrane marker Na, K-ATPase, which was used as an indicator of general brain development.

The detailed immunoblot analysis clearly showed that PM density of all $GABA_B$-R subunits was high at the birth (in fetuses D-1, PD1 and PD2) and subsequently it was largely decreased till PD15 (Fig. 1).

The $GABA_B$-R subunits in PM isolated from 15-days-old rats represented 55 % ($GABA_B$-R1a), 70 % ($GABA_B$-R1b) and 51 % ($GABA_B$-R2) of the level in newborn rats (100 %), respectively. The postnatal decrease of $GABA_B$-R1b subunit was relatively smaller when compared with $GABA_B$-R1a and $GABA_B$-R2. The decrease of $GABA_B$-R1a, $GABA_B$-R1b and $GABA_B$-R2 was accompanied by a decrease in the number of antagonist [^{3}H]CGP54626 binding sites, which was demonstrated in the presence of both calcium (2.5 mM $CaCl_2$) and magnesium (5 mM $MgCl_2$) ions. The ion-free buffer, which has been successfully used in μ-, δ- and κ-opioid receptor binding assays (Ko *et al.* 2003), was impropriate for radioligad binding assays of $GABA_B$-R.

In accordance with our data, the high levels of $GABA_B$-R1a in synaptic membranes isolated from brain cortex were also detected in the first postnatal days by Malitschek *et al.* (1998) and Fritschy *et al.* (1999) and these high levels of $GABA_B$-R1a were subsequently decreased till the adulthood. Both authors also described the different expression pattern for $GABA_B$-R1a and $GABA_B$-R1b isoforms. $GABA_B$-R1b was less abundant at birth than $GABA_B$-R1a, slightly increasing at postnatal days 10-14 and then decreasing till adulthood. Marked increase (3x) of PM density of Na, K-ATPase molecules was fully consistent with developmental study of Na, K-ATPase activity indicating manifold increase (5x) in membranes prepared by sucrose-density gradient centrifugation from the whole rat brain (Samson and Quinn 1967).

Our data thus indicated that the functional maturation of $GABA_B$-R signaling pathway is not finished at birth, in spite of the fact that these receptors are expressed in high amount (Fig. 1) and exhibit considerable ability to activate G-proteins with maximum of baclofen-stimulated [^{35}S]GTPγS binding at PD14-15 (Kagan *et al.* 2012). Increase of [^{35}S]GTPγS binding between the birth and PD14-15 was followed by a decrease in 18-day-old rats and further decrease till the adulthood (PD90). Accordingly, the peak value of [^{3}H]GABA binding was detected at PD14 in rat brain cortical slices by quantitative autoradiography and this high level of [^{3}H]GABA binding subsequently declined to the adult level (Turgeon and Albin 1994).

Contrarily, membrane density of all members of Gi/Go family of G-proteins was unchanged in the course of the whole postnatal development. The explanation why the "average" G-protein level in PM is unchanged in spite of the major change of G-protein function characterized by the peak level of baclofen- or SKF97541-stimulated [^{35}S]GTPγS binding at PD14-15 (Kagan *et al.* 2011), is unknown at present. It may be related to signaling *via* other effectors than AC (Ca_v and GIRKs); it may also reflect the fact that the data collected in mixture of all PM fragments do not reveal heterogeneities of protein composition in different PM compartments denominated as membrane domains/rafts (Moffett *et al.* 2000, Becher *et al.* 2001, 2004).

Conclusions

Our data indicate that the full complement of $GABA_B$-receptor protein molecules and cognate G-proteins exists in rat brain cortex already at birth. Functional maturation of $GABA_B$-R cascade in the course of the first two weeks of postnatal life was associated with a parallel decrease of plasma membrane density of $GABA_B$-R1a (55±15 %) and $GABA_B$-R2 (51±5 %) subunits; $G_i1/G_i2\alpha$, $G_i3\alpha$, $G_o\alpha$, $G_z\alpha$, $G_{12}\alpha$ and Gβ, $GABA_B$-R1b proteins were unchanged. Decrease of $GABA_B$-R subunits proceeded together with the decrease of antagonist [^{3}H]CGP54626 binding measured in ion-free, 2.5 mM $CaCl_2$ or 5 mM $MgCl_2$. The age interval between PD1 and PD14-15 represents the critical period for structural as well as functional maturation of $GABA_B$-R signaling cascade in rat brain cortex plasma membranes.

Conflict of Interest

There is no conflict of interest.

Acknowledgements

This work was supported by the GACR (P207/12/0919 and P304/12/G069) and by the Academy of Sciences of the Czech Republic (RVO: 67985823).

Abbreviations

Baclofen, β-p-chlorophenyl-GABA; Ca_v, voltage-dependent calcium channels; GABA, γ-aminobutyric acid; $GABA_B$-R, metabotropic receptor for GABA; GIRKs, inwardly rectifying potassium channels; GPCR, G-protein-coupled receptor; G-proteins, heterotrimeric guanine nucleotide-binding regulatory proteins; $G_s\alpha$, G-protein stimulating adenylyl cyclase activity; $G_i/G_o\alpha$, G-proteins inhibiting adenylyl cyclase activity in pertussis-toxin sensitive manner; $G_q/G_{11}\alpha$, G-proteins stimulating phoshoplipase C in pertussis-toxin independent manner; [^{35}S]GTPγS, guanosine-5′-[γ-^{35}S]

triphosphate; PD, postnatal day; P_i, inorganic phosphate; PMSF, phenylmethylsulfonyl fluoride; PTX, pertussis toxin; SKF 97541, aminopropyl (methyl) phosphinic acid; w.w., wet weight.

References

ASANO T, KAMIYA N, MORISHITA R, KATO K: Immunoassay for the beta gamma subunits of GTP-binding proteins and their regional distribution in bovine brain. *J Biochem* **103**: 950-953, 1988.

BACKLUND PS, AKSAMIT RR, UNSON CG, GOLDSMITH P, SPIEGEL AM, MILLIGAN G: Immunochemical and electrophoretic characterization of the major pertussis toxin substrate of the RAW264 macrophage cell line. *Biochemistry* **27**: 2040-2046, 1988.

BARRAL J, TORO S, GALARRAGA E, BARGAS J: GABAergic presynaptic inhibition of rat neostriatal afferents is mediated by Q-type Ca(2+) channels. *Neurosci Lett* **283**: 33-36, 2000.

BECHER A, GREEN A, IGE AO, WISE A, WHITE JH, MCILHINNEY RA: Ectopically expressed gamma-aminobutyric acid receptor B is functionally down-regulated in isolated lipid raft-enriched membranes. *Biochem Biophys Res Commun* **321**: 981-987, 2004.

BECHER A, WHITE JH, MCILHINNEY RAJ: The gamma-aminobutyric acid receptor B, but not the metabotropic glutamate receptor type-1, associates with lipid rafts in the rat cerebellum. *J Neurochem* **79**: 787-795, 2001.

BOEGE F, NEUMANN E, HELMREICH EJ: Structural heterogeneity of membrane receptors and GTP-binding proteins and its functional consequences for signal transduction. *Eur J Biochem* **199**: 1-15, 1991.

BORMANN J: Electrophysiology of GABAA and GABAB receptor subtypes. *Trends Neurosci* **11**: 112-116, 1988.

BOUROVA L, STOHR J, LISY V, RUDAJEV V, NOVOTNY J, SVOBODA P: Isolation of plasma membrane compartments from rat brain cortex; detection of agonist-stimulated G protein activity. *Med Sci Monit* **15**: BR111-BR122, 2009.

BOWERY NG, HILL DR, HUDSON AL: Characteristics of GABA B receptor binding sites on rat whole brain synaptic membranes. *Br J Pharmacol* **78**: 191-206, 1983.

BOWERY NG, HILL DR, HUDSON AL: [3H](-)Baclofen: an improved ligand for GABAB sites. *Neuropharmacology* **24**: 207-210, 1985.

BOWERY NG, HUDSON AL, PRICE GW: $GABA_A$ and $GABA_B$ receptor site distribution in the rat central nervous system. *Neuroscience* **20**: 365-383, 1987.

BRAY P, CARTER A, SIMONS C, GUO V, PUCKETT C, KAMHOLZ J, SPIEGEL A, NIRENBERG M: Human cDNA clones for four species of G alpha s signal transduction protein. *Proc Natl Acad Sci USA* **83**: 8893-8897, 1986.

BUSSIÈRES N, EL MANIRA A: GABA(B) receptor activation inhibits N- and P/Q-type calcium channels in cultured lamprey sensory neurons. *Brain Res* **847**: 175-185, 1999.

CHEN G, VAN DEN POL AN: Presynaptic GABAB autoreceptor modulation of P/Q-type calcium channels and GABA release in rat suprachiasmatic nucleus neurons. *J Neurosci* **18**: 1913-1922, 1998.

COUVE A, FILIPPOV AK, CONNOLLY CN, BETTLER B, BROWN DA, MOSS SJ: Intracellular retention of recombinant GABAB receptors. *J Biol Chem* **273**: 26361-26367, 1998.

DASCAL N: Signaling via the G protein-activated K^+ channels. *Cell Signal* **9**: 551-573, 1997.

DISCENNA PG, NOWICKY AV, TEYLER TJ: The development of GABAB-mediated activity in the rat dentate gyrus. *Brain Res Dev Brain Res* **77**: 295-298, 1994.

DOLPHIN AC: G protein modulation of calcium currents in neurons. *Annu Rev Physiol* **52**: 243-255, 1990.

DOLPHIN AC: Regulation of calcium channel activity by GTP binding proteins and second messengers. *Biochim Biophys Acta* **1091**: 68-80, 1991.

DUNLAP K, FISCHBACH GD: Neurotransmitters decrease the calcium conductance activated by depolarization of embryonic chick sensory neurones. *J Physiol* **317**: 519-535, 1981.

FERNÁNDEZ-ALACID L, AGUADO C, CIRUELA F, MARTÍN R, COLÓN J, CABAÑERO MJ, GASSMANN M, WATANABE M, SHIGEMOTO R, WICKMAN K, BETTLER B, SÁNCHEZ-PRIETO J, LUJÁN R: Subcellular compartment-specific molecular diversity of pre- and post-synaptic GABA-activated GIRK channels in Purkinje cells. *J Neurochem* **110**: 1363-1376, 2009.

FRITSCHY J-M, MESKENAITE V, WEINMANN O, HONER M, BENKE D, MOHLER H: $GABA_B$-receptor splice variants GB1a and GB1b in rat brain: developmental regulation, cellular distribution and extrasynaptic localization. *Eur J Neurosci* **11**: 761-768, 1999.

FUKUDA A, MODY I, PRINCE DA: Differential ontogenesis of presynaptic and postsynaptic GABAB inhibition in rat somatosensory cortex. *J Neurophysiol* **70**: 448-452, 1993.

GÄHWILER BH, BROWN DA: $GABA_B$-receptor-activated K^+ current in voltage-clamped CA3 pyramidal cells in hippocampal cultures. *Proc Natl Acad Sci USA* **82**: 1558-1562, 1985.

GALVEZ T, DUTHEY B, KNIAZEFF J, BLAHOS J, ROVELLI G, BETTLER B, PREZEAU L, PIN J-P: Allosteric interactions between GB1 and GB2 subunits are required for optimal $GABA_B$ receptor function. *EMBO J* **20**: 2152-2159, 2001.

GERHARDT MA, NEUBIG RR: Multiple Gi protein subtypes regulate a single effector mechanism. *Mol Pharmacol* **40**: 707-711, 1991.

GIERSCHIK P, MILLIGAN G, PINES M, GOLDSMITH P, CODINA J, KLEE W, SPIEGEL A: Use of specific antibodies to quantitate the guanine nucleotide-binding protein Go in brain. *Proc Natl Acad Sci USA* **83**: 2258-2262, 1986.

GOLDSMITH P, BACKLUND PSJ, ROSSITER K, CARTER A, MILLIGAN G, UNSON CG, SPIEGEL A: Purification of heterotrimeric GTP-binding proteins from brain: identification of a novel form of Go. *Biochemistry* **27**: 7085-7090, 1988.

GOLDSMITH P, GIERSCHIK P, MILLIGAN G, UNSON CG, VINITSKY R, MALECH HL, SPIEGEL AM: Antibodies directed against synthetic peptides distinguish between GTP-binding proteins in neutrophil and brain. *J Biol Chem* **262**: 14683-14688, 1987.

GUDERMANN T, SCHÖNEBERG T, SCHULTZ G: Functional and structural complexity of signal transduction via G-protein-coupled receptors. *Annu Rev Neurosci* **20**: 399-427, 1997.

HARHAMMER R, NÜRNBERG B, HARTENECK C, LEOPOLDT D, EXNER T, SCHULTZ G: Distinct biochemical properties of the native members of the G12 G-protein subfamily. Characterization of G alpha 12 purified from rat brain. *Biochem J* **319**: 165-171, 1996.

HARHAMMER R, NÜRNBERG B, SPICHER K, SCHULTZ G: Purification of the G-protein G13 from rat brain membranes. *Biochem J* **303**: 135-140, 1994.

HILDEBRANDT JD: Role of subunit diversity in signaling by heterotrimeric G proteins. *Biochem Pharmacol* **54**: 325-339, 1997.

HILL DR, BOWERY NG: 3H-baclofen and 3H-GABA bind to bicuculline-insensitive GABAB sites in rat brain. *Nature* **290**: 149-152, 1981.

IHNATOVYCH I, NOVOTNY J, HAUGVICOVA R, BOUROVA L, MARES P, SVOBODA P: Opposing changes of trimeric G protein levels during ontogenetic development of rat brain. *Brain Res Dev Brain Res* **133**: 57-67, 2002a.

IHNATOVYCH I, NOVOTNY J, HAUGVICOVA R, BOUROVA L, MARES P, SVOBODA P: Ontogenetic development of G protein-mediated adenylyl cyclase signaling in rat brain. *Brain Res Dev Brain Res* **133**: 69-75, 2002b.

JONES KA, BOROWSKY B, TAMM JA, DOUGLAS AC, DURKIN MM, DAI M, YAO WJ, JOHNSON M, GUNWALDSEN C, HUANG LY, TANG C, SHEN Q, SALON JA, MORSE K, LAZ T, SMITH KE, NAGARATHNAM D, NOBLE SA, BRANCHEK TA, GERALD C: GABAB receptors function as a heteromeric assembly of the subunits GABAB R1 and GABAB R2. *Nature* **396**: 674-678, 1998.

KAGAN D, DLOUHA K, ROUBALOVA L, SVOBODA P: Ontogenetic development of GABA(B)-receptor signaling cascade in plasma membranes isolated from rat brain cortex; the number of GABA(B)-receptors is high already shortly after the birth. *Physiol Res* **61**: 629-635, 2012.

KAMMERER RA, FRANK S, SCHULTHESS T, LANDWEHR R, LUSTIG A, ENGEL J: Heterodimerization of a functional GABAB receptor is mediated by parallel coiled-coil alpha-helices. *Biochemistry* **38**: 13263-13269, 1999.

KAUPMANN K, MALITSCHEK B, SCHULER V, HEID J, FROESTL W, BECK P, MOSBACHER J, BISCHOFF S, KULIK A, SHIGEMOTO R, KARSCHIN A, BETTLER B: GABAB-receptor subtypes assemble into functional heteromeric complexes. *Nature* **396**: 683-687, 1998.

KERR DI, ONG J: $GABA_B$ receptors. *Pharmacol Ther* **67**: 187-246, 1995.

KO MC, LEE H, HARRISON C, CLARK MJ, SONG HF, NAUGHTON NN, WOODS JH, TRAYNOR JR: Studies of mu-, kappa-, and delta-opioid receptor density and G protein activation in the cortex and thalamus of monkeys. *J Pharmacol Exp Ther* **306**: 179-186, 2003.

KUNER R, KÖHR G, GRÜNEWALD S, EISENHARDT G, BACH A, KORNAU HC: Role of heteromer formation in GABAB receptor function. *Science* **283**: 74-77, 1999.

LADERA C, DEL CARMEN GODINO M, JOSÉ CABAÑERO M, TORRES M, WATANABE M, LUJÁN R, SÁNCHEZ-PRIETO J: Pre-synaptic GABA receptors inhibit glutamate release through GIRK channels in rat cerebral cortex. *J Neurochem* **107**: 1506-1517, 2008.

MALITSCHEK B, RÜEGG D, HEID J, KAUPMANN K, BITTIGER H, FRÖSTL W, BETTLER B, KUHN R: Developmental changes of agonist affinity at $GABA_BR1$ receptor variants in rat brain. *Mol Cell Neurosci* **12**: 56-64, 1998.

MARGETA-MITROVIC M, JAN YN, JAN LY: A trafficking checkpoint controls GABA (B) receptor heterodimerization. *Neuron* **27**: 97-106, 2000.

MILLIGAN G: Techniques used in the identification and analysis of function of pertussis toxin-sensitive guanine nucleotide binding proteins. *Biochem J* **255**: 1-13, 1988.

MILLIGAN G: Immunological probes and the identification of guanine nucleotide-binding proteins. In: *G Proteins as Mediators of Cellular Signaling Processes*. HOUSLAY MD, MILLIGAN G (eds), John Wiley & Sons. Ltd., New York, 1990, pp 31-46.

MILLIGAN G: Regional distribution and quantitative measurement of the phosphoinositidase C-linked guanine nucleotide binding proteins G11 alpha and Gq alpha in rat brain. *J Neurochem* **61**: 845-851, 1993.

MISGELD U, BIJAK M, JAROLIMEK W: A physiological role for GABAB receptors and the effects of baclofen in the mammalian central nervous system. *Prog Neurobiol* **46**: 423-462, 1995.

MOFFETT S, BROWN DA, LINDER ME: Lipid-dependent targeting of G proteins into rafts. *J Biol Chem* **275**: 2191-2198, 2000.

MUMBY S, PANG IH, GILMAN AG, STERNWEIS PC: Chromatographic resolution and immunologic identification of the alpha 40 and alpha 41 subunits of guanine nucleotide-binding regulatory proteins from bovine brain. *J Biol Chem* **263**: 2020-2026, 1988.

PADGETT CL, SLESINGER PA: $GABA_B$ receptor coupling to G-proteins and ion channels. *Adv Pharmacol* **58**: 123-147, 2010.

PÉREZ-GARCI E, GASSMANN M, BETTLER B, LARKUM ME: The GABAB1b isoform mediates long-lasting inhibition of dendritic Ca2+ spikes in layer 5 somatosensory pyramidal neurons. *Neuron* **50**: 603-616, 2006.

PINARD A, SEDDIK R, BETTLER B: $GABA_B$ receptors: physiological functions and mechanisms of diversity. *Adv Pharmacol* **58**: 231-255, 2010.

POOLER AM, MCILHINNEY RA: Lateral diffusion of the $GABA_B$ receptor is regulated by the $GABA_{B2}$ C terminus. *J Biol Chem* **282**: 25349-25356, 2007.

RAYMOND JR: Multiple mechanisms of receptor-G protein signaling specificity. *Am J Physiol* **269**: F141-F158, 1995.

ROBERTSON B, TAYLOR WR: Effects of gamma-aminobutyric acid and (-)-baclofen on calcium and potassium currents in cat dorsal root ganglion neurones in vitro. *Br J Pharmacol* **89**: 661-672, 1986.

SAKABA T, NEHER E: Direct modulation of synaptic vesicle priming by GABA(B) receptor activation at a glutamatergic synapse. *Nature* **424**: 775-778, 2003.

SAMSON FE, QUINN DJ: Na+-K+-activated ATPase in rat brain development. *J Neurochem* **14**: 421-427, 1976.

SANTOS AE, CARVALHO CM, MACEDO TA, CARVALHO AP: Regulation of intracellular [Ca2+] and GABA release by presynaptic GABAB receptors in rat cerebrocortical synaptosomes. *Neurochem Int* **27**: 397-406, 1995.

SIMONDS WF: G protein regulation of adenylate cyclase. *Trends Pharmacol Sci* **20**: 66-73, 1999.

SUNAHARA RK, TAUSSIG R: Isoforms of mammalian adenylyl cyclase: multiplicities of signaling. *Mol Interv* **2**: 168-184, 2002.

SVOBODA P, AMLER E, TEISINGER J: Different sensitivity of ATP +Mg+Na (I) and Pi+Mg (II) dependent types of oubain binding to phospholipase A2. *J Membr Biol* **104**: 211-221, 1988.

TANG WJ, IÑIGUEZ-LLUHI JA, MUMBY S, GILMAN AG: Regulation of mammalian adenylyl cyclases by G-protein alpha and beta gamma subunits. *Cold Spring Harb Symp Quant Biol* **57**: 135-144, 1992.

TAUSSIG R, TANG WJ, HEPLER JR, GILMAN AG: Distinct patterns of bidirectional regulation of mammalian adenylyl cyclases. *J Biol Chem* **269**: 6093-6100, 1994.

TURGEON SM, ALBIN RL: Postnatal ontogeny of $GABA_B$ binding in rat brain. *Neuroscience* **62**: 601-613, 1994.

UJCIKOVA H, DLOUHA K, ROUBALOVA L, VOSAHLIKOVA M, KAGAN D, SVOBODA P: Up-regulation of adenylylcyclases I and II induced by long-term adaptation of rats to morphine fades away 20 days after morphine withdrawal. *Biochim Biophys Acta* **1810**: 1220-1229, 2011.

WATTS AE, WILLIAMS JT, HENDERSON G: Baclofen inhibition of the hyperpolarization-activated cation current, Ih, in rat substantia nigra zona compacta neurons may be secondary to potassium current activation. *J Neurophysiol* **76**: 2262-2270, 1996.

WHITE JH, WISE A, MAIN MJ, GREEN A, FRASER NJ, DISNEY GH, BARNES AA, EMSON P, FOORD SM, MARSHALL FH: Heterodimerization is required for the formation of a functional GABA(B) receptor. *Nature* **396**: 679-682, 1998.

XU J, WOJCIK WJ: Gamma aminobutyric acid B receptor-mediated inhibition of adenylate cyclase in cultured cerebellar granule cells: blockade by islet-activating protein. *J Pharmacol Exp Ther* **239**: 568-573, 1986.

Physiol. Res. 61: 629-635, 2012

Ontogenetic Development of $GABA_B$-Receptor Signaling Cascade in Plasma Membranes Isolated From Rat Brain Cortex; the Number of $GABA_B$-Receptors Is High Already Shortly After the Birth

D. KAGAN[1], K. DLOUHÁ[1], L. ROUBALOVÁ[1], P. SVOBODA[1]

[1]Institute of Physiology, Academy of Sciences of the Czech Republic, Prague, Czech Republic

Received March 19, 2012
Accepted July 23, 2012
On-line October 25, 2012

Summary

Our data indicate the significant intrinsic efficacy of $GABA_B$-receptors in rat brain cortex already at birth (PD1, PD2). Subsequently, baclofen- and SKF97541-stimulated G-protein activity, measured by agonist-stimulated, high-affinity [^{35}S]GTPγS binding assay, was increased; the highest level of both baclofen and SKF97541-stimulated [^{35}S]GTPγS binding was detected between PD10 and PD15. In older rats, baclofen- and SKF97541-stimulated [^{35}S]GTPγS binding was continuously decreased so, that the level in adult, 90-days old animals, was not different from that in newborn animals. The potency of G-protein response to baclofen (characterized by EC_{50} values) was also high at birth but unchanged by further postnatal development. An individual variance among different agonists was observed in this respect as the potency of SKF97541 response was decreased between the birth and adulthood. Accordingly, the highest plasma membrane density of $GABA_B$-R, determined by saturation binding assay with antagonist [^{3}H]CGP54626, was measured in 1-day old animals (2.27±0.08 pmol · mg^{-1}). The further development was reflected in a decrease of [^{3}H]CGP54626 binding as the B_{max} values of 1.38±0.05 and 0.93±0.04 pmol · mg^{-1} were determined in PM isolated from 13- and 90-days old rats, respectively.

Key words

Postnatal development • $GABA_B$-receptor • G-protein coupling/ activation • Baclofen • SKF97541

Corresponding author

P. Svoboda, Institute of Physiology, Academy of Sciences of the Czech Republic, Vídeňská 1083, 142 20 Prague 4, Czech Republic. Fax: + 420 24106 2488. E-mail: svobodap@biomed.cas.cz

Introduction

Historically, $GABA_B$ receptors were pharmacologically distinguished from $GABA_A$ receptors as bicuculline-insensitive GABA binding sites for which agonist is (-)-baclofen (Hill and Bowery 1981, Bowery *et al.* 1983, 1985, 1989, 1993, Hill *et al.* 1984, Hill 1985). After discovery of specific antagonists, $GABA_B$ receptors were defined as a class of bicuculline-insensitive GABA receptors for which (-)-baclofen is a specific agonist and phaclofen and 2-hydroxy-saclofen are specific antagonists (Kerr and Ong 1995). Later, more potent agonist SKF97541 was introduced and electrophysiologically characterized at pre- and postsynaptic binding sites on neurons in rat brain slices (Seabrook *et al.* 1990). $GABA_B$-receptors are not physically bound to an ionic channel and belong to the family of G-protein-coupled receptors, GPCRs (Bowery *et al.* 1983, 1985, 1989, 1993, Kerr and Ong 1995). Thus, the signal initiated by binding of GABA to these receptors is transmitted further downstream by trimeric G-proteins.

$GABA_B$-R agonist stimulation of G-protein activity (measured as high-affinity [^{35}S]GTPγS binding or [^{32}P-γ]GTPase assays) was important experimental evidence indicating that the effect of $GABA_B$-R agonists is mediated *via* trimeric G-proteins (Bowery *et al.* 1983, 1985, 1989, 1993). Close correlation between distribution of baclofen-stimulated GTPase activity and regional distribution of $GABA_B$-receptors in rat brain supported this idea. Furthermore, baclofen-stimulated GTPase *in vitro* was significantly inhibited by pertussis toxin (PTX) and specific antipeptide antisera oriented against $G_i\alpha$

subunit proteins (Sweeney and Dolphin 1992). Electrophysiological studies using specific antisera indicated that both PTX-sensitive $G_i\alpha$ and $G_o\alpha$ subunit proteins were activated by $GABA_B$-R agonists (Dolphin 1990, 1991).

With the aim to understand the maturation of $GABA_B$-R signaling cascade more fully, the early postnatal development of functional coupling between $GABA_B$-R and the cognate G-proteins was studied in plasma membranes isolated from rat brain cortex. The dose-response curves of the two potent agonists baclofen and SKF97541 were determined by high-affinity [^{35}S]GTPγS binding assay and compared in rats of different ages; the number of $GABA_B$-R was determined by saturation binding assay with specific antagonist [^{3}H]CGP54626.

Methods

Materials

$GABA_B$-receptor agonists baclofen (β-p-chlorophenyl-GABA), SKF97541 [3-aminopropyl (methyl) phosphinic acid] and antagonist [^{3}H]CGP54626 (41.5 Ci/mmol, cat. no. R1088) were purchased from Tocris. [^{35}S]GTPγS (1250 Ci/mmol) was from Perkin-Elmer (NEG030H). Complete protease inhibitor cocktail was from Roche Diagnostic (cat. no. 1697498). All other chemicals were of highest quality available.

Isolation of plasma membrane-enriched fraction from rat brain cortex

The experiments were approved by Animal Care and Use Committee of the Institute of Physiology, Academy of Sciences of the Czech Republic to be in agreement with Animal Protection Law of the Czech Republic as well as European Community Council directives 86/609/EEC.

Rat brain cortex was minced with razor blade on pre-cooled plate and diluted in STEM medium containing 250 mM sucrose, 20 mM Tris-HCl, 3 mM $MgCl_2$, 1 mM EDTA, pH 7.6, fresh 1 mM PMSF plus protease inhibitor cocktail. It was then homogenized mildly in loosely-fitting Teflon-glass homogenizer for 5 min (2 g w.w. per 10 ml) and centrifuged for 5 min at 3500 rpm. Resulting post-nuclear supernatant (PNS) was filtered through Nylon nets of decreasing size (330, 110 and 75 mesh, Nitex) and applied on top of Percoll in Beckman Ti70 tubes (30 ml of 27.4 % Percoll in STE medium). Centrifugation for 60 min at 30000 rpm (65000 x g) resulted in the separation of two clearly visible layers (Bourova *et al.* 2009). The upper layer represented plasma membrane fraction (PM); the lower layer contained mitochondria (MITO). The upper layer was removed, diluted 1:3 in STEM medium and centrifuged in Beckman Ti70 rotor for 90 min at 50000 rpm (175000 x g). Membrane sediment was removed from the compact, gel-like sediment of Percoll, re-homogenized by hand in a small volume of 50 mM Tris-HCl, 3 mM $MgCl_2$, 1 mM EDTA, pH 7.4 (TME medium), snap frozen in liquid nitrogen and stored at –80 °C.

Agonist-stimulated [^{35}S]GTPγS binding
Dose-response curves

Membranes prepared from 2-, 14- and 90-day-old rats of selected ages were incubated with (total binding, B_{total}) or without (basal binding, B_{basal}) increasing concentrations of $GABA_B$-R agonists baclofen and SKF97541 (10^{-10}-10^{-3} M) in final volume of 100 µl of reaction mix containing 20 mM HEPES, pH 7.4, 3 mM $MgCl_2$, 100 mM NaCl, 20 µM GDP, 0.2 mM ascorbate and [^{35}S]GTPγS (about 100-200,000 dpm per assay) for 30 min at 30 °C. The binding reaction was terminated by dilution with 3 ml of ice-cold 20 mM HEPES, pH 7.4, 3 mM $MgCl_2$ and filtration through Whatman GF/C filters on Brandel cell harvester. Radioactivity remaining on the filters was determined by liquid scintillation using Rotiszcint Eco Plus cocktail. Non-specific binding was determined in parallel assays containing 10 µM unlabelled GTPγS. Data were analyzed by GraphPad Prism 4 (GraphPad Software, San Diego, CA, USA) and B_{basal}, B_{max} and EC_{50}, values calculated according to the method of least-squares by fitting the data with sigmoidal dose-response curve.

"One-point assay"

With the aim to screen PM prepared from all age intervals under the same assay conditions, membranes (20 µg protein per assay) were incubated with ($B_{agonist}$) or without (B_{basal}) 1 mM baclofen or 100 µM SKF97541 in final volume of 100 µl of reaction mix containing 20 mM HEPES, pH 7.4, 3 mM $MgCl_2$, 20 µM GDP, 0.2 mM ascorbate and [^{35}S]GTPγS (1-2 nM) for 30 min at 30 °C. The binding reaction was discontinued by dilution with 3 ml of ice-cold 2 mM HEPES, pH 7.4, 0.15 mM $MgCl_2$ and immediate filtration through Whatman GF/C filters on Brandel cell harvester. Radioactivity remaining on the filters was determined by liquid scintillation using Rotiszcint Eco Plus cocktail. Non-specific GTPγS binding was determined in parallel assays containing

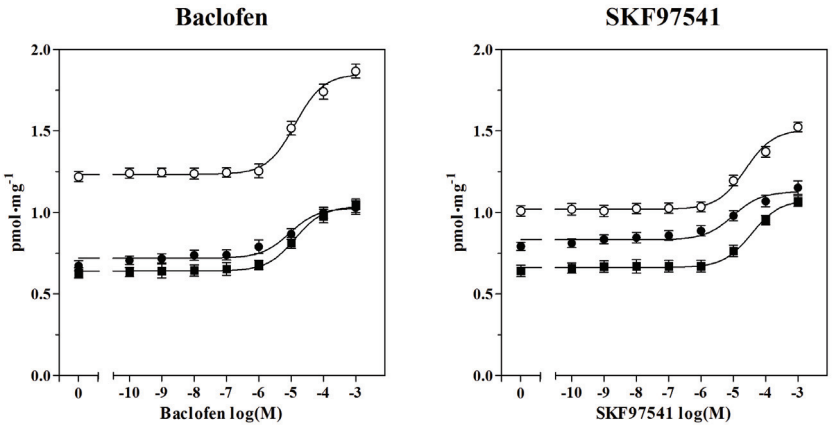

Fig. 1. Dose-response curves of baclofen and SKF97541-stimulated [^{35}S]GTPγS binding in PM isolated from 2-, 14- and 90-day-old rats. PM were isolated in parallel from brain cortex of 2 (●)-, 14 (○)- and 90 (■)-day-old rats and the high-affinity [^{35}S]GTPγS binding was measured in the presence of increasing concentrations of GABA$_B$-R agonists (-)-baclofen (left) or (-)-SKF97541 (right panel) in different age groups as described in Methods. The binding data were fitted by sigmoidal dose-response curves using GraphPad Prism 4 and represent the average of three experiments ± S.E.M. Differences between the averaged dose-response curves corresponding to PM prepared from 2-(PD2), 14-(PD14) and 90-days (PD90) old rats were statistically analyzed by one-way ANOVA followed by Bonferroni's *post-hoc* comparison test. **Left** (baclofen): PD2 (●) versus PD14 (○), p<0.0001, ****; PD14 (○) versus PD90 (■), p<0.0001, ****; PD2 (○) versus PD90 (■), NS, p>0.05. **Right** (SKF97541): PD2 (●) versus PD14 (○), p<0.05, *; PD14 (○) versus PD90 (■), p>0.05, NS; PD2 (○) versus PD90 (■), p<0.0001, ****.

10 μM GTPγS. The binding data were analyzed by GraphPad Prism 4 and represent an average ± S.E.M. of 3 experiments.

[^{3}H]CGP54626 binding; saturation binding study

Membranes (100 μg protein per assay) were incubated with increasing concentrations of GABA$_B$-antagonist [^{3}H]CGP54626 (0.06-36.8 nM) in final volume of 100 μl of binding mix containing 50 mM Tris-HCl (pH 7.4) plus 2.5 mM $CaCl_2$ for 60 min at 30 °C. The bound and free radioactivity was separated by filtration through Whatman GF/B filters in Brandel cell harvestor. Filters were washed 3x with 3 ml of ice-cold incubation buffer and radioactivity remaining and placed in 5 ml of scintillation cocktail (Rotiszint Eco Plus). The non-specific binding was determined in the presence of 1 mM GABA in binding mix. Data were analyzed by GraphPad Prism 4 and K_d and B_{max} values calculated according to the method of the least-squares by fitting the data with rectangular hyperbola.

Protein determination

The method of Lowry was used for determination of membrane protein. Bovine serum albumin (Sigma, Fraction V) was used as standard. Data were calculated by fitting the data with calibration curve as quadratic equation.

Results

The efficacy and potency of GABA$_B$-receptors in plasma membranes isolated from brain cortex of 2-, 14- and 90-days old rats was determined as baclofen- and SKF97541-stimulated, high-affinity [^{35}S]GTPγS binding in the presence of 20 μM GDP in reaction mix to suppress the low-affinity binding of this non-hydrolysable analog of GTP (Bourova *et al.* 2009). Dose-response curves were measured in 0.1 nM-1 mM range of baclofen or SKF97541 concentrations and the significance of differences among PM prepared from 2- (PD2), 14- (PD14) and 90-days (PD90) old rats was analyzed by one-way ANOVA followed by Bonferroni's *post-hoc* comparison test using GraphPad Prism 4 software (Fig. 1).

Both agonists exhibited the significant ability to increase the basal level of binding measured in the absence of agonist (B_{basal}) already in 2-day-old animals (PD2). This ability was further increased in the course of the first two weeks of postnatal life (compare PD2 and PD14, Fig. 1), but virtually unchanged when viewed over the whole period of brain development as the averaged dose-response curve corresponding to PD2 was not significantly different from that measured in adult rats (PD90). The same applied to the net-increment of agonist stimulation (Δ) and % stimulation of the basal level of [^{35}S]GTPγS binding (Table 1). The highest baclofen- and SKF97541-stimulated [^{35}S]GTPγS binding was measured between postnatal day 10 and 15 and than it steeply and continuously decreased towards the adult level (Fig. 2).

The potency (EC_{50} estimates) of G-protein response to baclofen was not significantly different in membranes prepared from 2-, 14- and 90-day-old rats, but decreased from the birth to adulthood in the case of SKF97541 (Table 1). This finding is compatible with electrophysiological studies of brain maturation indicating an altered sensitivity to different GABA$_B$-R agonists or antagonists and similar trends of postnatal changes of GABA$_B$-R efficacy (Bernasconi *et al.* 1992, Hosford *et al.* 1992, Marescaux *et al*. 1992, Lin *et al.* 1993, Kubová *et al*. 1996, Mareš 2008).

Table 1. Maximum response (B_{max}) and affinity (EC_{50}) of baclofen- and SKF97541-stimulated [^{35}S]GTPγS binding in PM isolated from 2-, 14- and 90-days old rats**.**

A(-)-baclofen	**2-days**	**14-days**	**90-days**
B_{basal}	0.72 ± 0.01	1.23 ± 0.02	0.64 ± 0.01
B_{max}	1.03 ± 0.02	1.85 ± 0.03	1.04 ± 0.01
$\Delta = B_{max} - B_{basal}$	0.31	0.62	0.40
$100 \times B_{max} / B_{basal}$	152 %	152 %	166 %
EC_{50} (μM)	9.00 (4.46-18.15)	13.34 (7.81-22.88)	13.26 (9.96-17.65)
B(-)-SKF97541			
B_{basal}	0.83 ± 0.01	1.02 ± 0.01	0.66 ± 0.01
B_{max}	1.13 ± 0.02	1.51 ± 0.02	1.08 ± 0.02
$\Delta = B_{max} - B_{basal}$	0.30	0.49	0.42
$100 \times B_{max} / B_{basal}$	142 %	152 %	168 %
EC_{50} (μM)	9.79 (5.30-18.10)	23.45 (14.34-38.35)	36.51 (21.87-60.95)

B_{basal} (pmol · mg^{-1}), binding in the absence of agonist; B_{max} (pmol · mg^{-1}), binding at saturating agonist concentration; $\Delta = B_{max} - B_{basal}$, net-increment of agonist stimulation; $100 \times B_{max} / B_{basal}$, % stimulation of the basal level by agonist. EC_{50} (μM), agonist concentration inducing half-maximum stimulation (95 % confidence limit). B_{max}, B_{basal} and EC_{50} values were determined by analysis of the sigmoidal dose-response curves of baclofen- (**A**) and SKF97541- (**B**) stimulated [^{35}S]GTPγS binding presented in Figure 1 by GraphPad Prism 4 and represent the average of three experiments ± S.E.M. The significance of difference between B_{basal}, B_{max} and EC_{50} values in PM prepared from 2 (PD2)-, 14 (PD14)- and 90 (PD90)-days-old rats was determined by one-way ANOVA followed by Bonferroni's *post-hoc* comparison test. **A (baclofen)**. B_{basal} (PD2 versus PD14, p<0.0001, ****; PD14 versus PD90, p<0.0001, ****; PD2 versus PD90, p>0.05, not significant. B_{max} (PD2 versus PD14, p<0.0001, ****; PD14 versus PD90, p<0.0001, ****; PD2 versus PD90, p>0.05, not significant. EC_{50} (PD2 versus PD14, p>0.05, NS; PD14 versus PD90, p>0.05, NS; PD2 versus PD90, p>0.05, NS. **B (SKF97541)**. B_{basal} (PD2 versus PD14, p<0.001, ***; PD14 versus PD90, p<0.0001, ****; PD2 versus PD90, p<0.001, ***. B_{max} (PD2 versus PD14, p<0.001, ***; PD14 versus PD90, p<0.0001, ****; PD2 versus PD90, p>0.05, NS. EC_{50} (PD2 versus PD14, p>0.05, NS; PD14 versus PD90, p>0.05, NS; PD2 versus PD90, p<0.01, **).

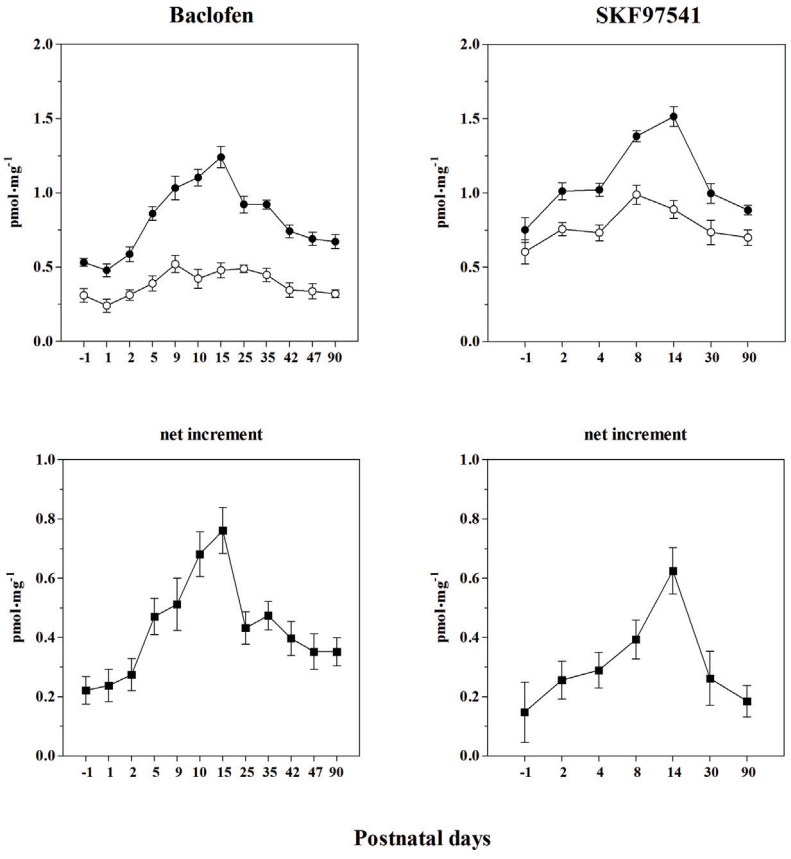

Fig. 2. Baclofen- and SKF97541-stimulated [^{35}S]GTPγS binding; one-point assay. **Upper panels.** PM were isolated from fetuses (-1) and from 1-, 2-, 4-, 5-, 9-, 10-, 14-, 15-, 25-, 30-, 35-, 42-, 47- and 90-days old rats, frozen in liquid nitrogen and used only once. Baclofen- and SKF97541-stimulated [^{35}S]GTPγS binding was determined in different age groups as described in Methods in the presence (●, $B_{agonist}$) or absence (○, B_{basal}) of 1 mM baclofen (**left panel**) or 100 μM SKF97541 (**right panel**). The significance of difference between the two sets of data ($B_{agonist}$ versus B_{basal}) at all age intervals was analyzed by Student s t-test using GraphPad Prism 4: baclofen, p<0.0001, ****; SKF97541, p<0.0022, **. The same type of comparison ($B_{agonist}$ versus B_{basal}) was also performed at individual age intervals: **baclofen** [day -1 (*), PD2 (**), PD5(****), PD9(***), PD10(****), PD15(**), PD25(***), PD35(****), PD42(***), PD47(**), PD90(***)]. **SKF97541** [day -1 (NS), PD2 (NS), PD4(*), PD8(*), PD14(**), PD30(NS), PD90(NS)]. **Lower panels.** Difference between agonist-stimulated ($B_{agonist}$) and basal (B_{basal}) level of binding was expressed as the net-increment of agonist stimulation $\Delta = B_{agonist} - B_{basal}$. Data represent the average ± S.E.M. of three experiments.

The existence of the maximum of GABA$_B$-R agonist-stimulated [^{35}S]GTPγS binding between PD10 and PD15 (Fig. 2) has to be considered together with our previous data indicating the striking maximum of basal, manganese-, fluoride- and forskoline-stimulated AC activity in 12-day-old rats (Ihnatovych *et al.* 2002; see discussion for further details). Thus, the increase of baclofen- and SKF97541-stimulated G-protein activity during the first two weeks of postnatal life, its maximum in 10-15-day-old rats and the subsequent decrease is related in time to the maximum and subsequent decrease of AC activity.

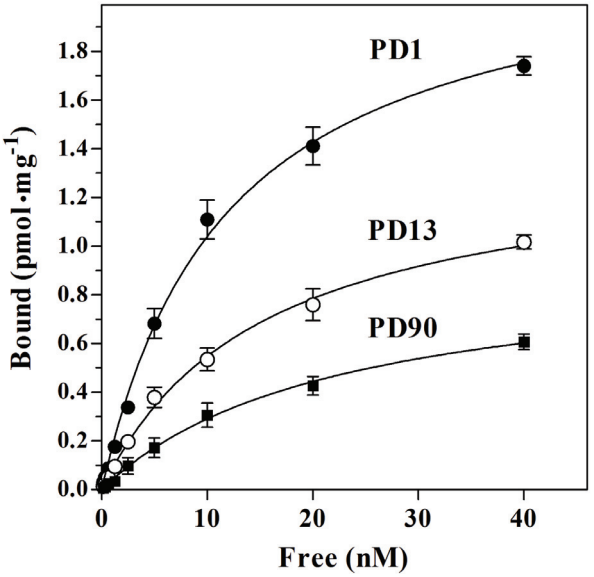

Fig. 3. Saturation of [^{3}H]CGP54626 binding sites in PM isolated from 1-, 13- and 90-day-old rats. Maximum number (B_{max}) and affinity (K_d) of specific [^{3}H]CGP54626 binding sites was determined in PM isolated in parallel from brain cortex of 1 (●)-, 13 (○)- and 90 (■)-days old rats by direct saturation binding assay as described in Methods. B_{max} (maximum binding capacity) and K_d (dissociation constant) of specific [^{3}H]CGP54626 binding sites were calculated by fitting the data by 1-site hyperbola by GraphPad Prism 4 and represent the average ± S.E.M. of 3 experiments. One-way ANOVA followed by Bonferroni's *post-hoc* comparison test was used for statistical analysis of the difference between B_{max} or K_d values in PM prepared from rats of different ages. B_{max} : PD1 versus PD13, $p<0.01$, **; PD13 versus PD90, $p<0.001$, ***; PD13 versus PD90, $p<0.05$, *. K_d: PD1 versus PD13, $p>0.05$, NS; PD13 versus PD90, $p<0.01$, **; PD13 versus PD90, $p<0.05$, *.

Plasma membrane density of GABA$_B$-R at different age intervals was measured by saturation binding study with specific antagonist [^{3}H]CGP54626. Data presented in Figure 3 indicated clearly that the highest PM density of GABA$_B$-R, estimated as the maximum binding capacity (B_{max}) of [^{3}H]CGP54626 binding sites, was detected in PM samples prepared from 1-day-old rats (2.27±0.08 pmol · mg^{-1}). The further development was reflected in a marked decrease of [^{3}H]CGP54626 binding as the B_{max} values of 1.38±0.05 and 0.93±0.04 pmol · mg^{-1} were determined in PM isolated from 13- and 90-days old rats, respectively. The dissociation constant (K_d) was increased from 11.8 nM (PD1) to 15.3 nM (PD13) and 22.1 nM (PD90), indicating the decreased affinity and qualitative change of GABA$_B$-R binding sites towards this antagonist in the course of rat brain cortex maturation.

Discussion

Data presented in this work (Figs 1 and 2) indicate a noticeable extent of compatibility of our present results with experimental data obtained by functional assays of adenylyl cyclase (AC) activity in the presence or absence of GABA$_B$-R agonists, which were previously reported by us (Ihnatovych *et al*. 2002). Maximum activation of baclofen- and SKF97541-stimulated [^{35}S]GTPγS binding coincided with the developmental profile of AC activity. The maximum of agonist-stimulated G-protein activity (Fig. 2) as well as basal, fluoride-, GTP- and forskoline-stimulated AC (Ihnatovych *et al*. 2002) was found in the same period of brain development, between PD10 and PD15. However, marked difference between the two sets of data was noticed as well. Maturation of functional coupling of GABA$_B$-R with G-proteins preceded maturation of AC system because AC activity was low at birth while both baclofen and SKF97541 exhibited significant efficacy already at PD2 (Fig. 1).

Plasma membrane density of GABA$_B$-R determined by saturation binding study with specific antagonist [^{3}H]CGP54626 was also high, virtually the highest, when compared with 13- and 90-day-old rats (Fig. 3). It may be therefore suggested that the physiological significance of the high receptor number and significant efficacy of coupling of GABA$_B$-R with G-proteins shortly after the birth (at PD1 and PD2) is related to some other effectors but AC-cAMP system. Ionic channels and electrophysiological effects of GABA$_B$-R stimulation mediated by $G_o\alpha$ and Gβ subunits represent the obvious choice (Newberry *et al.* 1984a,b, Gähwiler *et al.* 1985, Bormann 1988, Bowery *et al.* 1989).

Comparison of EC_{50} values of agonist-stimulated [^{35}S]GTPγS binding indicated no significant difference in PM isolated from 2-, 14- and 90-day-old rats for

baclofen, but EC_{50} values of SKF97541 were clearly increased from the birth to adulthood (Table 1). This result suggests a developmental decrease in affinity of $GABA_B$-R response for the latter agonist and it is compatible with electrophysiological studies of brain function indicating the differences in sensitivity of $GABA_B$-R to individual agonists (Bernasconi *et al.* 1992, Hosford *et al.* 1992, Lin *et al*. 1992, Marescaux *et al.* 1992). Furthermore, epileptological studies of brain function indicated that anticonvulsant action of baclofen was unchanged during postnatal period (Kubová *et al.* 1996) but the detailed ontogenetic profile of anticonvulsant action of SKF97541 was not identical with that of baclofen (Mareš 2008). The time-span between PD12 and PD18 represented the most critical period in this respect.

Conclusions

Our data indicate significant intrinsic efficacy of $GABA_B$-receptors in rat brain cortex already at the birth (PD1, PD2). Subsequently, baclofen and SKF97541-stimulated G-protein activity, measured by high-affinity [^{35}S]GTPγS binding assay, was increased; the highest level of agonist-stimulated [^{35}S]GTPγS binding was detected between PD10 and PD15. In older rats, both baclofen- and SKF97541-stimulated [^{35}S]GTPγS binding was continuously decreased so, that level in adult, 90-days old animals was not different from that in newborn animals. This profile of ontogenetic development of $GABA_B$-R was similar to the maturation of AC activity (Ihnatovych *et al.* 2002).

The potency of G-protein response to baclofen (characterized by EC_{50} values) was high at birth and unchanged by further development. An individual variance among different agonists was observed in this respect as the potency of SKF97541 response was decreased when compared in 2- and 90-days old rats. Surprisingly, the plasma membrane density of $GABA_B$-R, determined by saturation binding assay as maximum binding capacity (B_{max}) for specific antagonist [^{3}H]CGP54626, was highest in 1-day old and then decreased in 13- and 90-days old animals.

Conflict of Interest

There is no conflict of interest.

Acknowledgements

This work was supported by GACR (P207/12/0919 and P304/12/G069) and by Academy of Sciences of the Czech Republic (AV0Z50110509 and RVO: 67985823). The authors thank to Ing. Martin Chmátal and Kateřina Kašparovská for valuable help.

Abbreviations

AC, adenylyl cyclase; cAMP, cyclic 3´,5´-[α-^{3}H] adenosine monophosphate, baclofen, β-p-chlorophenyl-GABA; GABA, γ-aminobutyric acid, $GABA_B$-R, metabotropic receptor for GABA, GPCR, G-protein-coupled receptor; G-proteins, heterotrimeric guanine nucleotide-binding regulatory proteins; NS, not significant; PD, postnatal day; PBS, phosphate-buffered saline; PM, plasma membrane, PMSF, phenylmethylsulfonyl fluoride; PTX, pertussis toxin; SKF97541, aminopropyl (methyl) phosphinic acid; w.w., wet weight, TCA, trichloroacetic acid.

References

BERNASCONI R, LAUBER J, MARESCAUX C, VERGNES M, MARTIN P, RUBIO V, LEONHARDT T, REYMANN N, BITTIGER H: Experimental absence seizures: potential role of gamma-hydroxybutyric acid and $GABA_B$ receptors. *J Neural Transm* **35**: 155-177, 1992.

BORMANN J: Electrophysiology of $GABA_A$ and $GABA_B$ receptor subtypes. *Trends Neurosci* **11**: 112-116, 1988.

BOUROVA L, STOHR J, LISY V, RUDAJEV V, NOVOTNY J, SVOBODA P: Isolation of plasma membrane compartments from rat brain cortex; detection of agonist-stimulated G protein activity. *Med Sci Monit* **15**: BR111-BR122, 2009.

BOWERY NG: $GABA_B$ receptor pharmacology. *Annu Rev Pharmacol Toxicol* **33**: 109-147, 1993.

BOWERY NG, HILL DR, HUDSON AL: Characteristics of $GABA_B$ receptor binding sites on rat whole brain synaptosomes. *Br J Pharmacol* **78**: 191-206, 1983.

BOWERY NG, HILL DR, HUDSON AL: [3H](-) Baclofen: an improved ligand for $GABA_B$ sites. *Neuropharmacology* **24**: 207-210, 1985.

BOWERY NG: $GABA_B$ receptors and their significance in mammalian pharmacology. *Trends Pharmacol Sci* **10**: 401-407, 1989.

DOLPHIN AC: G protein modulation of calcium currents in neurons. *Annu Rev Physiol* **52**: 243-255, 1990.

DOLPHIN AC: Regulation of calcium channel activity by GTP binding proteins and second messengers. *Biochim Biophys Acta* **1091**: 68-80, 1991.

GÄHWILER BH, BROWN DA: GABAB-receptor-activated K^+ current in voltage-clamped CA3 pyramidal cells in hippocampal cultures. *Proc Natl Acad Sci U S A* **82**: 1558-1562, 1985.

HILL DR: $GABA_B$ receptor modulation of adenylate cyclase activity in brain slices. *Br J Pharmacol* **84**: 249-257, 1985.

HILL DR, BOWERY NG: ^{3}H-Baclofen and ^{3}H-GABA bind to bicuculline-insensitive $GABA_B$ sites in rat brain. *Nature* **290**: 149-152, 1981.

HILL DR, BOWERY NG, HUDSON AL: Inhibition of $GABA_B$ receptor binding by guanyl nucleotides. *J Neurochem* **42**: 652-657, 1984.

HOSFORD DA, CLARK S, CAO Z, WILSON WA JR, LIN FH, MORRISETT RA, HUIN A: The role of $GABA_B$ receptor activation in absence seizures of lethargic (lh/lh) mice. *Science* **257**: 398-401, 1992.

IHNATOVYCH I, NOVOTNY J, HAUGVICOVA R, BOUROVA L, MARES P, SVOBODA P: Ontogenetic development of the G protein-mediated adenylyl cyclase signaling in rat brain. *Brain Res Dev Brain Res* **133**: 69-75, 2002.

KERR DI, ONG J: GABAB receptors. *Pharmacol Ther* **67**: 187-246, 1995.

KUBOVÁ H, HAUGVICOVÁ R, MAREŠ P: Moderate anticonvulsant action of baclofen does not change during development. *Biol Neonate* **69**: 405-412, 1996.

LIN FH, CAO Z, HOSFORD DA: Increased number of $GABA_B$ receptors in lethargic (lh/lh) mouse model of absence epilepsy. *Brain Res* **608**: 101-106, 1993.

MARESCAUX C, VERGNES M, BERNASCONI R: $GABA_B$ receptor antagonists: potential new anti-absence drugs. *J Neural Transm Suppl* **35**: 179-188, 1992.

MAREŠ P: Anticonvulsant action of GABA-$_B$ receptor agonist SKF97541 differs from that of baclofen. *Physiol Res* **57**: 789-792, 2008.

NEWBERRY NR, NICOLL RA: Direct hyperpolarizing action of baclofen on hippocampal pyramidal cells. *Nature* **308**: 450-452, 1984a.

NEWBERRY NR, NICOLL RA: A bicuculline-resistant inhibitory post-synaptic potential in rat hippocampal pyramidal cells in vitro. *J Physiol* **348**: 239-254, 1984b.

SEABROOK GR, HOWSON W, LACEY MG: Electrophysiological characterization of potent agonists and antagonists at pre- and postsynaptic GABAB receptors on neurones in rat brain slices. *Br J Pharmacol* **101**: 949-957, 1990.

SWEENEY MI, DOLPHIN AC: 1,4-Dihydropyrines modulate GTP hydrolysis by Go in neuronal membranes. *FEBS Lett* **310**: 66-70, 1992.

Morphine, opioid-receptor signaling cascades and plasma membrane structure in rat cerebral cortex and model cell lines

H. UJCIKOVA[1], J. BREJCHOVA[1], M. VOSAHLIKOVA[1], D. KAGAN[1], K. DLOUHA[1], J. SYKORA[2], L. MERTA[1], Z. DRASTICHOVA[3], J. NOVOTNY[3], P. OSTASOV[1] L. ROUBALOVA[1], M. HOF[2], P. SVOBODA[1]

[1]Institute of Physiology, ASCR, Videnska 1084, 142 20 Prague 4, Czech Republic

[2]J. Heyrovsky Institute of Physical Chemistry, ASCR, Dolejskova 2155/3, 182 23 Prague 8, Czech Republic

[3]Department of Physiology, Faculty of Science, Charles University, Vinicna 7, 120 00 Prague 2, Czech Republic

---

Summary

Large number of extracellular signals is received by specific plasma membrane receptors which, upon activation, transduce information into the target cell interior *via* trimeric G-proteins (G-protein-coupled receptors, GPCR) and induce activation or inhibition of adenylylcyclase enzyme activity (AC). Receptors for opiopid drugs such as morphine (μ-OR, δ-OR and κ-OR) belong to rhodopsin family of GPCR. Our recent results indicated a specific up-regulation of adenylylcyclases I (8x) and II (2.5x) in plasma membranes (PM) isolated from rat brain cortex exposed to increasing doses of morphine (10-50 mg/kg) for 10 days. Increase of ACI and II represented the specific effect as the amount of ACIII-ACIX, of prototypical PM marker Na, K-ATPase and of trimeric G protein α and β subunits was unchanged. The up-regulation of ACI and ACII faded away after 20 days since the last dose of morphine.

Proteomic analysis of these PM indicated that the brain cortex of morphine-treated animals can not be regarded as being adapted to this drug as significant up-regulation of

proteins functionally related to oxidative stress and alternation of brain energy metabolism occurred. The number of δ-OR was increased 2x and their sensitivity to monovalent cations altered. Characterization of δ-OR-G-protein coupling in model HEK293 cell line indicated high ability of lithium to support potency /affinity of δ-OR response to agonist stimulation.

Our studies of plasma membrane structure and function in context with desensitization of GPCR action were extended by data indicating participation of cholesterol-enriched membrane domains /rafts in agonist-specific internalization of δ-OR. In HEK293 cells stably expressing δ-OR-$Gi_1\alpha$ fusion protein, depletion of PM cholesterol was associated with decrease (by two-orders of magnitude) in affinity /potency of G-protein-response to agonist stimulation; maximum response was unchanged. Hydrophobic interior of isolated PM became more "fluid", chaotically organized and more accessible to water molecules. Validity of this conclusion was supported by analysis of an immediate PM environment of cholesterol molecules in living δ-OR-$Gi_1\alpha$-HEK293 cells by fluorescent probes 22- and 25-NBD-cholesterol. Alternation of plasma membrane structure by decrease of cholesterol made the membrane more hydrated.

---

key-words: GPCR, morphine, μ-, δ- and κ-opioid receptors, rat brain cortex, adenylyl cyclase I and II, proteomic analysis, monovalent cations, agonist-induced internalization, plasma membrane structure, cholesterol, membrane domains, fluorescent probes.

Acknowledgements

This work was supported by Grant Agency of the Czech Republic (P207/12/0919, P304/12/G069) and by the Academy of Sciences of the Czech Republic (AV0Z50110509).

Introduction

Hormones, neurotransmitters and growth factors, bind to the cell surface membrane receptors, which may be divided into the three main families: i) coupled with guanine nucleotide-binding regulatory proteins (GPCR), ii) ionic channels, and iii) tyrosine-kinases. Binding of hormones or neurotransmitters to the stereo-specific site of receptor molecules, located at extracellular side of plasma membrane, represents the first step in complicated sequence of molecular events transmitting the signal into the cell interior and initiating the ultimate physiological response. In G-protein-mediated cascades, ligand binding induces conformational change of receptor molecule, which, in the next step, induces dissociation of trimeric G protein-complex (non-active) into the free, active Gα and Gβγ subunits. Subsequently, both Gα and Gβγ subunits activate variety of enzyme activities and/or ionic channels which regulate intracellular concentrations of secondary messengers such as cAMP, cGMP, diacylglycerol, IP_3, DAG, arachidonic acid, sodium, potassium or calcium cations (Svoboda et al., 2004; Drastichova et al., 2008).

Receptors for opiopid drugs, μ-OR, δ-OR and κ-OR were classified as members of rhodopsin family of GPCR. All these receptors are known to inhibit adenylyl cyclase activity in pertussis-toxin-dependent manner by activation of Gi/Go class of trimeric G proteins. These proteins (Gi1, Gi2, Gi3, Go1, Go2) are present in brain in large quantities and inhibit adenylyl cyclase activity or regulate ionic channels in pertussis-toxin-dependent manner.

Morphine binds to all three types of OR (μ-, and κ-OR) and represents one of the most effective painkillers. Repeated exposure of experimental animals to morphine results in *tolerance* to this drug, development of physical *dependence* and a *chronic relapsing disorder – drug addiction* [Contet et al., 2004]. Physical dependence contributes to a drug seeking behavior and the continuous drug use with the aim to prevent the onset of unpleasant *withdrawal* symptoms [Preston et al., 1991]. Morphine *withdrawal* generates a set of

symptoms like retches, vomiting, blood pressure increase, insomnia, intestines dysfunctions, body shaking and teeth chatter.

Drug addiction to morphine is characterized by a complex etiology including changes in psychology of experimental animals as well as physiology of their brain function. These changes proceed mainly in brain stem and hippocampus [Connor and Christie, 1999; Law et al., 2000; Chen et al., 2007; Law and Loh, 2000], however, some of the long-term behavioral consequences of repeated morphine exposure were related to reorganized patterns of synaptic connectivity in forebrain [Robinson et al., 1999]. Morphine-induced changes of brain function were also associated with alternations of neurotransmission, specific signaling cascades, energy metabolism and stability of protein molecules [Miller et al., 1972; Kim et al., 2005; Li et al., 2006; Li et al., 2009].

Hyper-sensitization or super-activation of adenyl cyclase (AC) activity by prolonged exposure of cultured cells or mammalian organism to morphine has been demonstrated in previous studies of mechanism of action of this drug [Contet et al. 2004; Preston 1991; Connor and Christie, 1999; Law et al., 2000; Law et al., 2004] and considered as biochemical basis for development of opiate *tolerance* and *dependence*.

Our previous work on isolated Percoll membranes (PM) prepared from brain cortex of rats exposed to morphine for 10 days (10-50 mg/kg) indicated a desensitization of G-protein response to μ-OR (DAMGO) and δ-OR (DADLE) stimulation [Bourova et al., 2010] and specific increase of ACI (8x) and ACII (2.5x) isoforms [Ujcikova et al., 2011]. The κ-OR (U-23554)-stimulated [^{35}S] GTPγS binding and expression level of ACIII-X in PM was unchanged. Behavioral tests of morphine-treated animals indicated that these animals were fully drug-dependent (*opiate abstinence syndrome*) and developed tolerance to subsequent drug addition (a*nalgesic tolerance* detected by hot-plate and hind paw withdrawal tests). The

increase of ACI and ACII was interpreted as a specific compensatory response to prolonged stimulation of brain cortex OR by morphine.

Proteomic analysis of membrane proteins in rat brain cortex; *changes induced by the long-term exposure to increasing doses to morphine*

The aim of the next step of our work was the description of an over-all change of membrane protein composition and recognition of proteins exhibiting the largest morphine-induced change. This was performed by proteomic analysis of post-nuclear supernatant (PNS) and plasma-membrane-enriched fraction isolated in Percoll gradient (PM). PNS was analyzed because it contains proteins of mitochondrial, endoplasmic reticulum, plasma membrane and cytoplasmic origin. Rats were adapted to morphine for 10 days [10 mg/kg (day 1 and 2), 15 mg/kg (day 3 and 4), 20 mg/kg (day 4 and 5), 30 mg/kg (day 6 and 7), 40 mg/kg (day 9) and 50 mg/kg (day 10)] and sacrificed 24 hours after the last dose (group +M10). Control animals were sacrificed in parallel with morphine-treated (group −M10). Post-nuclear supernatant fraction (PNS) was prepared from brain cortex of both groups and resolved by 2D-ELFO. The gels were stained by Coomassie brilliant blue (CBB) and the altered proteins detected by PDQuest software analysis.

The 10 up (↑)- or down (↓)-regulated proteins exhibiting the ***largest morphine-induced change*** were selected, excised manually from 2D-gel and identified by MALDI-TOF MS/MS. The identified proteins were: 1-(gi|148747414, Guanine deaminase), ↑2.5x; 2-(gi|17105370, Vacuolar-type proton ATP subunit B, brain isoform), ↑2.6x; 3-(gi|1352384, Protein disulfide-isomerase A3), ↑3.4x; 4-(gi|40254595, Dihydropyrimidinase-related protein 2), ↑3.6x; 5-(gi|149054470, N-ethylmaleimide sensitive fusion protein, isoform CRAa), ↑2.0x; 6-(gi|42476181, Malate dehydrogenase, mitochondrial precursor), ↑1.4x; 7-(gi|62653546, Glyceraldehyde-3-phosphate dehydrogenase), ↑1.6x; 8-(gi|202837, Aldolase A), ↑1.3x; 9-(gi|31542401, Creatine kinase B-type), ↓0.86x; 10-(gi|40538860, Aconitate

hydratase, mitochondrial precursor), ↑1.3x. Thus, the 10 most highly altered proteins in PNS were of cytoplasmic (1, 4, 5, 7, 9), cell membrane (2), endoplasmic reticulum (3) and mitochondrial (6, 8, 10) origin and the 9 of them were significantly increased by morphine, 1.3-3.6x. Correlation with functional properties of these proteins indicated up-regulation of proteins related to guanine degradation (1), vacuolar acidification (2), apoptotic cell death (3), oxidative stress (4, 6, 7, 10), membrane traffic (5) and glycolysis (8). The role in apoptosis has been also described for Glyceraldehyde-3-phosphate dehydrogenase (7), already mentioned as major target protein in oxidative stress [Hwang et al, 2009]. All together, the spectrum of altered proteins suggests a major change of energy metabolism of brain cortex tissue when exposed to increasing doses of morphine. Judged from functional point of view, the most significant change was up-regulation of proteins related to oxidative stress (4, 6, 7, 10) and apoptotic cell death.

We could therefore conclude that the brain cortex of rats exposed to increasing doses of morphine (10-50 mg/kg) for 10 days can not be regarded as being adapted to this drug. Significant up-regulation of proteins functionally related to oxidative stress and apoptosis indicates the state of severe "discomfort" of brain cells or even damage.

Identification of an *active*, minority pool of trimeric Gβ subunits responding to chronic morphine in rat brain cortex; *proteomic analysis of Percoll-purified membranes*

In Percoll-purified membranes (PM), the altered proteins were of plasma membrane [BASP1, Brain acid soluble protein, down regulated (↓) 2.1x; GBB, Guanine nucleotide-binding protein subunit beta-1, (↓) 2.0x], myelin membrane [MBP, Myelin basic protein S, (↓) 2.5x], cytoplasmic [KCRB, Creatine kinase B-type (EC 2.7.3.2), (↓) 2.6x; AINX, alpha-internexin, up-regulated (↑) 5.2x; DPYL2, Dihydropyrimidinase-related protein 2, (↑) 4.9x; SIRT2, NAD-dependent deacetylase sirtuin-2, (↑) 2.5x; SYUA, Alpha-synuclein, (↑) 2.0x; PRDX2, Peroxiredoxin-2, (↑) 2.2x; TERA, Transitional endoplasmic reticulum ATPase, (↑)

2.1x; UCHL1, Ubiquitin carboxyl-terminal hydrolase L1, (↑) 2.7x; COR1A, Coronin-1A, down 5.4x, SEP11, Septin-11, (↑) 2.2x; RL12, 60S ribosomal protein L12, (↑) 2.7x] and mitochondrial [DHE3, Glutamate dehydrogenase 1, (↑) 2.7x; SCOT1, Succinyl-CoA:3-ketoacid-coenzyme A, (↑) 2.2x; AATM, Aspartate aminotransferase**,** down 2.2x; PHB, prohibitin, (↑) 2.2x] origin.

The only member of GPCR-initiated signaling cascades identified by LC-MS/MS in PM was trimeric Gβ subunit (**2**-GBB) which was decreased 2x in samples of morphine-adapted rats. Similarly, proteomic analysis of protein alternations induced by long-term stimulation of HEK cells stably expressing TRH-receptor and G11α protein by TRH, indicated the change of 42 proteins, but not even one of these proteins represented the plasma membrane protein functionally related to G-protein mediated signaling cascades [Drastichova et al., 2010].

The immunoblot analysis of the same PM resolved by 2D-ELFO indicated that the "active" pool of Gβ subunits effected by morphine, which was decreased 2x, represented just a minor fraction of the total signal of Gβ subunits in 2D-gels (**Fig. 1**). The total signal of Gβ was decreased 1.2x only and dominant /major part of the total signal was unchanged. Accordingly, the immunoblot analysis of Gβ after resolution by 1D-SDS-PAGE in 10% w/v acrylamide/0.26% w/v bis-acrylamide or 4-12% (InVitroGene) gradient gels indicated no change of this protein. *We could therefore conclude that proteomic analysis represents a valuable tool for identification of membrane proteins. However, analysis of low-abundance proteins of OR-initiated signaling cascades in plasma membranes has to be accompanied by specific immublot analysis. Identification of an "active", minority pool of Gβ subunits down-regulated by morphine represents an original finding which has not been described in up-to-date literature dealing with drug addiction and morphine effect on mammalian brain.*

The effect of lithium and other monovalent ions on ligand binding and efficiency of δ-opioid receptor-G-protein coupling

Lithium is still one of the most effective therapies for depression. Comparison of the effect of lithium, sodium and potassium on δ-opioid receptor was studied in HEK293 cells stably expressing PTX-insensitive δ-OR-$G_i1\alpha$ (Cys^{351}-Ile^{351}) fusion protein. δ-OR-$G_i1\alpha$ (C^{351}-I^{351}) cells represent useful experimental tool as the covalent bond between δ-OR and $G_i1\alpha$ (C^{351}-I^{351}) provides the permanent and fixed, 1:1 stoichiometry and C^{351}-I^{351} mutation provides resistance to PTX together with extraordinary high efficacy of coupling between δ-OR and $G_i1\alpha$ (C^{351}-I^{351}) protein (Bourova et al. 2003; Brejchova et al. 2011).

Agonist [^{3}H]DADLE binding was decreased with the order: $Na^+ \gg Li^+ > K^+ > (+)$ NMDG. When plotted as a function of increasing NaCl concentrations, binding was best-fitted with a two phase exponential decay considering the two Na^+-responsive sites (r^2 = 0.99). High-affinity Na^+-sites were characterized by K_d = 7.9 mM and represented 25% of the basal level determined in the absence of ions. Remaining 75% represented the low-affinity sites (K_d = 463 mM). Inhibition of [^{3}H]DADLE binding by lithium, potassium and (+)-NMDG proceeded in low-affinity manner only. Preferential sensitivity of δ-OR-$G_i1\alpha$ to sodium was thus clearly manifested.

Surprisingly, the *affinity/potency* of DADLE-stimulated [^{35}S]GTPγS binding, quantitatively characterized by comparison of dose-response curves in different ion media (EC_{50} values), was increased in the reversed order: $Na^+ < K^+ < Li^+$. This result was demonstrated in PTX-treated as well as PTX-untreated cells (**Table 1**). Therefore, this finding is not restricted to $G_i1\alpha$ present in fusion protein, but is also valid for stimulation of endogenous G-proteins of Gi/Go family.

This surprising but fully reproducible result may be considered in connection with clinical usage of lithium in treatment of manic depression. In electrically active cells, Li^+

enters the intracellular compartment via “fast“ sodium channel (Richelson, 1977) and also via oubabain-sensitive K^+-influx catalyzed by Na,K-ATPase. However, the efflux of Li^+ via Na,K-ATPase is limited because ATP+Mg+Na-dependent phosphorylation proceeding at inner side of plasma membrane and out-ward oriented efflux of Na^+ cations via Na+-pump is strictly specific for sodium. Thus, if available in extracellular space, the intracellular Li^+ concentration will be slowly increased. It is reasonable to assume that such conditions may arise in neuronal or glial cells of depressive patients as the effective range of plasma concentrations of Li^+ used clinically is 0.6-1.0 mM. The 2 mM LiCl is regarded as toxic. In comparison with our results, this is exactly the concentration range in which the first significant inhibition of the basal level of [^{35}S]GTPγS binding was detected. The first significant decrease of the basal level of [^{35}S]GTPγS binding measured in the absence of cations was noticed at 1-2 mM NaCl, KCl and LiCl; the 50% inhibition was reached at 62 mM NaCl, 88 mM LiCl and 92 mM KCl, respectively (Vosahlikova and Svoboda, 2011). Thus, in treatment of acute depression, competitive effect of Li^+ on inverse agonist-like effect of Na^+ on δ-OR and, in parallel, on G_i/G_o class of G-proteins, might be considered as one plausible possibility for mechanism of action of lithium, i.e., besides numerous other effects on overall cell metabolism (Young, 2009).

The role of cholesterol, cholesterol depletion and membrane domains/rafts in structural organization of plasma membrane and trans-membrane signaling through G-protein-coupled receptors

Cholesterol constitutes a major component of mammalian plasma (cell) membrane. Its correct distribution among plasma membrane and intracellular membrane compartments is essential for the homeostasis of mammalian cells and intracellular membrane traffic plays a major role in the correct disposition of internalized cholesterol and in the regulation of cholesterol efflux (Scheidt et al., 2003; Maxfield and Wustner, 2002). Furthermore, lateral

and trans-bilayer organization of cholesterol molecules in the plasma membrane determines plasma membrane structure and dynamics. However, neither its intracellular pathways of trafficking nor its precise lateral organization in cholesterol-enriched microdomains such as membrane rafts and *caveolae* is fully understood. The same applies to the trans-bilayer distribution between the two leaflets of biological membranes (Simons and Ikonen, 1997; Brown and London, 1998; Anderson and Jacobson, 2002).

Cholesterol- and sphingolipid-enriched membrane domains, characterized by high content of cholesterol, saturated phospholipids, glycolipids and sphingomyelin, have been described as lipid platforms capable to harbor and confine trimeric G-proteins in high amounts (Simons and Ikonen, 1997; Brown and London, 1998; Anderson, 1998; Anderson and Jacobson, 2002; Moffett et al., 2000; Oh and Schnitzer, 2001; Pike, 2004; Quinton et al., 2005). Considering the function of trimeric G-proteins in membrane domains containing caveolin, heterologous desensitization of GPCR signaling was described as specific binding of G-proteins to caveolin (Murthy and Maclouf, 2000).

These structures were also reported to play an important role in both positive and negative regulation of trans-membrane signaling through G-protein-coupled receptors (Klein et al., 1995; Feron et al., 1997; De Weerd and Leeb-Lundberg, 1997; Gimpl et al., 1995; Gimpl and Farenholz, 2002; Schwencke et al., 1999; De Luca et al., 2000; Dessy et al., 2000; Lasley et al., 2000; Igarashi and Michel, 2000; Ostrom et al., 2000, 2001; Rybin et al., 2000, 2003; Ushio-Fukai et al., 2001; Sabourin et al., 2002; Ostrom and Insel, 2004; Pucadyil and Chattopadhyay, 2004, 2007; Monastyrskaya et al., 2005; Savi et al., 2006; Xu et al., 2006; Allen et al., 2007; Ostasov et al., 2007, 2008; Chini and Parenti, 2009). More specifically, the functional significance of OR presence in membrane domains is far from being understood as cholesterol reduction by methyl-β-cyclodextrin attenuated δ-OR-mediated signaling in neuronal cells but enhanced it in non-neuronal cells (Huang at al., 2007).

In HEK293 cells stably expressing δ-OR-$Gi_1α$ fusion protein, depletion of PM cholesterol was associated with decrease (by two-orders of magnitude) in affinity /potency of G-protein-response to agonist stimulation. The maximum response was unchanged (Brejchova et al., 2011). Hydrophobic interior of isolated PM became more "fluid", chaotically organized and more accessible to water molecules. Analysis of PM environment of fluorescent derivatives of cholesterol (22- and 25-NBD-cholesterol) in living δ-OR-$Gi_1α$-HEK293 cells confirmed these results as it indicated that alternation of plasma membrane structure by decrease of cholesterol makes the membrane more hydrated (Ostasov et al., 2013). Our data also indicated that small perturbation of PM structure by low, non-ionic detergent concentrations increased GPCR-G-protein coupling, while the high concentrations were strictly inhibitory (Sykora at al., 2009). The close-to-zero level of basal and agonist-stimulated G-protein activity is the typical feature of detergent-resistant membrane domains (DRMs) prepared at high detergent concentrations, 0.5-1% Triton X100 (Bourova at al., 2003).

Agonist-induced internalization of δ-opioid receptors

The first evidence for agonist-induced internalization of GPCR was brought by subcellular fractionation studies of cell homogenate using differential or sucrose density gradient centrifugation. The internalized, endosomal pool of receptor molecules was separated from the major pool of receptor molecules in plasma membranes and found to be increased by agonist stimulation (Waldo et al., 1983; Stadel et al., 1983; Hertel et al., 1985; Clark et al., 1985; Sibley et al., 1987). In intact cells, the specific, agonist-induced sequestration and internalization of GPCR was detected by immuno-fluorescence microscopy of cells expressing $β_2$-adrenergic receptors. $β_2$-AR were transferred from clathrine-coated pitts (in plasma membrane) to clathrine-coated vesicles, rab5-containing early endosomes and back to the plasma membrane (Zastrow and Kobilka, 1992, 1994; Moore et al., 1995; Pippig et al.,

1995). Cellular and molecular mechanisms of GPCR internalization are in focus of OR studies as one the leading theories of drug addiction is directly based on atypical parameters of μ-OR internalization (Whistler and von Zastrow, 1998; Whistler et al., 1999). When exposed to morphine, μ-OR remain at PM and in this way elude desensitization by β-arrestin.

Our analysis of HEK293 cells transiently expressing Flag-epitope tagged version of δ-OR indicated that cholesterol depletion alone induced transfer of receptor molecules into the cell interior (compare **Fig. 2A,** upper right and left panels). Incubation of cells with 10 mM β-CDX (30 minutes) caused significant increase of intracellular fluorescence ($p < 0.05$), while in control, β-CDX-untreated cells, the small intracellular signal distributed among numerous faint fluorescent patches was unchanged in the course of 30 min of incubation in serum-free medium alone (**Fig. 2B**). Massive transfer of receptor molecules from the cell surface (plasma membrane) into the intracellular compartments was noticed after agonist stimulation (100 nM DADLE). This transfer was decreased in β-CDX-treated cells (compare **Fig. 2A,** lower right and left panels). Difference between β-CDX-treated and β-CDX- plus DADLE-treated samples was highly significant, $p < 0.01$ (**Fig. 2B**).

We could therefore conclude that treatment of HEK293 cells with β-CDX alone, i.e., degradation of membrane domains, induced destabilization of HEK293 plasma membrane structure manifested as spontaneous transfer of a portion of δ-OR molecules into the cell interior. Massive internalization of δ-OR proceeding in the presence of specific agonist was suppressed by β-CDX. This part of internalized receptor molecules may be regarded as functionally related to membrane domains.

References

ALLEN JA, HALVERSON-TAMBOLI RA, RASENICK MM: Lipid raft microdomains and neutrotransmitter signaling. *Nat Rev Neurosci* **8**: 128-140, 2007.

ANDERSON RGW, JACOBSON K: A role for lipid shells in targeting proteins to caveolae, rafts, and other lipid domains. *Science* **296**: 1821-1825, 2002.

ANDERSON RGW: The caveolae membrane system. *Annu Rev Biochem* **67**: 199-225, 1998.

BOUROVA L, KOSTRNOVA A, HEJNOVA L, MORAVCOVA Z, MOON HE, NOVOTNY J, MILLIGAN G, SVOBODA P: delta-Opioid receptors exhibit high efficiency when activating trimeric G proteins in membrane domains. *J Neurochem* **85**: 34-49, 2003.

BOUROVA L, STOHR J, LISY, V., RUDAJEV V, NOVOTNY J, SVOBODA P: G-protein activity in Percoll-purified plasma membranes, bulk plasma membranes and low-density plasma membranes isolated from rat cerebral cortex. Medical Science Monitor (MCM), 15(4), BR111-122, 2009.

BOUROVA L, VOSAHLIKOVA M, KAGAN D, DLOUHA K, NOVOTNY J, SVOBODA P: Long-term adaptation to high doses of morphine causes desensitization of μ-OR- and δ-OR-stimulated G-protein response in forebrain cortex but does not decrease the amount of G-protein alpha subunit. *Med Sci Monit* **16**: 260-270, 2010.

BREJCHOVA J, SÝKORA J, DLOUHA K, ROUBALOVA L, OSTASOV P, VOSAHLIKOVA M, HOF M, SVOBODA P: Fluorescence spectroscopy studies of HEK293 cells expressing DOR-Gi1α fusion protein; the effect of cholesterol depletion. *Biochim Biophys Acta* **1808**: 2819-2829, 2011.

BROWN DA, LONDON E: Functions of lipid rafts in biological membranes. *Annu Rev Cell Dev Biol* **14**: 111-136, 1998.

CHEN XL, LU G, GONG YX, ZHAO LC, CHEN J, CHI ZQ, YANG YM, CHEN Z, LI QL, LIU JG: Expression changes of hippocampal energy metabolism enzymes contribute to behavioural abnormalities during chronic morphine treatment. *Cell Res* **17**: 689-700, 2007.

CHINI B, PARENTI M: G-protein-coupled receptors, cholesterol and palmitoylation: facts about fats. *J Mol Endocrinol* **42**: 371-379, 2009.

CLARK RB, FRIEDMAN J, PRASHAD N, RUOHO AE: Epinephrine-induced sequestration of the beta-adrenergic receptor in cultured S49 WT and cyc- lymphoma cells. *J Cyclic Nucleotide Protein Phosphor Res*. **10**, 97-119, 1985.

CONNOR M, CHRISTIE MD: Opioid receptor signaling mechanisms. *Clin Exp Pharmacol Physiol* **26**: 493-499, 1999.

CONTET C, KIEFFER BL, BEFORT K: Mu opioid receptor: a gateway to drug addiction. *Curr Opin Neurobiol* **14**: 370-378, 2004.

DE LUCA A, SARGIACOMO M, PUCA A, SGARAMELLA G, DE PAOLIS P, FRATI G, MORISCO C, TRIMARCO B, VOLPE M, CONDORELLI G: Characterization of caveolae from rat heart: localization of postreceptor signal transduction molecules and their rearrangement after norepinephrine stimulation. *J Cell Biochem* **77**: 529-539, 2000.

DE WEERD WFC, LEEB-LUNDBERG LMF: Bradykinin sequesters B2 bradykinin receptors and the receptor-coupled Galpha subunits Galphaq and Galphai in caveolae in DDT1 MF-2 smooth muscle cells. *J Biol Chem* **272**: 17858-17866, 1997.

DESSY C, KELLY RA, BALLIGAND JL, FERON O: Dynamin mediates caveolar sequestration of muscarinic cholinergic receptors and alternation in NO signaling. *EMBO J* **19**: 4272-4280, 2000.

DRASTICHOVA Z, BOUROVA L, LISY V, HEJNOVA L, RUDAJEV ., STOHR, J, DURCHANKOVA, D., OSTASOV P., TEISINGER J., SOUKUP T., NOVOTNY J., SBOBODA P: Subcellular redistribution of trimeric G-proteins – potential mechanism of

desensitization of hormone response; internalization, solubilisation, down-regulation. Phys. Res. 57 (Suppl.) S1-S10, 2008.

DRASTICHOVA Z, BOUROVA L, HEJNOVA L, JEDELSKY P, SVOBODA P, NOVOTNY J: Protein alterations induced by long-term agonist treatment of HEK293 cells expressing thyrotropin-releasing hormone receptor and $G_{11}\alpha$ protein. *J Cell Biochem* **109**: 255-264, 2010.

FERON O, SMITH TW, MICHEL T, KELLY RA: Dynamic targeting of the agonist-stimulated m2 muscarinic acetylcholine receptor to caveolae in cardiac myocytes. *J Biol Chem* **272**: 17744-17748, 1997.

GIMPL G, FAHRENHOLZ F: Cholesterol as stabilizer of the oxytocin receptor. *Biochim Biophys Acta* **1564**: 384-392, 2002.

GIMPL G, KLEIN U, REILÄNDER H, FAHRENHOLZ F: Expression of the human oxytocin receptor in baculovirus-infected insect cells: high-affinity binding is induced by a cholesterol-cyclodextrin complex. *Biochemistry* **34**: 13794-13801, 1995.

HERTEL C, COULTER SJ, PERKINS JP: A comparison of catecholamine-induced internalization of beta-adrenergic receptors and receptor-mediated endocytosis of epidermal growth factor in human astrocytoma cells. Inhibition by phenylarsine oxide. *J Biol Chem* **260**: 12547-12533, 1985.

HUANG P, XU W, YOON SI, CHEN C, CHONG PLG, LIU-CHEN LY: Cholesterol reduction by methyl-beta-cyclodextrin attenuates the delta opioid receptor-mediated signaling in neuronal cells and enhances it in non-neuronal cells. *Biochem Pharmacol* **73**: 534-549, 2007.

HWANG NR, YIM SH, KIM YM, JEONG J, SONG EJ, LEE Y, CHOI S, LEE KJ: Oxidative modifications of glyceraldehyde-3-phophate dehydrogenase play a key role in its multiple cellular functions. *Biochem J* **423**: 253-264, 2009.

IGARASHI J, MICHEL T: Agonist-modulated targeting of the EDG-1 receptor to plasmalemmal caveolae. eNOS activation by sphingosine 1-phosphate and the role of caveolin-1 in sphingolipid signal transduction. *J Biol Chem* **275**: 32363-32370, 2000.

KIM SY, CHUDAPONGSE N, LEE SM, LEVIN MC, OH JT, PARK HJ, HO IK: Proteomic analysis of phosphotyrosyl proteins in morphine-dependent rat brains. *Brain Res Mol Brain Res* **133**: 58-70, 2005.

KLEIN U, GIMPL G, FAHRENHOLZ F: Alteration of the myometrial plasma membrane cholesterol content with beta-cyclodextrin modulates the binding affinity of the oxytocin receptor. *Biochemistry* **34**: 13784-13793, 1995.

LASLEY RD, NARAYAN P, UITTENBOGAARD A, SMART EJ: Activated cardiac adenosine A(1) receptors translocate out of caveolae. *J Biol Chem* **275**: 4417-4421, 2000.

LAW PY, LOH HH, WEI LN: Insights into the receptor transcription and signaling: implications in opioid tolerance and dependence. *Neuropharmacology* **47**: 300-311, 2004.

LAW PY, WONG YH, LOH HH: Molecular mechanisms and regulation of opioid receptor signaling. *Annu Rev Pharmacol Toxicol* **40**: 389-430, 2000.

LI KW, JIMENEZ CR, VAN DER SCHORS RC, HORNSHAW MP, SCHOFFELMEER ANM, SMIT AB: Intermittent administration of morphine alters protein expression in rat nucleus accumbens. *Proteomics* **6**: 2003-2008, 2006.

LI Q, ZHAO X, ZHONG LJ, YANG HY, WANG Q, PU XP: Effects of chronic morphine treatment on protein expression in rat dorsal root ganglia. *Eur J Pharmacol* **612**: 21-28, 2009.

MAXFIELD FR, WÜSTNER D: Intracellular cholesterol transport. *J Clin Invest* **110**: 891-898, 2002.

MILLER AL, HAWKINS RA, HARRIS RL, VEECH RL: The effects of acute and chronic morphine treatment and of morphine withdrawal on rat brain in vivo. *Biochem J* **129**: 463-469, 1972.

MOFFETT S, BROWN DA, LINDER ME: Lipid-dependent targeting of G proteins into rafts. *J Biol Chem* **275**: 2191-2198, 2000.

MONASTYRSKAYA K, HOSTETTLER A, BUERGI S, DRAEGER A: The NK1 receptor localizes to the plasma membrane microdomains, and its activation is dependent on lipid raft integrity. *J Biol Chem* **280**: 7135-7146, 2005.

MOORE RH, SADOVNIKOFF N, HOFFENBERG S, LIU S, WOODFORD P, ANGELIDES K, TRIAL JA, CARSRUD ND, DICKEY BF, KNOLL BJ: Ligand-stimulated beta 2-adrenergic receptor internalization via the constitutive endocytotic pathway into rab5-containing endosomes. *J Cell Sci* **108**: 2983-2991, 1995.

MURTHY KS, MAKHLOUF GM: Heterologous desensitization mediated by G protein-specific binding to caveolin. *J Biol Chem* **275**: 30211-30219, 2000.

OH P, SCHNITZER JE: Segregation of heterotrimeric G proteins in cell surface microdomains: G(q) binds caveolin to concentrate in caveolae, whereas G(i) and G(s) target lipid rafts by default. *Mol Biol Cell* **12**: 685-698, 2001.

OSTASOV P, BOUROVA L, HEJNOVA L, NOVOTNY J, SVOBODA P: Disruption of the plasma membrane integrity by cholesterol depletion impairs effectiveness of TRH receptor-mediated signal transduction via G(q)/G(11)alpha proteins. *J Recept Signal Transduct Res* **27**: 335-352, 2007.

OSTASOV P, KRUSEK J, DURCHANKOVA D, SVOBODA P, NOVOTNY J: Ca2+ responses to thyrotropin-releasing hormone and angiotensin II: the role of plasma membrane integrity and effect of G11alpha protein overexpression on homologous and heterologous desensitization. *Cell Biochem Funct* **26**: 264-274, 2008.

OSTASOV P, SYKORA J, BREJCHOVA J, OLSZYNSKA A, HOF M, SVOBODA P: FLIM studies of 22- and 25-NBD-cholesterol in living HEK293 cells; *plasma membrane change induced by cholesterol depletion.* Chemistry and Physics of Lipids, 167-168, 62-69, 2013

OSTROM RS, GREGORIAN C, DRENAN RM, XIANG Y, REGAN JW, INSEL PA: Receptor number and caveolar co-localization determine receptor coupling efficiency to adenylyl cyclase. *J Biol Chem* **276**: 42063-42069, 2001.

OSTROM RS, INSEL PA: The evolving role of lipid rafts and caveolae in G protein-coupled receptor signaling: implications for molecular pharmacology. *Br J Pharmacol* **143**: 235-245, 2004.

OSTROM RS, POST SR, INSEL PA: Stoichiometry and compartmentation in G protein-coupled receptor signaling: implications for therapeutic interventions involving G(s). *J Pharmacol Exp Ther* **294**: 407-412, 2000.

PIKE LJ: Lipid rafts: heterogeneity on the high seas. *Biochem J* **378**: 281-292, 2004.

PIPPIG S, ANDEXINGER S, LOHSE MJ: Sequestration and recycling of beta 2-adrenergic receptors permit receptor resensitisation. *Mol Pharmacol* **47**: 666-676, 1995.

PRESTON KL: Drug abstinence effects: opioids. *Br J Addict* **86**: 1641-1646, 1991.

PUCADYIL TJ, CHATTOPADHYAY A: Cholesterol depletion induces dynamic confinement of the G-protein coupled serotonin(1A) receptor in the plasma membrane of living cells. *Biochim Biophys Acta* **1768**: 655-668, 2007.

PUCADYIL TJ, CHATTOPADHYAY A: Cholesterol modulates ligand binding and G-protein coupling to serotonin(1A) receptors from bovine hippocampus. *Biochim Biophys Acta* **1663**: 188-200, 2004.

QUINTON TM, KIM S, JIN J, KUNAPULI SP: Lipid rafts are required in Galpha(i) signaling downstream of the P2Y12 receptor during ADP-mediated platelet activation. *J Thromb Haemost* **3**: 1036-1041, 2005.

RICHELSON E: Lithium ion entry through the sodium channel of cultured mouse neuroblastoma cells: a biochemical study. *Science* **196**: 1001-1002, 1977.

ROBINSON TE, KOLB B: Morphine alters the structure of neurons in the nucleus accumbens and neocortex of rats. *Synapse* **33**: 160-162, 1999.

RYBIN VO, PAK E, ALCOTT S, STEINBERG SF: Developmental changes in beta2-adrenergic receptor signaling in ventricular myocytes: the role of Gi proteins and caveolae microdomains. *Mol Pharmacol* **63**: 1338-1348, 2003.

RYBIN VO, XU X, LISANTI MP, STEINBERG SF: Differential targeting of beta-adrenergic receptor subtypes and adenylyl cyclase to cardiomyocyte caveolae. A mechanism to functionally regulate the cAMP signaling pathway. *J Biol Chem* **275**: 41447-41457, 2000.

SABOURIN T, BASTIEN L, BACHVAROV DR, MARCEAU F: Agonist-induced translocation of the kinin B(1) receptor to caveolae-related rafts. *Mol Pharmacol* **61**: 546-553, 2002.

SAVI P, ZACHAYUS JL, DELESQUE-TOUCHARD N, LABOURET C, HERVÉ C, UZABIAGA MF, PEREILLO JM, CULOUSCOU JM, BONO F, FERRARA P, HERBERT JM: The active metabolite of Clopidogrel disrupts P2Y12 receptor oligomers and partitions them out of lipid rafts. *Proc Natl Acad Sci U S A* **103**: 11069-11074, 2006.

SCHEIDT HA, MULLER P, HERRMANN A, HUSTER D: The potential of fluorescent and spin-labeled steroid analogs to mimic natural cholesterol. *J Biol Chem* **278**: 45563-45569, 2003.

SCHWENCKE C, OKUMURA S, YAMAMOTO M, GENG YJ, ISHIKAWA Y: Colocalization of beta-adrenergic receptors and caveolin within the plasma membrane. *J Cell Biochem* **75**: 64-72, 1999.

SIBLEY DR, BENOVIC JL, CARON MG, LEFKOWITZ RJ: Molecular mechanisms of beta-adrenergic receptor desensitization. *Adv Exp Med Biol* **221**: 253-273, 1987.

SIMONS K, IKONEN E: Functional rafts in cell membranes. *Nature* **387**: 569-572, 1997.

STADEL JM, STRULOVICI B, NAMBI P, LAVIN TN, BRIGGS MM, CARON MG, LEFKOWITZ RJ: Desensitization of the beta-adrenergic receptor of frog erythrocytes. Recovery and characterization of the down-regulated receptors in sequestered vesicles. *J Biol Chem* **258**: 3032-3038, 1983.

SVOBODA P., TEISINGER J., NOVOTNY J., BOUROVA L, DRMOTA T, HEJNOVA L, MORAVCOVA Z, LISY V, RUDAJEV V, STOHR J, VOKURKOVA A, SVANDOVA I, DUSRCHANKOVA D: Biochemistry of trans-membrane signaling mediated by trimeric G-proteins. Physiol. Res. 53 (Suppl. 1), S141-S152, 2004.

SYKORA J, BOUROVA L, HOF M, SVOBODA P: The effect of detergents on trimeric G-protein activity in isolated plasma membranes from rat brain cortex; *correlation with studies of DPH and Laurdan fluorescence.* BBA Biomembranes, 1788, 324-332, 2009.

UJCIKOVA H, DLOUHA K, ROUBALOVA L, VOSAHLIKOVA M, KAGAN D, SVOBODA P: Up-regulation of adenylylcyclases I and II induced by long-term adaptation of rats to morphine fades away 20 days after morphine withdrawal. *Biochim Biophys Acta* **1810**: 1220-1229, 2011.

USHIO-FUKAI M, HILENSKI L, SANTANAM N, BECKER PL, MA Y, GRIENDLING KK, ALEXANDER RW: Cholesterol depletion inhibits epidermal growth factor receptor transactivation by angiotensin II in vascular smooth muscle cells: role of cholesterol-rich microdomains and focal adhesions in angiotensin II signaling. *J Biol Chem* **276**: 48269-48275, 2001.

VON ZASTROW M, KOBILKA BK: Antagonist-dependent and -independent steps in the mechanism of adrenergic receptor internalization. *J Biol Chem* **269**: 18448-18452, 1994.

VON ZASTROW M, KOBILKA BK: Ligand-regulated internalization and recycling of human beta2-adrenergic receptors between the plasma membrane and endosomes containing transferrin receptors. *J Biol Chem* **267**: 3530-3538, 1992.

VOSAHLIKOVA M, SVOBODA P: The influence of monovalent cations on trimeric G protein G(i)1α activity in HEK293 cells stably expressing DOR-G(i)1α (Cys(351)-Ile(351)) fusion protein. *Physiol Res* **60**: 541-547, 2011.

WALDO GL, NORTHUP JK, PERKINS JP, HARDEN TK: Characterization of an altered membrane form of the beta-adrenergic receptor produced during agonist-induced desensitization. *J Biol Chem* **258**: 13900-13908, 1983.

WHISTLER JL, VON ZASTROW M: Morphine-activated opioid receptors elude desensitization by beta-arrestin. Proc. Nat. Acad. Sci. USA 95, 9914-9919, 1998.

WHISTLER JL, CHUANG HH, CHU P, JAN LY, VON ZASTROW M: Functional dissociation of μ-opioid receptor signaling and receptor endocytosis: implications for the biology of opiate tolerance and addiction. Neuron 23, 737-746, 1999.

XU W, YOON SI, HUANG P, WANG Y, CHEN C, CHONG PL, LIU-CHEN LY: Localization of the kappa opioid receptor in lipid rafts. *J Pharmacol Exp Ther* **317**: 1295-1306, 2006.

YOUNG W: Review of lithium effects on brain and blood. *Cell Transplant* **18**: 951-975, 2009.

Table 1

DADLE-stimulated [^{35}S]GTPγS binding in membranes prepared from PTX-treated and PTX-untreated δ-OR-$G_i1\alpha$ - HEK293 cells

A PTX-treated

	EC_{50}		%		B_{basal}		B_{max}		Δ_{max}	
NaCl	5.1×10^{-8} M	**	350	**	0.143	**	0.499	*	0.356	**
KCl	9.6×10^{-9} M	* **	216	NS **	0.241	NS **	0.520	** NS	0.279	NS **
LiCl	5.4×10^{-9} M		231		0.209		0.481		0.272	

B PTX-untreated

	EC_{50}		%		B_{basal}		B_{max}		Δ_{max}	
NaCl	6.5×10^{-8} M	**	327	*	0.178	**	0.582	*	0.404	**
KCl	2.0×10^{-8} M	* **	237	NS *	0.222	NS **	0.526	NS *	0.304	NS **
LiCl	8.4×10^{-9} M		248		0.211		0.523		0.312	

[^{35}S]GTPγS binding was measured in P2 membrane fraction isolated from PTX-treated (A) or PTX-untreated cells (B) as described in methods. Binding assays were performed in 200 mM NaCl, KCl or LiCl. EC_{50} (M) and B_{max} (pmol x mg^{-1}) values were calculated by GraphPad*Prizm4*. B_{max} values were also expressed as the ratio (%) between maximum DADLE-stimulated (B_{max}) and the basal level (B_{basal}) of binding. Net-increment of agonist stimulation (Δ_{max}) was calculated as the difference between B_{max} and B_{basal} values. Numbers represent the means ± SEM of 3 binding assays, each performed in triplicates. Data were analyzed by one-way ANOVA followed by Neuman-Keuls post test (* $p<0.05$, ** $p<0.01$, NS non-significant).

(A) In PTX-treated membranes, [^{35}S]GTPγS binding in the absence of ions was 0.622 pmol × mg^{-1} and this level was decreased to 0.143 (NaCl), 0.241 (KCl) and 0.209 (LiCl) pmol × mg^{-1} by addition of 200 mM NaCl, KCl or LiCl, respectively.

(B) In PTX-untreated membranes, [^{35}S]GTPγS binding in the absence of ions was 0.809 pmol × mg^{-1} and this level was decreased to 0.178 (NaCl), 0.222 (KCl) and 0.211 (LiCl) pmol × mg^{-1} by addition of 200 mM NaCl, KCl or LiCl, respectively.

Figure legends

Fig. 1

Trimeric Gβ subunit protein; *immunoblot analysis of 2D-gels.*

A Two-dimensional resolution of Gβ protein content in PM isolated from control and morphine-adapted rats. PM protein (400 μg) was resolved by 2D electrophoresis using the pI range 3-11 for isoelectric focusing in the first dimension. The white small circle shows the small fraction of the total signal of Gβ which was taken into consideration when analyzed by LC-MS/MS. The second dimension was performed by SDS-PAGE in 10% w/v acrylamide/0.26% bis-acrylamide gels (Hoefer SE 600). Gβ was identified by immunoblotting with specific antibody oriented against C-terminal decapeptide of Gq/G11α. Numbers 1-8 represent spots of Gβ subunits which were subsequently analyzed by LC-MS/MS.

B The average of 3 immunoblots ± SEM. Difference between (-M10) and (+M10) was analyzed by Student´s *t*-test using GraphPad*Prizm4* and found not significant, NS ($p > 0.05$).

Fig.2

Agonist (DADLE)-induced internalization of δ-OR is attenuated by cholesterol depletion

HEK293T cells transiently transfected with FLAG-tagged δ-OR were *in vivo* labeled with the corresponding anti-tag antibodies, exposed to serum-free DMEM (Control), 10 mM β-CDX in serum-free DMEM (CDX), 100 nM DADLE (DADLE), or 10 mM β-CDX plus 100 nM DADLE in serum-free DMEM (CDX+DADLE) for 30 minutes, and fixed. After fixation the cells were subjected to indirect immunofluorescence with Alexa Fluor 488-conjugated secondary antibodies and imaged with laser scanning confocal microscopy.

Left panels **(A)** show representative micrographs of cells expressing FLAG-tagged δ-OR and treated as described above. Right panel (**B**) displays results from quantification of micrographs performed by ImageJ software. Fraction of internalized receptors was calculated as a ratio of intracellular to total signal determined in 8 cells per each condition, averaged and

normalized to values obtained by agonist (DADLE) stimulation. Data represent the average of 3 experiments, i.e., 3 independent transfections, ± S.E.M.. Statistical analysis was performed using one-way ANOVA repeated measurements with Bonferroni post test. *, **, represent the significant difference, $p<0.05$, $p<0.01$.

Fig.1

Morphine-induced decrease of trimeric Gβ subunits in plasma-membrane-enriched fraction; *resolution by 2D-electrophoresis*

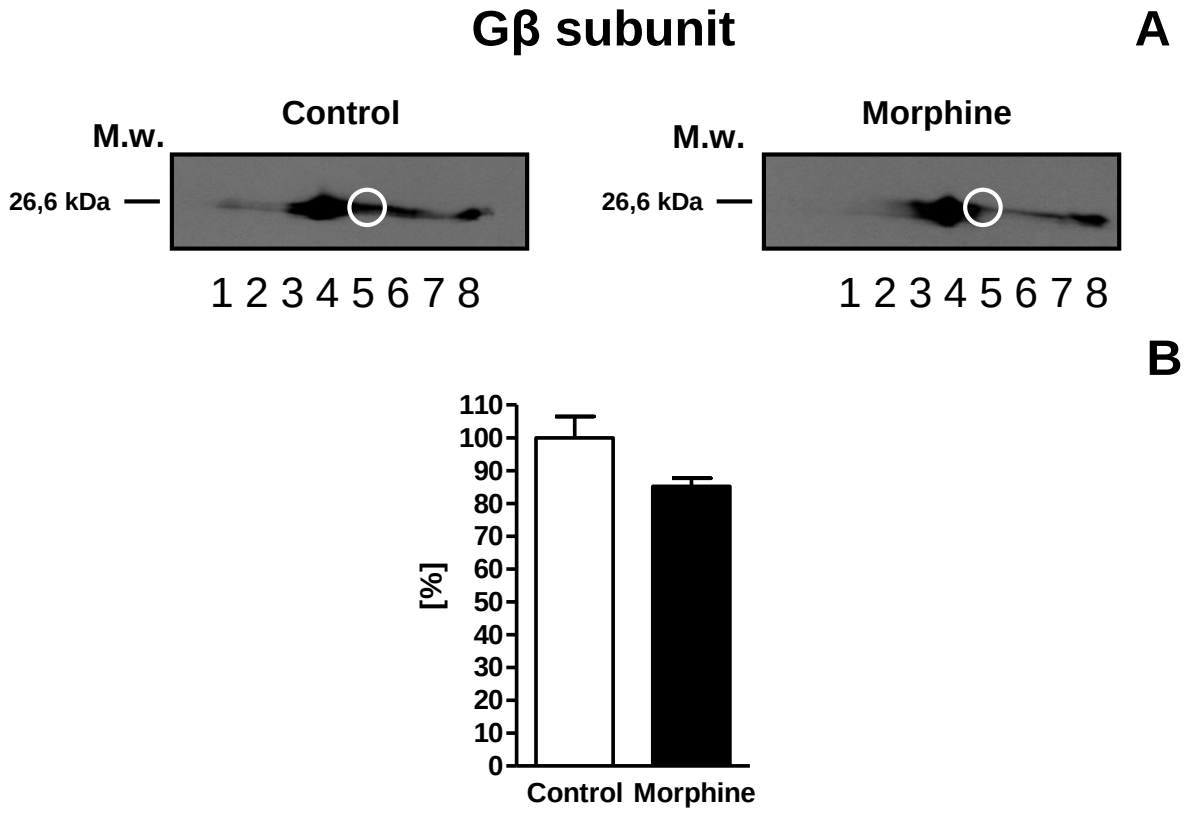

Fig. 2

Agonist-induced internalization of δ-opioid receptors in HEK cells transiently transfected with Flag-δ-OR

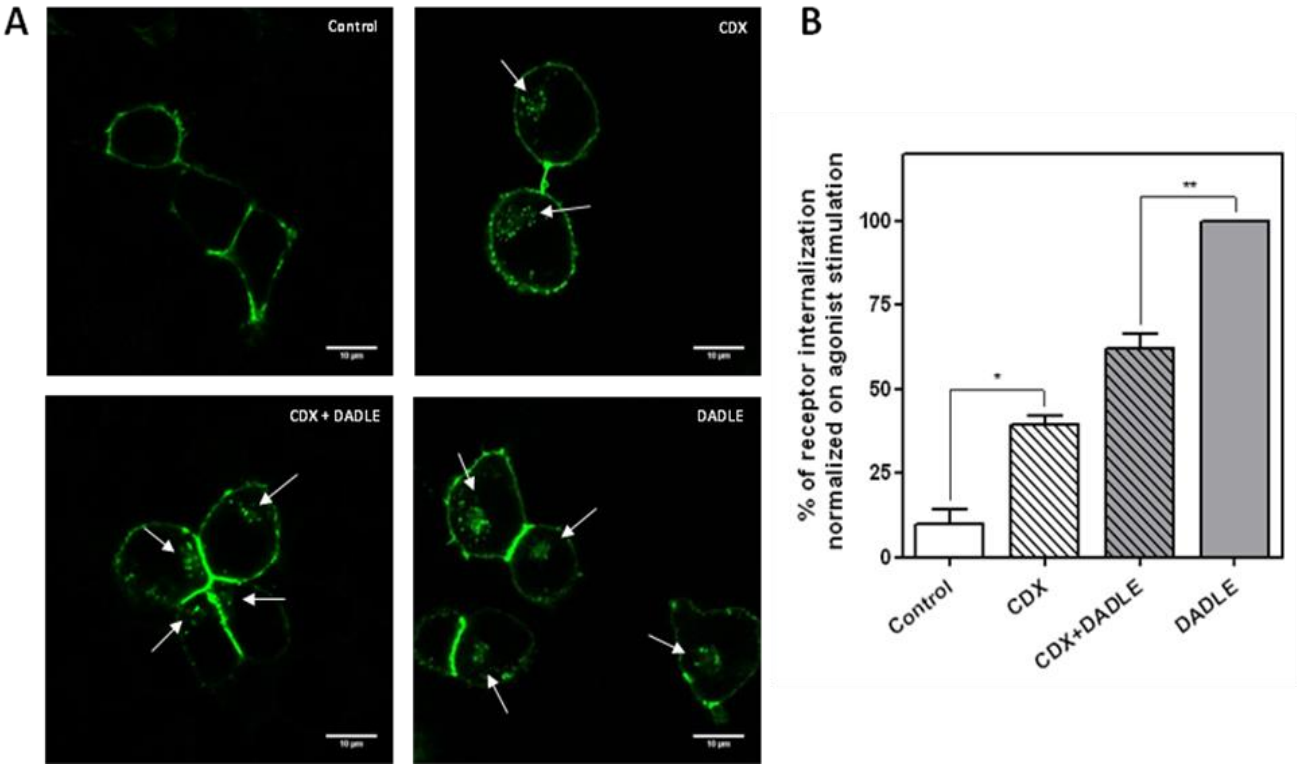

a

Biochimica et Biophysica Acta 1810 (2011) 1220–1229

Contents lists available at SciVerse ScienceDirect

Biochimica et Biophysica Acta

journal homepage: www.elsevier.com/locate/bbagen

Up-regulation of adenylylcyclases I and II induced by long-term adaptation of rats to morphine fades away 20 days after morphine withdrawal

Hana Ujcikova [a,b], Katerina Dlouha [a], Lenka Roubalova [a], Miroslava Vosahlikova [a], Dmytro Kagan [a], Petr Svoboda [a,b,*]

[a] Institute of Physiology, v.v.i., Academy of Sciences of the Czech Republic, Videnska 1083, 14220 Prague 4, Czech Republic
[b] Department of Physiology, Faculty of Science, Charles University, Vinicna 7, 12844 Prague 2, Czech Republic

ARTICLE INFO

Article history:
Received 21 April 2011
Received in revised form 12 September 2011
Accepted 27 September 2011
Available online 4 October 2011

Keywords:
Morphine
Long-term adaptation
Adenylyl cyclase isoforms I–IX
Forebrain cortex
Isolated plasma membranes

ABSTRACT

Background: Activation of adenylyl cyclase (AC) by prolonged exposure of mammalian organism to morphine was demonstrated in previous studies of mechanism of action of this drug. However, expression level of individual AC isoforms was not analyzed in crucial cell structure, plasma membrane (PM).
Methods: Rats were adapted to morphine for 10 days and sacrificed 24 h (group + M10) or 20 days (+M10/−M20) after the last dose. Control animals were sacrificed in parallel with morphine-treated (groups − M10 and (−M10/−M20)). Percoll®-purified PM were isolated from brain cortex and analyzed by immunoblotting and specific radioligand binding.
Results: ACI (ACII) was increased 8× (2.5×) in morphine-adapted rats (+M10) when compared with controls (−M10). Increase of ACI and II by long-term adaptation to increasing doses of morphine represented a specific effect as the amount of ACIII–ACIX, of prototypical PM marker, Na, K-ATPase and of trimeric G protein α and β subunits was unchanged. Increase of ACI and II was not detected in PM isolated from group (+M10/−M20). Thus, the marked increase of ACI and ACII faded away 20 days since the last dose of morphine.
Conclusions: We assume that the specific increase in expression level of ACI and ACII in brain cortex of morphine-adapted rats proceeds as a compensatory, homeostatic response to prolonged exposure to inhibitory drug, morphine.
General significance: Our findings demonstrate that the *dramatic and specific* change of the crucial component of the opioid receptor cascade in brain cortex, manifested as an increase in PM level of ACI and II, is reversible.

1. Introduction

Physiological action of opioid drugs requires an initial interaction with opioid receptors [1]. These receptors, MOR (μ-OR), DOR (δ-OR) and KOR (κ-OR) [2–9] are classified as members of rhodopsin family of G-protein coupled receptors, GPCRs. All these receptors are known to inhibit adenylyl cyclase activity in pertussis-toxin-dependent manner by activation of G_i/G_o class of trimeric G proteins [10]. These proteins (G_i1, G_i2, G_i3, G_o1, G_o2) are present in brain in large quantities and inhibit adenylyl cyclase activity or regulate ionic channels in pertussis-toxin-dependent manner [11–15].

Hyper-sensitization or super-activation of AC enzyme activity by prolonged exposure of cultured cells or mammalian organisms to morphine has been demonstrated in previous studies of mechanism of action of this drug representing the non-selective OR agonist [1,7,8,16–26]. Adenylyl cyclase is regulated by trimeric G-proteins, so any significant change of AC activity should be preceded by alternation of trimeric G-protein activity.

In our previous work [27], the purified membranes from brain cortex were used for determination of DAMGO (μ-OR)-, DADLE (δ-OR)-, and U-23554 (κ-OR)-stimulated [^{35}S] GTPγS binding which was used as an estimate of trimeric G protein activity. Membranes were isolated from forebrain cortex of control and morphine-treated rats. Results of this study indicated a clear desensitization of DAMGO- and DADLE-stimulated G protein response in membranes prepared from

Abbreviations: AC, adenylyl cyclase; β-AR, β-adrenergic receptor; DADLE, [2-D-alanine, 5-D-leucine]enkephalin = Tyr-D-Ala-Gly-Phe-D-Leu; DAMGO, [2-D-alanine, 4-N-methylphenylalanine, 5-glycinol]enkephalin = Tyr-D-Ala-Gly-N-methyl-Phe-Gly-ol; DOR, δ-opioid receptor; GPCR, G protein-coupled receptor; G proteins, heterotrimeric guanine nucleotide-binding regulatory proteins; $G_s\alpha$, G protein α subunit stimulating adenylyl cyclase activity; $G_i/G_o\alpha$, G protein α subunits inhibiting adenylyl cyclase activity in pertussis-toxin sensitive manner; $G_q/G_{11}\alpha$, G protein α subunits stimulating phoshoplipase C in pertussis-toxin independent manner; [^{35}S]GTPγS, guanosine-5′-[γ-^{35}S] triphosphate; KOR, κ-opioid receptor; PM, plasma (cell) membranes; MOR, μ-opioid receptor; Na,K-ATPase, sodium- plus potassium-activated, ouabain-dependent adenosine triphosphatase (EC 3.6.1.3); P_i, inorganic phosphate; OR, opioid receptor; PBS, phosphate-buffered saline; PM, plasma membrane; PMSF, phenylmethylsulfonyl fluoride; PTX, pertussis toxin; SLB, sample loading buffer; TBS, Tris-buffered saline; w.w., wet weight

* Corresponding author at: Institute of Physiology, Academy of Sciences of the Czech Republic, Videnska 1083, 14220 Prague 4, Czech Republic. Tel.: +420 2 41062533; fax: +420 2 41062488.
E-mail address: svobodap@biomed.cas.cz (P. Svoboda).

0304-4165/$ – see front matter © 2011 Elsevier B.V. All rights reserved.
doi:10.1016/j.bbagen.2011.09.017

morphine-treated rats [27]. U-23554-stimulated [^{35}S] GTPγS binding was unchanged. Our results were fully in line with data of Sim et al. [28], Sim-Selley et al. [29] and Maher et al. [30] indicating the desensitization of G protein response in specific areas of brain stem and hippocampus in morphine- as well as heroine-adapted rats.

In our present work, we have analyzed the content of *all* types of adenylyl cyclase protein molecules (ACI–IX) in PM isolated in the same way from morphine-adapted rats because the previous analyses of AC in drug-addicted state were preferentially oriented to functional assays of AC only and not to the quantitative determination of different isoforms of this enzyme in plasma membranes. Recent histochemical analysis of ACI–IX mRNA levels indicated that the expression level of ACI and II in rat brain cortex is high [31].

2. Material and methods

2.1. Chemicals

[^{3}H]-ouabain (30 mCi/mmol, NET211001MC), [^{3}H]DADLE (39.1 Ci/mmol, NET648250UC) and [^{3}H]DPDPE (45 Ci/mmol; NET922050UC) were purchased from Perkin Elmer. [α-^{32}P] ATP (adenosine-5′-[α-^{32}P] triphosphate, cat. no. 32007.2) was purchased from MP Biomedicals. [^{3}H]cAMP (cyclic 3′,5′-[α-^{3}H] adenosine monophosphate, cat. no. TRK498) was from Amersham. Complete protease inhibitor cocktail was from Roche Diagnostic, Mannheim, Germany (cat. no. 1697498). All other chemicals were of highest purity available.

2.2. Antisera

$G_i\alpha$ and $G_o\alpha$ subunit proteins were identified by antipeptide antibodies as originally described by Gierschik et al. [11], Goldsmith et al. [12], Backlund et al. [13] and Milligan [15]. Production of the rabbit polyclonal antisera anti-$G_i1/G_i2\alpha$, anti-$G_i3\alpha$, anti-G_o and anti-$G_q/G_{11}\alpha$ was performed according to Mitchell et al. [32,33], Mullaney and Milligan [34] and Mullaney et al. [35–37]. These antisera were previously characterized in our laboratory by Ihnatovych [38]. $G_s\alpha$ (G-5040) antibody was from Sigma. Rabbit polyclonal antibodies $G_z\alpha$ (I-20, sc-388), Gβ (T-20, sc-378), ACI (V-20, sc-586), ACII (C-20, sc-587), ACIII (C-20, sc-588), ACIV (C-20, sc-589), ACV/VI (C-17, sc-590), ACVII (M-20, sc-1966), ACVIII (C-17, sc-32131), ACIX (N-18, sc-8576) were purchased from Santa Cruz Biotechnology. Antibody oriented against α subunit of Na, K-ATPase (H-300, sc-28800) was also from Santa Cruz. Caveolin-1-oriented antibody C13630 was purchased from Transduction Laboratories [39].

2.3. Animals

All experiments were performed in accordance with the European Council Directive (86/609/EEC). Male Wistar rats (220–250 g) were killed by decapitation under ether narcosis, the frontal brain was rapidly removed, washed intensively from the remaining blood and cooled to 0 °C. The cerebral cortex was separated on the pre-cooled plate, snap frozen in liquid nitrogen and stored at −70 °C until use.

2.4. Morphine treatment of experimental animals

The animals were exposed to morphine by intra-muscular application according to the following protocol: 10 mg/kg (days 1 and 2), 15 mg/kg (days 3 and 4), 20 mg/kg (days 5 and 6), 30 mg/kg (days 7 and 8), 40 mg/kg (day 9) and, finally 50 mg/kg (day 10). The morphine-adapted rats were sacrificed 24 h (group + M10) or 20 days (group (+M10/−M20)) after the last dose of the drug. Control animals were injected with sterile PBS and sacrificed in parallel with morphine-adapted rats, i.e. 24 h (−M10) or 20 days (−M10/−M20) after the last dose.

An independent group of animals was exposed to the single dose (injection) of 10 mg/kg, 15 mg/kg, 20 mg/kg, 30 mg/kg, 40 mg/kg or 50 mg/kg of morphine (group + M1) and sacrificed for 24 h later. Control animals were injected with sterile PBS (group − M1). The aim of this *short term morphine exposure* experiment was to obtain an independent set of data on ACI and II levels in PM with the aim to compare these data with those collected from *morphine-adapted* rats for 10 days (group + M10).

2.5. Isolation of plasma membrane-enriched fraction from rat brain cortex

Rat brain cortex was minced with razor blade on pre-cooled plate and diluted in STEM medium containing 250 mM sucrose, 20 mM Tris–HCl, 3 mM $MgCl_2$, 1 mM EDTA, pH 7.6, fresh 1 mM PMSF plus protease inhibitor cocktail. It was then homogenized mildly in loosely-fitting Teflon-glass homogenizer for 5 min (2 g w. w. per 10 ml) and centrifuged for 5 min at 3500 rpm. Resulting post-nuclear supernatant (PNS) was filtered through Nylon nets of decreasing size (330, 110 and 75 mesh, Nitex) and applied on top of Percoll in Beckman Ti70 tubes (30 ml of 27.4% Percoll in STE medium). Centrifugation for 60 min at 30,000 rpm (65,000×*g*) resulted in the separation of two clearly visible layers [40]. The upper layer represented plasma membrane fraction (PM); the lower layer contained mitochondria (MITO). The upper layer was removed, diluted 1:3 in STEM medium and centrifuged in Beckman Ti70 rotor for 90 min at 50,000 rpm (175,000×*g*). Membrane sediment was removed from the compact, gel-like sediment of Percoll and re-homogenized by hand in a small volume of 50 mM Tris–HCl, 3 mM $MgCl_2$, 1 mM EDTA, pH 7.4 (TME medium).

2.6. SDS-PAGE and immunoblotting

The aliquots of membrane fractions were mixed 1:1 with 2× concentrated Laemmli buffer (SLB) and heated for 3 min at 95 °C. Standard (10% w/v acrylamide/0.26% w/v bis-acrylamide) SDS electrophoresis was carried out as described before [41–43]. Molecular mass determinations were based on pre-stained molecular mass markers (Sigma, SDS 7B). After SDS-PAGE, proteins were transferred to nitrocellulose and blocked for 1 h at room temperature in 5% (w/v) low-fat milk in TBS-Tween buffer [10 mM Tris–HCl, pH 8.0, 150 mM NaCl, 0.1% (v/v) Tween 20]. Antibodies were added in TBS-Tween containing 1% (w/v) low-fat milk and incubated for at least 2 h. The primary antibody was then removed and the blot washed extensively (3×10 min) in TBS-Tween. Secondary antibodies (donkey anti-rabbit IgG conjugated with horse-radish peroxidase) were diluted in TBS-Tween containing 1% (w/v) low-fat milk, applied for 1 h and after three 10 min washes the blots were developed by ECL technique using Super Signal West Dura (Pierce) as substrate. The developed blots were scanned with an imaging densitometer ScanJett 5370C (HP) and quantified by Aida Image Analyzer v. 3.28 (Ray test).

When indicated, membrane fractions were also analyzed by NuPAGE system (Invitrogen). Aliquots of membrane fractions were solubilized in NuPAGE LDS Sample Buffer (4×) with addition of NuPAGE Sample Reducing Agent (10×) according to manufacturer's instructions. Samples were heated at 70 °C for 10 min, loaded at 10 μg/well and resolved by NuPAGE 4–12% or 10% Bis-Tris polyacrylamide gels (10 wells,1 mm thick) using 3-(N-morpholino) propane sulfonic acid (MOPS), sodium dodecyl sulfate (SDS) running buffer with NuPAGE Antioxidant prior to blotting on nitrocellulose membranes (Protran, Schleicher & Schuell). Western blotting was carried out as described above.

2.7. Na, K-ATPase

All membrane preparations were screened for the content of PM marker, sodium- plus potassium-activated magnesium-dependent adenosine triphosphatase (EC 3.6.1.3). Na, K-ATPase was determined

by binding of radioactively labeled, selective inhibitor of this enzyme, [^{3}H]ouabain as described before by Svoboda et al. [44]. Membranes (50 μg) were incubated with 5 nM [^{3}H]ouabain for 90 min at 30 °C in total volume of 0.4 ml of 5 mM $NaHPO_4$, 5 mM $MgCl_2$, 50 mM Tris–HCl, pH 7.6 at 37 °C. Binding reaction was terminated by dilution with 5 ml of ice-cold buffer and filtration through Whatman GF/B filters. The filters were washed twice, dried overnight at laboratory temperature and the radioactivity was determined by liquid scintillation. Non-specific binding was determined in the presence of 1 μM unlabelled ouabain.

Membrane density of Na, K-ATPase molecules was detected by immunoblotting with antibodies oriented against α-subunit of this enzyme (sc-28800, Santa Cruz) as described above.

2.8. Adenylyl cyclase

Adenylyl cyclase enzyme activity was determined as described before by Bourova et al. [45]. Reaction mix was prepared according to Salomon [46]; separation of cyclic AMP from other nucleotides and inorganic phosphate was performed by dry alumina column chromatography as described by White [47].

2.9. δ-opioid receptors

Saturation binding experiments were performed using [^{3}H]DADLE or [^{3}H]DPDPE according to Bourova et al. [45] and Moon et al. [48]. The assay medium contained membrane protein (120 μg per tube) diluted in final volume of 100 μl of binding mix containing 50 mM Tris–HCl, 10 mM $MgCl_2$, 1 mM EDTA, pH 7.4 ± 100 mM NaCl plus increasing radioligand concentrations ([^{3}H]DADLE 0.1–34.4 nM; [^{3}H]DPDPE 0.1–57.3 nM). Specific binding of the radioligand was obtained as the difference between binding in the absence and presence of nonradioactive 10 μM DADLE or DPDPE. After incubation for 60 min at 30 °C, samples were diluted with 3 ml of ice-cold Mg-HEPES buffer, immediately filtered and washed 3× with 3 ml of Mg-HEPES buffer. Whatman GF/B filters mounted in Brandel cell harvester were used for separation of bound and free radioactivity. Radioactivity remaining on the filters was determined by liquid scintillation. Data were analyzed by GraphPad*Prizm4*.

2.10. Protein determination

The method of Lowry was used for determination of membrane protein. Bovine serum albumin (Sigma, Fraction V) was used as standard. Data were calculated by fitting the data with calibration curve as quadratic equation.

3. Results

3.1. Morphine-induced increase in plasma membrane density of adenylylcyclases I and II

The amount of adenylylcyclases I and II was determined first in plasma membrane fraction (PM) isolated from frontal brain cortex of rats adapted to increasing doses of morphine for 10 days and compared with PM isolated from control animals. Data presented in Fig. 1A (left panels) indicate clearly a large increase in membrane density of ACI. Quantitative analysis of 32 immunoblots performed with 50 μg or 100 μg of PM protein applied per gel indicated a highly significant difference between the two sets of data, $p<0.001$. Membranes isolated from morphine-adapted rats (group + M10) exhibited 8× higher density of ACI than membranes isolated from control animals (group − M10). The same type of analysis, when performed with ACII oriented antibody indicated 2.5× increase of this enzyme protein in membranes prepared from morphine-adapted rats when compared with controls (Fig. 1A, middle panels). The difference between the two groups was again highly significant, $p<0.01$.

The increased level of ACI and ACII in PM samples prepared from morphine-adapted animals was not observed in membranes isolated from animals exposed to morphine for 10 days but sacrificed 20 days since the last dose of morphine (group (+M10/−M20)), Fig. 1B. These samples exhibited the same amount of ACI and ACII as corresponding controls (group (−M10/−M20)); (compare left and middle panels in Fig. 1B). Thus, in drug addicted state, PM density of AC molecules was dramatically increased mainly as far as ACI isoform was involved. This increase, being clearly disproportionate between ACI (8×) and ACII (2.5×), faded away 20 days since application of the last dose of morphine. Obviously, the withdrawal of the drug for sufficiently long period of time resulted in reversal of the pathological change back to "normal" state as far as the levels of these two isoforms of AC were involved.

The increase of ACI and II observed after 10 days of adaptation to increasing doses of morphine represented the specific phenomenon as the PM level of ACIII, IV, V/VI, VII, VIII and IX was unchanged (Fig. 2A). Furthermore, analysis of ACI and II in membranes prepared from animals exposed to the same doses of morphine but for 24 h only, i.e. to the *single* injection of morphine 10, 15, 20, 30, 40 and 50 mg/kg (see Material and methods for details), indicated that this short-term exposure had no effect on the membrane density of ACI and ACII in brain cortex PM (Fig. 2B). Thus, the dramatic and specific increase of ACI (8×) observed after 10 days of step-wise adaptation to increasing doses of morphine does not represent an acute phenomenon and may be regarded as the long-term adaptation of experimental animals to this drug.

3.2. Unchanged level of Na, K-ATPase

The next part of our work was oriented to analysis of other PM signaling molecules distinct from AC. Therefore, in parallel membrane samples to those used for determination of ACI and ACII, the specific content of Na, K-ATPase was measured as a negative standard and prototypical plasma membrane marker which should not be affected by morphine treatment, (Fig. 1A–C, right panels). Quantitative analysis of immunoblot signals corresponding to α subunit of this enzyme indicated that the expression level of this protein in PM was unchanged after adaptation to morphine for 10 days (Fig. 1A). Accordingly, the membrane content of Na, K-ATPase in samples isolated from rats sacrificed 20 days after the last dose of morphine was the same as in controls (Fig. 1B, right panel).

Data obtained by immunoblot analysis of Na, K-ATPase protein content in PM were extended and verified by analysis of "functional" parameter of this marker molecule, the number and affinity of binding sites for its selective inhibitor [^{3}H] ouabain. The maximum number (B_{max}) and affinity (K_d) of binding of this radioligand represents the highly selective and sensitive method for detection of Na, K-ATPase molecules in a given membrane sample. Virtually the same results as those obtained by immunoblot analysis were obtained (Fig. 3). Maximum binding capacity B_{max} and dissociation constant K_d of this radioligand binding to membranes isolated from morphine-adapted rats ($B_{max} = 35.5 \pm 2.1$ pmol . mg^{-1}; $K_d = 20.8 \pm 2.3$ nM) were not different from those determined in membranes prepared from control animals ($B_{max} = 36.6 \pm 2.1$ pmol . mg^{-1}; $K_d = 26.2 \pm 3.1$ nM).

3.3. Unchanged level of trimeric G protein α and β subunits

Determination ACI–IX and Na, K-ATPase presented in the previous paragraphs (Figs. 1–3) was accompanied by analysis of G protein content in PM preparations isolated from the same rats as those used for determination of ACI and ACII. The reason why we have performed this analysis was that the change in functional activity of a given set of signaling molecules does not necessarily mean the change in its expression level or membrane density. As already mentioned in introduction section, our previous data indicated the desensitization of G

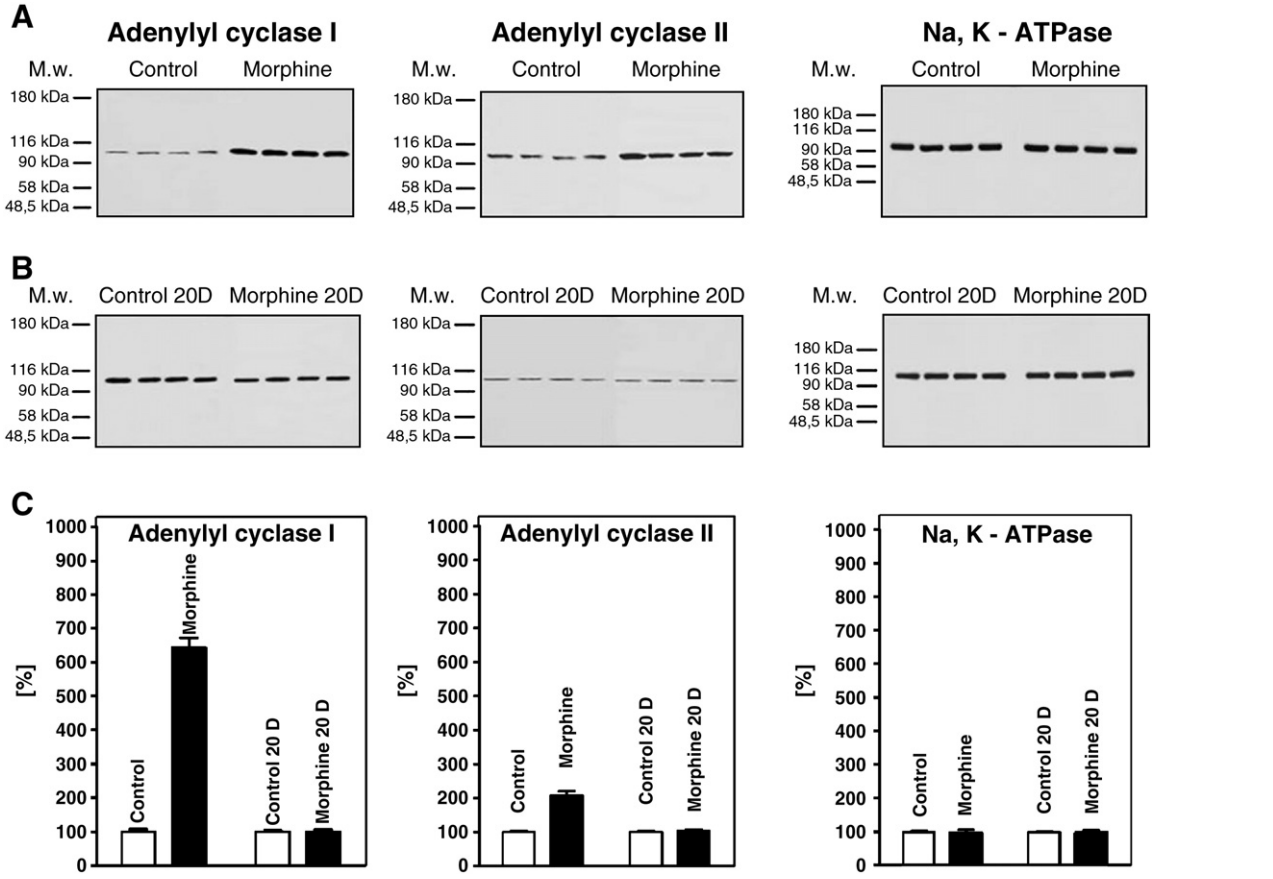

Fig. 1. Adenylyl cyclases I, II and Na, K-ATPase; *immunoblot analysis*. A. Membrane content of ACI (left), ACII (middle) and Na,K-ATPase (right panels) was determined by quantitative immunoblotting in PM isolated in parallel from brain cortex of control rats (group − M10) and rats adapted to increasing doses of morphine for 10 days (group + M10). Adaptation was performed according to the following protocol: 10 mg/kg (days 1 and 2), 15 mg/kg (days 3 and 4), 20 mg/kg (days 5 and 6), 30 mg/kg (days 7 and 8), 40 mg/kg (day 9) and 50 mg/kg (day 10). Control animals were injected with PBS at the same time intervals. Resolution of control and morphine-adapted samples by SDS-PAGE was always performed on the same gel and subsequently transferred to the same nitrocellulose sheet. Typical immunoblots performed with the same amount of protein in the two types of PM are shown: 4×(−M10) samples followed by 4×(+M10) samples from left to right. Control, membranes isolated from group (−M10); Morphine, membranes isolated from group (+M10). B. PM had been isolated from animals adapted to morphine according to the same protocol but further nurtured for 20 days in the absence of this drug (group (+M10/−M20)). Corresponding controls were represented by PM isolated from animals designated as (−M10/−M20), see Material and methods. Animals in this group were injected with PBS for 10 days and subsequently nurtured in the absence of any additions/injections for 20 days. Typical immunoblots performed with the same amount of PM protein resolved in the same gel [4×(−M10) plus 4×(+M10) samples] are shown. Control 20D, membranes isolated from group (−M10/−M20); Morphine 20D, membranes isolated from group (+M10/−M20). C. Statistical analysis of immunoblot signals collected from 32 (ACI), 26 (ACII) and 12 (Na, K-ATPase) immunoblots [4×(−M10) plus 4×(+M10) samples in each gel/blot]. Numbers represent the average + M10/−M10 ratio ± SEM expressed as% of control values, 100%.

protein response to OR stimulation in membranes isolated from morphine-adapted rats [27].

Data presented in Fig. 4 indicated clearly the unchanged level of all the major classes of trimeric G protein α and β subunits: $G_i1/G_i2\alpha$, $G_i3\alpha$, $G_o\alpha$, $G_z\alpha$, $G_s\alpha$, $G_q/G_{11}\alpha$ and Gβ. When normalized and compared in at least 3 immunoblots performed with different amounts of protein, the difference between morphine-treated and control samples (100%) was not significant: $G_i1/G_i2\alpha$ (100 ± 10%), $G_i3\alpha$ (109 ± 5%), $G_o\alpha$ (105 ± 2%), $G_z\alpha$ (100 ± 6%), $G_s\alpha$ (98 ± 4%), $G_q/G_{11}\alpha$ (96 ± 4%), Gβ (101 ± 7%). Membrane density of caveolin-1 was also unchanged — the level of this PM marker in morphine-adapted samples represented 89 ± 6% of the control level. The difference between control and morphine treated rats was analyzed by Student's *t*-test and expressed as% of control level. The numbers represent the average ± SEM of densitometric scans carried out in triplicate.

Results presented in Fig. 4 may be regarded as an additional support for desensitization mechanism of morphine action as more drastic adaptation should result in decrease of the amount of the cognate G protein α subunits in PM isolated from morphine-treated rats. This phenomenon, known as *down-regulation* of G proteins is well known, has been originally described by Milligan and Green [49] in white fat cells and later demonstrated in numerous GPCR-stimulated cascades both in cultured cells and intact tissue [35,36,49–56].

3.4. Adenylyl cyclase activity in morphine-adapted rats

The question, to what extend the increase of ACI and ACII in brain cortex of morphine-adapted rats (group + M10) is associated with or reflected in change of an overall adenylyl cyclase enzyme activity, was tested in parallel PM samples as those used before in immunoblot analysis of ACI–IX, Na, K-ATPase and G protein subunits. Data shown in Fig. 5 indicated that inhibitory effect of MOR and DOR agonists DAMGO and DADLE, which was manifested in control animals (group − M10), was not detected in morphine-adapted rats (group + M10). This result, demonstrated for basal as well as Forskolin-stimulated AC, supports the previously published data describing the decrease (desensitization) of G protein response to opioid stimulation in drug-addicted state [27–30,32] and is directly relevant and in agreement with principal finding of He and Whistler [57] indicating that chronic morphine resulted in a significant attenuation of the DAMGO-mediated inhibition of AC activity.

3.5. Increase in number of δ-opioid receptors (DOR)

In crude membrane preparations of monkey cortex and thalamus, the magnitude of MOR-, DOR- and KOR-stimulated G protein responses was proportional to the corresponding receptor densities

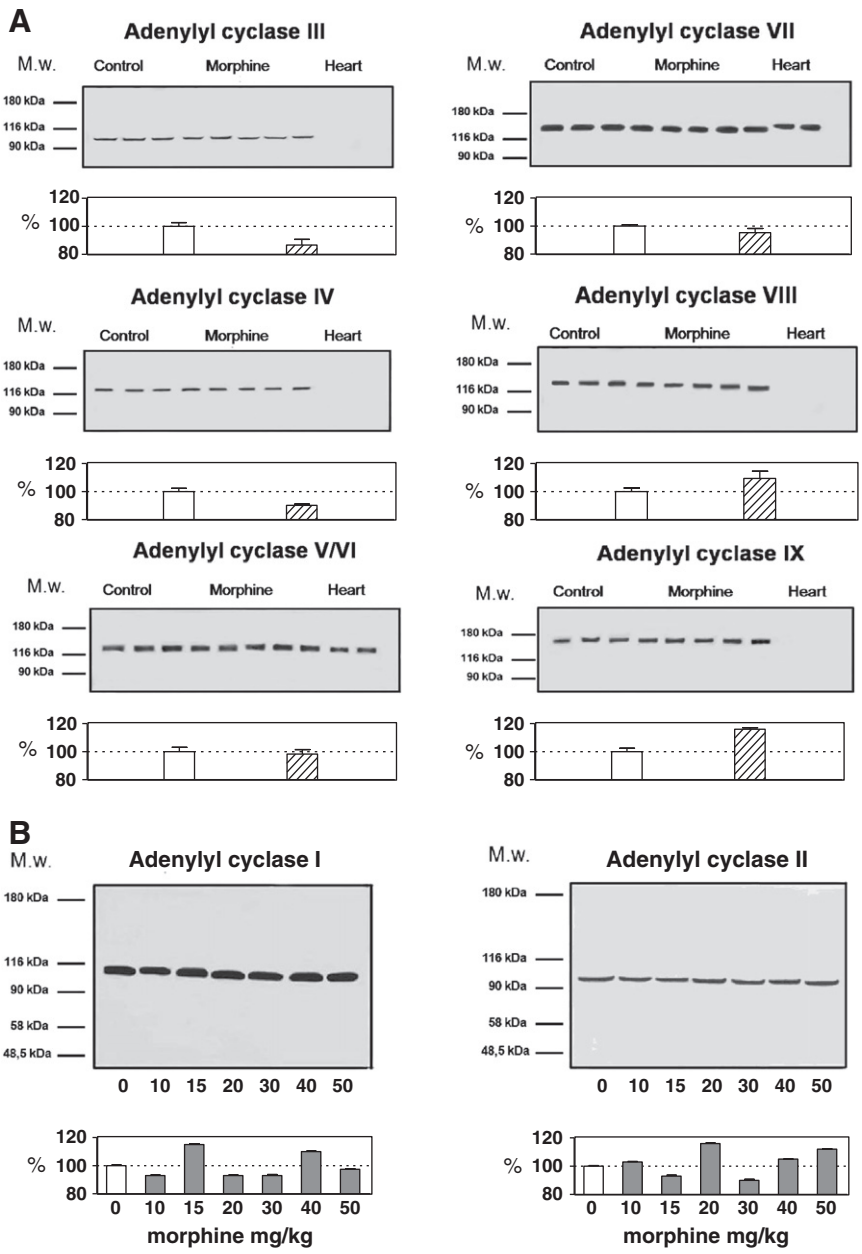

Fig. 2. Adenylyl cyclases III, IV, V/VI, VII, VIII and IX; *immunoblot analysis*. A. Membrane content of ACIII–IX was determined in PM isolated from brain cortex of morphine-adapted (group + M10) and control rats (group − M10) by quantitative immunoblotting. Typical immunoblots performed with the same amount of PM protein resolved in the same gel [4 × (− M10) plus 4 × (+ M10) samples] are shown. Statistical analysis was based on analysis of 3 immunoblots [4 × (− M10) plus 4 × (+ M10) samples in each gel/blot]. Numbers represent the average + M10/− M10 ratio ± SEM expressed as% of control (− M10) values, 100%. B. PM were isolated from animals exposed to the same doses of morphine (10, 15, 20, 30, 40 and 50 mg/kg) as in long-term adaptation experiment (Fig. 1), but for 24 h only (group + M1). Control animals were exposed to the single injection of PBS and sacrificed after 24 h (group − M1). As before, immunoblotting was performed with the same amount of PM protein resolved in the same gel [4 × (− M1) plus 4 × (+ M1). samples]. Both types of samples were run in parallel. Statistical analysis was based of comparison of (− M1) and (+ M1) samples in 3 immunoblots. Numbers represent the average + M1/− M1 ratio ± SEM expressed as% of control values, 100%.

[58]. Accordingly, the studies dealing with MOR in CHO cells [59] and in brain [60,61] indicated that the relationship between MOR occupancy and G protein activation depends on the receptor density [59–61]. As these studies were primarily oriented to MOR we decided to compare DOR density in PM prepared from control and morphine-adapted rat brain cortex.

DOR receptors in control (− M10) and morphine-treated (+ M10) brain cortex were characterized by saturation binding studies with DOR agonists [^{3}H]DADLE and [^{3}H]DPDPE. Saturation binding curves were measured in 0.1–34.4 nM ([^{3}H]DADLE) and 0.1–57.3 nM ([^{3}H] DPDPE) range of agonist concentrations in the presence or absence of 100 mM NaCl.

As shown in Fig. 6, maximum number of [^{3}H]DADLE binding sites in membranes isolated from morphine-adapted rats ($B_{max} = 0.115$ pmol . mg^{-1}) was 1.4× higher than in membranes isolated from control rats ($B_{max} = 0.083$ pmol . mg^{-1}). Surprisingly, 100 mM sodium chloride had no effect on [^{3}H]DADLE binding in morphine-adapted samples, but, as expected, it did inhibit radioligand binding to control membranes.

Morphine-induced increase of ligand binding to DOR was substantially higher when more specific ligand, [^{3}H] DPDPE, was

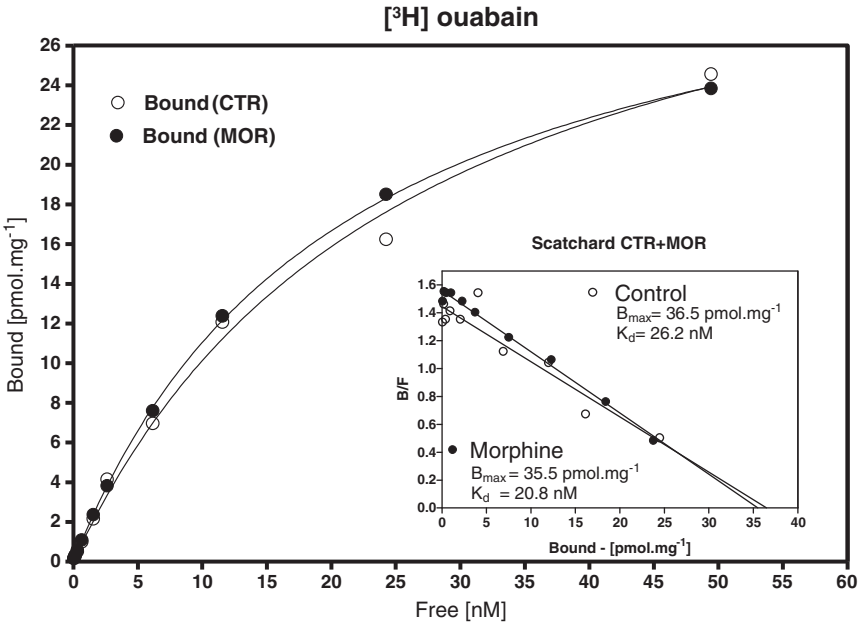

Fig. 3. Maximum binding capacity (B_{max}) and dissociation constant (K_d) of [^{3}H] ouabain binding sites in PM isolated from control and morphine-treated rats. Binding of selective Na, K-ATPase inhibitor [^{3}H] ouabain to PM isolated from brain cortex of control (−M10) and morphine-treated (+M10) rats was determined as described in Material and methods. Data were analyzed by GraphPad*Prism4*. B_{max} and K_d values represent the average of 3 experiments, each performed in triplicates.

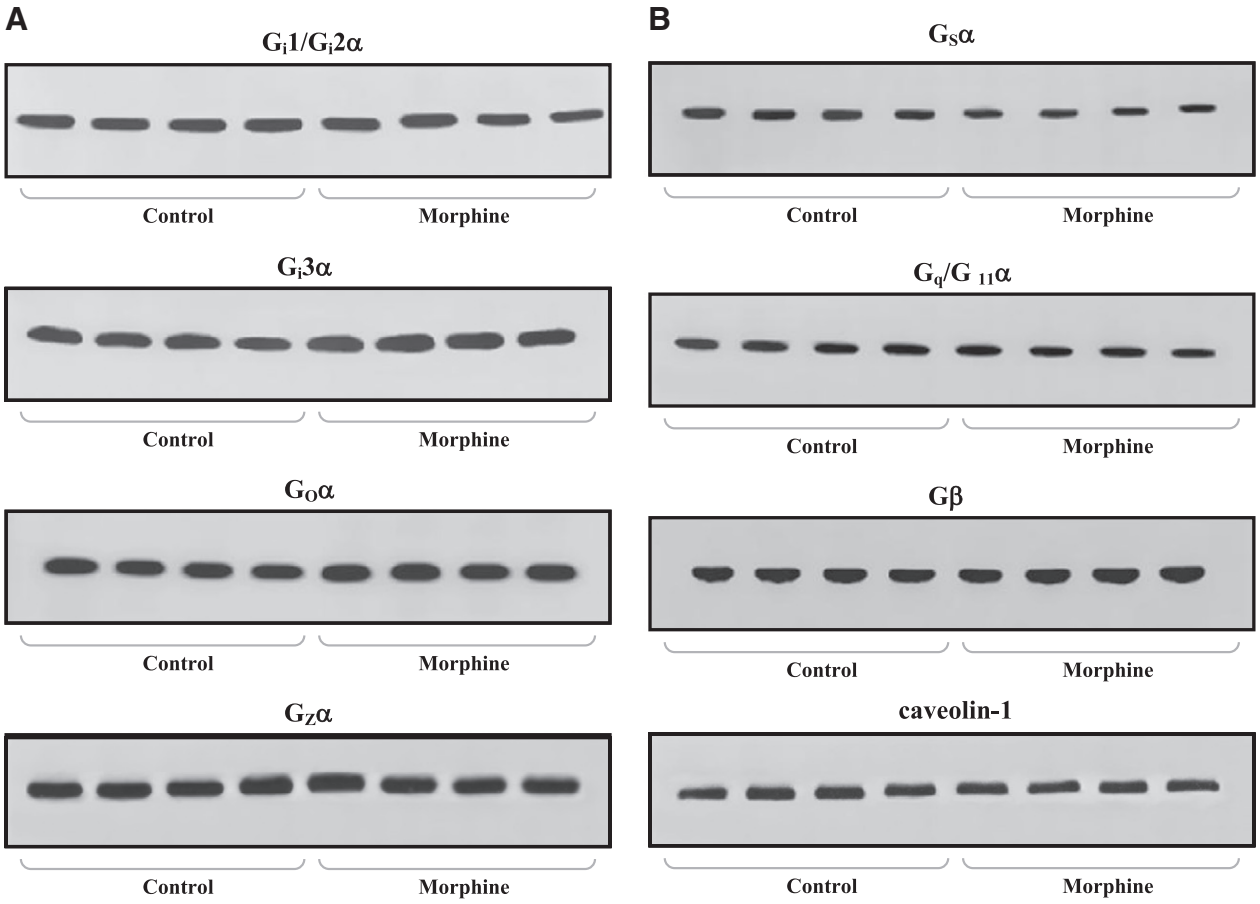

Fig. 4. Comparison of G protein content in PM isolated from control and morphine-adapted rats; $G_i1/G_i2\alpha$, $G_i3\alpha$, $G_z\alpha$, $G_s\alpha$, $G_q/G_{11}\alpha$, $G\beta$. PM protein (10 μg per well) was resolved by standard SDS-PAGE in Bio Rad Mini Protean II or by NuPAGE system (Invitrogen). G protein α and β subunits were identified by immunoblotting with specific antibodies as described in Material and methods. Caveolin-1 was determined as a marker of membrane domains. Data represent the typical immunoblots. $G_z\alpha$ and Gβ were resolved by NuPAGE electrophoretic system (Invitrogen); all other proteins were resolved by standard SDS-PAGE (BioRad). Statistical analysis was based on analysis of 3 immunoblots [4×(−M10) plus 4×(+M10) samples in each gel/blot]. Numbers represent the average + M10/−M10 ratio ± SEM expressed as% of control (−M10) values, 100%.

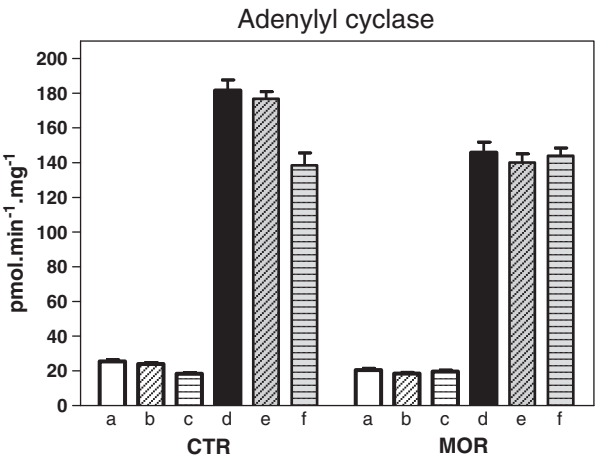

Fig. 5. Adenylyl cyclase enzyme activity. AC activity was measured in the absence (a, b, c) or presence of 10 μM Forskolin (d, e, f) in PM isolated from control (CTR, group − M10) or morphine-adapted (MOR, group + M10) rats as described in Material and methods. (a, d), basal activity, i.e. no additions; (b, e), 10 μM DADLE (δ-opioid agonist); (c, f), 10 μM DAMGO (μ-opioid agonist). Data represent the average of 3 experiments ± SEM.

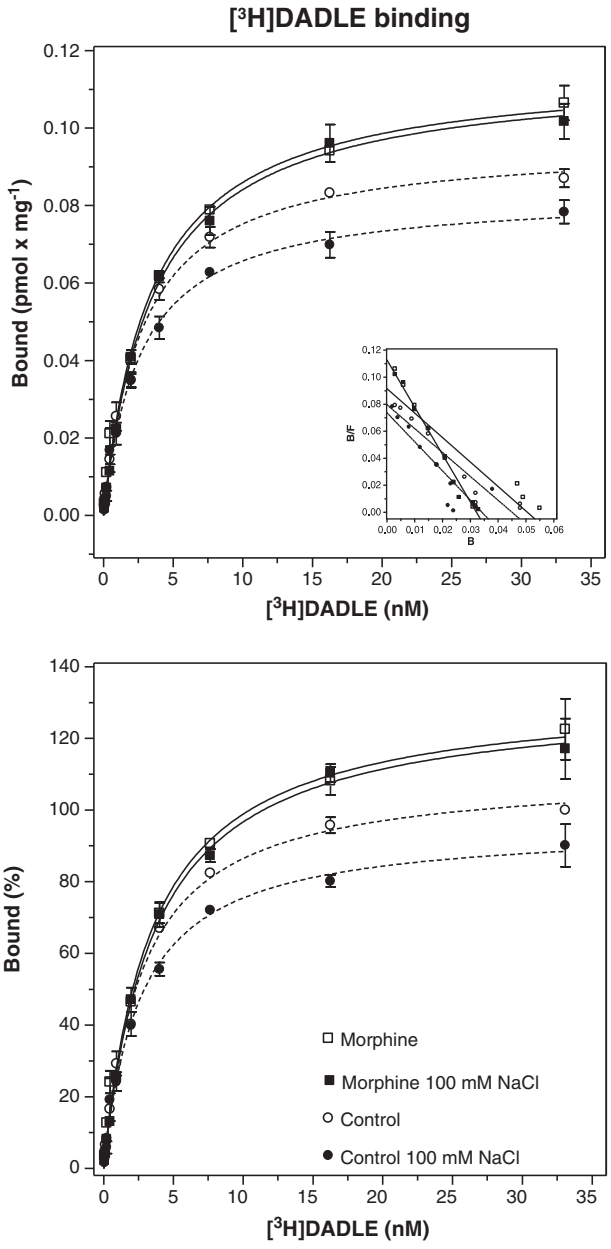

Fig. 6. Agonist binding characteristics of DOR; [^{3}H] DADLE. Saturation of specific [^{3}H] DADLE binding sites in control (− M10) and morphine-adapted (+ M10) plasma membrane samples was measured in 0.15–35 nM range of radioligand concentrations in the presence (+ NaCl) or absence (− NaCl) of 100 mM NaCl. The B_{max} and K_d values were calculated by GraphPad*Prizm4*. The data represent the average of three experiments performed in triplicates ± SEM. (○), controls, − NaCl; (●), controls, + NaCl; (□), morphine-adapted, − NaCl; (■), morphine-adapted, + NaCl.

used for determination of DOR in brain membranes. Maximum number of [^{3}H]DPDPE binding sites in morphine-treated membranes ($B_{max} = 0.057$ pmol . mg^{-1}) was 2.1× higher than in control ($B_{max} = 0.027$ pmol . mg^{-1}), Fig. 7. The effect of sodium chloride on [^{3}H]DPDPE binding was similar to that on [^{3}H]DADLE binding: inhibition was detected in control membranes only.

The difference between the two radioligands may be explained by higher specificity of [^{3}H]DPDPE to DOR in samples prepared from brain as the brain tissue contains, besides δ-opioid-receptors, high amount of μ- and κ-receptors [58]: maximum number of radioligand binding sites occupied by [^{3}H]DADLE was significantly higher than that recognized by [^{3}H]DPDPE. Therefore, morphine-induced increase of DOR detected by [^{3}H] DPDPE (2.1×) represents a "better estimate" of the actual increase of DOR density in PM isolated from morphine-adapted rats.

Sodium ions have been described as efficient inhibitors of agonist binding to numerous GPCR including OR causing the shift of receptor molecules towards the non-active state and uncoupling DOR from the cognate G protein, i.e. inverse agonist effect [62–65]. Sodium ions also decrease the basal GDP/GTP exchange of G_i/G_o proteins [66]. The low sensitivity of DOR to inhibitory effect of NaCl in morphine-adapted samples may be therefore interpreted as disturbance of equilibrium between active and non-active forms of receptor molecules.

4. Discussion

Opioid *addiction* has been long recognized as neurological disease involving the development of complex behavior characterized by drug tolerance, dependence and craving for the drug. The efforts to elucidate the molecular and cellular mechanisms of opioid *addiction* extend over many years and their results may be classified into two main hypotheses [1]:

(a) According to *homeostasis theory*, the drug disturbs cellular homeostasis and its effects are compensated by the activation of pathways that produce opposite effects and thus restore homeostasis.
(b) According to *desensitization theory*, the change of the drug–receptor interaction, receptor–G protein interaction or of some other, down-stream steps of OR-stimulated cascade renders the receptor less sensitive to the drug [1,7,57,67].

The *homeostasis* model involves an alteration of the amount of macromolecules in the cell, while the *desensitization* hypothesis does not because the negative change of drug–receptor interaction or subsequent steps of OR-initiated cascade may proceed with unchanged level of down-stream effectors. Our previous data [27] indicated that long-term adaptation of rats to increasing doses of morphine (according to the same protocol as that used in this work, group + M10) induces the *desensitization* of trimeric G protein response to MOR and DOR agonists (high-affinity GTPase and GTPγS binding assays). Desensitization of G protein response was demonstrated in plasma-membrane fraction isolated from rat brain cortex [27,40]. Furthermore, behavioral studies performed with the same group of animals indicated that these animals were fully "*drug*

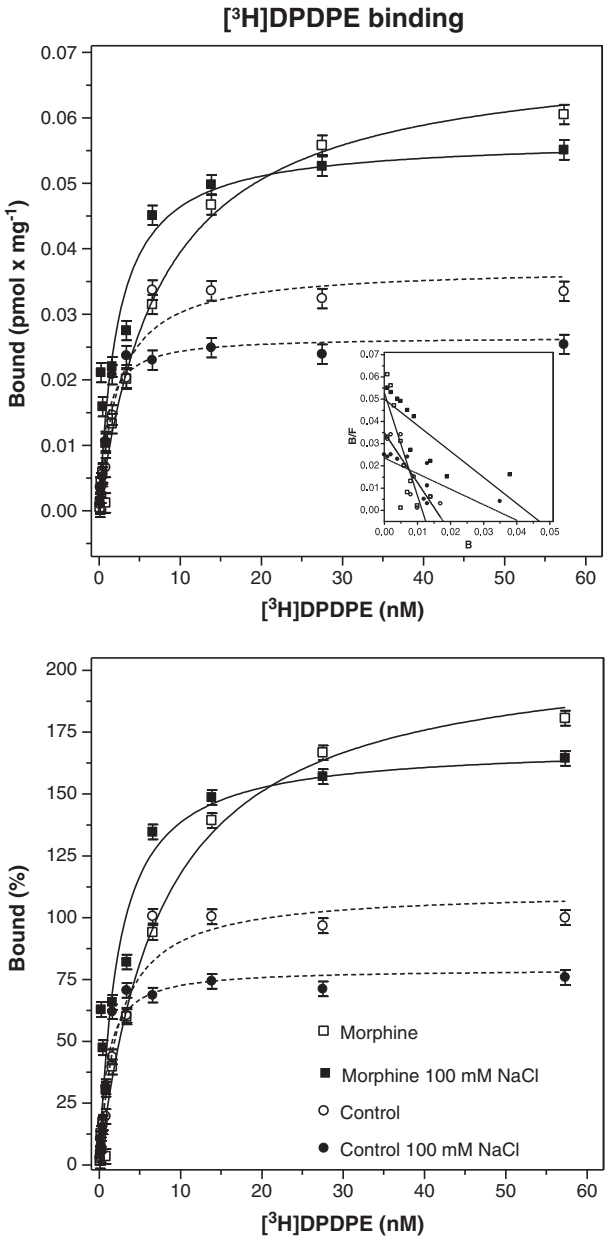

Fig. 7. Agonist binding characteristics of DOR; [^{3}H] DPDPE. Saturation of specific [^{3}H] DPDPE binding sites in control (−M10) and morphine-treated (+M10) plasma membrane samples was measured in 0.15–35 nM range of radioligand concentrations in the presence (+NaCl) or absence (−NaCl) of 100 mM NaCl. The B_{max} and K_d values were calculated by GraphPad*Prizm4*. The data represent the average of three experiments performed in triplicates ± SEM. (○), controls, −NaCl; (●), controls, +NaCl; (□), morphine-adapted, −NaCl; (■), morphine-adapted, +NaCl.

adapted" (*hot-plate* and *hind paw withdrawal* tests of tolerance). The state of *drug dependence* was also manifested by ptosis, chewing, diarrhea, increased sensitivity to touch and teeth clattering after drug withdrawal [27].

These results were fully compatible with data reported earlier by other authors who used auto-radiographic detection of the high-affinity [〈35〉S] GTPγS binding sites in different brain regions, mainly in specific areas of brain stem [28–30]. Thus, the decrease in functional response of G proteins persists in brain of animals fully adapted to morphine for prolonged period of time [27–30] and proceeds at the unchanged level of all the main classes of G proteins (Fig. 4). Accordingly, determination of AC activity in PM isolated from morphine-adapted rats indicated that inhibitory effect of opioid agonists, clearly manifested in control animals (group−M10), was *not* present in morphine-adapted rats (group+M10). This result has been demonstrated for basal as well as Forskolin-stimulated AC activity (Fig. 5) and was in full agreement with the data of He and Whistler [57].

Significance of the dramatic increase of ACI (8×) and ACII (2x) described in this work (Fig. 1A) was strongly supported by additional data indicating the specificity of this increase as the level of all other AC isoforms (AC III–IX) was unchanged (Fig. 2A) and that the increase of ACI and II was not detected in membranes exposed to the same doses of morphine, but for 24 h only (Fig. 2B).

It may be assumed that desensitization of G protein response for prolonged period of time (10 days) serves as an impulse for induction of compensatory response — proteosynthesis leading to specific increase of ACI and II in PM of morphine-adapted rats. This interpretation is fully in line with characteristics of molecular mechanisms of opioid tolerance and addiction as an example for homeostatic control aiming to keep the performance of target cell metabolism at unchanged level [1]. Finally, after withdrawal of the drug for 20 days, AC levels return back to the normal state (Fig. 1B).

Data presented in this work thus fall in line between the two above mentioned hypotheses of drug addiction as homeostatic mechanisms and activation of specific proteosynthetic pathways are obviously responsible for increase in plasma membrane density of ACI and ACII, simultaneously, the decrease of G protein response to OR stimulation detected in the same type of membranes [27], may be regarded as a part of desensitization mechanism of morphine action.

In brain, ACI and ACII represent the highly expressed and physiologically important species of this crucial regulatory enzyme of cAMP-dependent signaling cascades [31,68–70]. Sensitization, activation or over-shoot of AC activity after prolonged exposure of cultured cells or brain tissue to morphine has been demonstrated in previous studies of mechanism of action of this drug [1,7,8,16–23,26]. These data, however, were up to now not accompanied by the detailed analysis of the individual subtypes of AC protein molecules in plasma membranes isolated from brain cortex. Furthermore, the efforts to explain the molecular mechanism of the increase of AC activity by long-term morphine treatment have not so far resulted in a commonly accepted interpretation as widely different and even contradictory results were obtained [1,7,21,22,28,29,57].

The increase of ACI and II which has been clearly demonstrated in this work has to be considered together with the unchanged level of all other types of AC molecules and PM markers Na,K-ATPase, trimeric G protein subunits and caveolin-1. The unchanged level of these PM proteins brings strong evidence for the *specificity* of the long-term morphine effect on ACI and II. *Therefore, data presented in this work bring new and original evidence which so far has not been presented in the up-to-date literature and help for better understanding of the complicated pathological phenomenon denominated as drug addiction.*

We suggest that the positive as well as negative regulatory circuits exist at different steps of OR-induced signaling pathways when responding to prolonged exposure to morphine in the course of full adaptation to this drug. Decrease of G protein response to OR stimulation, *desensitization*, persists in animals adapted to morphine for 10- or 12 days [27–30], while the levels of all the main classes of G proteins remained unchanged (Fig. 4). Consequently, the decrease in inhibitory effect of G proteins on AC activity was measured in PM isolated from morphine-adapted rats (Fig. 5). It may be therefore assumed that the synthesis of new ACI and II molecules represents the *specific*, compensatory response leading to the increased plasma membrane density of these protein molecules (Fig. 1A, left panels).

Our results and interpretation are also relevant to analysis of drug tolerance and addiction states of mammalian organism as behavioral tests performed under in vivo conditions indicated that morphine-adapted animals have been fully *drug dependent* and developed *tolerance* to subsequent drug addiction [27].

Explanation why ACI and ACII differ when responding to the long-term morphine treatment can hardly be clear-cut and unequivocal as these two isoforms differ substantially when responding to different GPCR agonists and activated forms of G proteins [25,68–70]. ACI is known to be inhibited by free $G_o\alpha$ and $G\beta\gamma$ subunits [10,68,70], while ACII activity is dramatically activated/potentiated by $G\beta\gamma$ in the presence free $G_s\alpha$ subunits [21,22,25,69]. Nevertheless, we assume that the decreased response of PTX-sensitive G proteins of G_i/G_o family to MOR and DOR agonists in morphine-adapted rats (desensitization) represents the primary impulse for subsequent compensatory response increasing the expression level of ACI and II. Preferential increase of ACI (Fig. 1A) and attenuation of DAMGO-mediated inhibition of AC activity (Fig. 5) [57] suggests the primary involvement of "classical, inhibitory pathway" proceeding via MOR and inhibition of ACI activity [68,70].

5. Conclusions

Data presented in this work extend the knowledge and bring more close view to understanding of the long-term adaptation of mammalian organism to morphine and widely studied phenomena of drug addiction and tolerance.

We have found that:

- plasma membrane density of ACI and II molecules was increased largely and this increase was disproportionate between ACI (8×) and ACII (2.5×) in rats adapted to increasing doses of morphine for prolonged period of time, 10 days,
- increase of ACI and II represented the specific effect as the level of ACIII–IX was unchanged,
- levels of plasma membrane marker Na, K-ATPase and caveolin-1 were unchanged,
- membrane density of all the major classes of trimeric G proteins was unchanged;
- number of δ-opioid receptors was increased 2× and agonist binding to these receptor sites was not affected by sodium ions;
- difference in responsiveness of different AC isoforms to the long-term morphine treatment may be interpreted as preferential activation of specific synthetic pathway leading to production of new ACI and AC II molecules,
- increase of ACI and II was not detected in PM prepared from rats exposed to the same doses of morphine, but for 24 h only (short-term exposure),
- analysis of PM isolated from animals adapted to morphine for 10 days and subsequently nurtured for 20 days in the absence of the drug indicated that membrane density of both ACI and ACII returned fully to the control level observed in morphine-unexposed rats. *Thus, the major reorganization of the complement of AC molecules in plasma membrane, arising as a compensatory response to the long-term adaptation to morphine, was fully reversible.*

Acknowledgements

This work was supported by projects LC554 and LC06063 of MSMT, GACR (305/08/H037) and the Academy of Sciences of the Czech Republic (AV0Z50110509). The authors thank Ing. Martin Chmatal, CSc and Bc. Katerina Kasparovska for performing [^{3}H]ouabain binding assays and valuable help.

References

[1] P.Y. Law, H.H. Loh, L.N. Wei, Insights into the receptor transcription and signaling: implications in opioid tolerance and dependence, Neuropharmacology 47 (2004) 300–311.
[2] C.J. Evans, D.E. Keith, H. Morrison Jr., K. Magendzo, R.H. Edwards, Cloning of a delta opioid receptor by functional expression, Science 258 (1992) 1952–1955.
[3] B.L. Kieffer, K. Befort, C. Gaveriaux-Ruff, C.G. Hirth, The delta-opioid receptor: isolation of a cDNA by expression cloning and pharmacological characterization, Proc. Natl. Acad. Sci. U. S. A. 89 (1992) 12048–12052.
[4] B.L. Kieffer, Opioids: first lessons from knockout mice, Trends Pharmacol. Sci. 20 (1999) 19–26.
[5] Y. Chen, A. Mestek, J. Liu, J.A. Hurley, L. Yu, Molecular cloning and functional expression of a mu-opioid receptor from rat brain, Mol. Pharmacol. 44 (1993) 8–12.
[6] Y. Chen, A. Mestek, J. Liu, L. Yu, Molecular cloning of a rat kappa opioid receptor reveals sequence similarities to the mu and delta opioid receptors, Biochem. J. 295 (1993) 625–628.
[7] J.L. Whistler, M. von Zastrow, Morphine-activated opioid receptors elude desensitization by beta-arrestin, Proc. Natl. Acad. Sci. U. S. A. 95 (1998) 9914–9919.
[8] J.L. Whistler, H.H. Chuang, P. Chu, L.Y. Jan, M. von Zastrow, Functional dissociation of μ-opioid receptor signaling and receptor endocytosis: implications for the biology of opiate tolerance and addiction, Neuron 23 (1999) 737–746.
[9] C. Contet, B.L. Kieffer, K. Befort, Mu opioid receptor: a gateway to drug addiction, Curr. Opin. Neurobiol. 14 (2004) 370–378.
[10] B.D. Carter, F. Medzihradsky, Go mediates the coupling of the mu opioid receptor to adenylyl cyclase in cloned neural cells and brain, Proc. Natl. Acad. Sci. U.S.A. 90 (1993) 4062–4066.
[11] P. Gierschik, G. Milligan, M. Pines, P. Goldsmith, J. Codina, W. Klee, A. Spiegel, Use of specific antibodies to quantitate the guanine nucleotide-binding protein Go in brain, Proc. Natl. Acad. Sci. U. S. A. 83 (1986) 2258–2262.
[12] P. Goldsmith, P. Gierschik, G. Milligan, C.G. Unson, R. Vinitsky, H.L. Malech, A.M. Spiegel, Antibodies directed against synthetic peptides distinguish between GTP-binding proteins in neutrophil and brain, J. Biol. Chem. 262 (1987) 14683–14688.
[13] P.S. Backlund Jr., R.R. Aksamit, C.G. Unson, P. Goldsmith, A.M. Spiegel, G. Milligan, Immunochemical and electrophoretic characterization of the major pertussis toxin substrate of the RAW264 macrophage cell line, Biochemistry 27 (1988) 2040–2046.
[14] G. Milligan, Techniques used in the identification and analysis of function of pertussis toxin-sensitive guanine nucleotide binding proteins, Biochem. J. 255 (1988) 1–13.
[15] G. Milligan, Immunological probes and the identification of guanine nucleotide-binding proteins, in: M.D. Houslay, G. Milligan (Eds.), G proteins as Mediators of Cellular Signaling Processes, John Wiley & Sons. Ltd., New York, 1990, pp. 31–46.
[16] S.K. Sharma, M. Nierenberg, W.A. Klee, Morphine receptors as regulators of adenylate cyclase activity, Proc. Natl. Acad. Sci. U. S. A. 72 (1975) 590–594.
[17] S.K. Sharma, W.A. Klee, M. Nierenberg, Dual regulation of adenylate cyclase accounts for narcotic dependence and tolerance, Proc. Natl. Acad. Sci. U.S.A. 72 (1975) 3092–3096.
[18] B. Attali, Z. Vogel, Long-term opiate exposure leads to reduction of the alpha i-1 subunit of GTP-binding proteins, J. Neurochem. 53 (1989) 1636–1639.
[19] T. Avidor-Reiss, M. Baywatch, R. Levy, N. Matus-Leibovitch, I. Nevo, Z. Vogel, Adenylylcyclase super-sensitization in mu-opioid receptor-transfected Chinese hamster ovary cells following chronic opioid treatment, J. Biol. Chem. 270 (1995) 29732–29738.
[20] T. Avidor-Reiss, I. Nevo, R. Levy, T. Pfeuffer, Z. Vogel, Chronic opioid treatment induces adenylyl cyclase V superactivation. Involvement of Gβγ, J. Biol. Chem. 271 (1996) 21309–21315.
[21] H. Ammer, R. Schulz, Enhanced stimulatory adenylyl cyclase signaling during opioid dependence is associated with a reduction in palmitoylated Gs alpha, Mol. Pharmacol. 52 (1997) 993–999.
[22] H. Ammer, R. Schulz, Adenylyl cyclase super-sensitivity in opioid-withdrawn NG108-115 hybrid cells requires Gs but is not mediated by Gs alpha subunit, J. Pharmacol. Exp. Ther. 286 (1998) 855–862.
[23] M.L. Bayewitch, I. Nevo, T. Avidor-Reiss, R. Levy, W.F. Simonds, Z. Vogel, Alterations in detergent solubility of heterotrimeric G proteins after chronic activation of G(i/o)-coupled receptors: changes in detergent solubility are in correlation with onset of adenylyl cyclase superactivation, Mol. Pharmacol. 57 (2000) 820–825.
[24] H. Ammer, T.E. Christ, Identity of adenylyl cyclase isoform determines the G protein mediating chronic opioid-induced adenylyl cyclase supersensitivity, J. Neurochem. 83 (2002) 818–827.
[25] P.H. Tso, Y.H. Wong, Molecular basis of opioid dependence: role of signal regulation by G-proteins, Clin. Exp. Pharmacol. Physiol. 30 (2003) 307–316.
[26] E. Schallmach, D. Steiner, Z. Vogel, Adenylyl cyclase type II activity is regulated by two different mechanisms: implications for acute and opioid exposure, Neuropharmacology 50 (2006) 998–1005.
[27] L. Bourova, M. Vosahlikova, D. Kagan, K. Dlouha, J. Novotny, P. Svoboda, Long-term adaptation to high doses of morphine causes desensitization of μ-OR- and δ-OR-stimulated G protein response in forebrain cortex but not the decrease in the amount of G protein alpha subunits, Med. Sci. Monit. 16 (2010) BR260–BR270.
[28] L.J. Sim, D.E. Selley, S.I. Dworkin, S.R. Childers, Effects of chronic morphine administration on mu opioid receptor-stimulated [^{35}S] GTPgammaS autoradiography in rat brain, J. Neurosci. 16 (1996) 2684–2692.
[29] L.J. Sim-Selley, D.E. Selley, L.J. Vogt, S.R. Childers, T.J. Martin, Chronic heroin self-administration desensitizes mu opioid receptor-activated G-proteins in specific regions of rat brain, J. Neurosci. 20 (2000) 4555–4562.
[30] C.E. Maher, T.J. Martin, S.R. Childers, Mechanisms of mu opioid receptor/G-protein desensitization in brain by chronic heroin administration, Life Sci. 77 (2005) 1140–1154.
[31] C. Sanabra, G. Mengod, Neuroanatomical distribution and neurochemical characterization of cells expressing adenylyl cyclase isoforms in mouse and rat brain, J. Chem. Neuroanat. 41 (2011) 43–54.
[32] F.M. Mitchell, S.L. Griffiths, E.D. Saggerson, M.D. Houslay, J.T. Knowler, G. Milligan, Guanine-nucleotide-binding proteins expressed in rat white adipose tissue.

Identification of both mRNAs and proteins corresponding to Gi1, Gi2 and Gi3, Biochem. J. 262 (1989) 403–408.
[33] F.M. Mitchell, I. Mullaney, P.P. Godfrey, S.J. Arkinstall, M.J. Wakelam, G. Milligan, Widespread distribution of Gq alpha/G11 alpha detected immunologically by an antipeptide antiserum directed against the predicted C-terminal decapeptide, FEBS Lett. 287 (1991) 171–174.
[34] I. Mullaney, G. Milligan, Identification of two distinct isoforms of the guanine nucleotide binding protein Go in neuroblastoma × glioma hybrid cells: independent regulation during cyclic AMP-induced differentiation, J. Neurochem. 55 (1990) 1890–1898.
[35] I. Mullaney, M.W. Dodd, N. Buckley, G. Milligan, Agonist activation of transfected human M1 muscarinic acetylcholine receptors in CHO cells results in down-regulation of both the receptor and the alpha subunit of the G protein Gq, Biochem. J. 289 (1993) 125–131.
[36] I. Mullaney, F.M. Mitchell, J.F. McCallum, N.J. Buckley, G. Milligan, The human muscarinic M1 acetylcholine receptor when expressed in CHO cells, activates and down-regulates both Gq and G11 alpha equally and non-selectively, FEBS Lett. 324 (1993) 241–245.
[37] I. Mullaney, M.P. Caulfield, P. Svoboda, G. Milligan, Activation, cellular redistribution and enhanced degradation of the G proteins Gq and G11 by endogenously expressed and transfected phospholipase C-coupled muscarinic m1 acetylcholine receptors, Prog. Brain Res. 109 (1996) 181–187.
[38] I. Ihnatovych, J. Novotny, R. Haugvicova, L. Bourova, P. Mares, P. Svoboda, Ontogenetic development of G protein-mediated adenylyl cyclase signaling in rat brain, Brain Res. Dev. Brain Res. 133 (2002) 69–75.
[39] W.E. Evans, R.L. Coyer, M.F. Sandusky, M.J. Van Fleet, J.G. Moore, E. Nyquist, Characterization of membrane rats isolated from rat Sertoli cultures: caveolin and flotilin-1 content, J. Androl. 24 (2003) 812–821.
[40] L. Bourova, J. Stohr, V. Lisy, V. Rudajev, J. Novotny, P. Svoboda, Isolation of plasma membrane compartments from rat brain cortex; detection of agonist-stimulated G protein activity, Med. Sci. Monit. 15 (2009) BR111–BR122.
[41] Z. Moravcova, V. Rudajev, J. Stohr, J. Novotny, J. Cerny, M. Parenti, G. Milligan, P. Svoboda, Long-term agonist stimulation of IP prostanoid receptor depletes the cognate G(s)alpha protein in membrane domains but does not change the receptor level, Biochim. Biophys. Acta 1691 (2004) 51–65.
[42] P. Matousek, J. Novotny, P. Svoboda, Resolution of G(s)alpha and G(q)alpha/G (11)alpha proteins in membrane domains by two-dimensional electrophoresis: the effect of long-term agonist stimulation, Physiol. Res. 53 (2004) 295–303.
[43] P. Matousek, J. Novotny, V. Rudajev, P. Svoboda, Prolonged agonist stimulation does not alter the protein composition of membrane domains in spite of dramatic changes induced in a specific signaling cascade, Cell Biochem. Biophys. 42 (2005) 21–40.
[44] P. Svoboda, E. Amler, J. Teisinger, Different sensitivity of ATP + Mg + Na (I) and Pi + Mg (II) dependent types of oubain binding to phospholipase A2, J. Membr. Biol. 104 (1988) 211–221.
[45] L. Bourova, A. Kostrnova, L. Hejnova, Z. Moravcova, H.E. Moon, J. Novotny, G. Milligan, P. Svoboda, δ-opioid receptors exhibit high efficiency when activating trimeric G proteins in membrane domains, J. Neurochem. 85 (2003) 34–49.
[46] Y. Salomon, C. Londos, M. Rodbell, A highly sensitive adenylyl cyclase assay, Anal. Biochem. 58 (1974) 541–548.
[47] A.A. White, Separation and purification of cyclic nucleotides by alumina column chromatography, in: J.G. Hardman, B.W. O'Malley (Eds.), Methods in Enzymology, vol. 38C, Academic Press, 1974, pp. 41–46.
[48] H.E. Moon, A. Cavalli, D.S. Bahia, M. Hoffmann, D. Massotte, G. Milligan, The human δ opioid receptor activates Gi1α more efficiently than Go1α, J. Neurochem. 76 (2001) 1805–1813.
[49] G. Milligan, A. Green, Agonist control of G-protein levels, Trends Pharmacol. Sci. 12 (1991) 207–209.
[50] G. Milligan, Agonist regulation of cellular G protein levels and distribution: mechanisms and functional implications, Trends Pharmacol. Sci. 14 (1993) 413–418.
[51] F.M. Mitchell, N.J. Buckley, G. Milligan, Enhanced degradation of the phosphoinositidase C-linked guanine-nucleotide-binding protein Gq/G11 alpha following activation of the human M1 muscarinic acetylcholine receptor expressed in CHO cells, Biochem. J. 293 (1993) 495–499.
[52] F.R. McKenzie, G. Milligan, Prostaglandin E1-mediated, cyclic AMP-dependent down-regulation of Gs alpha in neuroblastoma × glioma hybrid cells, J. Biol. Chem. 265 (1990) 17084–17093.
[53] I. Mullaney, B.H. Shah, A. Wise, G. Milligan, Expression of the human β2-adrenoceptor in NCB20 cells results in agonist activation of adenylyl cyclase and agonist-mediated selective down-regulation of Gsα, J. Neurochem. 65 (1995) 545–553.
[54] P. Svoboda, L. Unelius, B. Cannon, J. Nedergaard, Attenuation of Gs alpha coupling efficiency in brown-adipose-tissue plasma membranes from cold-acclimated hamsters, Biochem. J. 295 (1993) 655–661.
[55] P. Svoboda, G.D. Kim, M.A. Grassie, K.A. Eidne, G. Milligan, Thyrotropin-releasing hormone-induced subcellular redistribution and down-regulation of G11 alpha: analysis of agonist regulation of co-expressed G11 alpha species variants, Mol. Pharmacol. 49 (1996) 646–655.
[56] P. Svoboda, L. Unelius, A. Dicker, B. Cannon, G. Milligan, J. Nedergaard, Cold-induced reduction in Gi alpha proteins in brown adipose tissue. Effects on the cellular hypersensitization to noradrenaline caused by pertussis-toxin treatment, Biochem. J. 314 (1996) 761–768.
[57] L. He, J.L. Whistler, The biochemical analysis of methadone modulation on morphine-induced tolerance and dependence in brain, Pharmacology 79 (2007) 193–202.
[58] M.C. Ko, H. Lee, C. Harrison, M.J. Clark, H.F. Song, N.N. Naughton, J.H. Woods, J.R. Traynor, Studies of mu-, kappa-, and delta-opioid receptor density and G protein activation in the cortex and thalamus of monkeys, J. Pharmacol. Exp. Ther. 306 (2003) 179–186.
[59] D.E. Selley, Q. Liu, S.R. Childers, Signal transduction correlates of mu opioid agonist intrinsic efficacy: receptor-stimulated [^{35}S]GTP gamma S binding in mMOR-CHO cells and rat thalamus, J. Pharmacol. Exp. Ther. 285 (1998) 496–505.
[60] L.J. Sim-Selley, J.B. Daunais, L.J. Porrino, S.R. Childers, Mu and kapp a1 opioid-stimulated [^{35}S]guanylyl-5′-O-(gamma-thio)-triphosphate binding in cynomolgus monkey brain, Neuroscience 94 (1999) 651–662.
[61] C.E. Maher, D.E. Selley, S.R. Childers, Relationship of mu opioid receptor binding to activation of G-proteins in specific rat brain regions, Biochem. Pharmacol. 59 (2000) 1395–1401.
[62] C.B. Pert, S.H. Snyder, Opiate receptor binding of agonists and antagonists affected differentially by sodium, Mol. Pharmacol. 10 (1974) 868–879.
[63] G. Koski, R.A. Streaty, W.A. Klee, Modulation of sodium-sensitive GTPase by partial opiate agonists. An explanation for the dual requirement for Na+ and GTP in inhibitory regulation of adenylate cyclase, J. Biol. Chem. 257 (1982) 14035–14040.
[64] H. Kong, K. Raynor, K. Yasuda, G.I. Bell, T. Reisine, Mutation of aspartate at residue 89 in somatostatine receptor subtype 2 prevents Na+ regulation of agonist binding but does not alter receptor–G protein interaction, Mol. Pharmacol. 44 (1993) 380–384.
[65] H. Kong, K. Raynor, K. Yasuda, S.T. Moe, P.S. Portoghese, G.I. Bell, T. Reisine, A single residue, aspartic acid 95, in the δ-opioid receptor specifies selective high affinity agonist binding, J. Biol. Chem. 268 (1993) 23055–23058.
[66] R. Seifert, K. Wenzel-Seifert, Constitutive activity of G-protein coupled receptors: cause of disease and common property of wild-type receptors, Naunyn-Schmiedeberg's Arch. Pharmacol. 366 (2002) 381–416.
[67] L. He, J.L. Whistler, An opiate cocktail that reduces morphine tolerance and dependence, Curr. Biol. 15 (2005) 1028–1033.
[68] J. Hanoune, N. Defer, Regulation and role of adenylyl cyclase isoforms, Annu. Rev. Pharmacol. Toxicol. 41 (2001) 145–174.
[69] R.K. Sunahara, R. Taussig, Isoforms of mammalian adenylyl cyclase: multiplicities of signaling, Mol. Interv. 2 (2002) 168–184.
[70] T.B. Patel, Z. Du, S. Pierre, L. Cartin, K. Scholich, Molecular biological approaches to unravel adenylyl cyclase signaling and function, Gene 269 (2001) 13–25.

Ujcikova et al. Proteome Science 2014, 12:11
http://www.proteomesci.com/content/12/1/11

PROTEOME SCIENCE

RESEARCH Open Access

Proteomic analysis of post-nuclear supernatant fraction and percoll-purified membranes prepared from brain cortex of rats exposed to increasing doses of morphine

Hana Ujcikova[1], Adam Eckhardt[2], Dmytro Kagan[1], Lenka Roubalova[1] and Petr Svoboda[1*]

Abstract

Background: Proteomic analysis was performed in post-nuclear supernatant (PNS) and Percoll-purified membranes (PM) prepared from fore brain cortex of rats exposed to increasing doses of morphine (10–50 mg/kg) for 10 days.

Results: In PNS, the 10 up (↑)- or down (↓)-regulated proteins exhibiting the *largest morphine-induced change* were selected, excised manually from the gel and identified by MALDI-TOF MS/MS: **1**-(gi|148747414, Guanine deaminase), ↑2.5×; **2**-(gi|17105370, Vacuolar-type proton ATP subunit B, brain isoform), ↑2.6×; **3**-(gi|1352384, Protein disulfide-isomerase A3), ↑3.4×; **4**-(gi|40254595, Dihydropyrimidinase-related protein 2), ↑3.6×; **5**-(gi|149054470, N-ethylmaleimide sensitive fusion protein, isoform CRAa), ↑2.0×; **6**-(gi|42476181, Malate dehydrogenase, mitochondrial precursor), ↑1.4×; **7**-(gi|62653546, Glyceraldehyde-3-phosphate dehydrogenase), ↑1.6×; **8**-(gi|202837, Aldolase A), ↑1.3×; **9**-(gi|31542401, Creatine kinase B-type), ↓0.86×; **10**-(gi|40538860, Aconitate hydratase, mitochondrial precursor), ↑1.3×. The identified proteins were of cytoplasmic (**1, 4, 5, 7, 9**), cell membrane (**2**), endoplasmic reticulum (**3**) and mitochondrial (**6, 8, 10**) origin and 9 of them were significantly increased, 1.3-3.6×. The 4 out of 9 up-regulated proteins (**4, 6, 7, 10**) were described as functionally related to oxidative stress; the 2 proteins participate in genesis of apoptotic cell death.
In PM, the 18 up (↑)- or down (↓)-regulated proteins were identified by LC-MS/MS and were of *plasma membrane* [Brain acid soluble protein, ↓2.1×; trimeric Gβ subunit, ↓2.0x], *myelin membrane* [MBP, ↓2.5×], *cytoplasmic* [Internexin, ↑5.2×; DPYL2, ↑4.9×; Ubiquitin hydrolase, ↓2.0×; 60S ribosomal protein, ↑2.7×; KCRB, ↓2.6×; Sirtuin-2, ↑2.5×; Peroxiredoxin-2, ↑2.2×; Septin-11, ↑2.2×; TERA, ↑2.1×; SYUA, ↑2.0×; Coronin-1A, ↓5.4×] and *mitochondrial* [Glutamate dehydrogenase 1, ↑2.7×; SCOT1, ↑2.2×; Prohibitin, ↑2.2×; Aspartate aminotransferase, ↓2.2×] origin. Surprisingly, the immunoblot analysis of the same PM resolved by 2D-ELFO indicated that the "active", morphine-induced pool of Gβ subunits represented just a minor fraction of the total signal of Gβ which was decreased 1.2x only. The dominant signal of Gβ was unchanged.

Conclusion: Brain cortex of rats exposed to increasing doses of morphine is far from being adapted. Significant up-regulation of proteins functionally related to oxidative stress and apoptosis suggests a major change of energy metabolism resulting in the state of severe brain cell "discomfort" or even death.

Keywords: Morphine, Long-term adaptation, Fore brain cortex, Isolated plasma membranes, Post-nuclear supernatant, 2D electrophoresis

* Correspondence: svobodap@biomed.cas.cz
[1]Laboratories of Biochemistry of Membrane Receptors, Institute of Physiology, v.v.i., Academy of Sciences of the Czech Republic, Videnska 1083, Prague 4 14220, Czech Republic
Full list of author information is available at the end of the article

Background

Morphine is one of the most effective painkillers. Repeated exposure of experimental animals to morphine results in tolerance to this drug, development of physical dependence and a chronic relapsing disorder – drug addiction [1-5]. Physical dependence contributes to a drug seeking behavior and the continuous drug use with the aim to prevent the onset of unpleasant withdrawal symptoms. To name just few, morphine-induced changes of brain function were associated with alternations of synaptic connectivity [6], neurotransmission [7], specific signaling cascades [8], energy metabolism [9] and stability of protein molecules [10].

Hyper-sensitization or super-activation of adenyl cyclase (AC) activity by prolonged exposure of cultured cells or mammalian organism to morphine has been demonstrated in previous studies of mechanism of action of this drug [1-5] and considered as biochemical basis for development of opiate *tolerance* and *dependence*.

Our previous work on isolated Percoll® membranes (PM) prepared from brain cortex of rats exposed to morphine for 10 days (10–50 mg/kg) indicated a desensitization of G-protein response to μ-OR (DAMGO) and δ-OR (DADLE) stimulation [11] and specific increase of ACI (8x) and ACII (2.5×) isoforms [12]. The κ-OR (U-23554)-stimulated [^{35}S] GTPγS binding and expression level of ACIII-IX in PM was unchanged. Behavioral tests of morphine-treated animals indicated that these animals were fully drug-dependent (opiate abstinence syndrome) and developed tolerance to subsequent drug addition (analgesic tolerance - hot-plate and hind paw withdrawal tests). The increase of ACI and ACII was interpreted as a specific compensatory response to prolonged stimulation of brain cortex OR by morphine.

Proteomic analysis represents a useful approach for an investigation of the overall changes of protein composition induced by the short-term or prolonged use of drugs. The aim of our present work was to identify proteins which are significantly altered in brain cortex of rats exposed to the increasing, high doses of morphine for prolonged period of time (10 days). For this aim, the post-nuclear supernatant fraction (PNS) was analyzed because it contains proteins of mitochondrial, endoplasmic reticulum, plasma membrane as well as cytoplasmic origin. In the second part of our work, we extended these studies by analysis of protein composition in membrane fraction isolated in Percoll gradient (PM).

Results

Two-dimensional electrophoresis and protein identification in post-nuclear supernatant prepared from brain cortex of control and morphine-treated rats; *analysis by MALDI-TOF MS/MS*

Samples of PNS were extracted in ice-cold aceton/TCA/96% ethanol, resolved by 2D-ELFO in linear IPG strips (pH 3–11) and 10% w/v acrylamide/0.26% w/v bis-acrylamide gels as described in methods and stained with silver or colloidal Coomassie blue. The stained 2D gels were scanned with an imaging densitometer and quantified by PDQuest software.

About 440 protein spots were recognized by silver staining and PDQuest analysis of gels in both types of PNS (Figure 1, left panels); when stained in colloidal Coomassie blue, about 200 spots were recognized. In CBB-stained gels, proteins 1–10 with different mobility in (+M10) and (−M10) samples were selected for identification by MALDI-TOF MS/MS as described in methods (Figure 1, right panels). The detailed list of the altered and identified proteins is presented in Additional file 1: Table S1 and Table 1. These tables also include description of the subcellular localization and function of these proteins.

The identified proteins were of cytoplasmic (**1**-Guanine deaminase, ↑2.5×; **4**-Dihydropyrimidinase-related protein 2,↑3.6×; **5**-N-ethylmaleimide sensitive fusion protein, isoform CRAa, ↑2.0×; **7**-Glyceraldehyde-3-phosphate dehydrogenase, ↑1.6×; **9**-Creatine kinase B-type, ↓0.86), cell membrane (**2**-Vacuolar-type proton ATPase, subunit B, brain isoform), ↑2.6x), endoplasmic reticulum (**3**-Protein disulfide-isomerase A3, ↑3.4×) and mitochondrial (**6**-Malate dehydrogenase, mitochondrial precursor, ↑1.4x; **8**-Aldolase A, ↑1.3×; **10**-Aconitate hydratase, mitochondrial precursor, ↑1.3x) origin. The 9 of them were significantly increased, 1.3-3.6x. Correlation with functional properties of these proteins indicated up-regulation of proteins related to guanine degradation (**1**), vacuolar acidification (**2**), apoptotic cell death (**3**), oxidative stress (**4, 6, 7, 10**), membrane traffic (**5**) and glycolysis (**8**). All together, the spectrum of the altered proteins suggests a major alternation of brain cortex tissue when exposed to increasing doses of morphine. *The most significant change from functional point of view was up-regulation of proteins related to oxidative stress (see discussion for further details).*

Two-dimensional electrophoresis and protein identification in Percoll-purified membranes isolated from brain cortex of control and morphine-treated rats; *analysis by LC-MS/MS*

PM samples were resolved by 2D-electrophoresis in the same way as described for PNS. The resolution in 10% w/v acrylamide/0.26% w/v bis-acrylamide gels was used in the case of silver staining; 12.0% w/v acrylamide/0.32% w/v bis-acrylamide gels were used for staining in CBB. About 300 protein spots were recognized by silver (Figure 2, left panels); when stained in CBB, the total number of detected protein spots was 490 (Figure 2, right panels). Proteins 1–18 with an altered mobility in (+M10) versus (−M10) samples were excised from in

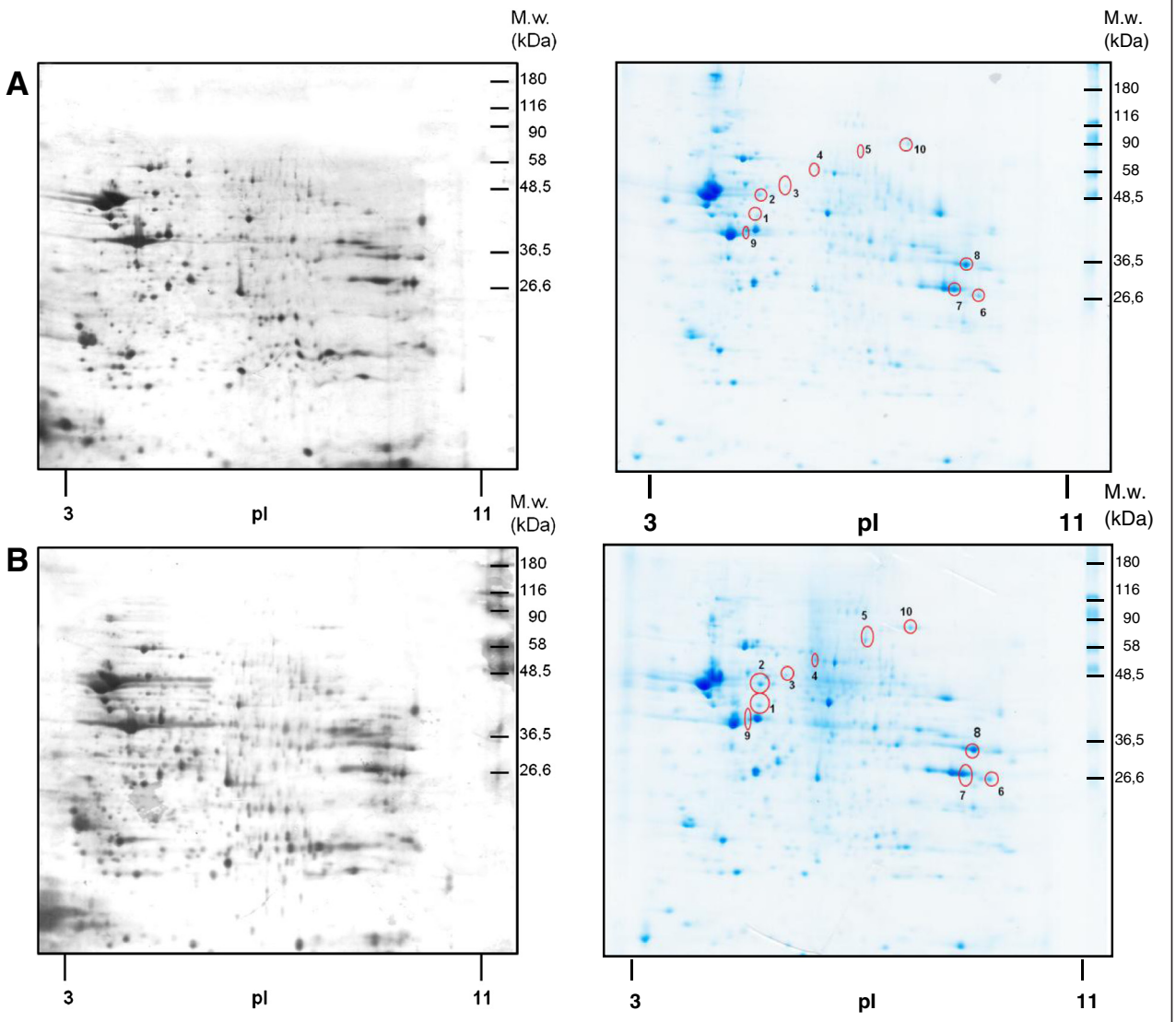

Figure 1 Two-dimensional gel electrophoresis maps of PNS prepared from control (A) and morphine-treated (B) rats. Protein samples (600 μg for both Silver and CBB staining) were separated in the first dimension on pH 3–11 IPG strips. For resolution in the second dimension, SDS-PAGE was performed in 10% w/v acrylamide/0.26% w/v bis-acrylamide gel. The stained 2D gels were scanned in an imaging densitometer and quantified by PDQuest software. The process of quantification of the difference between morphine-treated (+M10) and control (–M10) samples included spot detection, gel matching and spot quantification. Master gel was constructed for each group (+M10) or (–M10) as a synthetic image that contains the spot data from all the gels in the MatchSet. At least four replicates were performed for each group/sample. All matched and unmatched spots were then checked in a manual manner. Protein levels altered at least two-fold were taken into consideration. About 200 protein spots totally were recognized by CBB silver staining by PDQuest analysis. Proteins 1–10 with an altered mobility in (+M10) versus (–M10) samples were excised from in CBB-stained gels and identified by MALDI TOF/TOF analyzer as described in methods. *Left panels*, Silver staining; *Right panels*, CBB staining.

CBB-stained gels and identified by LC-MS/MS. The list of altered and identified proteins is presented in Additional file 2: Table S2 and Table 2. These tables also include a brief description of subcellular localization and function of these proteins as well as quantitative estimate of their relative change induced by morphine-treatment.

The identified up (↑)- or down (↓)-regulated proteins were of *plasma membrane* [**1**-BASP1, Brain acid soluble protein 1, ↓2.1×; **2**-GBB1, Guanine nucleotide-binding protein subunit beta-1, ↓2.0×], *myelin membrane* [**17**-MBP, Myelin basic protein S, ↓2.5×], *cytoplasmic* [**3**-KCRB, Creatine kinase B-type (EC 2.7.3.2), ↓2.6x; **4**-AINX, Alpha-internexin, ↑5.2×; **5**-DPYL2, Dihydropyrimidinase-related protein 2, ↑4.9×; **6**-SIRT2, NAD-dependent deacetylase sirtuin-2, ↑2.5×; **7**-SYUA, Alpha-synuclein, ↑2.0×; **8**-PRDX2, Peroxiredoxin-2, ↑2.2×; **9**-TERA, Transitional endoplasmic reticulum ATPase, ↑2.1×; **13**-UCHL1,

Table 1 Functional significance of proteins identified in PNS as altered by chronic morphine

Protein name	Change (dependence vs.control)	Subcellular localization	Functional category	Protein characterization - PNS
Guanine deaminase	Up-regulated	Cytoplasm	Metabolism	Purine metabolism, guanine degradation [13]
V-type proton ATP subunit B, brain isoform	Up-regulated	Cell membrane	Trafficking	ATP hydrolysis coupled proton transport, vacuolar acidification [14]
Protein disulfide-isomerase A3	Up-regulated	Endoplasmatic reticulum lumen	Cellular development and regulation	Up-regulation of this protein causes apoptotic cell death [15], alterations in its level were revealed during neurodegenerative processes [16]
Dihydropyrimidinase-related protein 2	Up-regulated	Cytoplasm	Neuronal development and regulation	Neuronal development and polarity [8], cone collapse and cell migration; one of major determinants in the control of oxidative stress [17]
N-ethylmaleimide sensitive fusion protein, isoform CRA_a	Up-regulated	Cytoplasm	Trafficking	ATP binding, regulating protein membrane trafficking, involved in vesicle priming [18]
Malate dehydrogenase, mitochondrial precursor	Up-regulated	Mitochondrion matrix	Metabolism	L-malate dehydrogenase activity, protein self-association; up-regulation of the mitochondrial malate dehydrogenase is caused by oxidative stress [19]
Glyceraldehyde-3-phosphate dehydrogenase	Up-regulated	Cytoplasm	Metabolism	Glyceraldehyde-3-phosphate dehydrogenase and nitrosylase activities; surprising role in apoptosis [20]; is known as a major target protein in oxidative stress [21]
Aldolase A	Up-regulated	Mitochondrion	Metabolism	Role in glycolysis and gluconeogenesis, scaffolding protein; potential role in regulating the free intracellular concentration of InsP3, and subsequently intracellular calcium dynamics[22,23]; the expression of aldolase A may be regulated by chronic lithium administration [24]
Creatine kinase B-type	Down-regulated	Cytoplasm	Metabolism	Energy-related (skeletal muscle, heart, brain and spermatozoa), brain development [25]
Aconitate hydratase, mitochondrial precursor	Up-regulated	Mitochondrion	Metabolism	Isomerization of citrate to isocitrate via cis-aconitate;an iron-sulfur protein, the particular susceptibility to oxidative damage may be related to the iron-sulfur cluster [4Fe-4S]in its active site [26]

Ubiquitin carboxyl-terminal hydrolase L1, ↓2.0×; **15**-COR1A, Coronin-1A, ↓5.4×, **16**-SEP11, Septin-11, ↑2.2×; **18**-RL12, 60S ribosomal protein L12, ↑2.7×] and *mitochondrial* [**10**-DHE3, Glutamate dehydrogenase 1, ↑2.7×; **11**-SCOT1, Succinyl-CoA:3-ketoacid-coenzyme A transferase 1, ↑2.2×; **12**-AATM, Aspartate aminotransferase**,** ↓2.2×; **14**-PHB, Prohibitin, ↑2.2×] origin.

Thus, the only member of GPCR-initiated signaling cascades identified by LC-MS/MS was trimeric Gβ subunit, which was decreased 2× in PM samples prepared from morphine-adapted rats. The morphine-induced decrease of Gβ subunit in PM was subsequently verified by immunoblot analysis of the same 2D-gels as those used for preparation of samples for LC-MS/MS (Figure 3). The spot 2 (compare with Figure 2) represented just a small fraction of the total signal of Gβ subunits which was distributed over wider range of pI. The total signal of Gβ was decreased 1.2x only. We have divided the signal of Gβ in CBB-stained gels into 8 small spots according to immunoblot signal (Figure 3) in order to verify it. Proteomic analysis was performed by LC-MS/MS and positive signal was detected in spots 3, 4, 5, 7 and 8 (Table 3).

Therefore, the decrease of Gβ determined by proteomic analysis (2×) has to be regarded as an alternation of relatively small fraction of numerous forms of Gβ resolved by 2D-ELFO. Morphine-induced decrease of Gβ is selectively oriented to specific, minority component of this protein; the dominant pool of Gβ subunits is unchanged.

Discussion

Opium extracts from the plant Papaver somniferum have been used for therapeutic and recreational purposes for thousands of years. Opioid alkaloids and related pharmaceuticals are the most effective analgesics for the treatment of acute and chronic pain. They also represent one of the largest components of the illicit drug market worldwide, generating revenue of approximately $70 billion in 2009, much of which supports crime, wars and terrorism. Intravenous use of opioid drugs is a leading cause of death by overdose in Europe and North America, and a major contributing factor to the worldwide AIDS epidemic [50,51].

Morphine and codeine are the main active opioid alkaloids in opium. In humans, they act on the central nervous system to produce a wide range of effects including analgesia, euphoria, sedation, respiratory depression and cough suppression. Chronic opiate administration results

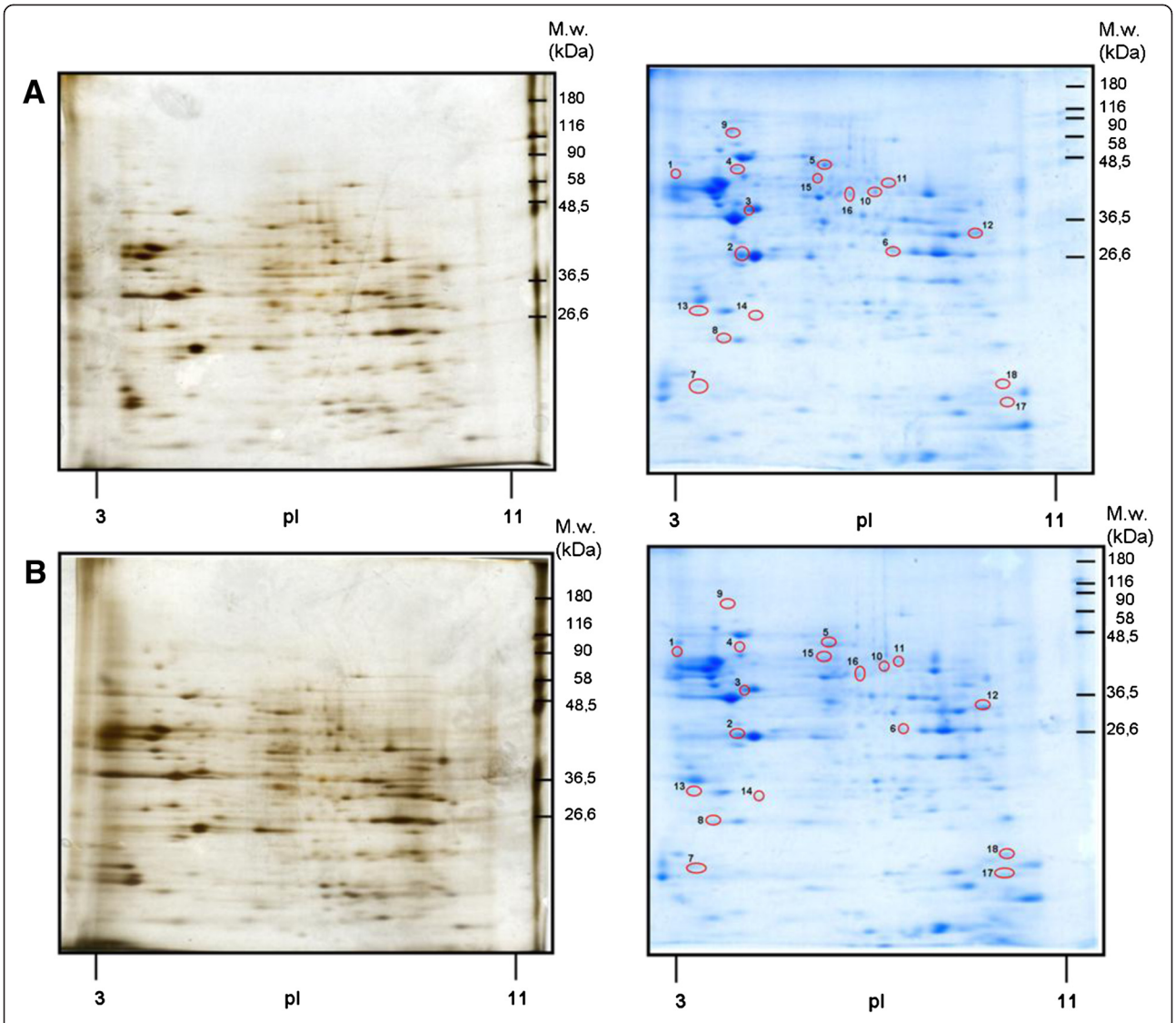

Figure 2 Two-dimensional gel electrophoresis maps of protein extracts prepared from PM of control (A) and morphine-treated (B) rats. Protein samples (400 μg for Silver staining; 2 mg for CBB staining) were separated in the first dimension on pH 3–11 IPG strips. For resolution in the second dimension, SDS-PAGE was performed in 10% w/v acrylamide/0.26% w/v bis-acrylamide gel (silver staining) or in 12.5% w/v acrylamide/0.0625% w/v bis-acrylamide gel (CBB staining). The stained 2D gels were scanned in an imaging densitometer and quantified by PDQuest software. The process of quantification of the difference between morphine-treated (+M10) and control (–M10) samples included spot detection, gel matching and spot quantification. Master gel was constructed for each group (+M10) or (–M10) as a synthetic image that contains the spot data from all the gels in the MatchSet. At least four replicates were performed for each group/sample. All matched and unmatched spots were then checked in a manual manner. Protein levels altered at least two-fold were taken into consideration. About 500 protein spots totally were recognized by CBB staining by PDQuest analysis. Proteins 1–18 with an altered mobility in (+M10) versus (–M10) samples were excised from in CBB-stained gels and identified by LC-MS/MS as described in methods. *Left panels*, Silver staining. *Right panels*, Coomassie staining.

in the development of tolerance and dependence, but the regulation of MOR and DOR function during this process is not clearly understood.

To localize changes of MOR-stimulated G-protein activity in various brain regions after chronic morphine treatment, Sim et al. [52] examined [^{35}S]GTPγS binding to brain sections by in vitro autoradiography. Rats were treated for 12 d with increasing doses (10–320 mg . kg^{-1} . d^{-1}) of morphine. Control rats were injected with either saline or a single acute injection of morphine (20 mg/kg). [^{35}S]GTPγS binding was measured in the presence or absence of MOR-selective agonist DAMGO. In rats injected with a *single acute dose* of morphine, no significant changes were detected in basal or DAMGO-stimulated [^{35}S]GTPγS binding in any brain region. In *chronic morphine-treated rats*, however, DAMGO-stimulated [^{35}S]GTPγS binding in cerebral cortex was significantly decreased when compared with control rats. Similar data were obtained in analysis of

Table 2 Functional significance of proteins identified in PM fraction as altered by chronic morphine

Protein name	Change (dependence vs.control)	Subcellular localization	Functional category	Protein characterization - PM
Brain acid soluble protein 1	Down-regulated	Cell membrane; Lipid anchor	Neuronal development and regulation	Associated with the membranes of growth cones that form the tips of elongating axons, DNA-dependent, localizes in the membrane raft domain with a cholesterol-dependent manner; changes in the localization during the development of neuronal polarity [27]
Guanine nucleotide-binding protein subunit beta-1	Down-regulated	Cell membrane	Signaling	Gβ1 is required for neural tube closure, neural progenitor cell proliferation and neonatal development [28]; stimulated ACII, ACIV, ACVII, inhibited ACI, ACV/VI, ACVIII [29,30]
Creatine kinase B-type	Down-regulated	Cytoplasm	Metabolism	Energy-related (skeletal muscle, heart, brain and spermatozoa), brain development [25], aging [31]; one of major determinants in the control of oxidative stress [17]
Alpha-internexin	Up-regulated	Cytoplasm	Neuronal development and regulation	Copurifies with intermediate filaments from rat spinal cord and optic nerve, developmental protein involved in morphogenesis of neurons [32]
Dihydropyrimidinase-related protein 2	Up-regulated	Cytoplasm	Neuronal development and regulation	Neuronal development and polarity [8], cone collapse and cell migration; one of major determinants in the control of oxidative stress [17]
NAD-dependent deacetylase sirtuin-2	Up-regulated	Cytoplasm	Cellular development and regulation	Colocalizes with microtubules; NAD-dependent deacetylase, involved in the control of mitotic exit in the cell cycle; up-regulation may protect the brain against incurred oxidative damage [33]
Alpha-synuclein	Up-regulated	Cytoplasm	Neuronal development and regulation	Specifically expressed in neuronal cell bodies and synapses, negative regulation of neuron apoptosis, aging; role in the pathogenesis of Parkinson's disease [34]
Peroxiredoxin-2	Up-regulated	Cytoplasm	Neuronal development and regulation	Involved in redox regulation of the cell, negative regulation of neuron apoptosis; the relative abundance appears to protect cellular components by removing the low levels of hydroperoxides and peroxinitrites produced as a result of normal cellular metabolism in the cytosol [35]
Transitional endoplasmic reticulum ATPase	Up-regulated	Cytoplasm Nucleus	Cellular development and regulation	Involved in the formation of the transitional endoplasmatic reticulum, necessary for the fragmentation of Golgi stacks during mitosis and for their reassembly after mitosis [36]; interacts with neurofibromin to control the density of dendritic spines [37]
Glutamate dehydrogenase 1, mitochondrial	Up-regulated	Mitochondrion matrix	Metabolism	Glutamate catabolic process, long-term memory, in rat brain the glutamate dehydrogenase reaction operates in the direction of ammonia production [38]
Succinyl-CoA:3-ketoacid-coenzyme A transferase 1, mitochondrial	Up-regulated	Mitochondrion matrix	Metabolism	A mitochondrial ketone body-activating enzyme [39]; brain development, response to drug
Aspartate aminotransferase, mitochondrial	Down-regulated	Mitochondrion matrix	Metabolism	Amino acid metabolism, metabolite exchange between mitochondria and cytosol, fatty acid transport; its activity is related with the maintenance of amino acid homeostasis and might be an indicator of mitochondrial injury [40]
Ubiquitin carboxyl-terminal hydrolase isozyme L1	Down-regulated	Cytoplasm Endoplasmatic reticulum membrane	Deubiquitination Neuronal development and regulation	Involved both in the processing of ubiquitin precursors and of ubiquitinated proteins; the ubiquitination/proteasome pathway involved in synaptic plasticity [41]
Prohibitin	Up-regulated	Mitochondrion inner membrane	Cellular development and regulation	Antiproliferative activity, role in regulating mitochondrial respiration activity and aging, response to drug [42-44]; down-regulation of prohibitin renders neurons more vulnerable to injury and reactive oxygen species production, whereas up-regulation appears to be neuroprotective [45]
Coronin-1A	Down-regulated	Cytoplasm	Cellular development and regulation	Invagination of plasma membrane, forming protrusions of plasma membrane involved in cell locomotion; coronin-1A activity is spatially and temporally regulated by phosphoinositides [46]

Table 2 Functional significance of proteins identified in PM fraction as altered by chronic morphine *(Continued)*

Septin-11	Up-regulated	Cytoplasm	Cellular development and regulation	Filament-forming cytoskeletal GTPase, cell division; it is involved in dendritic maturation [47]
Myelin basic protein S	Down-regulated	Myelin membrane	Neuronal development and regulation	Myelination, negative regulation of axonogenesis; morphine exposure colud result in a decreased number of myelinated axons [48]
60S ribosomal protein L12	Down-regulated	Cytoplasm	Regulatory	Binds directly to 26S ribosomal RNA; it accesses the importin 11 pathway as a major route into the nucleus [49]

MOR-stimulated [^{35}S]GTPγS binding after chronic heroin administration [53,54]. Accordingly, our analysis of PM isolated from cerebral cortex of rats exposed to morphine for 10 days (10–50 mg/kg) indicated significant desensitization of G-protein response to MOR and DOR stimulation [11] and up-regulation of ACI and II [12].

Proteome changes after prolonged morphine exposure have been so far investigated in "frozen tissue powders" of the rat cerebral cortex, hippocampus, striatum [55,56] and nucleus accumbens [7] or in the "whole-cell lysates" of striatal neuronal cell cultures [57]. Therefore, the aim of our work was to perform proteomic analysis in *more defined* preparations: post-nuclear supernatant (PNS) and membranes isolated in Percoll® gradient (PM). The morphine-induced changes in protein composition (proteom) of PNS and PM were determined by 2D-electrophoresis resolution and PDQuest analysis; the altered proteins were identified by MALDI-TOF MS/MS or LC-MS/MS.

Proteomic analysis of PNS indicated a marked increase of proteins of mitochondrial and cytoplasmic origin (Additional file 1: Table S1 and Table 1). The 9 out of 10 proteins exhibiting the largest morphine-induced change in Coomassie stained gels were increased *by* morphine: **1**-Guanine deaminase, ↑2.5×; **2**-Vacuolar-type proton ATP subunit B, brain isoform ↑2.6×; **3**-Protein disulfide-isomerase A3, ↑3.4×; **4**-Dihydropyrimidinase-related protein 2, ↑3.6x; **5**-N-ethylmaleimide sensitive fusion protein, isoform CRAa, ↑2.0×; **6**-Malate dehydrogenase, mitochondrial precursor, ↑1.4×; **7**-Glyceraldehyde-3-phosphate dehydrogenase, ↑1.6×; **8**-Aldolase A, ↑1.3×; **10**-Aconitate hydratase, mitochondrial precursor, ↑1.3×**.** The 4 out of 9 up-regulated proteins (**4**, **6**, **7**, **10**) were described as functionally related to manifestation of oxidative stress conditions [17,19,21,26]. Marked increase of Protein disulfide-isomerase A3 (**3**) causing apoptotic cell death [15] should be also noticed. The role in apoptosis has

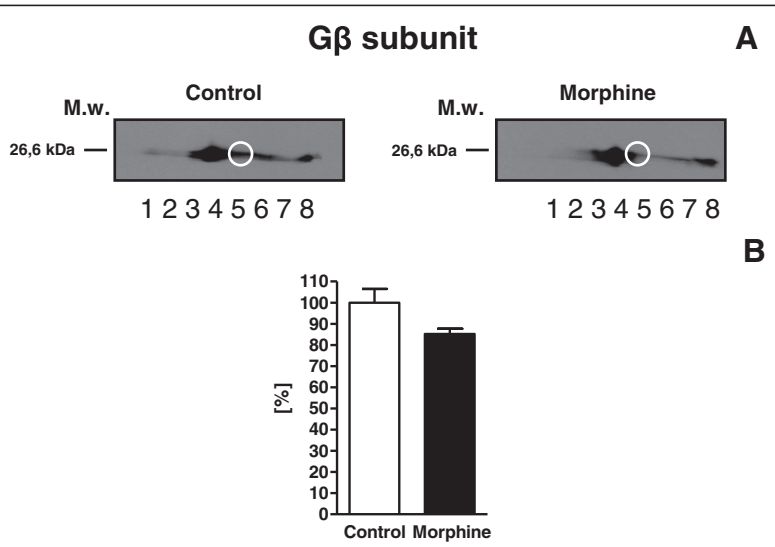

Figure 3 Gβ subunit protein; ***immunoblot analysis of 2D-gels.*** **A** Two-dimensional resolution of Gβ protein content in PM isolated from control and morphine-adapted rats. PM protein (400 μg) was resolved by 2D electrophoresis using the pI range 3–11 for isoelectric focusing in the first dimension. The white small circle shows the small fraction of the the total signal of Gβ which was taken into consideration when analyzed by LC-MS/MS. The second dimension was performed by SDS-PAGE in 10% w/v acrylamide/0.26% bis-acrylamide gels (Hoefer SE 600). Gβ was identified by immunoblotting with specific antibody as described in Material and methods. The numbers 1–8 represent spots of Gβ subunits which were subsequently analyzed by LC-MS/MS. **B** The average of 3 immunoblots ± SEM. Difference between (–M10) and (+M10) was analyzed by Student's *t*-test using GraphPad*Prizm4* and found not significant, NS ($p > 0.05$).

Table 3 Proteomic analysis of Gβ subunits isolated from brain cortex of control and morphine-treated rats

Spot	Accession number	Protein name	Mascot score	Matched peptides	Peptides	SC[a] [%]	MW[b] (kDa)	pI[c]
3	GBB1_RAT	**Guanine nucleotide-binding protein subunit beta-1**	184.3	6	R.LFDLR.A R.LLVSASQDGK.L K.LWDVR.E K.IYAMHWGTDSR.L + Oxidation (M) K.ACADATLSQITNNIDPVGR.I K.VHAIPLR.S	16.8	37.4	5.6
4	GBB1_RAT	**Guanine nucleotide-binding protein subunit beta-1**	471	12	K.ACADATLSQITNNIDPVGR.I R.LFVSGACDASAK.L K.IYAMHWGTDSR.L + Oxidation (M) R.LFDLR.A K.IYAMHWGTDSR.L R.LLVSASQDGK.L K.LWDVR.E R.KACADATLSQITNNIDPVGR.I R.LLLAGYDDFNCNVWDALK.A K.VHAIPLR.S K.LIIWDSYTTNK.V R.ELAGHTGYLSCCR.F	32.9	37.4	5.6
4	GBB2_RAT	**Guanine nucleotide-binding protein subunit beta-2**	413.9	10	R.TFVSGACDASIK.L K.ACGDSTLTQITAGLDPVGR.I K.IYAMHWGTDSR.L + Oxidation (M) R.LFDLR.A K.IYAMHWGTDSR.L R.LLVSASQDGK.L K.LWDVR.D K.VHAIPLR.S K.LIIWDSYTTNK.V R.LLLAGYDDFNCNIWDAMK.G + Oxidation (W)	14.4	37.3	5.6
5	GBB1_RAT	**Guanine nucleotide-binding protein subunit beta-1**	199.1	5	R.AGVLAGHDNR.V R.LFVSGACDASAK.L R.LFDLR.A K.IYAMHWGTDSR.L + Oxidation (M) R.LLVSASQDGK.L	14.1	37.4	5.6
5	GBB2_RAT	**Guanine nucleotide-binding protein subunit beta-2**	188.7	5	R.AGVLAGHDNR.V R.TFVSGACDASIK.L R.LFDLR.A K.IYAMHWGTDSR.L + Oxidation (M) R.LLVSASQDGK.L	3.5	37.3	5.6
7	GBB (1–4)_RAT	**Guanine nucleotide-binding protein subunit beta-3**	22.4	1	K.LLVSASQDGK.L	2.9	37.2	5.4
8	GBB (1–4)_RAT	**Guanine nucleotide-binding protein subunit beta-3**	34.7	1	K.LLVSASQDGK.L	2.9	37.2	5.4

[a]Sequence coverage.
[b]Theoretical molecular weight.
[c]Theoretical isoelectric point.

been also described for Glyceraldehyde-3-phosphate dehydrogenase (**7**), already mentioned as major target protein in oxidative stress [21]. The 4 out of 9 up-regulated proteins (**4**, **6**, **7**, **10**) were thus functionally related to manifestation of the state of oxidative stress/oxidative damage in brain of morphine-exposed rats and 2 proteins were related to apoptotic cell death.

More detailed analysis of Percoll-purified membranes indicated a complex reorganization of PM protein composition. The list of proteins presented in Additional file 2: Table S2 and Table 2 indicates that morphine-induced alternation included increase as well as decrease of wide range of proteins functionally and structurally related to plasma, myelin, endoplasmic reticulum and mitochondrial membranes. Numerous soluble enzymes present in soluble, cytosol fraction or in mitochondrial matrix were also altered by chronic morphine. Surprisingly, with the exception of trimeric Gβ subunit, not just one of these proteins was functionally related to GPCR- or ionic-channel-activated signaling cascades. Similarly, proteomic analysis of protein alternations induced in the long-term TRH-treatment of HEK cells expressing TRH-R and G11α protein indicated the change of 42 proteins, but not even one of these proteins represented plasma membrane protein functionally related to GPCR-initiated signaling cascades [58].

Our results indicate that the energy metabolism of rat brain cortex exposed to increasing doses of morphine (10–50 mg/kg, 10 days) is shifted far from the normal, physiological state. Using other words, brain cortex of rats exposed to morphine according to our protocol is far from being adapted. It may be suggested that the both neuronal and glial cells undergo a drastic reorganization as consequence of cell discomfort and, subsequently, oxidative stress. Simultaneous activation of all types of opioid receptors (μ-, δ- and κ-OR) by high doses of morphine results in high energy demand of neurons [59,60]. Consequently, glycogen in astrocytes as the single largest energy reserve in the brain is mobilized with the aim to match these increased energy requirements [61]. After depletion of glycogen in astrocytes, the state of oxidative stress appears [62] as the full supply of oxygen to brain mitochondria is not accompanied by transfer of the sufficient number of "reducing equivalents" into the mitochondrial matrix.

Conclusions

Proteomic analysis of rat brain cortex of rats exposed to morphine for 10 days (10–50 mg/kg) indicated a significant morphine-induced change of membrane protein composition. Changes in *post-nuclear supernatant* were exclusively based on increase (1.3-3.6×) of proteins of mitochondrial and cytoplasmic origin. In isolated *plasma membranes* (PM), morphine-induced alternation included increase as well as decrease of wide range of proteins functionally and structurally related to plasma, myelin, endoplasmic reticulum and mitochondrial membranes. Numerous soluble enzymes present in soluble, cytosol fraction or in mitochondrial matrix were also altered by chronic morphine. The only member of GPCR-initiated signaling cascades identified by LC-MS/MS in Percoll-purified membranes was trimeric Gβ subunit (**2**-GBB) which was decreased 2x in samples prepared from morphine-adapted rats. This "active" component of Gβ subunits, however, represented a minor pool of total complement of Gβ molecules in PM, which was unchanged.

Material and methods

Chemicals

Acrylamide, bis-acrylamide and Coomassie Blue G-250 were from SERVA (Heidelberg, Germany), nitrocellulose membrane was from Whatman (Germany). Immobiline Dry-Strips, Pharmalyte buffer, and secondary anti-rabbit antibody labeled with horseradish peroxidase were purchased from GE Healthcare (Piscataway, NJ). Complete protease inhibitor cocktail was from Roche Diagnostic, Mannheim, Germany (cat. no. 1697498). All others chemicals were from Sigma-Aldrich and were of highest purity available. Primary antibody oriented against trimeric Gβ subunit protein (T-20, sc-378) was from Santa Cruz.

Animals

Male Wistar rats (220-250 g) were killed by decapitation under ether narcosis, the frontal brain was rapidly removed, washed intensively from the remaining blood and cooled to 0°C. The cerebral cortex was separated on the pre-cooled plate, snap frozen in liquid nitrogen and stored at −70°C until use. The experiments were approved by Animal Care and Use Committee of the Institute of Physiology, Academy of Sciences of the Czech Republic to be in agreement with Animal Protection Law of the Czech Republic as well as European Comunity Council directives 86/609/EEC.

Morphine treatment of experimental animals

The animals were exposed to morphine by intra-muscular application according to the following protocol: 10 mg/kg (day 1 and 2), 15 mg/kg (day 3 and 4), 20 mg/kg (day 4 and 5), 30 mg/kg (day 6 and 7), 40 mg/kg (day 9) and, finally 50 mg/kg (day 10). The *morphine-adapted* rats were sacrificed 24 hours after the last dose of the drug (group + M10). Control animals were injected with sterile PBS and sacrificed in parallel with morphine-treated rats, i.e. 24 hours (group – M10) after the last dose [12].

Subcellular fractionation of rat brain cerebral cortex; preparation of post-nuclear supernatant (PNS) and percoll-purified membranes (PM)

Rat brain cortex was minced with razor blade on pre-cooled plate and diluted in STEM medium containing 250 mM sucrose, 20 mM Tris–HCl, 3 mM $MgCl_2$, 1 mM EDTA, pH 7.6, fresh 1 mM PMSF plus protease inhibitor cocktail. It was then homogenized mildly in loosely-fitting Teflon-glass homogenizer for 5 min (2 g w. w. per 10 ml) and centrifuged for 5 min at 3500 rpm (1200 × *g*). Resulting post-nuclear supernatant (PNS) was filtered through Nylon nets of decreasing size (330, 110 and 75 mesh, Nitex) and applied on top of Percoll in Beckman Ti70 tubes (30 ml of 27.4% Percoll in STE medium). Centrifugation for 60 min at 30000 rpm (65000 × *g*) resulted in the separation of two clearly visible layers (Bourova et al., 2009). The upper layer represented plasma membrane fraction (PM); the lower layer contained mitochondria (MITO). The upper layer was removed, diluted 1:3 in STEM medium and centrifuged in Beckman Ti70 rotor for 90 min at 50000 rpm (175000 × *g*). Membrane sediment was removed from the compact, gel-like sediment of Percoll and re-homogenized by hand in a small volume of 50 mM Tris–HCl, 3 mM $MgCl_2$, 1 mM EDTA, pH 7.4 (TME medium).

SDS-PAGE and immunoblotting

The aliquots of membrane fractions were mixed 1:1 with 2x concentrated Laemmli buffer (SLB) and heated for 3 min at 95 °C. Standard (10% w/v acrylamide/0.26% w/v bis-acrylamide) SDS electrophoresis was carried out as described before [63-65]. Molecular mass determinations were based on pre-stained molecular mass markers (Sigma, SDS 7B). After SDS-PAGE, proteins were transferred to nitrocellulose and blocked for 1 h at room temperature in 5% (w/v) low-fat milk in TBS-Tween buffer [10 mM Tris–HCl, pH 8.0, 150 mM NaCl, 0.1% (v/v) Tween 20]. Antibodies were added in TBS-Tween containing 1% (w/v) low-fat milk and incubated for at least 2 h. The primary antibody was then removed and the blot washed extensively (3x10 min) in TBS-Tween. Secondary antibodies (donkey anti-rabbit IgG conjugated with horseradish peroxidase) were diluted in TBS-Tween containing 1% (w/v) low-fat milk, applied for 1 h and after three 10 min washes, the blots were developed by ECL technique using Super Signal West Dura (Pierce) as substrate. The developed blots were scanned with an imaging densitometer ScanJett 5370C (HP) and quantified by Aida Image Analyzer v. 3.28 (Ray test).

Sample preparation for isoelectric focusing

Samples of PNS or PM containing 400–600 μg protein or 2 mg protein, respectively, were precipitated with ice cold aceton overnight at – 20°C. After centrifugation at 16 000 × *g* for 20 min at 4°C, the supernatant was removed and the pellet was precipitated with ice-cold 6% TCA for 1.5 h on ice. After centrifugation at 16 000 × *g* for 10 min at 4°C, the supernatant was discarded and the pellet washed with 400 μl of ice-cold 96% ethanol for 1 h at room temperature. The mixture was centrifuged at 16 000 × *g* for 10 min at 4°C and the remaining pellet was solubilizated with 250 μl IEF sample buffer containing 7 M urea, 2 M thiourea, 4% CHAPS, 1% DTT, 1% ampholines pH 3–10 and 0.01% bromphenol blue for 3 h at room temperature. After a brief centrifugation (16 000 × *g*, 1 min), the sample was transferred into a groove of the Immobiline DryStrip Reswelling Tray (GE Healthcare).

Two-dimensional electrophoresis (2D-ELFO)

Immobiline DryStrips (linear pH gradient 3–11 NL, 13 cm) were placed into the Immobiline DryStrip Reswelling Tray containing protein samples and rehydrated overnight.

Isoelectric focusing was performed using the Multiphor II system (GE Healthcare) at 15°C in the following manner: 150 V for 5 h, 500 V for 1 h, 3500 V for 12 h and 500 V for 3 h. The focused strips were stored at – 20°C or immediately used.

Strips were rinsed thoroughly with ultrapure water, dried quickly on filter paper and equilibrated in 4 ml of equilibration buffer (50 mM Tris–HCl pH 6.8, 6 M urea, 0.1 mM EDTA, 2% SDS, 30% glycerol and 0.01% bromophenol blue) containing 1% DTT for 15 min in order to reduce disulphide bridges and other oxidized groups. Subsequently, the strips were alkylated in equilibration buffer containing 2.5% iodoacetamide for 15 min. Molecular weight markers were loaded onto a piece of filter paper and placed close to the alkaline side of the strip. The strip and molecular marker were covered with 0.5% agarose. Gels were run vertically at a constant current of 10 mA for 20 min and then at 80 mA for 2 h till the bromophenol blue dye reached the end of the gel. The apparatus was cooled to 15°C using the Hoefer SE 600 unit (GE Healthcare).

Silver staining

Silver staining was performed by ProteoSilver™ Plus Silver Stain Kit (Sigma-Aldrich) according to the manufacturer's instructions [66-68]. Briefly, the gel was fixed in 40% ethanol/10% acidic acid overnight and then washed by 30% ethanol for 10 min and once by ultrapure water for 10 min. The gels were incubated for 10 min with 1% Sensitizer solution and washed twice with 200 ml of ultrapure water for 10 min. The gels were submerged in 1% Silver solution for 10 min, washed with 200 ml of ultrapure water for 1 min and developed with 100 ml of the Developer solution until the desired

intensity of spots was attained. The ProteoSilver Stop solution was added to the Developer solution and gels were incubated for 5 min. All steps were carried out at room temperature on an orbital shaker at 60 to 70 rpm. The gels were stored in fresh, ultrapure water or dried in 3% glycerol/25% methanol.

Colloidal coomassie staining

For MS analysis, the gels were stained by colloidal Coomassie Blue G-250 [69]. The gel was fixed in 40% methanol/5% orthophosphoric acid for 12 h and incubated with colloidal Coomassie Blue (17% ammonium sulphate, 34% methanol, 3% orthophosphoric acid and 0.1% Coomassie G-250) for 48 h. After staining, the gels were kept in 1% acetic acid at 4°C.

Image analysis

The stained 2D gels were scanned with an imaging densitometer ScanJett 5370C (HP) and quantified by PDQuest software (Bio-Rad, version 7.3.1). The process included spot detection, gel matching and spot quantification. Master gel was constructed as a synthetic image that contains the spot data from all the gels in the MatchSet. At least four replicates were performed for each sample. All matched and unmatched spots were then checked in a manual manner. Protein levels altered at least two-fold were taken into consideration.

Preparation of samples for MALDI-TOF MS/MS; *analysis of post-nuclear fraction*

Mass spectrometric analysis MALDI-TOF was performed as described before [58]. The peak lists from the MS spectra were generated by 4000 Series Explorer V 3.5.3 (Applied Biosystems/MDS Sciex) without smoothing, peaks with local signal to noise ratio greater than 5 were picked and searched by local Mascot v. 2.1 (Matrix Science) against nonredundant NCBI database of protein sequences (11186807 sequences; 3815639892 residues). Database search criteria were as follows-enzyme: trypsin, taxonomy: *Rattus norvegicus* (66703 sequences), fixed modification: carbamidomethylation, variable modification: methionine oxidation, peptide mass tolerance: 120 ppm, one missed cleavage allowed. Only hits that were scored as significant ($P < 0.001$) were included.

In-gel digestion and preparation of samples for LC-MS/MS; *analysis of percoll-purified membranes (PM)*

Protein spots (from 2-DE: ca 1–2 mm in diameter) were excised from the Coomassie-stained gels, and then processed as described by Shevchenko et al. [70]. Briefly, the spots were first destained by incubation in 100 μl of 100 mM ammonium bicarbonate/acetonitrile (1:1, v/v) with occasional shaking for 1 hour. After destaining, the gel pieces were shrunk by dehydration in 500 μl of acetonitrile, which was then removed and the gel pieces were dried in a vacuum centrifuge. In further step, 100 μl of 10 mM DTT in 100 mM ammonium bicarbonate was added, and the proteins were reduced for 1 hour at 56°C. After cooling to room temperature, the DTT solution was replaced by roughly the same volume of 55 mM iodoacetamide in 100 mM ammonium bicarbonate, and the gels were incubated at ambient temperature for 45 min in the dark. Then the gel pieces were washed with 100 μl of 100 mM ammonium bicarbonate, and dehydrated by addition 500 μl of acetonitrile. Subsequently, the liquid phase was removed and the gel pieces were dried in a vacuum centrifuge.

Before the in-gel digestion, the gel pieces were cooled in an ice-cold bath and swollen in a 100 μl of digestion buffer containing trypsin (20 μg/ml) in 50 mM ammonium bicarbonate, and the gel pieces were sonicated (5 min), placed to air circulation thermostat, and incubated overnight at 37°C. The volumes of solutions needed for processing of the protein bands were four-fold larger than the volumes for processing of the spots. The supernatant of each spot was then transferred to a new vial. The in-gel digestion was performed once more the same way. The resulting tryptic peptides were extracted with sonication (15 min) by 150 μl of extraction buffer (5% formic acid/acetonitrile, 1:2, v/v). Then the solution was spun, the supernatants were transferred, pooled and concentrated to dryness by lyophilization. Dried extracts were stored at −80°C before analysis.

Analysis of tryptic digests with LC-MS/MS

Dried protein digests were dissolved in 20 μl of 1% formic acid, centrifuged (10 000 × *g*, 5 min, 4°C) and the supernatant transferred to inserts in vials. The nano-HPLC apparatus used for protein digests analysis was a Proxeon Easy-nLC (Proxeon, Odense, Denmark) coupled to a maXis Q-TOF (quadrupole – time of flight) mass spectrometer with ultrahigh resolution (Bruker Daltonics, Bremen, Germany) by nanoelectrosprayer. The nLC-MS/MS instruments were controlled with the software packages HyStar 3.2 and micrOTOF-control 3.0. The data were collected and manipulated with the software packages ProteinScape 2.0 and DataAnalysis 4.0 (Bruker Daltonics).

The 3 μl of the peptide mixture were injected into a NS-AC-11-C18 Biosphere C18 column (particle size: 5 μm, pore size: 12 nm, length: 150 mm, inner diameter: 75 μm), with a NS-MP-10 Biosphere C18 pre-column (particle size: 5 μm, pore size: 12 nm, length: 20 mm, inner diameter: 100 μm), both manufactured by NanoSeparations (Nieuwkoop, Netherlands).

The separation of peptides was achieved via a linear gradient between mobile phase A (water) and B (acetonitrile), both containing 0.1% (v/v) formic acid. Separation was

started by running the system with 5% mobile phase B, followed by gradient elution to 30% B at 70 min. The next step was gradient elution to 50% B in 10 min, and then a gradient to 100% B in 8 min was used. Finally, the column was eluted with 100% B for 2 min. Equlibration before the next run was achieved by washing the column with 5% mobile phase B for 10 min. The flow rate was 0.25 μl min^{-1}, and the column was held at ambient temperature (25°C).

On-line nano-electrospray ionization (easy nano-ESI) in positive mode was used. The ESI voltage was set at +4.5 kV, scan time 1.3 Hz. Operating conditions: drying gas (N_2), 1 l min^{-1}; drying gas temperature, 160°C; nebulizer pressure, 0.4 bar. Experiments were performed by scanning from 100 to 2200 m/z. The reference ion used (internal mass lock) was a monocharged ion of $C_{24}H_{19}F_{36}N_3O_6P_3$ (m/z 1221.9906). Mass spectra corresponding to each signal from the total ion current chromatogram were averaged, enabling an accurate molecular mass determination. All LC-MS/MS analyses were done in duplicates.

Database searching

Data were processed using ProteinScape software. Proteins were identified by correlating tandem mass spectra to SwissProt databases, using the MASCOT searching engine (http://www.matrixscience.com); *Rattus norvegicus* as species. Trypsin was chosen as the enzyme parameter. One missed cleavage was allowed, and an initial peptide mass tolerance of ±10.0 ppm was used for MS and ±0.05 Da for MS/MS analysis. Cysteines were assumed to be carbamidomethylated, proline and lysine to be hydroxylated, serine, threonine and tyrosine to be phosphorylated, and methionine was allowed to be oxidated. All these possible modifications were set to be variable. Monoisotopic peptide charge was set to 1+, 2+ and 3+. The Peptide Decoy option was selected during the data search process to remove false-positive results. Only significant hits (MASCOT score ≥60, http://www.matrixscience.com) were accepted.

Statistical analysis

In immunoblot assays, the significance of difference between data collected in control and morphine-treated samples was analyzed by Student's t-test by GraphPad-*Prizm4*. Results represent the average ± S.E.M.

Protein determination

The method of Lowry was used for determination of membrane protein. Bovine serum albumin (Sigma, Fraction V) was used as standard. Data were calculated by fitting the data with calibration curve as quadratic equation.

Additional files

Additional file 1: Table S1. Proteomic analysis of post-nuclear supernatant prepared from brain cortex of control and morphine-treated rats.

Additional file 2: Table S2. Proteomic analysis of PM fraction isolated from brain cortex of control and morphine-treated rats.

Abbreviations

AC: Adenylyl cyclase; CBB: Coomassie brilliant blue; d: Day; DAMGO: [(2-D-alanine2-4-methylphenylalanine-5-glycineol)-enkefalin]; DADLE: [(2-D-alanine-5-D-leucine)-enkefalin]; DOR: δ-opioid receptor; DTT: Dithiothreitol; EDTA: Ethylenediamine-tetraacetic acid; ELFO: Electrophoresis; GPCR: G protein-coupled receptor; G proteins: Heterotrimeric guanine nucleotide-binding regulatory proteins; CHAPS: 3-[(3-cholamidopropyl) dimethylammonio]-1-propanesulfonate; DTT: Dithiothreitol; IEF: Isoelectric focusing; KOR: κ-opioid receptor; LC-MS/MS: Liquid chromatography–mass spectrometry; MALDI-TOF MS/MS: Matrix-assisted laser desorption/ionization time-of-flight mass spectrometry; MOR: μ-opioid receptor; PBS: Phosphate-buffered saline; PM: Percoll®-purified membranes; PMSF: Phenylmethylsulfonyl fluoride; PNS: Post-nuclear supernatant; SLB: Sample loading buffer; TBS: Tris-buffered saline; w.w.: Wet weight; TCA: Trichloroacetic acid; TRH-R: Thyrotropin-releasing hormone receptor.

Competing interests

The authors declare that they have no competing interests.

Authors' contributions

HU performed the experiments, analyzed the data and participated in writing the manuscript. AE performed proteomic analysis of plasma membrane proteins by LC-MS/MS. DK and LB were responsible for application of morphine to rats according to experimental protocol described in Methods and prepared membrane fractions by differential or density gradient centrifugation. PS conceived the study, designed the experiments and wrote the manuscript. All authors have read and approved the final manuscript.

Acknowledgements

This work was supported by the GACR (P207/12/0919), Centrum of Neurosciences (P304/12/G069) and by Academy of Sciences of the Czech Republic (RVO: 67985823). The authors thank to Silvia Bezouskova for useful practical experience, Petr Jedelsky for performing MALDI -TOF MS/MS and Karel Harant for valuable assistance.

Author details

[1]Laboratories of Biochemistry of Membrane Receptors, Institute of Physiology, v.v.i., Academy of Sciences of the Czech Republic, Videnska 1083, Prague 4 14220, Czech Republic. [2]Analysis of Biologically Important Compounds, Institute of Physiology, v.v.i., Academy of Sciences of the Czech Republic, Videnska 1083, Prague 4 14220, Czech Republic.

Received: 2 July 2013 Accepted: 3 February 2014
Published: 14 February 2014

References

1. Contet C, Kieffer BL, Befort K: **Mu opioid receptor: a gateway to drug addiction.** *Curr Opin Neurobiol* 2004, **14:**370–378.
2. Preston KL: **Drug abstinence effects: opioids.** *Br J Addict* 1991, **86:**1641–1646.
3. Connor M, Christie MD: **Opioid receptor signalling mechanisms.** *Clin Exp Pharmacol Physiol* 1999, **26:**493–499.
4. Law PY, Wong YH, Loh HH: **Molecular mechanisms and regulation of opioid receptor signaling.** *Annu Rev Pharmacol Toxicol* 2000, **40:**389–430.
5. Law PY, Loh HH, Wei LN: **Insights into the receptor transcription and signaling: implications in opioid tolerance and dependence.** *Neuropharmacology* 2004, **47:**300–311.
6. Robinson TE, Kolb B: **Morphine alters the structure of neurons in the nucleus accumbens and neocortex of rats.** *Synapse* 1999, **33:**160–162.

7. Li KW, Jimenez CR, van der Schors RC, Hornshaw MP, Schoffelmeer ANM, Smit AB: **Intermittent administration of morphine alters protein expression in rat nucleus accumbens.** *Proteomics* 2006, **6:**2003–2008.
8. Kim SY, Chudapongse N, Lee SM, Levin MC, Oh JT, Park HJ, Ho IK: **Proteomic analysis of phosphotyrosyl proteins in morphine-dependent rat brains.** *Brain Res Mol Brain Res* 2005, **133:**58–70.
9. Miller AL, Hawkins RA, Harris RL, Veech RL: **The effects of acute and chronic morphine treatment and of morphine withdrawal on rat brain in vivo.** *Biochem J* 1972, **129:**463–469.
10. Li Q, Zhao X, Zhong LJ, Yang HY, Wang Q, Pu XP: **Effects of chronic morphine treatment on protein expression in rat dorsal root ganglia.** *Eur J Pharmacol* 2009, **612:**21–28.
11. Bourova L, Vosahlikova M, Kagan D, Dlouha K, Novotny J, Svoboda P: **Long-term adaptation to high doses of morphine causes desensitization of μ-OR- and δ-OR-stimulated G-protein response in forebrain cortex but does not decrease the amount of G-protein alpha subunit.** *Med Sci Monit* 2010, **16:**260–270.
12. Ujcikova H, Dlouha K, Roubalova L, Vosahlikova M, Kagan D, Svoboda P: **Up-regulation of adenylylcyclases I and II induced by long-term adaptation of rats to morphine fades away 20 days after morphine withdrawal.** *Biochim Biophys Acta* 1810, **2011:**1220–1229.
13. Paletzki RF: **Cloning and characterization of guanine deaminase from mouse and rat brain.** *Neuroscience* 2002, **109:**15–26.
14. Toei M, Saum R, Forgac M: **Regulation and isoform function of the V-ATPases.** *Biochemistry* 2010, **49:**4715–4723.
15. Tanaka S, Uehara T, Nomura Y: **Up-regulation of protein-disulfide isomerase in response to hypoxia/brain ischemia and its protective effect against apoptotic cell death.** *J Bioch Chem* 2000, **275:**10388–10393.
16. Conn KJ, Gao W, McKee A, Lan MS, Ullman MD, Eisenhauer PB, Fine RE, Wells JM: **Identification of the protein disulfide isomerase family member PDIp in experimental Parkinson's disease and Lewy body pathology.** *Brain Res* 2004, **1022:**164–172.
17. Drabik A, Bierczynska-Krzysik A, Bodzon-Kulakowska A, Suder P, Kotlinska J, Silberring J: **Proteomics in neurosciences.** *Mass Spectrom Rev* 2007, **26:**432–450.
18. Abul-Husn NS, Annangudi SP, Ma'ayan A, Ramos-Ortolaza DL, Stockton SD Jr, Gomes I, Sweedler JV, Devi LA: **Chronic morphine alter the presynaptic protein profile: identification of novel molecular targets using proteomics and network analysis.** *PLoS One* 2011, **6:**e25535.
19. Shi Q, Gibson GE: **Up-regulation of the mitochondrial malate dehydrogenase by oxidative stress in mediated by miR-743a.** *J Neurochem* 2011, **118:**440–448.
20. Chuang DM, Hough C, Senatorov VV: **Glyceraldehyde-3-phosphate dehydrogenase, apoptosis, and neurodegenerative diseases.** *Annu Rev Pharmacol Toxicol* 2005, **45:**269–290.
21. Hwang NR, Yim SH, Kim YM, Jeong J, Song EJ, Lee Y, Choi S, Lee KJ: **Oxidative modifications of glyceraldehyde-3-phophate dehydrogenase play a key role in its multiple cellular functions.** *Biochem J* 2009, **423:**253–264.
22. Koppitz B, Vogel F, Mayr GW: **Mammalian aldolases are isomer-selective high-affinity inositol polyphosphate binders.** *Eur J Biochem* 1986, **161:**421–433.
23. Baron CB, Tolan DR, Choi KH, Coburn RF: **Aldolase A Ins(1,4,5)P_3-binding domains as determined by site-directed mutagenesis.** *Biochem J* 1999, **341:**805–812.
24. Hua LV, Green M, Warsh JJ, Li PP: **Lithium regulation of aldolase A expression in the rat frontal cortex: identification by differential display.** *Biol Psychiatry* 2000, **48:**58–64.
25. Shen W, Willis D, Zhang Y, Schlattner U, Wallimann T, Molloy GR: **Expression of creatine kinase isoenzyme genes during postnatal development of rat brain cerebellum:evidence for transcriptional regulation.** *Biochem J* 2002, **367:**369–380.
26. Perluigi M, Poon HF, Maragos W, Pierce WM, Klein JB, Calabrese V, Cini C, De Marco C, Butterfield DA: **Proteomic analysis of protein expression and oxidative modification in R6/2 transgenic mice.** *Mol Cell Proteomics* 2005, **4:**1849–1861.
27. Kashihara M, Miyata S, Kumanogoh H, Funatsu N, Matsunaga W, Kiyohara T, Sokawa Y, Maekawa S: **Changes in the localization of NAP-22, a calmodulin binding membrane protein, during the development of neuronal polarity.** *Neurosci Res* 2000, **37:**315–325.
28. Okae H, Iwakura Y: **Neural tube defects and impaired neural progenitor cell proliferation in Gβ_1-deficient mice.** *Dev Dyn* 2010, **239:**1089–1101.
29. Sunahara RK, Taussig R: **Isoforms of mammalian adenylylcyclase: multiplicities of signaling.** *Mol Interv* 2002, **2:**168–184.
30. Wang HY, Burns LH: **Gβγ that interacts with adenylyl cyclase in opioid tolerance originates from a Gs protein.** *J Neurobiol* 2006, **12:**1302–1310.
31. Perluigi M, Domenico FD, Giorgi A, Shininà ME, Coccia R, Cini C, Bellia F, Cambria MT, Cornelius C, Butterfield DA, Calabrese V: **Redox proteomics in aging rat brain involvement of mitochondrial reduced glutathione status and mitochondrial protein oxidation in the aging process.** *J Neurosci Res* 2010, **88:**3498–3507.
32. Kaplan MP, Chin SSM, Fliegner KH, Liem RKH: **α-internexin, a novel neuronal intermediate filament protein, precedes the low molecular weight neurofilament protein (NF-L) in the developing rat brain.** *J Neurosci* 1990, **10:**2735–2748.
33. Wu A, Ying Z, Gomez-Pinilla F: **Oxidative stress modulates Sir2α in rat hippocampus and cerebral cortex.** *Eur J Neurosci* 2006, **22:**5213–5216.
34. Maries E, Dass B, Collier TJ, Kordower JH, Steece-Collier K: **The role of α-synuclein in Parkinson's disease: insights from animal models.** *Nat Rev Neurosci* 2003, **4:**727–738.
35. Rhee SG, Chae HZ, Kim K: **Peroxiredoxins: a historical overview and speculative preview of novel mechanisms and emerging concepts in cell signaling.** *Free Radic Biol Med* 2005, **38:**1543–1552.
36. Woodman PG: **p97, a protein coping with multiple identities.** *J Cell Sci* 2003, **116:**4283–4290.
37. Wang HF, Shih YT, Chen CY, Chao HW, Lee MJ, Hsueh YP: **Valosin-containing protein and neurofibromin interact to regulate dendritic spine density.** *J Clin Invest* 2011, **121:**4820–4837.
38. Cooper AJL: **^{13}N as a tracer for studying glutamate metabolism.** *Neurochem Int* 2011, **59:**456–464.
39. Ohnuki M, Takahashi N, Yamasaki M, Fukui T: **Different localization in rat brain of the novel cytosolic ketone body-utilizing enzyme, acetoacetyl-CoA synthetase, as compared to succinyl-CoA:3 –oxoacid CoA-transferase.** *Biochim Biophys Acta* 2005, **1729:**147–153.
40. Das SK, Hiran KR, Mukherjee S, Vasudevan DM: **Oxidative stress is the primary event: effects of ethanol consumption in brain.** *Indian J Clin Biochem* 2007, **22:**99–104.
41. Murphey RK, Godenschwege TA: **New roles for ubiquitin in the assembly and function of neuronal circuits.** *Neuron* 2002, **36:**5–8.
42. Artal-Sanz M, Tavernarakis N: **Prohibitin couples diapause signalling to mitochondrial metabolism during ageing in *C.elegans*.** *Nature* 2009, **461:**793–797.
43. Merkwirth C, Langer T: **Prohibitin function within mitochondria: essential roles for cell proliferation and cristae morphogenesis.** *Biochim Biophys Acta* 2009, **1793:**27–32.
44. Mishra S, Ande SR, Nyomba BL: **The role of prohibitin in cell signaling.** *FEBS J* 2010, **277:**3937–3946.
45. Zhou P, Qian L, D'Aurelio M, Cho S, Wang G, Manfredi G, Pickel V, Iadecola C: **Prohibitin reduces mitochondrial free radical production and protects brain cells from different injury modalities.** *J Neurosci* 2012, **32:**583–592.
46. Tsujita K, Itoh T, Kondo A, Oyama M, Kozuka-Hata H, Irino Y, Hasegawa J, Takenawa T: **Proteome of acidic phospholipid-binding proteins: spatial and temporal regulation of coronin 1A by phosphoinositides.** *J Biol Chem* 2010, **285:**6781–6789.
47. Tada T, Simonetta A, Batterton M, Kinoshita M, Edbauer D, Sheng M: **Role of septin cytoskeleton in spine morphogenesis and dendrite development in neurons.** *Curr Biol* 2007, **17:**1752–1758.
48. Traudt CM, Tkac I, Ennis KM, Sutton LM, Mammel DM, Rao R: **Postnatal morphine administration alters hippocampal development in rats.** *J Neurosci Res* 2012, **90:**307–314.
49. Plafker SM, Macara IG: **Ribosomal protein L12 uses a distinct nuclear import pathway mediated by importin 11.** *Mol Cell Biol* 2002, **22:**1266–1275.
50. Filizola M, Devi LA: **Structural biology: how opiod drugs bind to receptors.** *Nature* 2012, **485:**314–317.
51. Manglik A, Kruse AC, Kobilka TS, Thian FS, Mathiesen JM, Sunahara RK, Pardo L, Weis WI, Kobilka BK, Granier S: **Crystal structure of the μ-opioid receptor bound to a morphinan antagonist.** *Nature* 2012, **485:**321–326.
52. Sim LJ, Selley DE, Dworkin SI, Childers SR: **Effects of chronic morphine administration on μ opioid receptor-stimulated [^{35}S]GTPγS autoradiography in rat brain.** *J Neurosci* 1996, **16:**2684–2692.

53. Maher CE, Martin TJ, Childers SR: **Mechanisms of mu opioid receptor/G-protein desensitization in brain by chronic heroin administration.** *Life Sci* 2005, **77:**1140–1154.
54. Sim-Selley LJ, Selley DE, Vogt LJ, Childers SR, Martin TJ: **Chronic heroin self-administration desensitizes μ opioid receptor-activated G-proteins in specific regions of rat brain.** *J Neurosci* 2000, **20:**4555–4562.
55. Bierczynska-Krzysik A, Bonar E, Drabik A, Noga M, Suder P, Dylag T, Dubin A, Kotlinska J, Silberring J: **Rat brain proteome in morphine dependence.** *Neurochem Int* 2006, **49:**401–406.
56. Bierczynska-Krzysik A, Pradeep John JP, Silberring J, Kotlinska J, Dylag T, Cabatic M, Lubec G: **Proteomic analysis of rat cerebral cortex, hippocampus and striatum after exposure to morphine.** *Int J Mol Med* 2006, **18:**775–784.
57. Bodzon-Kułakowska A, Suder P, Mak P, Bierczynska-Krzysik A, Lubec G, Walczak B, Kotlinska J, Silberring J: **Proteomic analysis of striatal neuronal cell cultures after morphine administration.** *J Sep Sci* 2009, **32:**1200–1210.
58. Drastichova Z, Bourova L, Hejnova L, Jedelsky P, Svoboda P, Novotny J: **Protein alterations induced by long-term agonist treatment of HEK293 cells expressing thyrotropin-releasing hormone receptor and $G_{11}\alpha$ protein.** *J Cell Biochem* 2010, **109:**255–264.
59. Kraus MA, Piper JM, Kornetsky C: **Persistent increases in basal cerebral metabolic activity induced by morphine sensitization.** *Pharmacol Biochem Behav* 1997, **57:**89–100.
60. Magistretti PJ, Pellerin L: **Cellular mechanisms of brain energy metabolism and their relevance to functional brain imaging.** *Philos Trans R Soc Lond B Biol Sci* 1999, **354:**1155–1163.
61. Magistretti PJ, Allaman I: **Glycogen: a Trojan horse for neurons.** *Nat Neurosci* 2007, **10:**1341–1342.
62. Guzman DC, Vazquez IE, Brizuela NO, Alvarez RG, Mejia GB, Garcia EH, Santamaria D, La Rosa De Apreza M, Olguin HJ: **Assessment of oxidative damage induced by acute doses of morphine sulfate in postnatal and adult rat brain.** *Neurochem Res* 2006, **31:**549–554.
63. Matousek P, Novotny J, Svoboda P: **Resolution of G(s)alpha and G(q)alpha/G(11)alpha proteins in membrane domains by two-dimensional electrophoresis: the effect of long-term agonist stimulation.** *Physiol Res* 2004, **53:**295–303.
64. Matousek P, Novotny J, Rudajev V, Svoboda P: **Prolonged agonist stimulation does not alter the protein composition of membrane domains in spite of dramatic changes induced in a specific signaling cascade.** *Cell Biochem Biophys* 2005, **42:**21–40.
65. Moravcova Z, Rudajev V, Stohr J, Novotny J, Cerny J, Parenti M, Milligan G, Svoboda P: **Long-term agonist stimulation of IP prostanoid receptor depletes the cognate G(s)alpha protein in membrane domains but does not change the receptor level.** *Biochim Biophys Acta* 2004, **1691:**51–65.
66. Gharahdaghi F, Weinberg CR, Meagher DA, Imai BS, Mische SM: **Mass spectrometric identification of proteins from silver-stained polyacrylamide gel: a method for the removal of silver ions to enhance sensitivity.** *Electrophoresis* 1999, **20:**601–605.
67. Shevchenko A, Wilm M, Vorm O, Mann M: **Mass spectrometric sequencing of proteins from silver-stained polyacrylamide gels.** *Anal Chem* 1996, **68:**850–858.
68. Sinha P, Poland J, Schnölzer M, Rabilloud T: **A new silver staining apparatus and procedure for matrix-assisted laser desorption/ionization-time of flight analysis of proteins after two-dimensional electrophoresis.** *Proteomics* 2001, **1:**835–840.
69. Fountoulakis M, Takács MF, Berndt P, Langen H, Takács B: **Enrichment of low abundance proteins of Escherichia coli by hydroxyapatite chromatography.** *Electrophoresis* 1999, **20:**2181–2195.
70. Shevchenko A, Tomas H, Havlis J, Olsen JV, Mann M: **In-gel digestion for mass spectrometric characterization of proteins and proteomes.** *Nat Protoc* 2006, **1:**2856–2860.

doi:10.1186/1477-5956-12-11
Cite this article as: Ujcikova *et al.*: Proteomic analysis of post-nuclear supernatant fraction and percoll-purified membranes prepared from brain cortex of rats exposed to increasing doses of morphine. *Proteome Science* 2014 **12**:11.

Mol Cell Biochem (2011) 347:157–162
DOI 10.1007/s11010-010-0623-2

Early postnatal development of rat brain is accompanied by generation of lipofuscin-like pigments

Jiří Wilhelm · Joško Ivica · Dmytro Kagan · Petr Svoboda

Received: 9 June 2010 / Accepted: 6 October 2010 / Published online: 19 October 2010

Abstract The increased generation of free radicals results in the formation of fluorescent end-products of lipid peroxidation, lipofuscin-like pigments (LFPs). The authors observed that LFPs are generated in rat brain after a normal birth during 5 postnatal days. The experimental design of the study comprised 10 groups of animals. The authors measured prenatal values 1 day and 7 days before birth, and then the animals were sampled on postnatal day 1, 2, 5, 10, 15, 25, 35, and 90. Maximum LFP concentration is achieved on the postnatal day 2. Starting from postnatal day 10, LFP concentration returns to prenatal values. A new rise in LFP concentration is observed at 3 months of age. This is associated with the beginning of the aging process. LFPs were characterized by fluorescence spectroscopy using tridimensional excitation spectra, synchronous spectra and their derivatives, and HPLC with fluorescence detection. It was possible to discern several tens of fluorescent compounds of unknown structure that are generated and metabolized during early development. The authors suggest that LFPs are formed after respiratory burst of microglia phagocytosing apoptotic cells.

Keywords Brain · Early development · Lipofuscin-like pigments · Fluorescence · Rat

J. Wilhelm (✉) · J. Ivica
Department of Medical Chemistry and Biochemistry, 2nd Medical School, Charles University, Plzeňská 221, 150 00 Prague 5, Czech Republic
e-mail: jiri.wilhelm@lfmotol.cuni.cz

D. Kagan · P. Svoboda
Institute of Physiology, CR Academy of Sciences, Vídeňská 1083, 142 20 Prague 4, Czech Republic

Introduction

The increased generation of free radicals and non-radical intermediates of oxygen reduction, collectively known as reactive oxygen species (ROS), constitutes the condition of oxidative stress that is considered as a major factor in the aging process and has formed the basis for explaining the mechanism of aging [1, 2]. The main quantitative source of ROS in mammalian organism is represented by mitochondria [3]. The effect of oxidative stress on the aging process is therefore widely recognized [4] in the brain tissue containing abundant mitochondria and highly active respiratory enzymes [5].

Immediately after birth, brain oxygen concentration undergoes dramatic changes that, from the quantitative point of view, are comparable to the exposure of experimental animals to hyperoxia. This pathological state was documented as a cause of brain oxidative damage [6], and an increase in ROS production in brain after birth is, therefore, to be expected.

As earlier studies indicated that brain mitochondrial enzymes in rats are fully active only after postnatal day 10 [7, 8], the direct role of mitochondria in neonatal ROS production is uncertain. Another possible source of ROS is represented by brain phagocytes, microglia. During mammalian brain development, both neurons and glia are produced in overabundance, and approximately half of them are eliminated by apoptosis [9]. Apoptotic cells are phagocytosed by microglia with concomitant production of ROS. Superoxide was detected by staining living brain slices with nitroblue tetrazolium, and microglial respiratory burst was revealed in vivo using a fluorescent probe [10].

There are many products formed during oxidative free radical damage to cells. Widely used as markers of free radical attack are the aldehydes originating from membrane

lipid peroxidation, especially malonaldehyde and 4-hydroxynonenal [11]. These aldehydes are relatively short-lived because of their high reactivity, and their determination by the thiobarbituric acid assay has several draw-backs. The most serious problem is the fact that positive reaction is also given by substances not related to free radicals [12]. A more reliable group of markers of free radical damage is represented by lipophilic fluorescent end-products, originally termed lipofuscin-like pigments (LFPs) [13]. They are relatively stable and long-lived. LFPs were originally named on the basis of the similarity of their fluorescence properties with those of lipofuscin—the pigment of old age. However, later studies showed that they are not directly related to lipofuscin formation but are rather the result of free radical-initiated oxidative damage to membrane lipids [14].

The presence of LFP has been widely used as an indicator of oxidative damage in various biological systems induced by such diverse triggers as hyperoxia or hypoxia [6, 15, 16], ionizing radiation [17–19], phagocytosis of oxidized proteins [20], and physical activity [21].

The aim of this study was to investigate the formation of LFP in frontal rat brain cortex in the neonatal period and during early development to assess the extent of oxidative damage after birth. For a more detailed characterization of fluorescent properties of LFP, the authors used various spectral methods comprising tridimensional spectral arrays, synchronous fluorescence spectra, and their derivatives. The LFPs were resolved into several fractions by means of HPLC with fluorescence detection. The results confirm that the highest accumulation of oxidative products takes place immediately after birth; they also indicate that brain LFPs constitute a complex mixture of chemical compounds whose composition is changing during development.

Methods

The study was conducted in accordance with the *Guide for the Care and Use of Laboratory Animals* published by the US National Institutes of Health (NIH publication No. 85-23, revised 1996).

Animals

A total of 70 pregnant female Wistar rats were used throughout the experiments. They had free access to water and standard laboratory diet. The offsprings of both sexes were divided into 10 groups. Group A (110 foetuses) was sampled 7 days before birth, group B (110 foetuses) 1 day before birth, group C (50 animals) on postnatal day 1, group D (50 animals) on postnatal day 2, group E (50 animals) on postnatal day 5, group F (50 animals) on postnatal day 10, group G (50 animals) on postnatal day 15, group H (30 animals) on postnatal day 25, group I (30 animals) on postnatal day 35, and group J (20 animals) 3 months after birth. The animals were euthanized by decapitation in ether narcosis. The frontal brain was rapidly removed, separated from white matter if possible, snap-frozen in liquid nitrogen, and stored at −70°C until use.

LFP fluorescence measurement

The technique described by Goldstein and McDonagh [22], modified in [16], was used for the analysis of LFP in brain homogenates. Approximately 30 mg of frozen brain sample was weighed, chopped to fine pieces, and transferred into a glass-stoppered test tube containing 6 ml of chloroform–methanol mixture (2:1, v/v). After 1-h extraction on a motor-driven shaker, 2 ml of double distilled water was added, the sample was agitated, and the ensuing mixture was centrifuged (400 g, 10 min). After centrifugation, the lower chloroform phase was separated and used for measurements.

Fluorescence excitation and synchronous spectra were measured on an Aminco-Bowman series 2 spectrofluorometer and recorded and analyzed using AB-2 computer program that also organized the spectra into tridimensional spectral arrays. The excitation spectra were measured in the range of 250–400 nm for emission adjusted between 400 and 500 nm in steps of 10 nm. The quantitative estimation of LFP was based on excitation and emission maxima found in tridimensional spectral arrays. The authors identified three major fluorophores F325/380, F335/410, and F355/440 (excitation/emission, nm). The fluorometer was calibrated based on the standard No. 5 of the instrument manufacturer, and the LFP concentration was expressed in arbitrary units per mg tissue wet weight. The statistical evaluations were made using ANOVA with Scheffe post-hoc test, and the results are shown as means ± SEM.

The synchronous emission spectra were measured in the range of 350–550 nm, with a constant difference of 50 nm between excitation and emission wavelengths. Their second derivatives were obtained using the AB-2 software.

HPLC analysis

Brain chloroform extracts were evaporated under the stream of nitrogen. The evaporated sample was dissolved in approximately 1 ml of running phase used in isocratic HPLC separation. A mixture of acetonitrile–methanol–water (50:10:40, v/v) was used for separation of LFP. A Jasco HPLC instrument equipped with fluorescence detector was set at the excitation and emission maxima of the three major fluorophores. A C18 column (4 × 250 mm)

was used for the analysis. Isocratic elution gave optimum separation at 0.2 ml/min.

Results

Fluorescence measurements

In the first step of our study, the authors analyzed the chloroform extracts obtained from brains of animals of different age by measuring tridimensional fluorescence spectral arrays. These spectral arrays are capable of revealing many fluorophores contained in the studied mixture. Each age group was characterized by a specific spectral pattern. For the sake of illustration, Fig. 1 shows the examples of spectra of whole-brain chloroform extracts from animals 7 days before birth (A), 2 days after birth (D), and then 3 months old (J). The shapes of the spectra indicate the presence of many fluorophores and their changes in the course of development. The general appearance of the spectra is a sort of a "fingerprint" characteristic for given mixture. Thus, even a subtle difference between groups A and D indicates a change in composition. This conclusion is further confirmed by the second derivatives of synchronous spectra shown in Fig. 3.

Figure 2 documents the evolution of the three major fluorophores used for the quantitation—F325/380, F335/410, and F355/440 (excitation/emission)—during the development. It is apparent that the pattern of changes is similar for all of them. On the postnatal day 1 (group C), there is an increase in concentration that is statistically significant in relation to prenatal group A. On the postnatal day 2 (group D), the concentration reaches its maximum, and on postnatal day 5 (group E), it is still significantly increased in relation to prenatal situation. Starting from postnatal day 10 (group F) up to day 35 (group I), the concentrations of the fluorophores are decreased to prenatal levels. A new rise of fluorophore concentration appears at 3 months of age (group J).

As the shape of the spectra of Fig. 1 implies the presence of several fluorophores, the authors attempted to further resolve the mixture by spectral and chromatographic techniques. Figure 3 presents the synchronous fluorescence spectra in the left-hand panels and their second derivatives in the right-hand panels. Especially the second derivative of the synchronous spectra has a great resolving power. The vertical arrows indicate the emission maxima of major peaks. It is apparent from the comparison of prenatal (group A) and 2-day-old animals (group D) that the greatest changes are observed between emissions in the range of 410–470 nm, i.e., in the region characteristic for fluorescent products of lipid peroxidation. Comparison with 5-day-old animals (group E) indicates dynamic changes in the fluorophore composition that persist until 90 days of age (group J).

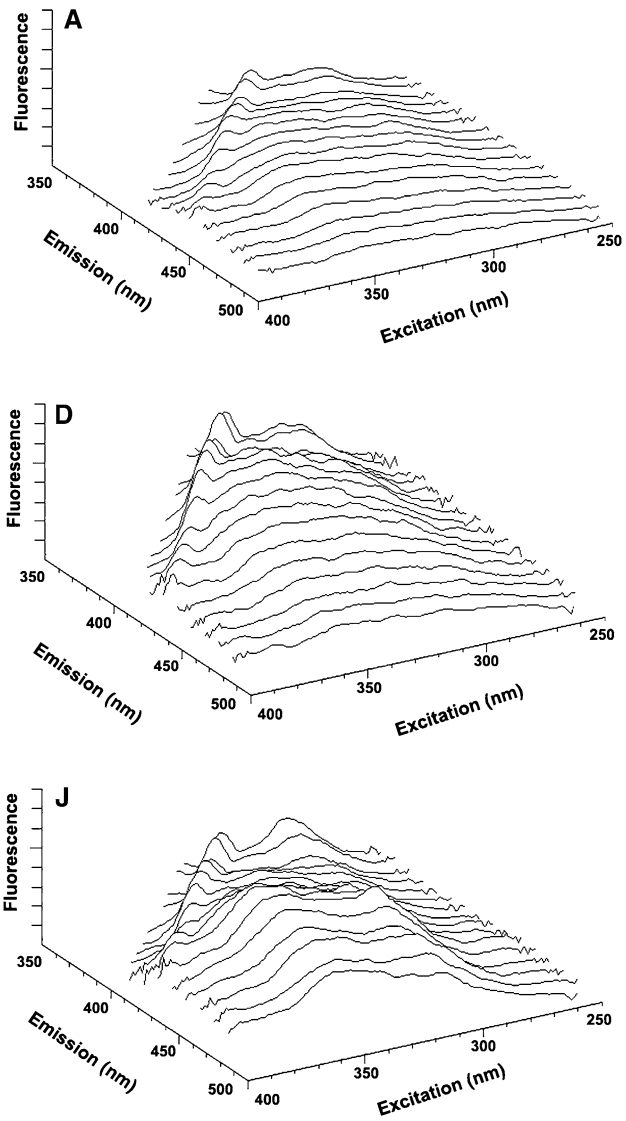

Fig. 1 Examples of 3D fluorescence excitation spectra of brain chloroform extracts. **A** 7 days before birth, **D** postnatal day 2, **J** 3-month-old animals

HPLC analysis

The authors further resolved spectrally characterized fluorophores by HPLC. Figure 4 documents that one fluorophore can be resolved into several chromatographically distinct species. Again, the fractionation pattern is different throughout the development indicating changes in the composition of these free radical products. Figure 4 illustrates the fractionation of the fluorophore F355/410, but other fluorophores can also be fractionated in a similar way. This means that several tens of fluorescent radical

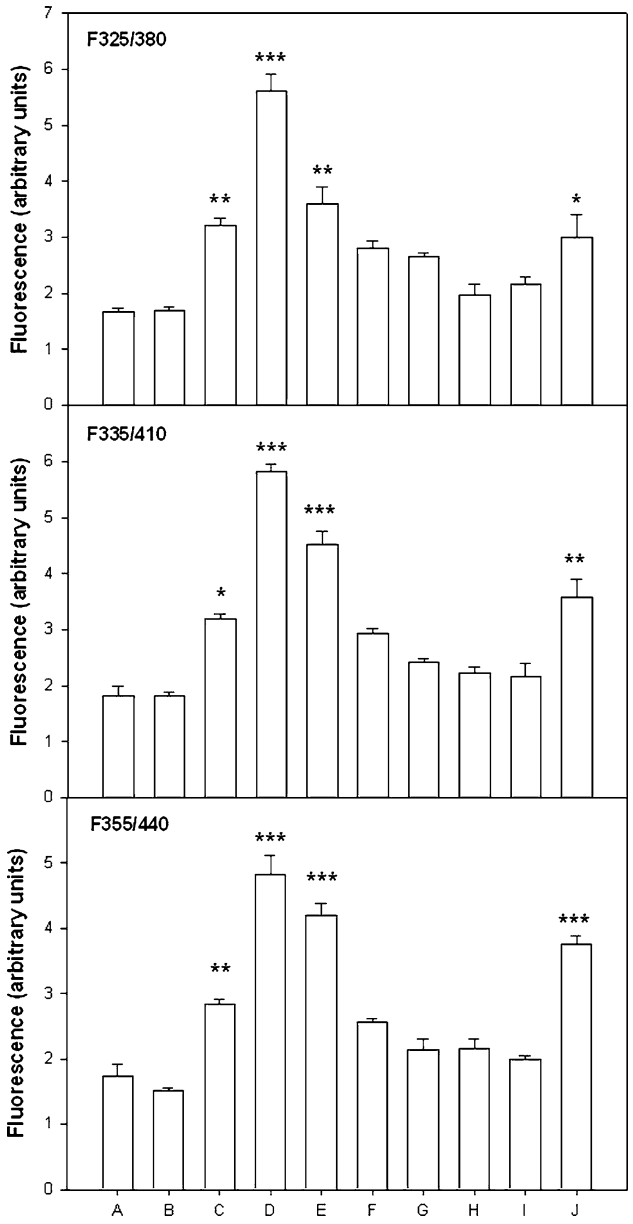

Fig. 2 Quantitative presentation of three major LFP fluorophores found in 3D spectra. For the group description, see Methods section. Statistical significance related to group A: * $P < 0.05$, ** $P < 0.01$, *** $P < 0.001$

products are generated and metabolized during brain development.

Discussion

Although the increased free radical generation after birth is to be expected because of rapid increase in oxygen concentration, the problem has not been extensively studied. An important study in this regard showed ROS-mediated oxidative damage to DNA in rat liver, kidney, and skin during the first few hours after normal birth. Lungs were not affected. The lesions were considered substantial, having been similar to or exceeding the levels in 24-month-old rats [23]. The concept of oxidative stress after normal birth was supported by the finding of pronounced neonatal decreases in the hepatic GSH/GSSG ratio in rats [24, 25]. Also the product of membrane lipid peroxidation, malonaldehyde, exhibited a transient rise after birth in rat liver and kidney [26]. The tissue specificity of oxidative damage may be explained by differences in both oxidative metabolism and antioxidant protection. Unfortunately, no such studies were undertaken in brain.

Our results indicate a transient accumulation of oxidative products occurring in neonatal rat brain. LFPs, which represent the end-products of membrane lipid peroxidation, appeared on the day 1 after birth, were at a maximum on the day 2, and decreased to prenatal concentrations after postnatal day 5. A new rise of LFP production appeared in 3-month-old animals. Thus, our results correlate with oxidative damage to DNA observed in a previous study [23]. The fact that all fluorophores have similar, though not identical, kinetics is biologically relevant. It might mean that they originate from the same kind of processes or are localized to the same compartment.

In a parallel study, the authors have investigated LFPs in neonatal rat heart, and found that the kinetics is similar to that of brain. The manuscript is in preparation for publication.

Though mitochondria are the first suspects when it comes to ROS generation in brain, their role in early postnatal brain is uncertain, as previous studies have documented fully active mitochondrial enzymes only after postnatal day 10 [7, 8]. It suggests that mitochondria are not responsible for the aforementioned oxidative damage. It appears that the real culprit might be microglia phagocytosing apoptosed brain cells. In mice, it was shown that maximum phagocytosis associated with ROS production occured on postnatal day 3 [10]. This time period corresponds well with maximum LFP production between postnatal day 1 and day 5 in this study. Thus, the authors suggest that the early production of LFP in brain is connected with the activity of microglia. Transition from hypoxia to normoxia triggers increased production of free radicals [16]. Delivery is accompanied with the increase in oxygen partial pressure which might support free radical generation. In that case, LFPs would increase immediately after birth; however, the authors have found maximum LFP formation on the postnatal day 2. It is possible that hypoxic/normoxic transition can contribute to the process of LFP formation, but it will not be the major factor.

The patterns of tridimensional spectral arrays, synchronous spectra, and their derivatives all indicate the presence of many fluorescent species belonging to the category of

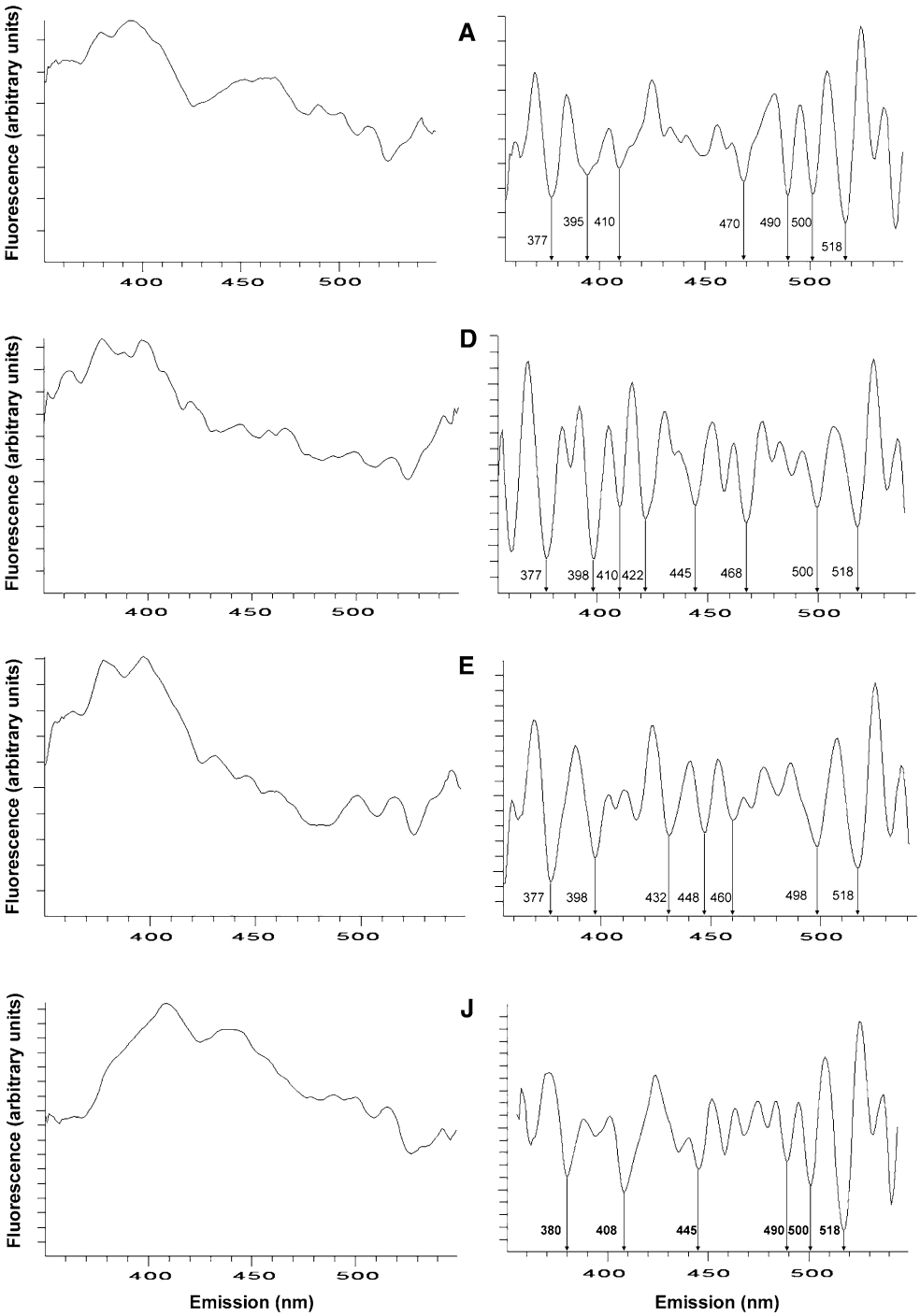

Fig. 3 Examples of synchronous fluorescence spectra (*left-hand panels*) and their second derivatives (*right-hand panels*). **A** 7 days before birth, **D** postnatal day 2, **E** postnatal day 5, **J** 3-month-old animals. *Vertical arrows* in the second derivatives of the spectra indicate the emission maxima of the resolved fluorophores

LFP. Each spectrally characterized species can be further resolved into several chromatographically distinct compounds. Taken together, LFPs represent several tens of unknown compounds that are related to brain oxidative damage after normal birth in rats. The changes in their concentration are accompanied by dynamic changes in their composition. Apparently, therefore, there is a dynamic metabolism of these compounds in the neonatal period. Unfortunately, the chemical composition of these compounds is not known, nor are their biological effects. Further studies should, therefore, be aimed at their detailed characterization that would enable us elucidate on their biological role.

The formation of LFPs in 3-month-old animals, when aging starts in rats, might depend on ROS generated by mitochondria [5]. Since that time, these products only cumulate [27]. The levels of LFP generated in the early neonatal period are higher than in 3-month-old animals,

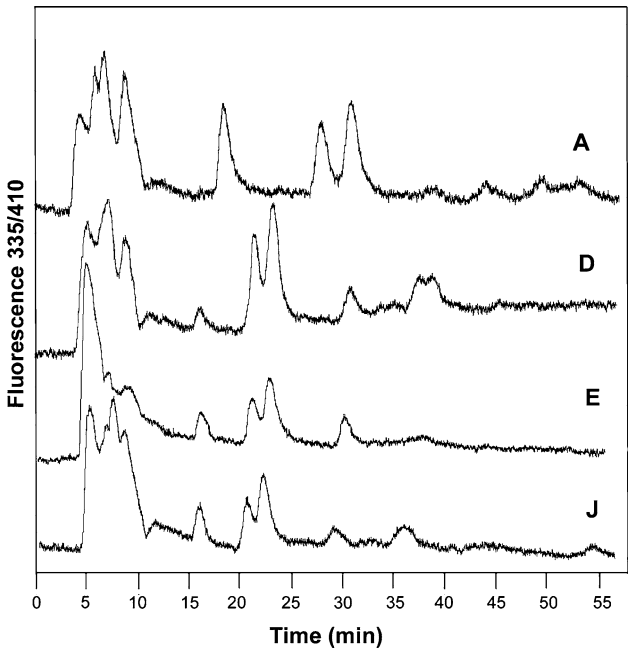

Fig. 4 Examples of the HPLC tracings of the fluorophore F355/410 in brain chloroform extracts of animals of different age: (*A*) 7 days before birth, (*D*) postnatal day 2, (*E*) postnatal day 5, (*J*) 3-month-old animals

but they return to basal value on day 10. The authors believe that this effect is caused by short-term ROS production. When apoptosis is terminated, newly growing brain cells—not producing ROS—"dilute" LFP generated during the respiratory burst. In our opinion, this kinetics support our view that early LFPs are the by-products of microglial phagocytosis of apoptosed brain cells.

Acknowledgments This study was supported by Grant Agency of AS CR (IAA500110606), The Centre of Neurosciences (project of Ministry of Education of the Czech Republic LC 554), and by the Academy of Sciences of the Czech Republic (AV0Z50110509).

References

1. Harman D (1956) Aging: a theory based on free radical and radiation chemistry. J Gerontol 11:298–300
2. Harman D (2003) The free radical theory of aging. Antioxid Redox Signal 5:557–561
3. Chance B, Sies H, Boveris A (1979) Hydroperoxide metabolism in mammalian organs. Physiol Rev 59:527–605
4. Navarro A, Boveris A (2004) Rat brain and liver mitochondria develop oxidative stress and lose enzymatic activities on aging. Am J Physiol Regul Integr Comp Physiol 287:R1244–R1249
5. Kann O, Kovács R (2007) Mitochondria and neuronal activity. Am J Physiol Cell Physiol 292:C641–C657
6. Jamieson DD (1991) Lipid peroxidation in brain and lungs from mice exposed to hyperoxia. Biochem Pharmacol 41:749–756
7. Svoboda P, Lodin Z (1972) Postnatal development of some mitochondrial enzyme activities of cortical neurons and glial cells. Physiol Bohemoslov 21:457–465
8. Svoboda P, Lodin Z (1973) Ontogenic development of oxidative capacity of the brain. Physiol Bohemoslov 23:434
9. Kuan CY, Roth KA, Flavell RA et al (2000) Mechanisms of programmed cell death in the developing brain. Trends Neurosci 23:291–297
10. Marín-Teva JL, Dusart I, Collin C et al (2004) Microglia promote the death of developing Purkinje cells. Neuron 41:535–547
11. Witz G, Lawrie NJ, Zaccaria A et al (1986) The reaction of 2-thiobarbituric acid with biologically active alpha, beta-unsaturated aldehydes. Free Radic Biol Med 2:33–39
12. Weber GF (1990) The measurement of oxygen-derived free radicals and related substances in medicine. J Clin Chem Clin Biochem 28:569–603
13. Chio KS, Reiss V, Fletcher B et al (1969) Peroxidation of subcellular organelles: formation of lipofuscin-like pigments. Science 166:1535–1536
14. Armstrong D, Wilhelm J, Smid F et al (1992) Chromatography and spectrofluorometry of brain fluorophores in neuronal ceroid lipofuscinosis (NCL). Mech Ageing Dev 64:293–302
15. Wihlmark U, Wrigstad A, Roberg K et al (1996) Lipofuscin formation in cultured retinal pigment epithelial cells exposed to photoreceptor outer segment material under different oxygen concentrations. APMIS 104:265–271
16. Wilhelm J, Herget J (1999) Hypoxia induces free radical damage to rat erythrocytes and spleen: analysis of the fluorescent end-products of lipid peroxidation. Int J Biochem Cell Biol 31: 671–681
17. Bonnefont-Rousselot D, Gardes-Albert M, Lepage S et al (1992) Effect of pH on low-density lipoprotein oxidation by O_2^-/HO_2 free radicals produced by gamma radiolysis. Radiat Res 132: 228–236
18. Wilhelm J, Brzak P, Rejholcova M (1989) Changes in lipofuscin-like pigments in erythrocytes and spleen after whole-body gamma irradiation of rats. Radiat Res 120:227–233
19. Wilhelm J, Sonka J (1981) Time-course of changes in lipofuscin-like pigments in rat liver homogenate and mitochondria after whole body gamma irradiation. Experientia 37:573–574
20. Shimasaki H, Maeba R, Tachibana R et al (1995) Lipid peroxidation and ceroid accumulation in macrophage cultured with oxidized low density lipoprotein. Gerontology 41(Suppl 2):39–48
21. Vasankari T, Kujala U, Heinonen O et al (1995) Measurement of serum lipid peroxidation during exercise using three different methods: diene conjugation, thiobarbituric acid reactive material and fluorescent chromolipids. Clin Chim Acta 234:63–69
22. Goldstein BD, McDonagh EM (1976) Spectrofluorescent detection of in vivo red cell lipid peroxidation in patients treated with diaminodiphenylsulfone. J Clin Investig 57:1302–1307
23. Randerath E, Zhou G-D, Randerath K (1997) Organ-specific oxidative DNA damage associated with normal birth in rats. Carcinogenesis 18:859–866
24. Sastre J, Asensi M, Rodrigo F et al (1994) Antioxidant administration to the mother prevents oxidative stress associated with birth in the neonatal rat. Life Sci 54:2055–2059
25. Pellardo FV, Sastre J, Asensi M et al (1991) Physiological changes in glutathione metabolism in fetal and newborn liver. Biochem J 274:891–893
26. Gunther T, Hollriegl V, Vormann J (1993) Perinatal development of iron and antioxidant defense systems. J Trace Elem Electrolytes Health Dis 7:47–52
27. Brunk UT, Terman A (2002) Lipofuscin: mechanisms of age-related accumulation and influence on cell function. Free Radic Biol Med 33:611–619